CHAPTER 1

INTRODUCTION

1.1 Background

Due to the continued growth in ageing population, report from World Health Organization forecasted the neurodegenerative disorders will rise above cancer in the next 30 years, as a second leading cause of death following cardiovascular disease. More than 600 disorders afflict the nervous system especially Alzheimer's disease and Parkinson’s disease, as the world's leading cause of approximately 50-75 % dementia that have been associated with free radical generation. Growing substantial evidences have shown that various neurodegenerative diseases arise as a result from free radical generation. On the other hand, reactive oxygen species-induced oxidative stress has been implicated in various neurodegenerative diseases namely Alzheimer's disease, Parkinson's disease, Huntington's disease, amyotrophic lateral sclerosis, Friedreich's ataxia, Lewy body disease, and spinal muscular atrophy with serious and life-threatening consequences. Neurodegenerative disorders involved the dysfunction in central and peripheral nervous system which might cause failure in movement, balance, speaking, breathing and heart function. Yet, most of the neurodegenerative diseases have no cure and subject to solemn negative side effects after drugs treatment. Also, their etiology is poorly understood and complicated. In view of that, a raise in the efforts to seek natural-based treatment is enforced for the sake of overcoming neurodegenerative diseases in a manner of side effects-free. Phytochemical plays an important role in phytotheraphy particularly in neurodegenerative diseases as most of the antioxidants have been proven scientifically for their significant potential in the contribution of neuroprotection. Extensive natural product researches have been

identified in the exploration of effective neuroprotective agent as an urgent need to resolve the burden raise in the neurodegeneration phenomenon lately. For that reason, a Chinese folk medicine, *L. parasiticus* has been selected to investigate the antioxidative and neuroprotective activities in an oxidative stress-induced neuroprotection model in the present study, hypothesing that *L. parasiticus* in exhibiting significant antioxidative and neuroprotective properties as well as a novel molecular therapeutic target site in *L. parasiticus*-mediated neuroprotective mechanism to be established.

1.2 Objectives

1.2.1 Overall objective

The present work was performed to investigate the antioxidative and neuroprotective activities of *L. parasiticus* against hydrogen peroxide (H_2O_2)-induced oxidative stress in NG108-15 cells, as well as to identify the most potent neuroprotective compound through bioactivity-guided isolation approach and subsequently to elucidate the underlying neuroprotective mechanisms of the most potent neuroprotective compound isolated from *L. parasiticus* in NG108-15 neuroprotection model.

1.2.2 Specific objectives

The specific objectives of the present study were the following:

a. to evaluate the antioxidative activities of *L. parasiticus*

b. to investigate the neuroprotective effects of *L. parasiticus* against H_2O_2-induced

oxidative damage in NG108-15 cells via 3-(4,5-domethylthiazol-2-yl)-2,5-diphenyltetrazolim (MTT) cell viability assay

c. to determine the H_2O_2-induced apoptotic effect and neuroprotective effect of *L. parasiticus* on nuclear morphological changes by 4',6-diamidino-2-phenylindole (DAPI) staining in NG108-15 cells

d. to elucidate and confirm the neuroprotective mechanisms via the antiapoptotic effects of *L. parasiticus* through the alteration in intracellular glutathione (GSH) level, intracellular reactive oxygen species level, externalization of phosphatidylserine, change in mitochondrial membrane potential, and cell cycle distribution in H_2O_2-induced oxidative damaged NG108-15 cells

e. to isolate and elucidate the chemical structure of the most potent neuroprotective compound from *L. parasiticus* against H_2O_2-induced oxidative damage in NG108-15 cells, via neuroprotective activity-guided fractionation approach

f. to elucidate the neuroprotective mechanisms via the antiapoptotic effects of (+)-catechin through the alteration in intracellular reactive oxygen species level, externalization of phosphatidylserine, change in mitochondrial membrane potential, cell cycle progression, and intracellular antioxidant enzymes (SOD and GPx) in H_2O_2-induced oxidative damaged NG108-15 cells

g. to investigate the neuroprotective effects of (+)-catechin on the expression level of Bax and Bcl-2 following H_2O_2-induced oxidative damage in NG108-15 cells

h. to investigate the role of neuronal chemokine CCL21 in the neuroprotective action of (+)-catechin in H_2O_2-induced oxidative damaged NG108-15 cells

CHAPTER 2

LITERATURE REVIEW

2.1 Neurodegeneration

By 2040, World Health Organization forecasts that neurodegenerative diseases will have overtaken cancer to become the world's second leading cause of death following cardiovascular disease, as an outcome of continual growth in ageing population. Yet, distinct from the condition in cancer and cardiovascular disease, governments and pharmaceutical sectors have yet to make a major commitment in treating neurodegenerative diseases.

According to the National Institute of Neurological Disorders and Stroke, more than 600 neurologic disorders afflict the nervous system, with approximately 50 million Americans affected every year. Among the neurological disorders, oxidative stress plays a prominent role in all type of dementia which leads to the amendment in one's memory, activity, behaviour and ability to think clearly.

Neurons are building blocks of the nervous system that contain the brain and spinal cord. Generally, neuronal cells are not able to reproduce themselves and unable to replace by the body as well in the context of neuronal damage. Neurodegenerative diseases can be defined as sporadic and hereditary circumstances that are characterized by progressive dysfunction of nervous system. Generally, neurodegenerative diseases are incurable which result in progressive degeneration and death of nerve cells, embracing a situation in which nerve cells from brain and central nervous system are lost leading to either sensory dysfunction (dementia) or functional loss (ataxia).

Oxidative stress has long been implicated in numerous neurodegenerative diseases such as Parkinson's disease (Seaton, 1997; Smith and Bennett, 1997; Cassarino et al.,

1997; Merad-Boudia et al., 1998; Merad-Saidoune et al., 1999; Thomas et al., 2000), Alzheimer's disease (Mecocci et al., 1994; Mecocci et al., 1997a; Mecocci et al., 1997b), amyotrophic lateral sclerosis (Yim et al., 1996; Yim et al., 1997; Wiedau-Pazos et al., 1996; Warita et al., 2001), Huntington's disease (Schapira, 1998; Polidori et al 1999; Browne et al., 1997), and Friedreich's ataxia (Rotig et al., 1997; Pandolfo, 1998) which coupled with the onset of mechanisms between increment of reactive oxygen species production, depletion of intracellular antioxidant enzymes, abnormal mitochondrial function, modulation of Bcl-2 family members, regulation of neuronal chemokines, and eventually neuronal cell death.

2.1.1 Brain and nervous system

Brain, the center of nervous system consists of high level of unsaturated fatty acids that are vulnerable to peroxidation and oxidative modification, which consumes an inordinate fraction (20 %) of total oxygen consumption for its relatively small weight (2 %). Unsaturated fatty acids with double bonded chemical structure prompts the brain to be more susceptible to free radical harass and therefore accounts for the onset of chain reaction to further damage the adjacent unsaturated fatty acids (Butterfield et al., 2002). Moreover, the neuronal cells in brain are low in antioxidant activity and antioxidant defenses compared with other tissues. These abnormal neuronal biochemical compositions in brain have been claimed from various researchers in regards to its sensitivity to oxidative stress (Chance et al., 1979; Floyd and Carney, 1992; Zaleska and Floyd, 1985). Also, long-term impact of the increased deleterious effects of reactive oxygen species generation (Schaffer et al., 2006) leading to a cascade of oxidative stress-induced apoptosis in brain (Salganik, 2001).

2.1.2 Reactive oxygen species

Under physiological circumstance, 1-2 % of oxygen consumed is converted to reactive oxygen species. However, this percentage rises up due to the decrease observation of antioxidants and low regenerative capacity in aged brain (Lepoivre et al., 1994). The generation of reactive oxygen species required metabolic system to facilitate the interaction of organic molecules with oxygen in vivo. Also, molecular oxygen has to be activated and cellular system needs to evolve range of metallo-enzymes which assists reactive oxygen species formation during the interaction of redox metals with oxygen by a range of catalytic pathways. Under normal biological conditions, cells have proficient regulatory system and defense system for the interaction between metal ion and oxygen causing the formation of reactive oxygen species as well as free radicals (Bush, 2000).

Reactive oxygen species consist of highly reactive hydroxyl radicals ($OH^{\bullet}$), superoxide anions (O_2^{-}), nitric oxide (NO), and H_2O_2. Damaged mitochondria and activated microglia acts as reservoir of reactive oxygen species. Formerly reactive oxygen species formation was understood to be an imbalance outcome between elimination and generation of reactive oxygen species and reactive nitrogen species but recently many molecular biology and chemistry revealed the regulatory role of reactive oxygen species in modulating key cellular functions (Klaus and Heribert, 2004). For instance, Haber Weiss and Fenton reaction (Figure 1) kick off the free radicals and reactive oxygen species formation to trigger mitogen activated protein kinase cascade, excitotoxic calcium mobilization and eventually apoptotic cell death (Hyman, 2004). The toxicity effect of free radicals have been reported for their significant contribution to neuronal loss in Alzheimer's disease, Parkinson's disease, cerebral ischemia, schizophrenia, and seizure disorders (Cadet, 1998; Demopoulos et al., 1980).

The nature of neuronal biochemical composition is vulnerable to reactive

oxygen species since it involves pool of unsaturated lipids which are labile to oxidative damage. As evident from terminology, reactive oxygen species are highly reactive to various cellular elementary molecules to initiate cascade of biochemical reactions simultaneously which leading to neuronal cell death eventually. Under oxidative stress circumstance, oxidation of lipids, proteins, and DNA occurred in neuronal microenvironment and produces numerous byproducts such as aldehydes, peroxides, ketones, cholesterol oxide, and alcohols which are toxic to macrophages and blood lymphocyte, paralyzing the defense system in vivo (Ferrari, 2000).

2.1.3 Oxidative stress

The term ‘oxidative stress’ was first coined by Sies to account for the imbalance between reactive oxygen species and the antioxidant opposing forces (Sies, 1985). Oxygen is essential for all living cells including neuronal cells but absurdly, it produces reactive oxygen species which are extremely toxic to cells as a by-product. Reactive oxygen species are predominantly vigorous in the nervous system as neurotransmitters and excitatory amino acids, whose metabolism is the factory of reactive oxygen species, serve as sources of oxidative stress. Excess in reactive oxygen species generation caused an imbalance of intracellular antioxidant enzymes and overwhelms antioxidant defensive system. Toxic accumulation of reactive oxygen species which subsequently leads to the occurrence of oxidative stress persist in the contribution of various neurodegenerative diseases (Halliwell, 1994; Sies, 1997). In most cases, low degree of reactive oxygen species act as signaling molecules and modulators whereas high degree of reactive oxygen species causes oxidative stress, and eventually leading to neuronal apoptosis (Dumont et al., 1999; Slater et al., 1995).

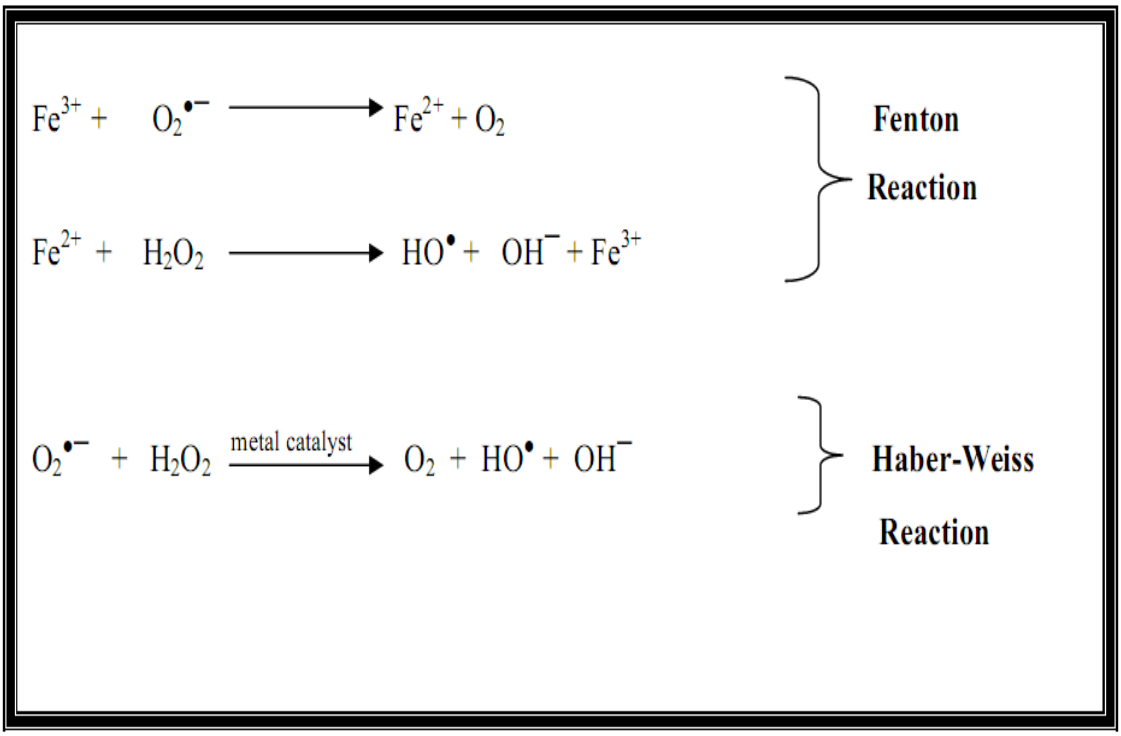

Figure 1. Free radical and reactive oxygen species formation as shown in equations (Kehrer, 2000)

Oxidative stress has long been postulated to play a vital role in aging process (Harman, 1956). In aged brain, oxidative stress levels were high and intracellular antioxidant enzymes such as catalase, superoxide dismutase, glutathione reductase and glutathione peroxidase were greatly reduced associated with the increased in oxidized glutathione levels, lipid peroxidation, and protein oxidation (Sugaya et al., 1996; Tian et al., 1998) in aged rodents (Mo et al., 1995).

Apart from its role in aging, oxidative stress has also been implicated in various neurodegenerative diseases. For instance, high levels of oxidized nuclear DNA (Gabbita et al., 1998) and mitochondrial DNA (Mecocci et al., 1994) have been shown in the central nervous system of Alzheimer's patients. Also, augmented protein oxidation was found in the central nervous system of Alzheimer's patients, especially in the region of hippocampus (Hensley et al., 1995). Furthermore, dinitrotyrosine and nitrotyrosine (Su et al., 1997) are found to be elevated in the central nervous system (particularly in the hippocampus and neocortex) and ventricular cerebrospinal fluid of Alzheimer's patients (Good et al., 1996; Smith et al., 1997; Hensley et al., 1998). Furthermore, oxidized mitochondrial DNA has been found in the central nervous system of Huntington's patients (Polidori et al., 1999) as well.

2.1.4 Mitochondria in relation to neurodegeneration

During the second half of the 20th century, mitochondria were considered entirely as the cell’s powerhouse, organelles with particular biochemical composition and architecture which serve only one main principle specifically in energy production by oxidative phosphorylation. In the year of 1995, mitochondria were being discovered a second vital role, called the control of cell death. Until now, it is complicated to disregard that cell death, in both its pathological and physiological occurrence, is intimately correlated to mitochondrial structure and dysfunction. The context of control

cell death in mitochondrial is crucial to recognize the complexity of mitochondrial life and death decision making devoid of getting lost in details.

In healthy cells, the inner mitochondrial membrane, the frontier between the intermembrane or intercristae space and the matrix, is nearly impermeable to all ions, including protons. This permits complexes I–IV of the mitochondrial respiratory chain to develop, across the inner mitochondrial membrane, the proton gradient which is required for oxidative phosphorylation (Mitchell and Moyle, 1965a; Mitchell and Moyle, 1965b). The imbalance of charge that results from the formation of an electrochemical gradient across the inner mitochondrial membrane forms the basis of the inner mitochondrial transmembrane potential. In the end, the proton gradient is exploited by complex V of the respiratory chain to force the synthesis of ATP. Thus, the maintenance of proton gradient is pivotal for cellular bioenergetics (Mitchell and Moyle, 1965a; Mitchell and Moyle, 1965b), in which all the elements of mitochondrial matrix as well as all metabolites that cross the inner mitochondrial membrane are well regulated by specific transport proteins and highly selective channels. Even though a transient loss of the mitochondrial transmembrane potential, through the “flickering” of one or several inner mitochondrial membrane pores, may occur in physiological circumstances (Kroemer et al., 1998; Zoratti and Szabo, 1995), a long-lasting or permanent mitochondrial transmembrane potential depolarization is frequently related to cell death (Marchetti et al., 1996; Zamzami et al., 2005).

The outer mitochondrial membrane permeability that delimits the outer contour of mitochondria is also well regulated in both normal life and the onset of cell death. During cell death circumstance, there was an increment in the outer mitochondrial membrane permeability which permits the release of soluble proteins that generally are retained within mitochondria, in the intermembrane space. The death-associated outer mitochondrial membrane permeabilization is also a tightly regulated process with major

consequences in health and various diseases.

Mitochondria play an imperative role in cell death regulation, a key feature of both acute and chronic neuronal death (Mattson and Kroemer, 2003). Accumulated experimental evidences support the death of neurons occurs via mitochondrial pathways following an acute stroke or a traumatic injury (Fiskum, 2000; Mattson, 2000). Even though apoptosis is not the only cell death mode in all brain regions (Friberg et al., 1999), the majority of neuronal death occurred via apoptosis pathway, exhibiting the typical features of nuclear shrinkage, chromatin condensation, caspase activation, and DNA fragmentation. Fascinatingly, mitochondrial membrane potential modulators which inhibit mitochondrial apoptosis are able to proficiently suspend neuronal cell death following hypoglycemic insult or stroke (Cao et al., 2002; Friberg et al., 1998) and actively participated in models of spinal cord injury and traumatic brain as well (Nesic-Taylor et al., 2005; Sato et al., 2003).

Conclusively, mitochondria function as ATP and Ca^{2+} generator as well as altering the reduction-oxidation potential of cells. Mitochondria also release proteins that activate caspases family of proteases (Folio, 2003). However, oxidative damage occurs mainly via mitochondrial electron transport chain. Generally, cells convert a small portion of oxygen into superoxide in the mitochondrial electron transport chain (Turrens et al., 1985; Nohl et al., 1996; Loschen et al., 1974; Dalton et al., 1999; Ksenzenko et al., 1983) as reactive oxygen species are normal byproducts of mitochondrial respiratory chain activity. Nevertheless, over production of reactive oxygen species leads to oxidative damage condition in mitochondria, cellular lipids, proteins, and nucleic acids, causing a shutdown in mitochondrial energy production (Reddy and Beal, 2005; Reddy, 2006). Additionally, high polyunsaturated level of mitochondrial phospholipids in brain prompt them to the activity of peroxidation and therefore, brain mitochondria are more vulnerable to neurological disorders which

evolved through the mechanisms of mitochondrial oxidative damage (Brookes et al., 1998).

2.1.5 Apoptosis in neuronal cell death

Programmed cell death is a genetically controlled and highly selective progression of cell deletion whereas cellular necrosis is a passive type of cellular injury which leads to the loss of membrane integrity and subsequently cell lysis (Wyllie, 1980). Programmed cell death is an essential element in the progression of the nervous system (Lo and Anderson, 1995) and also in numerous pathophysiological circumstances that result in neurodegeneration. Neuronal programmed cell death is thought to match neuronal number to target size and to rid the neurons from appropriate neuronal connections. Characteristics of neuronal programmed cell death such as plasma membrane blebbing, neuronal soma shrinkage with intact organelles, DNA fragmentation into oligonucleosomes, and nuclear condensation are the hallmarks of apoptosis, a mode of cell death seen during both development and normal tissue maintenance (Kerr et al., 1972).

In general, apoptosis can be elicited by two prominent molecular pathways namely the extrinsic (death receptor) pathway and intrinsic (mitochondrial) pathway (Figure 2). Apoptosis is activated at the death receptors of the cell surface via the ligand-induced activation in the extrinsic pathway. Death receptors consist of tumor necrosis factor (TNF) receptor-1, TNF-related apoptosis inducing ligand receptors, and cluster of differentiation (CD) 95/Fas receptor. On the other hand, apoptosis is triggered from mitochondrial membrane permeabilization via an intracellular cascade of events in intrinsic pathway (Scaffidi et al., 1998).

Both extrinsic and intrinsic routes to apoptotic cell death can be divided at least in three distinct phases: initiation, integration/decision, and execution/degradation

(Kroemer et al., 1997). During the initiation phase, the occurrence of apoptosis is extremely heterogeneous which depends on either extrinsic or intrinsic death signals. In the integration/decision phase, the death signals are transmitted into a complex molecular interplay and “point of no return” is set for the cells to undergo apoptosis. Lastly, the execution/degradation phase involved the damage of cellular function and structure which is subsequently causing the biochemical and morphological phenotypes of apoptosis (Kroemer et al., 1997). The typical morphological characteristic of extrinsic and the intrinsic pathways in apoptosis are membrane blebbing, phosphatidylserine exposure, cell shrinkage, DNA fragmentation, and chromatin condensation (Zamzami et al., 1996).

The caspases, a specific class of proteases are mandatory in the execution of apoptosis. Nevertheless, only a limited subset of caspases is activated particularly caspases-3, caspases-6, and caspases-7 (Fuentes-Prior and Salvesen, 2004), which belong to the “executioner” caspases by mediating their effects through the cleavage of specific cellular substrates. Initiator caspases-8, caspases-9, and caspases-10 that activate executioner caspases-3 and caspases-7 were identified as the most common apoptotic pathways.

Throughout the extrinsic pathway which initiated by the ligation of death receptors, the oligomerization and recruitment of Fas-associated protein with death domain (FADD) within the death-inducing signaling complex took place, in which the FADD attaches to the initiator caspases-8 and caspases-10 and leading to the event of dimerization and activation in apoptosis (Debatin and Krammer, 2004). Alternatively, dependency receptors can also be triggered in extrinsic pathway to activate a cascade of caspases as well without the ligand-induced activation event, and subsequently turn on cell death via a state of cellular dependence from their ligands (Mehlen and Bredesen, 2004).

However, most cell death is activated via the intrinsic or mitochondrial pathway of apoptosis (Green and Kroemer, 2004). Here, the multimerization on the apoptosis protease activating factor (APAF) 1 triggers the cleavage and activation of executioner caspases via the initiator caspase-9, within a multiprotein complex called “apoptosome.” APAF1 appeared as a monomer in cytosol and activated in the existence of cytochrome c and ATP/dATP (Cain et al., 2002). The production of apoptosome depends on the release of cytochrome c (Bernardi and Azzone, 1981). For this reason, mitochondrial membrane permeabilization is the decisive matter in accounting for the caspases activation in the intrinsic pathway. Moreover, mitochondrial membrane permeabilization can lead to cell death even in the event of caspases inactivation. The occurrence of “caspase-independent death” (Chipuk and Green, 2005; Kroemer and Martin, 2005) is due to the mitochondrial release of caspase independent death effectors such as apoptosis-inducing factor (AIF) (Susin et al., 1999), endonuclease G (Li et al., 2001), and others (Chipuk and Green, 2005; Kroemer and Martin, 2005), and also an irreversible functional loss of mitochondrial.

Neuronal programmed cell death can be induced via various toxic insults, for example nitric oxide exposure (Palluy and Rigaud, 1996; Maiese, 1998; Vincent and Maiese, 1999), excitotoxicity (Didier et al., 1996), cerebral ischemia (Hara et al., 1997), and oxidative stress (Bei et al., 2004; Kang et al., 2004; Yoon et al., 2000). Reactive oxygen species-induced oxidative stress plays an important role in neuronal apoptosis. For example, over expression in sympathetic neurons of Bcl-2 with known antioxidant properties (Hockenbery et al., 1993; Kane et al., 1993), delays the process of apoptosis with regards to nerve growth factor deprivation (Garcia et al., 1992), signifying the role of reactive oxygen species in neuronal apoptosis. Additionally, high oxygen-induced oxidative stress in different culture system (Enokido and Hatanaka, 1993) with beta-amyloid (Forloni et al., 1993; Loo et al., 1993; Behl et al., 1994), and transient ischemia

(Linnik et al., 1993; Okamoto et al., 1993; MacManus et al., 1994) exposure have been shown to activate apoptotic course in different neuronal types. A role for reactive oxygen species in motor neuron death has been suggested by the identification of mutations in copper/zinc SOD linked to familial amyotrophic lateral sclerosis (Deng et al., 1993; Rosen et al., 1993; Robberecht et al., 1994). Reactive oxygen species are also play an important function in lymphocyte programmed cell death as the over expression of either Bcl-2 or GPx delays the interleukin-3 deprivation-induced apoptosis in a B-cell line (Hockenbery et al., 1990).

2.1.6 Cell cycle event

Cell cycle, a precisely regulated process by cell cycle related proteins, is critical in the development, differentiation, proliferation and cellular death. Increasing empirical evidences indicate that activation of aberrant cell cycle elements in neuronal cells plays a vigorous role in many neurodegenerative diseases (Hoglinger et al., 2007; Osuga et al., 2000). Inappropriate activation of cell cycle regulators has been associated with a broad pathophysiology related central nervous system diseases, as well as both acute and chronic neurological disorders.

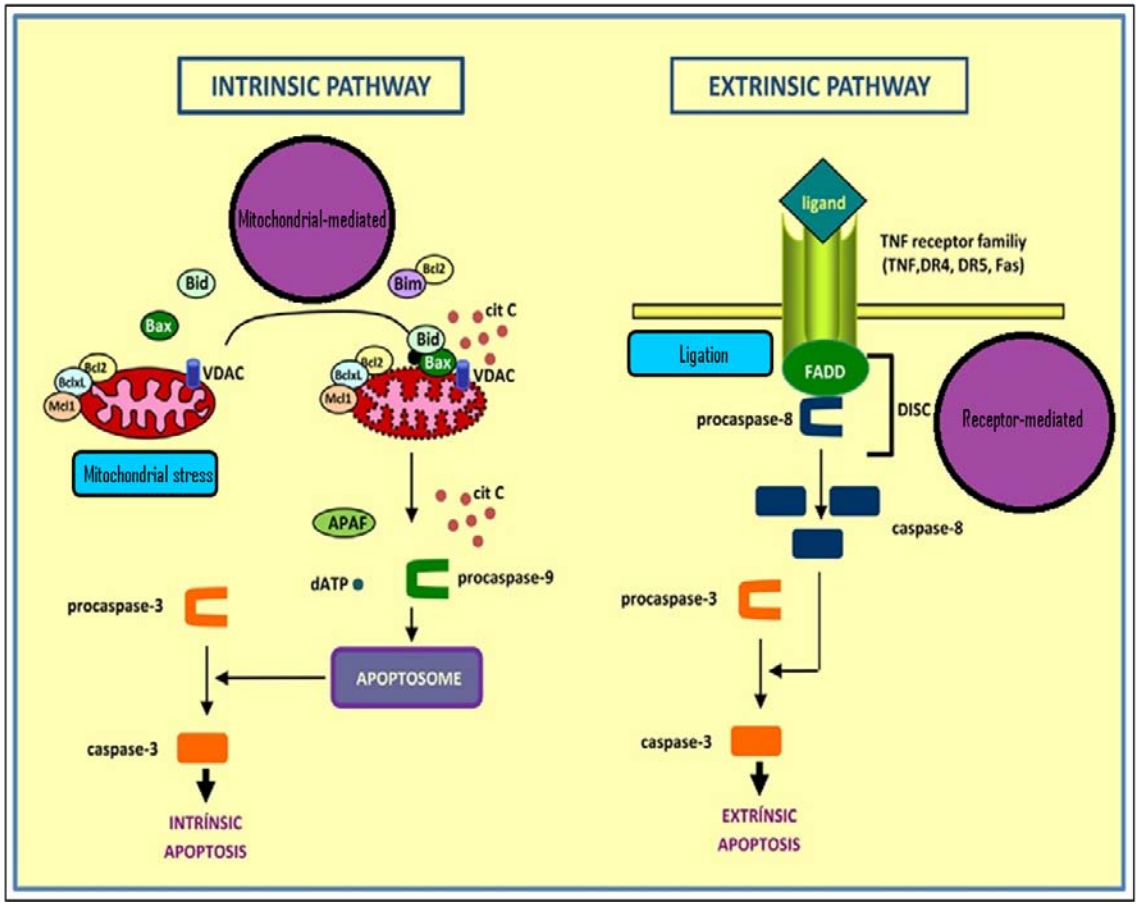

Figure 2. Two major apoptotic signaling routes: extrinsic (death receptor-mediated) pathway and intrinsic (mitochondrial-mediated) pathway (Gomez-Sintes et al., 2011)

Neurons and glia are the fundamental components of the central nervous system. Central nervous system progression is a complicated process that involves cell proliferation, differentiation, migration, and apoptosis of progenitor cells in an extremely regulated mode. Approximately half of neuronal cells formed during neurogenesis undergo cell death via apoptosis prior to the maturation of nervous system. Oxidative stress-induced DNA damage has been shown to trigger programmed cell death via the activation of cell cycle. Activated cell cycle associated molecules subsequently amend the transcription of several genes, such as bax and AIF to initiate apoptosis (Lossi and Merighi, 2003; Simonati et al., 1999). Furthermore, cell cycle components take part in the development of distinct regions in the central nervous system. For instance, gene targeting experiments revealed that cyclin-dependent kinase (CDK) 5 is a requisite in the progression of axonal migration, neurite outgrowth, control of cell adhesion, cortical lamination, synaptic activity, axonal transport, motor functions, and neuronal adaptive changes (Dhavan and Tsai, 2001).

In general, cell division in a cell cycle is typically divided into four phases: G1, S, G2, and M (Figure 3). G1 phase is the primary and main growth phase where the cells are preparing for DNA synthesis. In the S phase, the cells start to undergo DNA replication. G2 phase is the secondary growth phase where the cells are preparing for mitosis. In the M phase, the cells divide into two daughter cells. Briefly, G1, S, and G2 phases are recognized as interphase whereas M phase can be subdivided into prophase (condensation of chromosomes), metaphase (attachment of chromosomes to mitotic spindle), anaphase (separation of sister chromatids to opposite poles), and telophase (division into two daughter cells). The activation and expression of cell cycle proteins such as cyclins, CDKs, and CDK inhibitors drive these essential cell cycle events to generate a highly complicated biological coordination (Kohn, 1999). Hence, the core of

the cell cycle machinery accounts with the ordered and periodic activation or inactivation of CDKs (Han et al., 2005).

Neurons are classically illustrated as terminally differentiated that are permanently held at the G1 phase of the cell cycle. However, current findings have revealed that post-mitotic neurons attempt to re-enter the cell cycle in numerous pathological conditions (Malik et al., 2008; Osuga et al., 2000; Timsit et al., 1999). For instance, expression of CDK1/cyclin B1 complex (G2/M phase transition marker) has been demonstrated in Alzheimer's disease (Vincent et al., 1997) and also in vivo evidence has reported that S phase re-entry in ischemic neurons (Kuan et al., 2004). Nonetheless, cell cycle reactivation (S phase re-entry) in neuronal cells initiates the signals for neuronal death as opposed to neuronal proliferation.

Several studies have established the connection between neuronal cell death and dysregulation of cell cycle events (Yang and Herrup, 2007), both in acute neurodegenerative diseases such as trauma and stroke (Di Giovanni et al., 2005; Osuga et al., 2000) and chronic neurodegenerative diseases including Alzheimer's disease (Busser et al., 1998; Vincent et al., 1997), Parkinson's disease (Hoglinger et al., 2007; Jordan-Sciutto et al., 2003), amyotrophic lateral sclerosis (Nguyen et al., 2001; Ranganathan and Bowser, 2003), and Niemann-Pick disease type C (Bu et al., 2002a; Bu et al., 2002b). However, the exact cell cycle mechanisms leading to neuronal cell death are not entirely understood.

Cell cycle progression is tightly regulated by a family of protein kinases called CDKs. For instance, activation of CDK4 has been shown in the blockade of G1/S phase which is associated with neuronal apoptosis, in an acute central nervous system model (Di Giovanni et al., 2005; Osuga et al., 2000). Conversely, in chronic neurodegenerative diseases, neuronal cells may have passed through G1/S checkpoint to enter S phase of the cell cycle for DNA replication. The cell cycle machinery at this stage drives the

neuronal cells into G2/M transition accompany with highly activated CDK1. However, these highly expressed CDK1 were mislocated in cytoplasm and undergo a cascade of phosphorylation that subsequently arrested the neuronal cells at G2/M transition and contribute to the neuronal apoptosis (Vincent et al., 1997).

2.2 Neuroprotection

Neuroprotection is the strategies and mechanisms utilized in the protection of neuronal cells against neuronal injury or degeneration both in acute disorders and in chronic diseases. Neuroprotection approach is aim to limit neuronal dysfunction and neuronal death following central nervous system injury as well as to preserve a highest integrity and regulatory cellular communications within the nervous system.

Since oxidative stress have been recognized as the principle pathological cause of neurodegeneration, antioxidants as inhibitors of the process of oxidation, are proposed as therapeutic options to balance the formation of free radical. In general, antioxidative system includes both non-enzymatic (α-tocopherol, β-carotene, ascorbic acid, GSH, uric acid) and enzymatic systems (SOD, GPx, catalase), as well as some hormones (estrogen, angiotensin) which are capable of removing reactive oxygen species generated in cells and thus protecting against oxidative damage (Tawaha et al., 2007). Antioxidants have currently turned into a therapeutic focus against solemn neuronal injury or neuronal apoptosis, as they possessed the ability to neutralize free radicals. Also, antioxidants are capable to battle with other oxidizable substrates at relatively low concentrations to inhibit the oxidation event (Halliwell and Gutteridge, 1999). Recognition of upstream and downstream antioxidant remedy with regards to oxidative stress is essential to prevent free radicals-induced oxidative stress in neuronal damage.

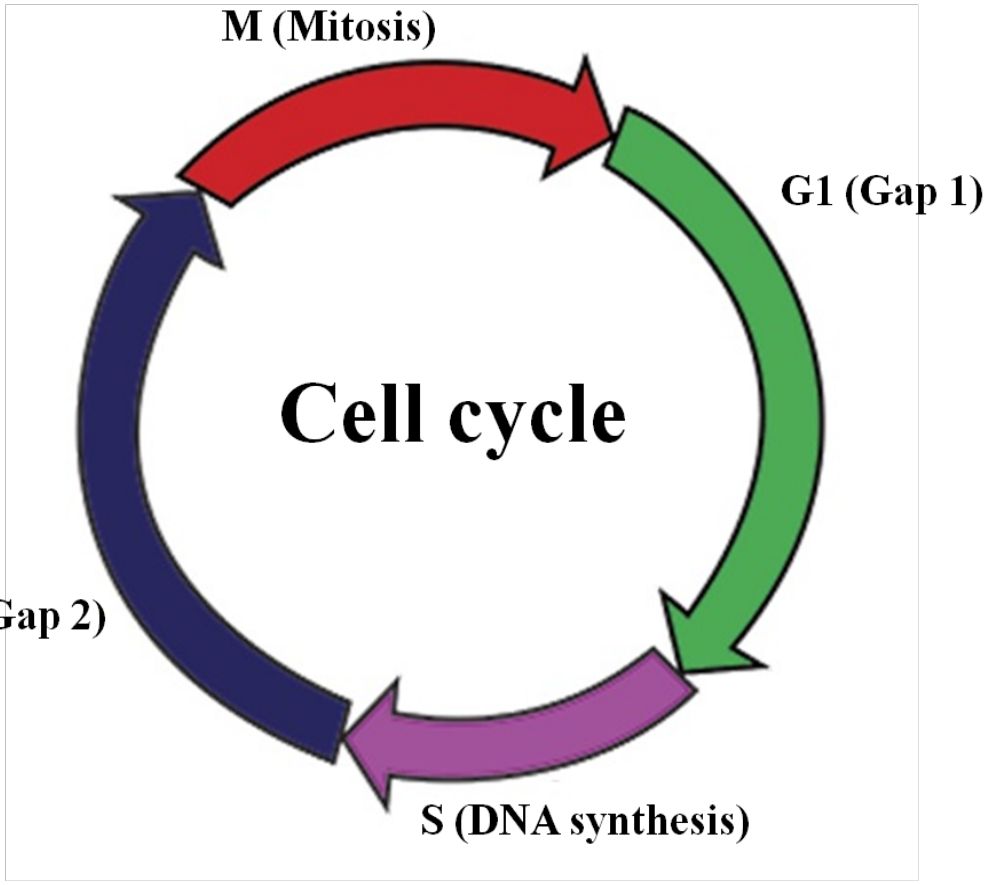

Figure 3. Phases of cell cycle

In view of that, effective neuroprotection therapy is essential in the context of neurodegenerative diseases. Antioxidants play a crucial role in neuroprotection by exhibiting neuroregenerative properties in preventing neuronal apoptosis (Moosmann and Behl, 2002). Antioxidants can be classified into endogenous antioxidants and exogenous antioxidants in nature. Endogenous antioxidants consist of intracellular enzymes (SOD, GPx, and catalase) and proteins (albumin, ceruloplasmin, transferrin, haptoglobin, and metallothionein). On the other hand, exogenous antioxidants include phytochemicals (flavonoids, polyphenols, catechins, quinones, terpenoids, and coumarins) and smaller molecules (ascorbic acid, beta-carotene, and alpha-tocopherol).

The process of antioxidant can occur in cytoplasm, plasma, and mitochondria (Larson, 1988; Namiki et al., 1993; Berger, 2005). Antioxidants, particularly plant-derived antioxidants present a promising therapy in various neurodegenerative diseases such as Alzheimer's disease, Parkinson's disease, Huntington's disease, amyotrophic lateral sclerosis, ischaemic, and haemorrhagic stroke (Maxwell, 1995; Floyd, 1999; Mattson, 2000; Moosmann and Behl, 2002; Nair et al., 2003; Berger, 2005). The free radical scavenging properties afforded by antioxidants to limit the production of reactive oxygen species slow the development of neurodegenerative diseases (Halliwell, 2001; Singh et al., 2004). Given that endogenous antioxidants defense system is not entirely effective with the increase of oxidative stress environment exposure, exogenous antioxidants play a critical and pivotal role in combating the accumulated effects of oxidative damage (Gilgun-Sherki et al., 2001). Additionally, the focus of medication has shifted from treatment to prevention, particularly the naturally derived phytochemicals with the four pillars of phytochemistry, phytopharmacy, phytopharmacology, and phytotherapy have come into consideration as the key contribution in neuroprotection (Weiss and Fintelmann, 2000). A statistic has been reported in the developing countries that approximately 80 % of the people believe in

phytomedicine for the basic healthcare intended for man and livestock (Plotkin, 1992; McCorkle et al., 1996).

2.2.1 Phytochemicals as neuroprotective agents

Majority of neuroprotectants are antioxidants. Food is the main source of antioxidants particularly diets that comprise natural phytochemicals has its significant contribution in neuroprotection presently. Plants have established an array of defense strategies (antioxidant system) to cope with oxidative stress. Extensive free radical scavenging molecules including phenolic compounds (phenolic acids, flavones, quinones, flavonoids, lignans, coumarins, tannins, stilbenes), nitrogen compounds (amines, alkaloids, betalains), terpenoids, vitamins, and other endogenous metabolites that possess antioxidant properties, can be found in medicinal herbs, fruits, and vegetables (Cai et al., 2003; Cotelle et al., 1996; Velioglu et al., 1998; Zheng and Wang, 2001). Polyphenolic compounds protect neuronal cells against oxidative stress-induced cell death via different molecular mechanisms as antioxidants are good source of neuroprotective agents in nature. For instance, hydroxyl groups of catechins may be critical for various biological activities including the antioxidative and free radical scavenging activities (van Acker et al., 1996; Nanjo et al., 1996), and subsequently impacted on the cellular events leading to apoptosis. Likewise, naturally derived antioxidants have been demonstrated to serve as singlet and triplet oxygen quenchers, free radical scavengers, enzyme inhibitors, peroxide decomposers, and synergists (Manach et al., 1998), and compounds belonging to several classes of phytochemical components such as phenols, flavonoids, and carotenoids are able to scavenge free radical in plasma (Gutteridge and Halliwell, 2000).

2.2.2 Catechins

Traditional Chinese medicine played an imperative role in the health care needs of Chinese and other oriental countries for thousands of years. As a result, traditional Chinese herbs have gained interest from the international medical, biomedical and pharmaceutical institutions due to the valuable phytochemicals contain in developing new antioxidants and neuroprotectants (Tawaha et al., 2007; Bouayed et al., 2006). This interest needed to apply modern research and development and to explore the full medical potential of resources from Chinese traditional herbs in the contribution to manage oxidative stress-related neurodegenerative diseases.

According to Chinese history, a cup of tea daily could dissolve body poisons as declared by emperor Sin-Non more than 3000 years ago. Tea consumption has been traditionally believed in oriental cultures to possess a variety of medicinal efficacies in the prevention and treatment of numerous diseases as well as to promote longevity (Liao, 2001). Conventionally, the consumption of green tea by the Chinese and Japanese communities is perhaps the most consumed beverage after water for centuries (Zaveri, 2006). Lately, green tea has gained significant attention in the contribution of health benefits for various diseases both in consumer as well as scientific communities, leading to the insertion of green tea extract in supplementation market and an increment in green tea consumption by the general and patient population. To date, the health benefits of green tea catechin are mainly based on the presence of polyphenolic compounds, particularly catechins that comprise 30 % of the dry weight of green tea leaves (Graham, 1992). Several polyphenolic catechins of green tea have been identified, for instance, (+)-catechin, (+)-gallocatechin, (−)-epicatechin, (−)-epicatechin-3-gallate, (−)-epigallocatechin, and (−)-epigallocatechin-3-gallate (EGCG) (Figure 4-9).

Green tea catechins have been reported to protect neuronal cells in Alzheimer's disease, Parkinson's disease, and ischemic damage significantly among the neurological

diseases (Mandel and Youdim, 2004). Green tea catechins are known to function as a pro-survival role in neuroprotection by showing their far lower treatment concentration than antitumor activities (Mandel et al., 2004). The neuroprotective mechanism of green tea catechins in neuronal cultures is principally due to the antioxidant properties to scavenge reactive oxygen species (Yang, 1999) and metal chelating activity (Brown et al., 1998; Hider et al., 2001; Kumamoto et al., 2001). However, experimental data proposed that catechins are able to trigger or activate a variety of signaling pathways leading to neuroprotection (Weinreb et al., 2003; Mandel et al., 2003). For example, green tea catechins exhibited a reduction in the expression of proapoptotic genes bad, bax, p21, and caspases at significantly low doses of treatment concentration in neuronal cells (Levites et al., 2002; Weinreb et al., 2003). Furthermore, green tea catechins also revealed to promote amyloid precursor protein processing through the nonamyloidogenic α-secretase pathway (Levites et al., 2003) as well as to inhibit the β-secretase pathway which leads to the development of β-amyloid fibrils (Jeon et al., 2003b), signifying a pro-survival neuroprotective effect afforded by green tea catechins in brain.

More recently, green tea catechins shown to attenuate neuronal death signals in a mouse amyotrophic lateral sclerosis model (Koh et al., 2006), enhanced learning ability and spatial cognition in a rodent model (Haque et al., 2006), decreased cerebral amyloidosis in an Alzheimer's transgenic mice model (Rezai-Zadeh et al., 2005), promoted neurorescue activity and neurite outgrowth in a serum deprived PC12 model (Reznichenko et al., 2005), and rapid degradation of Bad protein mediated by protein kinase C via ubiquitin proteasome system in culture cells (Kalfon et al., 2007).

Green tea catechin has been scientifically proven via various mechanisms of action in the contribution of neuroprotection particularly the most abundant catechin in green tea, EGCG. Nonetheless, little has been known about (+)-catechin. (+)-Catechin is

a flavanol, a class of flavonoids which attributed to the building blocks of proanthocyanidins. (+)-Catechin, an established powerful antioxidant compound that can be found abundantly in tea, particularly green tea (Manning and Roberts, 2003), is well-known for its anti-carcinogenesis, anti-cancer, and neuroprotection properties. (+)-Catechin has been reported to exhibit a variety of other pharmacological properties such as inhibition of intestinal tumor, depression ultraviolet B-induced skin stress, and treatment of viral hepatitis (Jeon et al., 2003a; Suzuki et al., 1986; Wcyant et al., 2001). Alternatively, (+)-catechin has also been revealed to possess neuropharmacological function in several neuroprotection model (Bastianetto et al., 2000; Conte et al., 2003; Inanami et al., 1998; Nobre Junior et al., 2003). Conversely, none has been reported on the effects of (+)-catechin against H_2O_2-induced oxidative damage in NG108-15 cells. Furthermore, the underlying neuroprotective mechanism afforded by (+)-catechin under oxidative stress condition remains unclear and has not been fully discovered. In view of that, investigating the role of (+)-catechin will be indispensable for the input of future therapeutic neuroprotective agent.

2.2.3 The role of intracellular GSH in neuroprotection

GSH was discovered in 1888 by de Rey Pailhade as an extract from baker's yeast, called "philothione", that had the ability to reduce sulphur to hydrogen sulphide (Meister, 1988). GSH is a major antioxidant in the brain (Dringen, 2000), with a concentration of approximately 2-3 mM, which is much higher than that in blood or cerebrospinal fluid (Cooper and Kristal, 1997). GSH exerts its functions via several mechanisms.

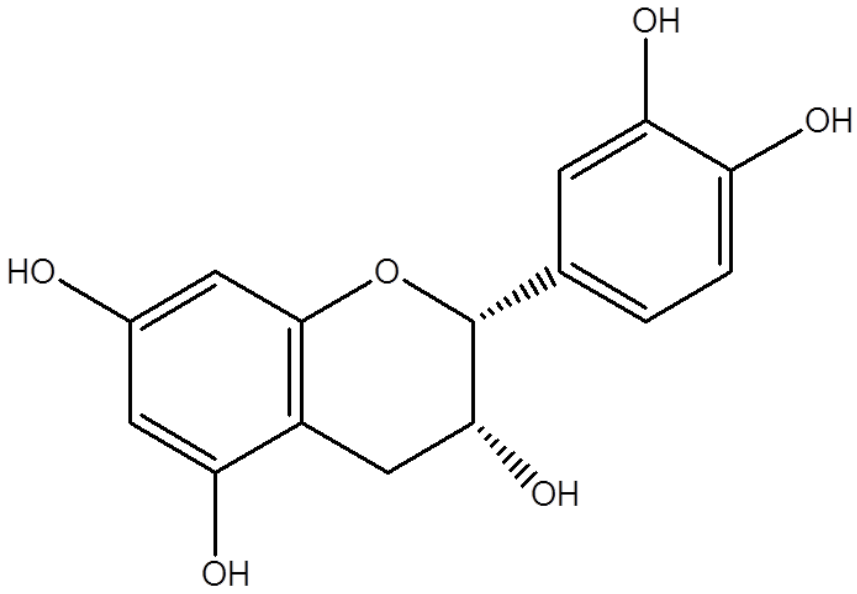

Figure 4. Chemical structure of (-)-epicatechin

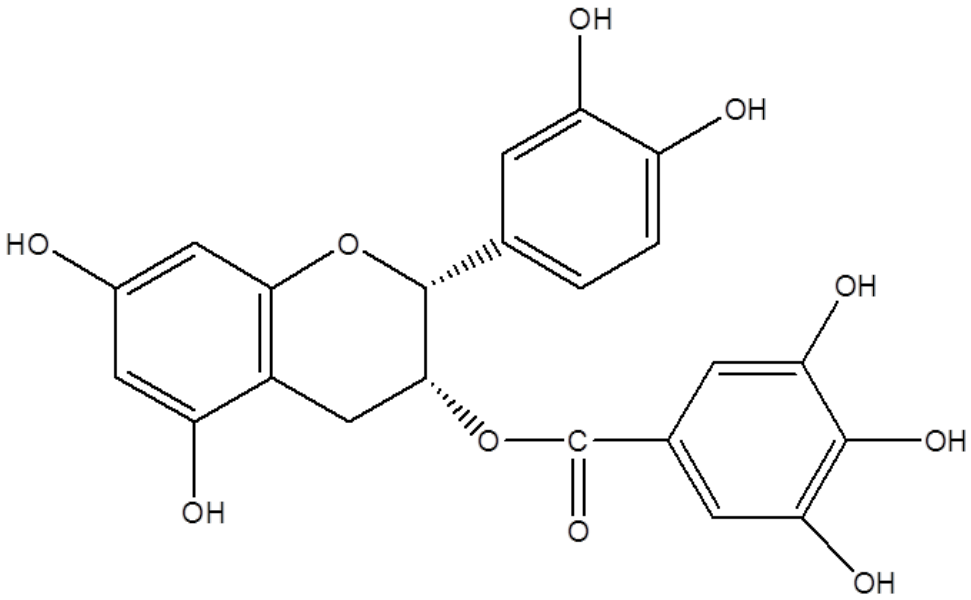

Figure 5. Chemical structure of (-)-epicatechin gallate

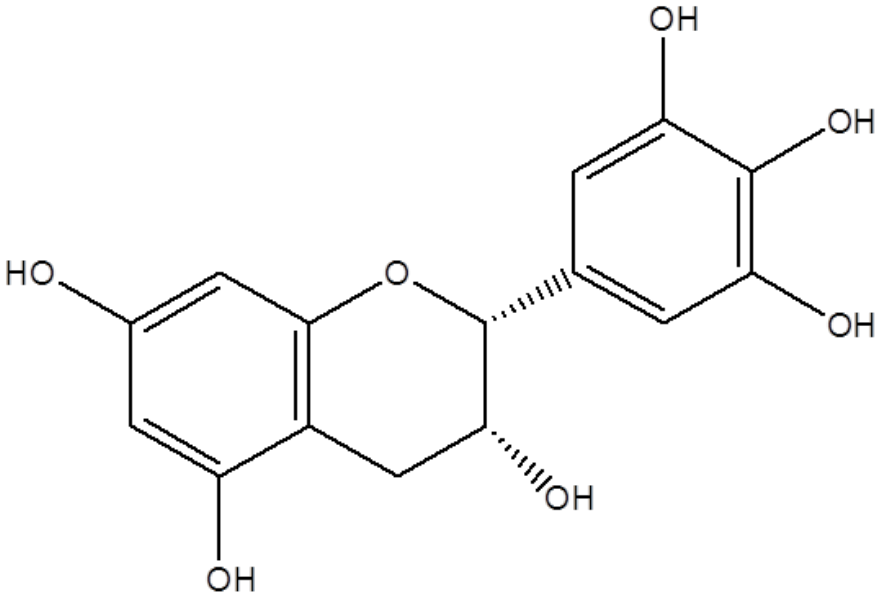

Figure 6. Chemical structure of (-)-epigallocatechin

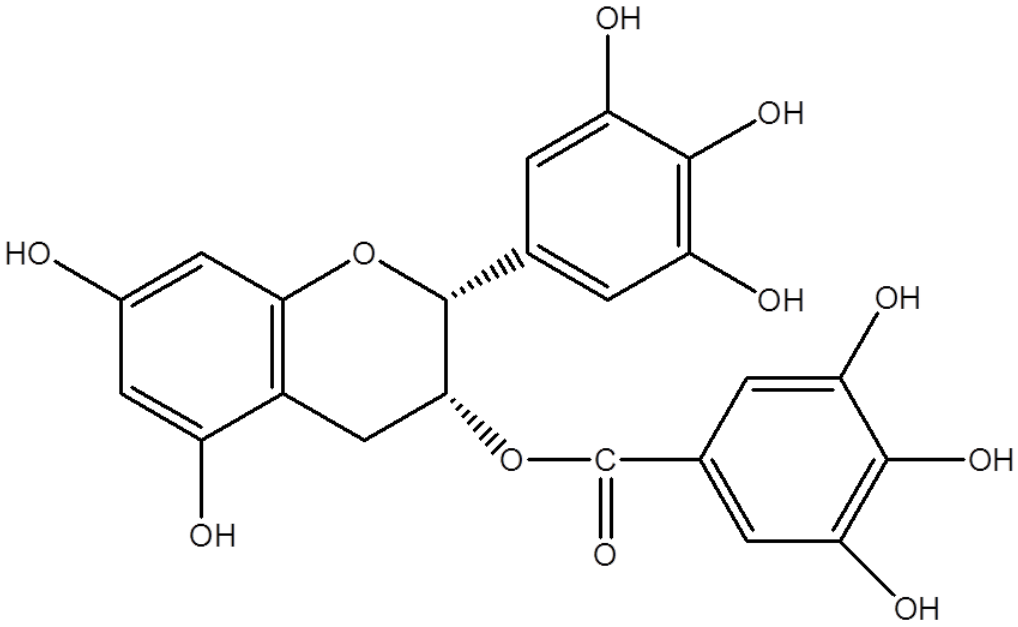

Figure 7. Chemical structure of (-)-epigallocatechin gallate

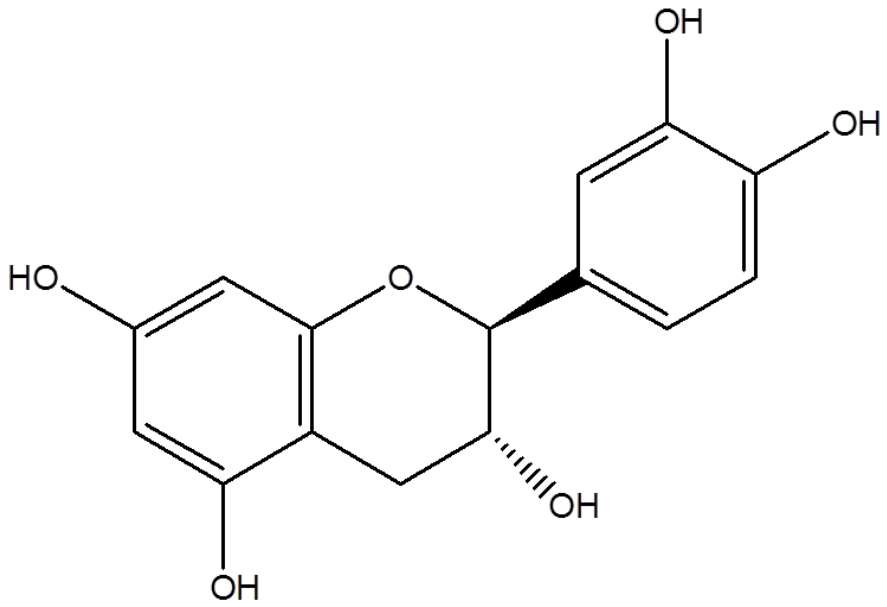

Figure 8. Chemical structure of (+)-catechin

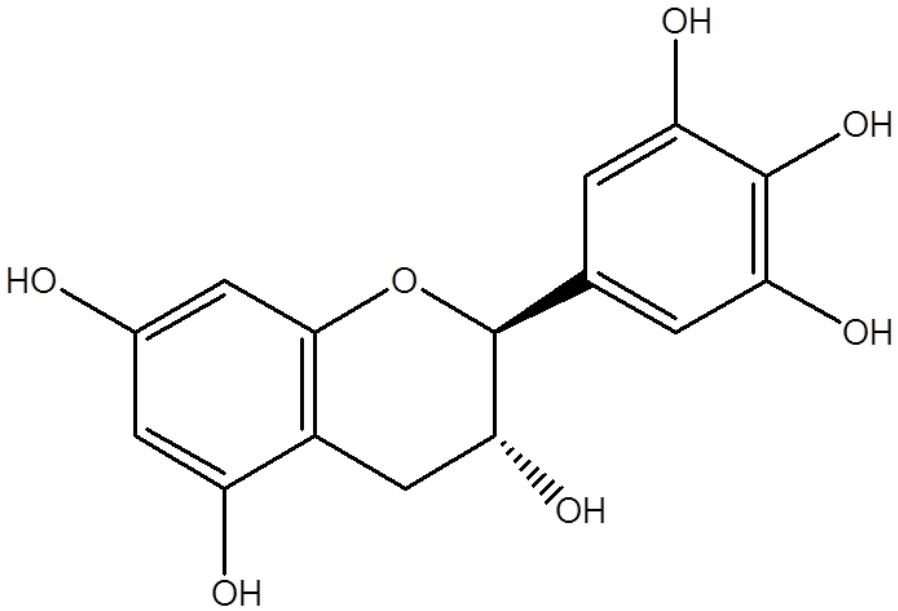

Figure 9. Chemical structure of (+)-gallocatechin

First, GSH reacts with O_2^- (Winterbourn and Metodiewa, 1994), NO (Clancy et al., 1994), peroxynitrite ($ONOO^-$) (Koppal et al., 1999), and $OH^\bullet$ (Bains and Shaw, 1997) non-enzymatically. In particular, GSH has a higher ability to scavenge O_2^- than cysteine (Hussain et al., 1996). Furthermore, there is no known enzymatic defense against $OH^\bullet$, making GSH the only compound capable of scavenging these radicals (Bains and Shaw, 1997).

Second, GSH serves as an essential cofactor for a number of enzymes. As an electron donor, GSH plays a vital role in the reduction of H_2O_2 or other peroxides catalyzed by GPx (Chance et al., 1979). The brain has a relatively high level of GPx as compared with that of catalase (Maher, 2005). H_2O_2 is reduced to water (H_2O) via the reaction of GPx with GSH, which is oxidized to GSH disulfide (GSSG) (Dringen, 2000). GSSG is subsequently reduced back to GSH, a step catalyzed by GSH reductase (GR) with nicotinamide adenine dinucleotide phosphate (NADPH), and is then reused as a GPx substrate. The relative ratio of the reduced/oxidized forms is over 100 under normal conditions, but is decreased to 49 under stressed conditions (Maher, 2005), serving as an indicator in the cellular redox environment (Schafer and Buettner, 2001). GSH reacts with a range of xenobiotic and endogenous compounds mediated through glutathione-S-transferase (GST) (Commandeur et al., 1995) to form mixed disulfides that are exported to the outer of the cell. GSH can also react with 4-hydroxy-2-nonenal (HNE) via the action of GST to form GSH-HNE adduct (Xie et al., 1998) in cellular detoxification.

A third important role of GSH is serving as a carrier /storage form for cysteine. Cysteine itself has neurotoxic effects mediated by free radical generation, increasing extracellular glutamate, and triggering overactivation of N-methyl-D-aspartate (NMDA) receptors (Janaky et al., 2000). GSH is a non-toxic cysteine storage form with 10-100 times higher concentrations in mammalian tissues than cysteine (Cooper and Kristal,

1997). Approximately one-third to one-half of the total liver GSH serves as a cysteine reservoir that can be released, when necessary (Tateishi et al., 1977).

Fourth, GSH is the key redox buffer in the maintenance of intracellular redox homeostasis. During oxidative stress circumstances, GSH is able to cause the reversible generation of mixed disulfides between protein thiol groups (S-glutathionylation), a crucial process in the inhibition of irreversible protein oxidation (Giustarini et al., 2004). Thus, GSH modulates a variety of protein functions via S-glutathionylation.

Fifth, GSH can serve as a neuromodulator and neurotransmitter. GSH binds via its gamma-glutamyl moiety to NMDA receptors (Janaky et al., 1999). GSH is thought to exert agonistic as well as antagonistic actions on neuronal responses mediated by NMDA receptors in the brain. GSH also serves as an endogenous NO reservoir to form S-nitrosoglutathione (Singh et al., 1996). S-nitrosoglutathione can release NO under certain conditions with biological effects, while S-nitrosoglutathione has a protective effect in the brain under oxidative stress conditions (Rauhala et al., 1998).

Moreover, GSH is important in the neuronal differentiation and cell proliferation (Poot et al., 1995; Sagara and Makino, 2008). GSH is a low mass molecule with thiol-containing tripeptide of glutamate-cysteine-glycine through the -SH oxidation in the cysteine residue, leading to the formation of disulphide bridge (Halliwell and Gutteridge, 1999). Hence, cysteine residue is the rate-limiting substrate in the synthesis of GSH within neurons. GSH is in existence in aerobic bacteria, plants, animals, and humans with high concentration which involved many vital roles in cellular functions and biochemical pathways such as antioxidant, cysteine storage form, enzyme cofactor, major redox buffer, neuromodulator, and also to interact with $OH^{\bullet}$ to become a GSH radical that can be restored back to its reduced form (Gul et al., 2000; Halliwell and Gutteridge, 1999). However, GSH deficiency has been implicated in several neurodegenerative diseases. For instance, a significant reduction in GSH level has been

revealed to induce programmed cell death in dopaminergic neurons and conversely, addition of GSH reversed the effects by preventing dopamine-dependent neurotoxicity (Emdadul Haque et al., 2003; Canals et al., 2001; Stokes et al., 2000).

2.2.4 The role of intracellular antioxidant enzymes in neuroprotection

Generally, living organisms are able to decompose H_2O_2 enzymatically. Enzymes are belonging to a class of spheroproteins play a pivotal role in a variety of chemical and biochemical activities of organisms. Enzymes can serve as catalysts to accelerate chemical and biochemical reactions without being damaged or distorted. Also, enzymes are tremendously efficient and a single enzyme might catalyze thousands reactions per second.

A dual stage reaction is involved in the detoxification of O_2^- generated in ischemia reperfusion injury. Firstly, SOD catalyzes the reduction of O_2^- to H_2O_2 throughout the Fenton reaction (Cuzzocrea et al., 2001). The later stage involves the reduction of H_2O_2 to H_2O via GPx and catalase (Figure 10). In brief, SOD catalyses the conversion of O_2^- to H_2O_2 and H_2O (Malstrom et al, 1975). Subsequently, GPx as the major H_2O_2 detoxifying enzyme in neurons (De Haan et al., 1998) continues where SOD leaves off by catalyzing the reduction of H_2O_2 to H_2O at the expense of GSH (Comhair and Erzurum, 2005).

Also, catalase is a homotetrameric enzyme that is primarily located in peroxisomes (Chance et al., 1979). This enzyme catalyses the decomposition of H_2O_2 to oxygen and H_2O, providing a substantial protection against toxic effects from oxygen radical. Furthermore, catalase enzyme which plays a vital role in promoting cell survival as well as in preventing tumor proliferation supports the antioxidant function of this enzyme (Jones et al., 1985; Lewis, 1985; Agar et al., 1986).

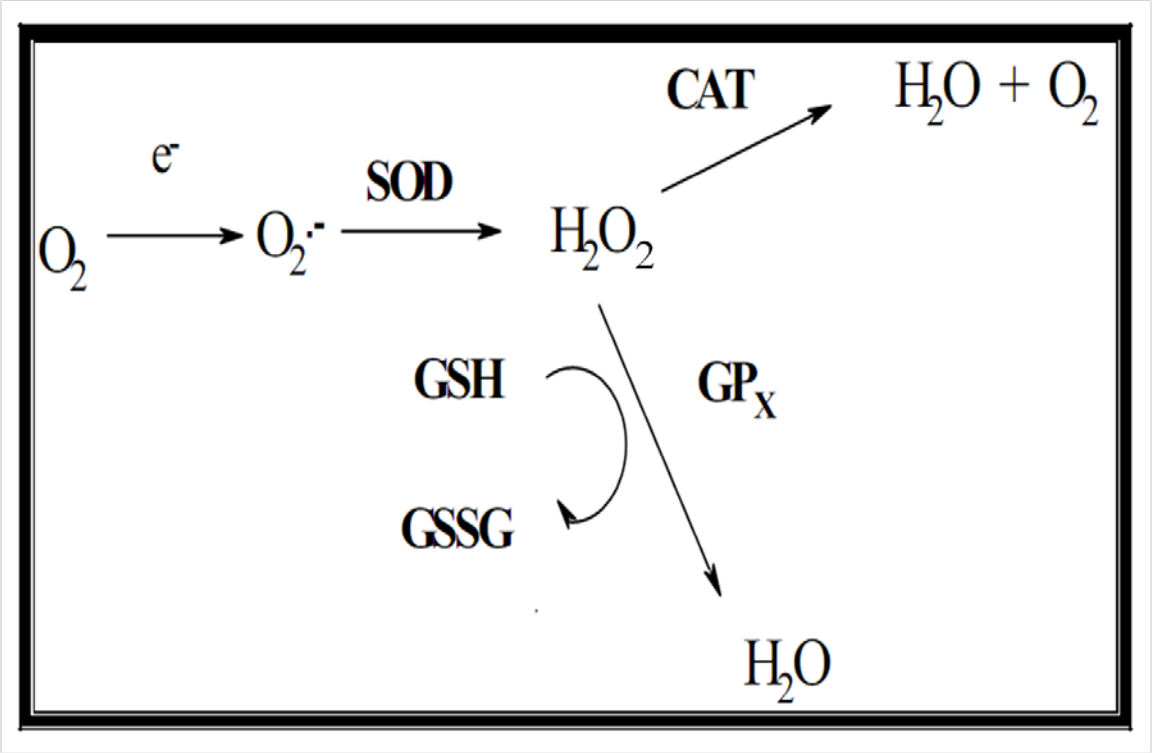

Figure 10. Outline of main intracellular antioxidant enzymes namely SOD, GPx, and catalase involved in the prevention of reactive oxygen species (Reiter, 1995)

2.2.5 Bcl-2 family members as regulators of apoptosis

Apoptosis, a form of programmed cell death, is a highly regulated process via the activation and expression of numerous proteins and genes (Steller, 1995), especially the Bcl-2 family members. The Bcl-2 family members of related genes encoding proteins that either promote (pro-apoptotic) or suppress (anti-apoptotic) programmed cell death in the regulation of apoptosis (Hockenbery, 1995). Bcl-2 family members share one or among the four characteristic homology domains termed the Bcl-2 homology (BH) domains, namely BH1, BH2, BH3, and BH4 to form either homodimers or heterodimers. Under BH domains, Bcl-2 family members can be categorized into three groups. First, the pro-apoptotic members with multi-domain (consist of BH1, BH2 and BH3): Bax, Bok, Bak. Second, the pro-apoptotic members with only BH-3 domain: Bad, Bid, Bik, Bim, Bcl-xS, Bmf, Hrk, Puma, and Noxa. Third, the anti-apoptotic members with BH1, BH2, BH3, and BH4 domains: Bcl-2, Bcl-xL, Bcl-W, A1, and Mcl-1 (Adams and Cory, 1998; Danial, 2007). In an apoptotic cascade, life and death of a cell's fate is mainly based on the balance between the pro-apoptotic and anti-apoptotic proteins of the Bcl-2 family members. The ratio of Bax/Bcl-2 is superior to the absolute concentrations of Bax or Bcl-2 alone and whichever changes in the Bax/Bcl-2 ratio will influence the cell's life and death decision (Cory and Adams, 2002).

2.2.5.1 Bcl-2

Bcl-2, a proto-oncogene which was first cloned in a B-cell lymphoma line (Vaux et al., 1988), has been known in the regulation of apoptosis. Bcl-2 protein is localized at the outer membranes of both nuclei and mitochondria, together with a family of proteins to form heterodimers which consist of a unique helical domain called BH3. Bcl-2 gene encodes 26 kDa protein with 239 amino acids. The recognition of Bcl-2 kicks off a

novel category in the context of oncogenes in which most of the oncogenes promote cell proliferation whereas the Bcl-2 inhibits cell death by halting the cell propagation (Korsmeyer, 1992; Nunez et al., 1990; Vaux et al., 1988). Bcl-2 is expressed in the growth of fetal survival cells (LeBrun et al., 1993; Novack and Korsmeyer, 1994) and prevented programmed cell death in a range of in vitro systems (Vaux et al., 1988; Hockenbery et al., 1990; Sentman et al., 1991). The changes in the mitochondrial membrane permeability are highly manipulated via Bcl-2 by triggering the mitochondrial to inhibit the release of apoptotic factors such as AIF and cytochrome c, and also to activate the caspases (Antonsson and Martinou, 2000). Additionally, the anti-apoptotic Bcl-2 protein significantly protects neuronal cells against a variety of stimuli-induced neuronal apoptosis such as deprivation of nerve growth factor (Garcia et al., 1992), deprivation of neurotrophic factors (Allsopp et al., 1993), serum deprivation (Batistatou et al., 1993), afferent neuron deprivation (Mostafapour et al., 2002), reactive oxygen species generation (Kane et al., 1993), glucose withdrawal, serum withdrawal, membrane peroxidation, as well as growth factor withdrawal (Zhong et al., 1993). For example, Bcl-2 upregulation has been reported in the protection of neuronal cells against oxidative damage-induced neuronal apoptosis such as $ONOO^-$ (Spear et al., 1998), H_2O_2 (Satoh et al., 1996; Bruce-Keller et al., 1998; Distelhorst et al., 1996), beta-amyloid (Ivins et al., 1999), and NO (Melkova et al., 1997; Bonfoco et al., 1996). Also, the overexpression of Bcl-2 improved the endogenous antioxidant defense system to protect the cells from reactive oxygen species by decreasing the accumulation of reactive oxygen species. Hence, the raise in Bcl-2 expression will cause the cells to be more resistant to reactive oxygen species and resistance to various types of oxidative stress (Hockenbery et al., 1993). Also, overexpression of Bcl-2 increased survival and delayed the onset of symptoms in SOD1 transgenic mice (Azzouz et al., 2000), prevented the occurrence of apoptosis during early neuronal development

(Putcha and Johnson, 2004), and decreased the infarct size in areas of ischemic insult in sublethally injured neurons (Ferrer and Planas, 2003).

2.2.5.2 Bax

Bax, a Bcl-2 associated protein was the first identified pro-apoptotic member of the Bcl-2 family proteins via the co-immunoprecipitation with Bcl-2 (Oltvai et al., 1993). Bax is a 21 kDa protein with 191 amino acids which shares 21 % identical amino acids with Bcl-2 protein. Bax is generally localized in the cytosol of healthy cells. However, a conformational change occurs and leads to an insertion of Bax into the organelle membranes particularly the outer membrane of mitochondrial, upon the induction of apoptosis (Wolter et al., 1997).

Bax is known in promoting apoptosis as the key activator in mitochondria-dependent signaling pathway. During the onset of apoptosis, Bax triggers the formation of oligomeric pores at the outer membranes of mitochondria, leading to the release of cytochrome c as well as other pro-apoptotic factors from mitochondria. The change in the mitochondrial membrane permeability by Bax subsequently activates the caspases and causes the occurrence of apoptosis. Therefore, Bax as a death promoter works directly on the mitochondrial membrane potential to accelerate apoptosis by antagonizing the death inhibitory effects of Bcl-2 via its BH1 and BH2 domains (Yin et al., 1994). Also, Bax has been revealed to enhance the rate of cell death in an interleukin 3-dependent cell line without the surviving factor. However, upregulation of Bax has been shown to counteract with death repressor activity of Bcl-2 (Oltvai et al., 1993) in which direct binding of Bcl-2 to Bax was necessary for the death repressor activity of Bcl-2 (Yin et al., 1994). Hence, the balance between the Bax and Bcl-2 indicates a crucial decision of a cell to either undergo survival or death.

2.2.6 The role of neuronal chemokines in neuroprotection

Chemokines are a class of proteins that are secrected by cells. Chemokines can be defined as a small cytokines family with chemotactic effect, which is associated with the chemotaxis capability to induce the neighboring cells. Ever since the first protein detected with chemotactic activity (Yoshimura et al., 1987), around 50 chemokines (Laing and Secombes, 2004) and 20 receptors (Murphy, 2002) have been discovered in the family of chemokines. In general, based on the position of four conserved cysteine residues at the N-terminal region of the protein, chemokines can be categorized into four groups, namely CXC, CC, CX3C, and C. The CXC and CC belong to the bigger groups of chemokines as the first two cysteines in the CXC chemokine are separated by an amino acid residue while the first two cysteines in the CC chemokine are next to each other (Fernandez and Lolis, 2002; Rossi and Zlotnik, 2000). On the other hand, the CX3C and C belong to the smaller groups of chemokines as the first two cysteines in the CX3C chemokine are separated by three amino acids residues whereas only one cysteine at the N-terminal region in the C chemokine (Rossi and Zlotnik, 2000).

Chemokine receptors are designated in accordance with the preferential binding of chemokine groups. For instance, the CC chemokines will be binding to CC receptors. Nevertheless, an exceptional chemokine, CCL21 binds not only to CCR7 receptor but also involved in the binding of CXCR3 receptor (Biber et al., 2002; Dijkstra et al., 2004; Soto et al., 1998). Commonly, all chemokine receptors can be categorized in the G-protein coupled receptors (GPCRs) family. Various G-proteins can bind to GPCRs and trigger a range of intracellular signaling pathways (Neves et al., 2002). For example, chemokine receptors have been shown in the activation of intracellular molecules like phospholipases, adenylcyclase, phosphatidyl inositol-3 kinases, and mitogen-activated protein kinases (Balkwill, 1998; Mellado et al., 2001). The chemokine receptors are able to trigger a broad intracellular signaling pathway as well as participating in cellular

migration to activate distinct pathways, chemokine receptors are proficient to serve in a vast spectrum of cellular functions (Laudanna and Alon, 2006; Rittner and Brack, 2006).

Chemokines are capable in mediating all leukocyte migration and play critical roles in the pathogenesis of numerous human diseases, from AIDS to atherosclerosis to autoimmune disorders (Alkhatib et al., 1996; Baggiolini and Dahinden, 1994; Dragic et al., 1996; Feng et al., 1996; Furie and Randolph, 1995; Hosaka et al., 1994; Kukielka et al., 1995). Chemokines have been reported in the regulation of peripheral immune cell trafficking under both pathological and physiological circumstances (Baggiolini, 1998; Moser and Loetscher, 2001; Rot and von Andrian, 2004). Also, chemokines have been implicated in diverse cellular functions, for example wound healing (Charo and Ransohoff, 2006; Kunkel, 1999), asthma (Murray et al., 2006), angiogenesis (Mackay, 2001; Benelli et al., 2006), pain and analgesia (Rittner and Brack, 2006), allergic (Pease and Williams, 2006), metastasis (Zlotnik, 2006), and tumor growth (Rossi and Zlotnik, 2000). As a result, chemokines can serve as versatile messengers due to the capability in managing the interaction among a broad distinctive cell lines. In neurons, chemokines are being expressed not only at the peripheral nervous system but also at the central nervous system which represents a vital role in both pathological and physiological circumstances, like synaptic transmission, neuroinflammation associated diseases, injury, homeostasis, and development (Charo and Ransohoff, 2006; Ubogu et al., 2006; Bertollini et al., 2006). Even though microglia and astrocytes represent the principal source of chemokines, neurons secrete and express chemokines as well, pointing to chemokine signaling via neuronal contribution.

2.2.7 Chemokine CCL21

CCL21, a chemokine ligand 21, is a small cytokine belonging to the family of CC chemokine. Since chemokine CCL21 has six conserved cysteine residues rather than four typical cysteine residues, it is also known as 6Ckine, secondary lymphoid-tissue chemokine, and exodus-2 (Hedrick and Zlotnik, 1997; Hromas et al., 1997; Nagira et al., 1997). The expression of chemokine CCL21 is based on the binding onto chemokine receptors such as CCR7 and CXCR3 which are localized at the cell surface (Yoshida et al., 1998). Increasing evidence supports the role of chemokines in providing neuroprotective effects in endangered neurons, particularly chemokine CCL21. During oxidative stress circumstances, neurons exclusively express the microglia-activating CCL21 (Biber et al., 2001; Dijkstra et al., 2004; Rappert et al., 2002; Rappert et al., 2004). Neuronal chemokines CCL21 are distributed throughout neuronal cells in vesicle-like structures and suggested to serve as a neuronal signal to activate microglia from primary lesion at distant sites (De Jong et al., 2005). Therefore, neuronal chemokine CCL21 is responsible in neuron-microglia signaling as the chemokine CC21 has the ability to activate microglia particularly in endangered neurons of the brain region.

2.3 Mistletoes

Mistletoes, semiparasitic plants distributed mainly in China, Korea, and Japan have long been recognized as therapeutic herbs (Li, 1975). Mistletoes are traditionally used as sedative, analgesic, spasmolytic, cardiac and anticancer agent; the herbs are also used to tone the liver and kidneys, strengthen tendons and bones, expel pathogens associated with rheumatism, stabilise the fetus and cause lactogenesis. The use of mistletoes as a remedy for circulatory and nervous disorders dates from antiquity.

2.3.1 The plant, *L. parasiticus*

Loranthus parasiticus grows on mulberry (*Morus alba* L.) and sapodilla (*Manilkara zapota*) in Southern China and Malaysia, respectively. The broad leaves are ovate or oblong and are arranged oppositely or alternately. The red brown flowers are bisexual and umbrella-shaped. The elliptical berries are ripening in autumn.

2.3.2 Ethnopharmacological uses of *L. parasiticus*

Loranthus parasiticus belongs to the family Loranthaceae according to the taxonomy. *Loranthus parasiticus* is commonly known as benalu teh (in Malay), baso-kisei (in Japan), and Sang Ji Sheng (in Chinese), which is distributed in south and southwest region of China, has been utilized as a traditional medicine for the treatment of schizophrenia in southwest China (Okuda et al., 1987). *Loranthus parasiticus* has been used as folk medicine for brain, bone, liver, kidney, prevents miscarriage, and expels wind-damp.

2.3.3 Reported phytochemical and biological activities of *L. parasiticus*

Among the semiparasitic plants, *Loranthus* species have been reported to produce various bioactive compounds; i.e., (+)-catechin, 3,4-dimethoxycinnamyl alcohol, and 3,4,5-trimethoxycinnamylalcohol from *L. globosus* for the antifungal and antimicrobial activities (Sadik et al., 2003). Also, chemical components like triterpenoids from *L. falcatus* (Anjaneyulu et al., 1977) and *L. grewinkii* (Rahman et al., 1973), flavonoids from the leaves of *L. europaeus* (Harvala et al., 1984) and *L. kaoi* (Lin and Lin, 1999), and phenolics from *L. longiflorus* (Indrani et at., 1980) have been reported up to this point. However, sesquiterpene lactones (coriamyrtin, tutin, coriatin, and corianin) and flavonoids (avicularin, quercetin, and quercetin-3-arabinoside) (Tseng and Chen, 1957; Wang and Yuan, 1980; Wu et al., 1982; Wu and Zhang, 1984; Okuda

et al., 1987) have been isolated so far from *L. parasiticus* (Figure 12-18). Also, sesquiterpene lactones from have been shown to be effective in managing schizophrenia disease (Okuda et al., 1987). In addition, *L. parasiticus* also demonstrated the highest total phenolic content and antioxidant activities among the 50 tested medicinal plants, which could provide a rich natural resource of antioxidant (Gan et al., 2010; Cha et al., 2003). Moreover, *L. parasiticus* efficiently improved the rate of tissue regeneration in damaged bones (Yao et al., 2005) and possessed inhibitory activity on avian myeloblastosis virus -reverse transcriptase (Kusumoto et al., 1992).

2.4 NG108-15 neuroprotection model

NG108-15 cell line, an adherent culture, was initially termed 108CC15 and developed by Bernd Hamprecht. NG108-15 hybridoma cell line was produced via the inactivated Sendai virus fusion of mouse N18TG2 neuroblastoma cells and rat C6-BV-1 glioma cells (Hamprecht et al., 1985). NG108-15 cells represent a useful model for study of neuroprotection because all cells are identical and show synchronous propagation in culture dishes which has been utilized as neuroprotection model by many researchers (Sukma and Siripong, 2006; Dakshinamurti et al., 2003; Vajragupta et al., 2003; Suma et al., 1997; Tanaka et al., 2001).

NG108-15 hybridoma cell line was designed in an attempt to increase the range of neuronal properties available in one hybrid clone. Also, NG108-15 cells offer advantage over the parent neuroblastoma cells on the enhancement in the expression of neuronal properties (Harvey, 1984). Therefore, NG108-15 hybridoma cell line has been widely used as neuronal model (Bei et al., 2005; Cheng Chew et al., 2003; Tetich et al., 2003; Mahakunakorn et al., 2004; Kawpoomhae et al., 2010) due to the simultaneous presence in one cell of various properties observed in neurons. Moreover, their

superiority to neuroblastoma cells is also based on such neuronal properties that are more strongly expressed in the hybrids than in the neuroblastoma clones (Harvey, 1984). In view of that, NG108-15 cell line has been employed as present neuroprotection model towards the investigation of neuroprotective potential exhibited by *L. parasiticus* against H_2O_2-induced oxidative damage (Figure 19).

Figure 11. Image of *Loranthus parasiticus*

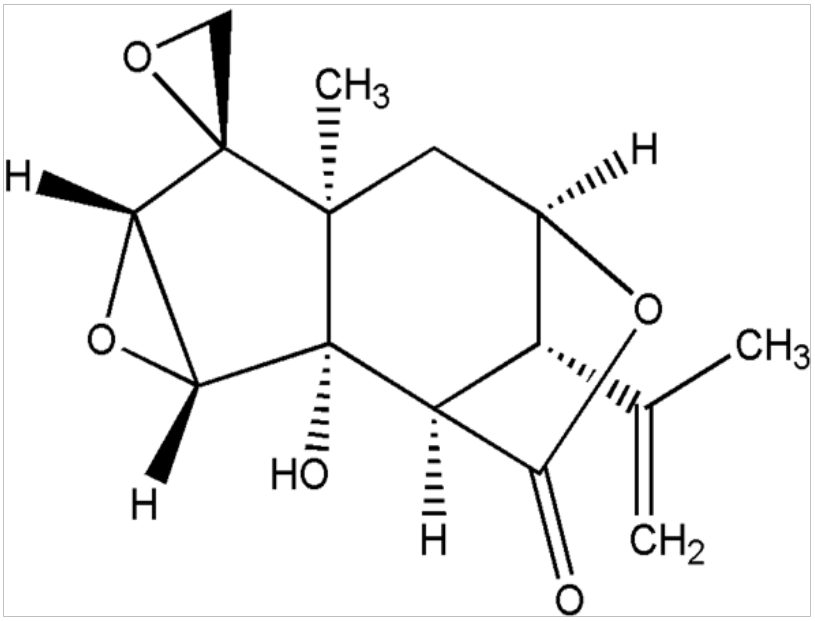

Figure 12. Chemical structure of coriamyrtin

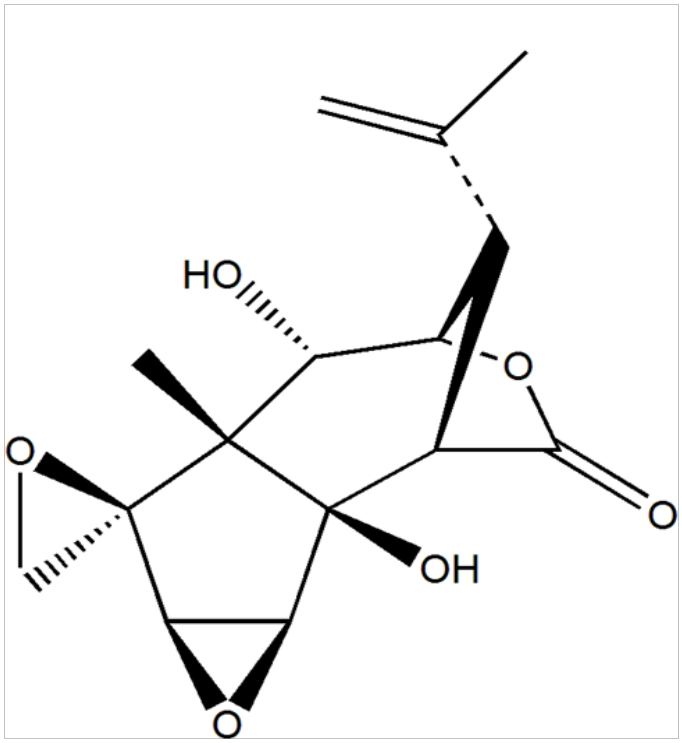

Figure 13. Chemical structure of tutin

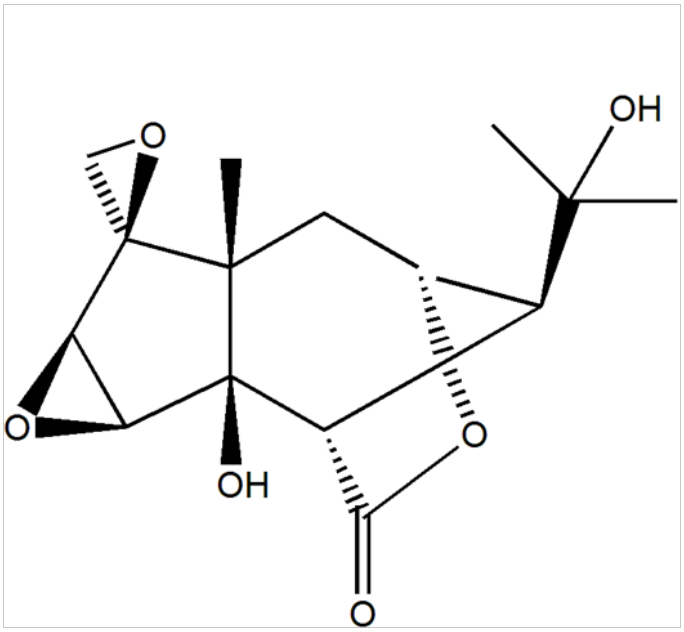

Figure 14. Chemical structure of coriatin

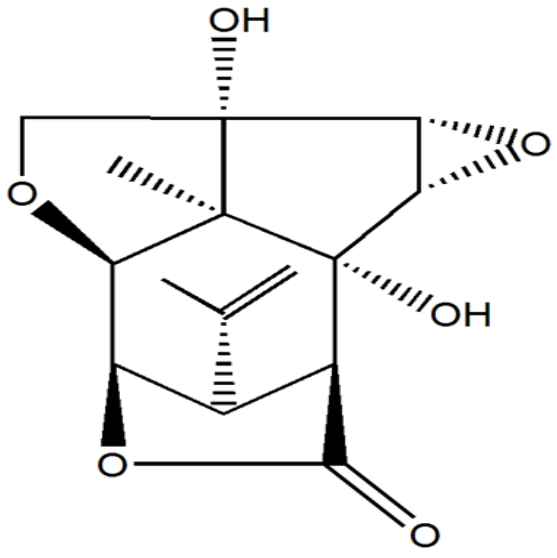

Figure 15. Chemical structure of corianin

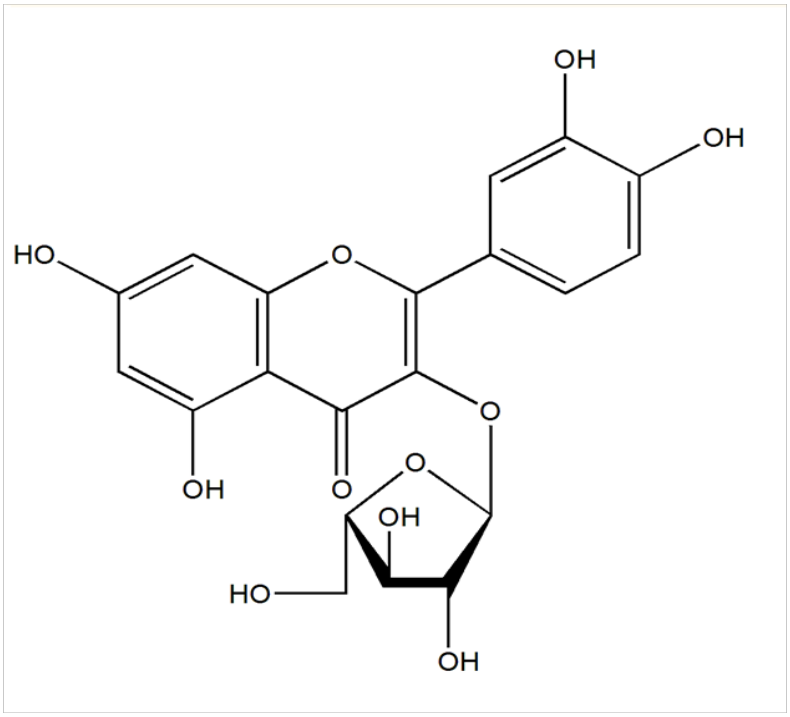

Figure 16. Chemical structure of avicularin

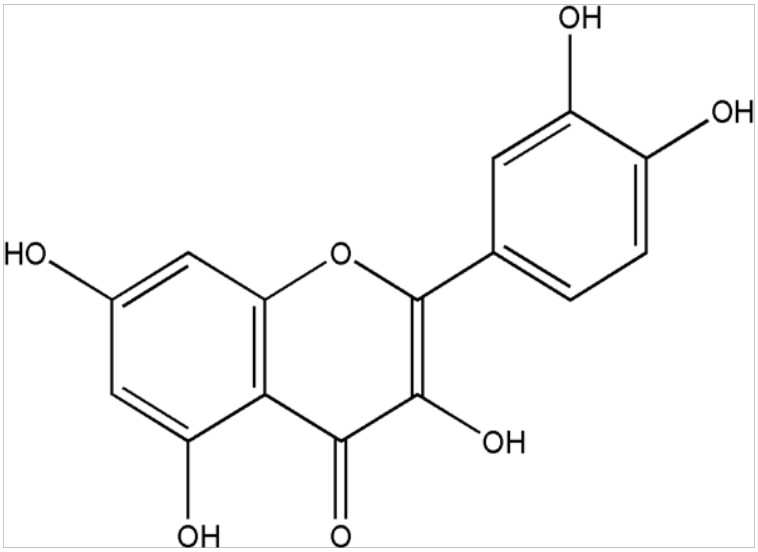

Figure 17. Chemical structure of quercetin

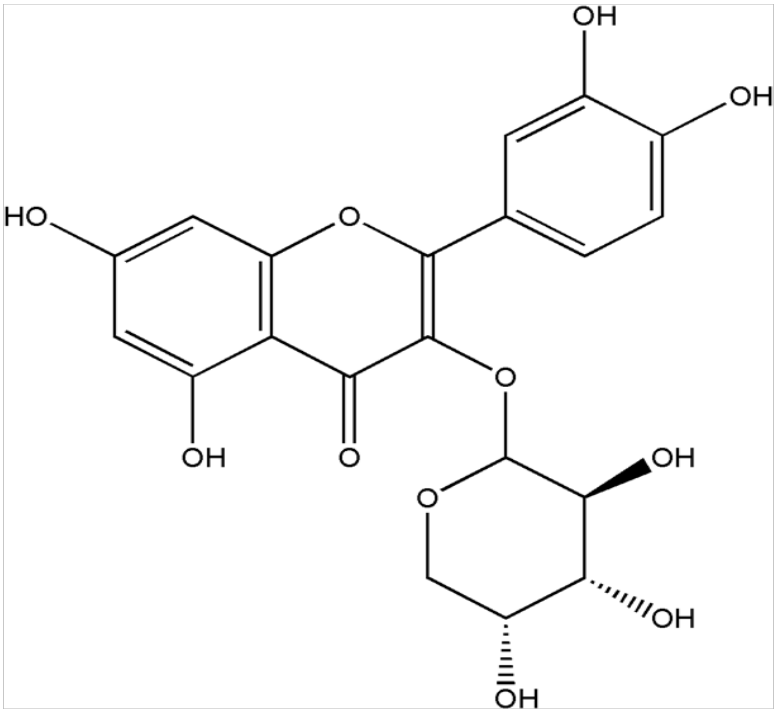

Figure 18. Chemical structure of quercetin-3-arabinoside

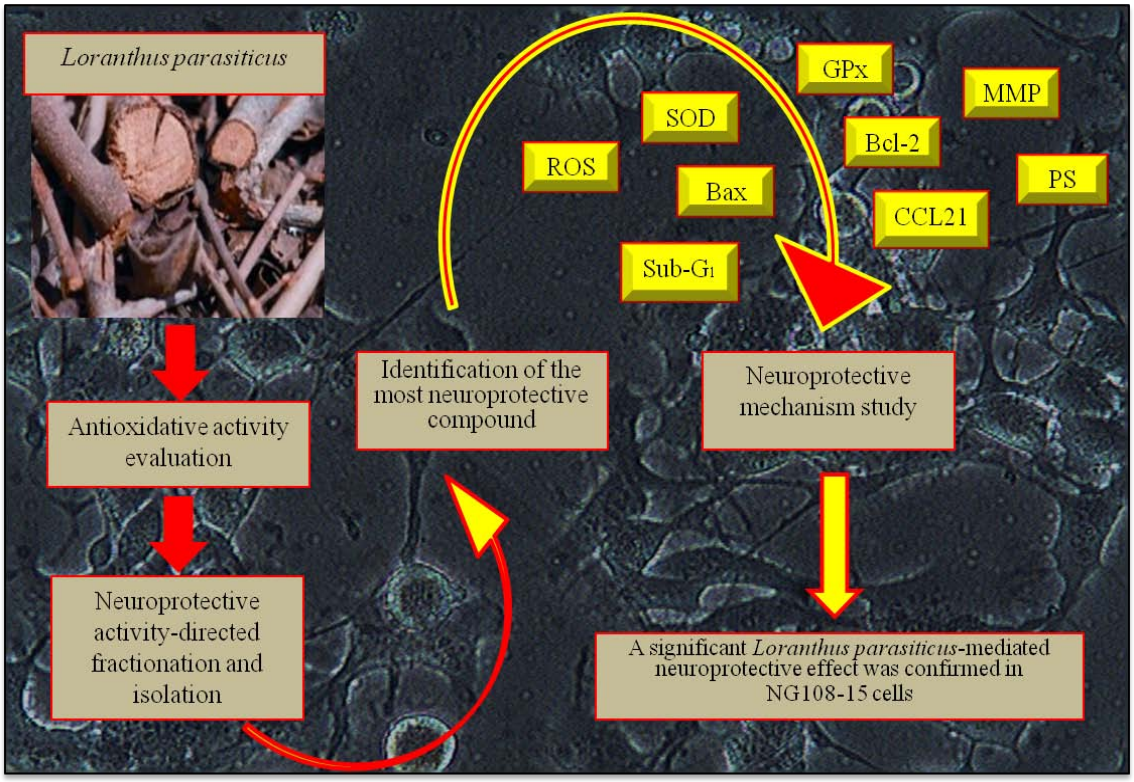

Figure 19. Graphical abstract illustrating experimental design

CHAPTER 3

MATERIALS AND METHODS

3.1 Materials

3.1.1 Solvents

Methanol, ethanol, ethyl acetate, acetone, chloroform, benzene-ethyl formate-formic acid, benzene-ethyl formate-formic acid, ferric chloride ($FeCl_3$), and ferrous sulfate ($FeSO_4$) were purchased from Merck, United States of America. Sulfuric acid (H_2SO_4) was obtained from Fisher Scientific, United States of America.

3.1.2 Cell line

NG108-15 was acquired from American Type Culture Collection (ATCC), United States of America, with catalogue number HB-12317.

3.1.3 Culture medium

Hypoxanthine-aminopterin-thymidine (HAT), Dulbecco's modified Eagle's medium (DMEM), penicillin/streptomycin (100x), amphotericin B (250 μg/mL), and fetal bovine serum (FBS) were provided by PAA Laboratories, United Kingdom. Accutase was purchased from Innovative Cell Technologies, Inc, United States of America.

3.1.4 Reagents and chemicals

Dimethyl sulfoxide (DMSO) and trichloroacetic acid (TCA) were purchased from Merck, United States of America. Phosphate buffer saline (PBS), MTT, 2,2-diphenyl-1-picrylhydrazyl (DPPH), Folin-Ciocalteu's phenol reagents, butylated hydroxytoluene (BHT), curcumin, gallic acid, GSH, 5',5'-dithio-bis(2-nitrobenzoic acid) (DTNB),

NADPH, ethylenediaminetetraacetic acid (EDTA), GR, 5-sulfosalicylic acid, sodium citrate, RNAse, Triton-X-100, propidium iodide (PI), and DAPI were provided by Sigma-Aldrich, United States of America. H_2O_2, sodium dihydrogen phosphate (NaH_2PO_4), disodium hydrogen phosphate (Na_2HPO_4), sodium carbonate (Na_2CO_3), and thiobarbituric acid (TBA) were bought from Systerm®, Malaysia. 2,7 dichlorofluorescein diacetate (DCF-DA), fluorescein isothiocyanate (FITC)-labeled annexin V, annexin V binding buffer, 5,5',6,6'-tetrachloro-1,1',3,3'-tetraethylbenzimidazolylcarbocyanine iodide (JC-1), JC-1 solution were obtained from Becton Dickinson (BD), United States of America. All solvents and chemicals used were all of analytical grade without further purification.

3.1.5 Biochemical assay kits

Intracellular SOD and GPx activity determination kits were bought from Sigma-Aldrich, United States of America. RNAqueous-4PCR kit was obtained from Applied Biosystem, United States of America. SensiMix One-Step Kit for real time-polymerase chain reaction (Q-PCR) was procured from Quantace, United Kingdom. Intracellular flow cytometry system was bought from Santa Cruz Biotechnology, Inc, United States of America. Lightning-Link^{TM} fluorescein conjugation kit was acquired from Innova Biosciences Ltd, United Kingdom.

3.1.6 Oligonucleotides

Forward and reverse primer sequences of Bax, Bcl-2, chemokine CCL21, and hydroxymethylbilane synthase (HMBS) were synthesized from 1st BASE, Singapore, as listed in Table 1.

3.1.7 Antibodies

FITC-conjugated Bax mouse monoclonal antibody and phycoerythrin (PE)-conjugated Bcl-2 mouse monoclonal antibody were purchased from Santa Cruz Biotechnology, Inc, United States of America. Rabbit anti-murine exodus-2 CCL21 polyclonal antibody was bought from Peprotech Inc, United States of America. Rabbit immunoglobulin G (IgG) isotype control was acquired from Abcam plc, United States of America.

3.1.8 Instruments/Equipments

Rotary evaporator (Buchi, Switzerland), spectrophotometer (Amersham Biosciences Ultrospec 2100 pro, Sweden), CO_2 incubator chamber (RS Biotech, United Kingdom), inverted microscope (Motic, Hong Kong), microplate reader (Asys UVM 340, United Kingdom), flow cytometry (BD FACSCalibur, United States of America), fluorescence microscope (Nikon, Japan), thin layer chromatography (TLC) (Merck, United States of America), Sephadex LH-20 (Amersham Biosciences, Sweden), Diaion HP20SS column (Supelco, United States of America), ^{1}H nuclear magnetic resonance (NMR) and ^{13}C NMR spectroscopic were recorded in ppm (δ), acetone-d_6 and DMSO-d_6 by a Bruker DRX 300 NMR spectrometer, Germany. Liquid chromatography mass spectroscopy (LC-MS) analysis was carried out via Thermo Scientific LTQ Orbitrap mass spectrometer at 30,000 resolutions (Thermo Fisher Scientific, Breman, Germany) fitted with an electrospray interface.

Table 1. Primer sequence for Bax, Bcl-2, CCL21, and HMBS

Genes	Function	Sequence
Bax	Forward	5'-GCA GGG AGG ATG GCT GGG GAG-3'
	Reverse	5'-TCC AGA CAA GCA AGC AGC CGC TCA CG-3'
Bcl-2	Forward	5'-CAC CCC TGG CAT CTT CTC CT-3'
	Reverse	5'-GTT GAC GCT CCC CAC ACA CA-3'
CCL21	Forward	5'-TGC CTT AAG TAC AGC CAG AAG-3'
	Reverse	5'-TTC CTC AGG GTT TGC ACA TAG-3'
HMBS	Forward	5'-CCG AGC CAA GGA CCA GGA TA-3'
	Reverse	5'-CTC CTT CCA GGT GCC TCA GA-3'

3.2 Methods

3.2.1 Extraction and fractionation of *L. parasiticus*

3.2.1.1 Collection of *L. parasiticus*

Leaves of *L. parasiticus* were obtained from a licensed Chinese medicine outlet in the state of Selangor, Malaysia, due to the limited availablility of the fresh sample in Malaysia. *Loranthus parasiticus* grows on mulberry (*Morus alba* L.) and the leaves of *L. parasiticus* originated from Wuzhou, province of Guangxi, China.

3.2.1.2 Preparation of *L. parasiticus*

Leaves of *L. parasiticus* (10 kg) were ground into fine powder by dry grinder. The ground dried leaves were soaked in 95 % ethanol for three days at ambient temperature followed by the addition of activated charcoal to get rid of the chlorophyll. The extract was filtered by Whatman No.1 filter paper and evaporated at 40 °C by a rotary evaporator under reduced pressure. The remaining residues were re-extracted twice with 95 % ethanol and accumulated as crude *L. parasiticus* ethanol extract (LPEE).

3.2.1.3 Solvent extraction and fractionation of *L. parasiticus*

Leaves of *L. parasiticus* were extracted as crude LPEE after repeated extraction with ethanol solvent. Crude LPEE was subsequently partitioned between ethyl acetate and water to form an ethyl acetate-soluble fraction. The ethyl acetate-soluble fraction was evaporated while the water-soluble fraction was freeze-dried to yield *L. parasiticus* ethyl acetate fraction (LPEAF) and *L. parasiticus* aqueous fraction (LPAF), respectively. LPEE, LPEAF, and LPAF were dissolved in DMSO (less than 0.5 % v/v) and subjected to antioxidative and neuroprotective activities screening.

3.2.2 Antioxidant studies

3.2.2.1 DPPH free radical scavenging activity assay

DPPH free radical scavenging assay was performed according to the method described by Blois (1958). Briefly, 1.0 ml LPEE, LPEAF, and LPAF with various concentrations (15, 30, 60, 120, 240 and 480 µg/mL in ethanol) were added with 1.0 ml 0.2 mM DPPH solution and incubated in the dark at ambient temperature for 30 min. BHT with various concentrations (15, 30, 60, 120, 240 and 480 µg/mL in ethanol) was used as a positive control. Absorbance at 517 nm was measured using spectrophotometer. The percentage of antioxidant activity was calculated as below:

$$\% \text{ of antioxidant activity} = [1- A_S/A_C] \text{ X } 100 \%$$

Where A_S is the absorbance of LPEE, LPEAF, and LPAF or BHT and Ac is the absorbance of control (DPPH solution + ethanol)

3.2.2.2 Reducing power activity assay

Reducing power assay was performed according to the method reported by Karawita et al. (2005) with some modifications. 1.0 ml of LPEE, LPEAF, and LPAF (15, 30, 60, 120, 240, 480 and 960 µg/mL in ethanol) was added to 1.0 ml sodium phosphate buffer (0.2 M, pH 6.6) and 1.0 ml potassium ferricyanide (10 mg/mL in distilled water). The mixture was incubated at 50 °C for 20 min. After incubation, 1.0 ml TCA (100 mg/mL in distilled water) was added to LPEE, LPEAF, and LPAF and centrifuged at 1500 rpm for 8 min. 1.0 ml of supernatant was transferred into 1.0 ml distilled water, followed by 0.1 ml of $FeCl_3$ (1.0 mg/mL in distilled water). BHT (15, 30, 60, 120, 240, 480 and 960 µg/mL in ethanol) was used as positive control. Absorbance at 700 nm was measured

after 10 min. The higher absorbance represents the stronger reducing power activity.

3.2.2.3 Lipid peroxidation inhibitory assay

Lipid peroxidation assay was conducted according to the method modified from Kuppusamy et al. (2002). Egg yolk homogenates which mainly comprised of phospholipids, triacyglycerols and proteins were used as an alternative to rodent liver microsomes and linoleic acid. Reaction mixture for the induction of lipid peroxidation consisted of 1.0 ml egg yolk emulsified with PBS (0.1 M, pH 7.4), to give a concentration of 12.50 g/L. 0.1 ml of serial concentrations of LPEE, LPEAF, and LPAF ranging from 0.3125 mg/mL to 10 mg/mL was then added to the buffered egg yolk. 0.2 ml of 3.0 mM $FeSO_4$ was added to the mixture and incubated at 37 °C for 1 h. After incubation, the mixture was treated with 0.5 ml of 15 % TCA and 1.0 ml of 1 % TBA. The reaction tubes were kept for 10 min in boiling water bath and centrifuged at 3,500 g for 10 min upon cooling to get rid of the precipitated proteins. Absorbance was determined at 532 nm. Curcumin with various concentrations (0.3125, 0.625, 1.25, 2.5 and 5 mg/mL in ethanol) was used as positive control. The percentage of inhibition was calculated from the following equation:

$$\% \text{ inhibition} = [(A_C - A_S)/A_C] \text{ X } 100 \%$$

Where A_S is the absorbance of LPEE, LPEAF, and LPAF or curcumin and Ac is the absorbance of control (buffered egg + $FeSO_4$)

3.2.2.4 Total phenolic content

Total phenolic content was determined by the method of Lee et al. (2004) with some modifications. 200 µl of 100 µg/mL LPEE, LPEAF, and LPAF as well as various

concentrations of gallic acid (3.75, 7.5. 15, 30, 60, 120 and 240 μg/mL in ethanol) were prepared. 1.5 ml of Folin-Ciocalteu's phenol reagent (10x dilutions in distilled water) was added into LPEE, LPEAF, and LPAF to incubate at ambient temperature for 5 min. After incubation, 1.5 ml sodium carbonate (60 mg/mL in distilled water) was added and the final mixture was incubated in darkness for an additional 2 h at ambient temperature. Absorbance at 725 nm was measured and total phenolic content was determined from the gallic acid calibration curve. Results were expressed as milligram of gallic acid equivalent per gram of dry weight of plant (GAE/g_{DW}).

3.2.3 Cell culture

3.2.3.1 Maintenance of cells

NG108-15 hybridoma cells were cultured in DMEM supplemented with 2 % penicillin/streptomycin, 1 % amphotericin B, 10 % heat inactivated FBS, and HAT as a complete medium. The cells were maintained and cultured at 37 °C in 5 % CO_2 atmosphere with 95 % humidity incubator chamber.

3.2.3.2 Cryopreservation of cells

NG108-15 cells were observed under an inverted microscope to confirm the cultures were in a healthy, log phase of growth, and absence of bacterial or fungal contaminants. Cells were harvested with accutase, washed with PBS, and centrifuged to obtain the cell pellet. 1.0 ml of freezing medium which consisted of 70 % basic medium, 20 % FBS, and 10 % DMSO was added and aliquoted into a cryoprotective ampoule. Cells were then cooled down gradually and stored in a liquid nitrogen tank eventually for preservation.

3.2.3.3 Reviving of cells

To revive frozen NG108-15 cells from liquid nitrogen, cryoprotective ampoule which consisted of cells was thawed rapidly by transferring directly from liquid nitrogen tank to a water bath at 37 °C. Cells were pipetted to a Falcon tube consisting of fresh pre-warmed medium as soon as they are defrosted. Cells were subsequently centrifuged to discard the old medium containing DMSO (as growth inhibitor) and pipetted gently into a 25 cm^3 or 75 cm^3 culture flask consisting complete growth medium to grow.

3.2.3.4 Subculturing of cells

Flasks with actively growing NG108-15 cells of 80-90 % confluence were harvested with accutase. Cells were observed under inverted microscope for detachment. If the cells were detached lesser than 90 %, a longer incubation period was added. Detached cells were centrifuged to discard the used medium and cell pellet was subsequently transferred into several culture flasks as desired. Cells were usually subcultured every 3-4 days.

3.2.3.5 Counting of cells

NG108-15 cells that achieved 80-90 % confluency were selected for assay. Cells were harvested with accutase and centrifuged to collect the cell pellet. Cells were then resuspended in 1.0 ml fresh medium and 20 µl of cell suspension was subjected to tryphan blue exclusion assay in which, live cells with intact cell membranes excluded tryphan blue dye while dead cells did not. In another words, viable cells possess clear cytoplasm whereas non-viable cells stain blue under inverted microscope. Cell count was visualized utilizing haemocytometer under an inverted microscope. Viable (unstained) and non-viable (stained) cells were counted separately in hemocytometer to obtain the total number of cells and subsequently aliquoted to desired concentrations in

various assays.

3.2.4 Neuroprotective experimental design

3.2.4.1 Induction of oxidative damage

Oxidative stress treatment was initiated by adding the H_2O_2 in NG108-15 cells. Cells were treated with serial concentrations of H_2O_2 prepared in complete medium for up to 10 h.

3.2.4.2 MTT cell viability assay

NG108-15 cell viability in neuroprotection was analyzed by MTT assay (Mosmann, 1983). This test is based on a reduction of tetrazolium salts into purple formazan derivatives in intact mitochondria of viable cells. Cells were raised to confluence, harvested by accutase, rinsed with PBS and plated at a density of $5x10^3$ cells/well in 96-well plate. The cells were incubated at 37 °C with 5 % CO_2 for 48 h. After the incubation period, cells were pretreated with varying concentrations of LPEE, LPEAF, and LPAF for 2 h at 37 °C with 5 % CO_2 followed by 10 h H_2O_2-induced oxidative damage. After 10 h exposure to H_2O_2, tetrazolium salt solution was added into each well and incubated for subsequent 4 h. Plates were analyzed in microplate reader at 570 nm with 650 nm as reference wavelength. Resveratrol was used as positive control. Percentage of cell viability was calculated according to the equation below:

$$\% \text{ of cell viability} = [A_s/A_C] \times 100\ \%$$

Where A_s is the absorbance of LPEE, LPEAF, and LPAF pretreated cells and Ac is the absorbance of control cells

3.2.5 Bioassay-guided isolation of neuroprotective compounds from LPAF

3.2.5.1 Fractionation and purification of LPAF

LPEE, LPEAF and LPAF were subjected to neuroprotective activity screening by MTT cell viability assay. Results indicated that LPAF exhibited the strongest neuroprotective activity and thus, LPAF was further fractionated via neuroprotective activity-directed fractionation and purification. Firstly, LPAF was purified utilizing Diaion HP20SS column with the elution of a constant gradient solvent system from 0 to 100 % with 10 % methanol increment in water to elute the compounds with different polarity. The chemical composition of fractions was determined using TLC. TLC was carried out on pre-coated silica gel 60 F_{254} plates (0.2 mm thick, Merck) with $CHCl_3$-MeOH-H_2O (7:3:0.5 or 6:4:1 v/v) or C_6F_6-HCOOEt-HCOOH (1:7:1 v/v) and spots were detected under ultraviolet illumination (254nm and 365nm) and sprayed with 10 % H_2SO_4 followed by heating or sprayed with 2 % ethanolic $FeCl_3$ reagent. After evaporation under reduced pressure, ten fractions (designated as LPAF1, LPAF2, LPAF3, LPAF4, LPAF5, LPAF6, LPAF7, LPAF8, LPAF9, and LPAF10) were collected from Diaion HP20SS column and subjected to neuroprotective activity screening subsequently. Both LPAF6 and LPAF7 showed the strongest neuroprotective activity with the highest percentage cell viability following H_2O_2 insult and hence, LPAF6 and LPAF7 were subjected to further fractionation. LPAF6 was purified using Sephadex LH-20 column with the elution of a constant gradient solvent system from 0 to 100 % with 10 % methanol increment in water. Eight fractions (designated as LPAF61, LPAF62, LPAF63, LPAF64, LPAF65, LPAF66, LPAF67, and LPAF68) were yielded and the most active fraction (LPAF66) was further fractionated on Sephadex LH-20 column using methanol-water solvent system from 20 to 100 % with 10 % methanol increment in water. A total of five fractions (designated as LPAF661, LPAF662, LPAF663,

LPAF664, and LPAF665) were collected. LPAF662 with the strongest activity was identified through LC-MS, ^{1}H NMR, and ^{13}C NMR. On the other hand, LPAF7 was purified using Sephadex LH-20 column with the elution of a constant gradient solvent system from 20 to 100 % with 10 % methanol increment in water. Eight fractions (designated as LPAF71, LPAF72, LPAF73, LPAF74, LPAF75, LPAF76, LPAF77, and LPAF78) were yielded and the most active fraction (LPAF76) was further fractionated on Sephadex LH-20 column using the identical methanol-water solvent system. A total of four fractions (designated as LPAF761, LPAF762, LPAF763, and LPAF764) were collected. LPAF762 with the strongest neuroprotective activity was identified through LC-MS, ^{1}H NMR, and ^{13}C NMR. The stationary phase consisted of a glass column packed with either Diaion HP20SS or Sephadex LH-20 while the mobile phase comprised a constant gradient combination of methanol and water with the gradually eluting strength increment in the percentage of more polar solvent. The initial solvent composition was water (100 %, 300 ml), and subsequently changed to chloroform-methanol-water (5:5:1.5, v/v/v, 200 ml), followed by chloroform-methanol-water (7:3:0.5, v/v/v, 200 ml), chloroform-methanol-water (6:4:1, v/v/v, 200 ml), benzene-ethyl formate-formic acid (1:7:1, v/v/v, 200 ml), and benzene-ethyl formate-formic acid (1:7:2, v/v/v, 200 ml).

3.2.5.2 Thin layer chromatography

TLC was performed by TLC aluminum sheets coated with silica gel 60 F_{254} 6 cm x 6 cm. Standard fractions chromatograms were prepared by inducing a few drops of solution onto a silica gel TLC plate and developing by distinct solvent systems to improve the separation under saturated conditions. Separated bands were detected under ultraviolet light with 254 nm and 365 nm.

3.2.5.3 Liquid chromatography mass spectroscopy

Mass spectra of the isolated compounds were recorded via electrospray ionization fitted with Finnigan LTQ orbitrap mass spectrometer. LC-MS was carried out in positive ion mode through the setting of needle voltage at 4000 V, capillary voltage at 35 V, and capillary temperature at 285 °C.

3.2.5.4 NMR spectroscopy

^{1}H NMR and ^{13}C NMR spectra of the isolated compounds were recorded using Bruker DRX 300 NMR spectrometer with 300 MHz and 75 MHz for ^{1}H-NMR and ^{13}C-NMR, respectively.

3.2.5.4.1 AC trimer

Tan amorphous powder, $C_{45}H_{38}O_{18}$: $[M+H]^+$ peak at *m/z* 867.21. ^{1}H-NMR (Acetone-d_6 + D_2O, 300 MHz) δ: 4.88 (1H, d, *J* = 6.0 Hz, H-2); ^{13}C-NMR (Acetone-d_6 + D_2O, 75 MHz) δ: 101.4 (C-10), 100.7 (C-10', 10''), 81.6 (C-2), 76.6 (C-2', 2''), 72.8 (C-3''), 71.3 (C-3'), 67.5 (C-3), 36.8 (C-4', 4'').

3.2.5.4.2 (+)-Catechin

White amorphous powder, $C_{15}H_{14}O_6$: $[M+H]^+$ peak at *m/z* 291.09. ^{1}H-NMR (Acetone-d_6, 300 MHz) δ: 6.87 (1H, d, *J* = 1.8 Hz, H-2'), 6.77 (1H, d, *J* = 8.1 Hz, H-5'), 6.71 (1H, dd, *J* = 2.1, 8.1 Hz, H-6'), 5.99 (1H, d, *J* = 2.4 Hz, H-8), 5.83(1H, d, *J* = 2.4 Hz, H-6), 4.50 (1H, d, *J* = 7.8 Hz, H-2), 3.95 (1H, m, H-3), 2.88 (1H, dd, *J* = 5.4, 15.9 Hz, H-4b), 2.48 (1H, dd, *J* = 8.7, 15.9 Hz, H-4a); ^{13}C-NMR (Acetone-d_6, 75 MHz) δ: 157.5 (C-7), 157.1 (C-5), 156.6 (C-9), 145.6 (C-3'), 145.5 (C-4'), 131.7 (C-1'), 119.8 (C-6'), 115.5 (C-5'), 115.1 (C-2'), 100.3 (C-10), 95.9 (C-6), 95.0 (C-8), 82.4 (C-2), 68.0 (C-3), 28.7 (C-4).

3.2.6 Fluorescence microscopy detection of DAPI nuclear stain

NG108-15 cells were cultured on cover slips and pretreated with LPAF for 2 h at various treatment concentrations followed by H_2O_2 insult for subsequent 10 h. Upon treatment, cells were rinsed with PBS and fixed for 30 min in ice cold acetone. Fixed cells were rinsed with PBS and stained with DAPI solution for 30 min at 4 ^{o}C. Cover slips were mounted onto the glass microscope slides subsequently and analyzed via fluorescence microscope with the excitation and emission fluorescent filter at 350 nm and 460 nm, respectively.

3.2.7 Measurement of total intracellular GSH content

Intracellular GSH level was determined through the method of Griffith (1980). In brief, total GSH content was measured via enzymatic recycling method by DTNB and GR in which GSH is oxidized by DTNB and reduced by NADPH in the presence of GR. NG108-15 cells were pretreated with LPAF for 2 h followed by the induction of H_2O_2 for subsequent 10 h. Upon treatment, cells were harvested, rinsed with ice-cold PBS, and resuspended in 500 µl 5 % 5-sulfosalicylic acid on ice for 15 min. Cells were centrifuged for 15 min at 10000 rpm after 15 min incubation on ice and supernatant was utilized in the measurement of total GSH content. Reaction mixture consisting of NADPH, DTNB, and GSH standards in phosphate buffer was prepared and initiated by the addition of GR. Final concentrations of each component in the reaction mixture were 0.038 mg/mL (48 µM) NADPH, 0.95 mM EDTA, 0.031 mg/mL DTNB, 0.115 units/mL GR, 0.24 % 5-sulfosalicylic acid, and 95 mM potassium phosphate buffer with pH 7.0. Absorbance was measured for 10 min with 1 min intervals at 405 nm via microplate reader, and compared with GSH standard curve.

3.2.8 Determination of intracellular reactive oxygen species using DCF-DA stain

Intracellular oxidative stress level was determined by fluorescent probe, DCF-DA. NG108-15 cells were pretreated with various concentrations of LPAF and (+)-catechin for 2 h followed by H_2O_2-induced oxidative stress for 10 h. After treatment, cells were harvested, rinsed, and incubated in the existence of 10 μM DCF-DA at 37 °C for 30 min in cell loading medium. PI solution of 10 μg/mL was added subsequently for 5 min at ambient temperature. Lastly, fluorescence was determined by flow cytometry with 490 nm excitation and 520 nm emission fluorescent filter.

3.2.9 Assessment of externalization of phosphatidylserine using annexin V/PI labeling

To confirm the occurrence of apoptosis in NG108-15 cells, annexin V/PI dual staining was carried out based on the membrane phosphatidylserine translocation. Annexin V/PI double stained cells were elucidated with FITC-labeled annexin V (green fluorescence), simultaneously with dye exclusion of PI (negative for red fluorescence). Upon treatment with LPAF and (+)-catechin for 2 h at various concentrations and subsequently 10 h oxidative stress induction by H_2O_2, cells were harvested, pelleted, and resuspended in annexin V binding buffer followed by annexin V and PI staining for 30 min at ambient temperature in dark. Finally, cells were examined by flow cytometry.

3.2.10 Detection of mitochondrial membrane potential by JC-1 stain

Mitochondrial membrane potential was assayed by a mitochondrial-specific and cell-permeable fluorescent probe, JC-1 according to the method of Reers et al. (1995). JC-1

probe is a cationic and lipophilic dye that goes into mitochondria in proportion to the membrane potential and forms J-aggregates at high mitochondrial membrane potential. After pretreatment with LPAF and (+)-catechin at various concentrations for 2 h followed by H_2O_2 insult for subsequent 10 h, NG108-15 cells were harvested, resuspended in JC-1 solution and incubated for 15 min at 37 °C in the CO_2 incubator. Cells were rinsed twice with fresh media and resuspended in fresh medium. The ratio of green/red fluorescence of each cell that indicates mitochondrial membrane potential was evaluated via flow cytometry. In healthy cells, JC-1 forms J-aggregates within mitochondria spontaneously which fluoresces red and detected in FL-2 channel. In unhealthy or apoptotic cells, JC-1 cannot accumulate within mitochondria and remains monomeric form in cytoplasm which shows only green fluorescence, were detected in FL-1 channel.

3.2.11 Analysis of cell cycle events using PI stain

Cell cycle distribution and DNA content were evaluated via PI staining (Nicoletti et al., 1991). NG108-15 cells were pretreated with various concentrations of LPAF and (+)-catechin for 2 h followed by H_2O_2-induced oxidative damage for subsequent 10 h. After treatment, cells were harvested, rinsed with PBS, and fixed with ice-cold absolute ethanol at -20 °C overnight. Fixed cells were rinsed and resuspended in PI solution containing 0.1 % sodium citrate, 0.1 % Triton-X-100, 100 μg/mL RNAse, and 10 mg/mL PI to incubate in dark for 30 min at ambient temperature. PI-stained cells were ready to be examined using flow cytometry. The percentage of apoptotic and non-apoptotic populations in every cell cycle phase was measured and the arrest at sub-G_1 phase reflected on the apoptotic population.

3.2.12 SOD enzyme activity assay

SOD enzyme activity assay was assessed based on the manufacturer's protocol. After 2 h pretreatment with various concentrations of (+)-catechin followed by 10 h H_2O_2-induced oxidative stress, NG108-15 cells were harvested and lysed to obtain the supernatant for SOD enzyme activity assay. SOD assay kit utilizes Dojindo's highly water-soluble tetrazolium salt, 2-(4-Iodophenyl)-3-(4-nitrophenyl)-5-(2,4-disulfophenyl)-2H-tetrazolium, monosodium salt (WST-1) which forms a water-soluble formazan dye during the reduction with a O_2^-. The O_2 reduction rate is proportional to xanthine oxidase (XO) activity which is inhibited by SOD, as shown in Figure 20. Hence, the IC_{50} of SOD can be measured by a colorimetric method. SOD enzyme activity was expressed in percentage of inhibition. Hence, one unit of SOD is defined as the amount of the enzyme which inhibits the reduction of WST-1 with O_2^-.

3.2.13 GPx enzyme activity assay

GPx enzyme activity was assayed based on the manufacturer's protocol. Upon pretreatment with (+)-catechin at various concentrations for 2 h followed by H_2O_2 insult for subsequent 10 h, NG108-15 cells were harvested and lysed to acquire the supernatant for GPx enzyme activity assay. GPx assay kit determines the GPx level indirectly via a coupled reaction with GR. During the reduction of an organic hydroperoxide by GPx, GSSG is formed and recycled to its reduced state by NADPH and GR. The decrease in NADPH absorbance was measured at 340 nm upon the oxidation of NADPH to $NADP^+$ is an indicator of GPx enzyme activity as shown in Figure 21, since GPx is the rate limiting factor of the coupled reactions. The level of GPx enzyme activity was expressed as nmol/min/ml. Hence, one unit of GPx will cause

the formation of $NADP^+$ from NADPH per minute at pH 8.0 at 25 °C in the presence of reduced glutathione, GR, and organic hydroperoxide.

3.2.14 Analysis of Bax, Bcl-2, and CCL21 gene expression via Q-PCR

To examine the role of Bax, Bcl-2, and CCL21 in the present NG108-15 neuroprotection model, we determined the gene expression of Bax, Bcl-2, and CCL21 via Q-PCR. A density of $0.5x10^6$ cells were exposed to desired treatment. Upon pretreatment with (+)-catechin for 2 h followed by H_2O_2 for subsequent 10 h, total RNA was isolated using RNAqueous-4PCR kit according to the manufacturer's protocol. Bax, Bcl-2, and CCL21 gene expression were evaluated using one-step SYBR Green relative Q-PCR and normalized to HMBS as reference gene. The reactions were performed in a total volume of 25 μl by SensiMix One-Step Kit. The Q-PCR amplification conditions for Bax was 40 cycles of 10 seconds at 95 ^oC, 45 seconds at 60 ^oC and 10 seconds at 72 ^oC, whereas Bcl-2 was 40 cycles of 10 seconds at 95 ^oC, 45 seconds at 51 ^oC and 10 seconds at 72 ^oC, while for CCL21 was 40 cycles of 10 seconds at 95 ^oC, 45 seconds at 45 ^oC and 10 seconds at 72 ^oC. Fluorescence threshold Ct values and ΔCt values were calculated by the formula $\Delta Ct = Ct_{\text{Bax or Bcl-2 or CCL21}} - Ct_{\text{HMBS.}}$ The ΔΔCt values were calculated subsequently based on formula ΔΔCt = ΔCt treated - ΔCt untreated. The expression levels of Bax, Bcl-2, and CCL21 in the treated cells was measured relative to the level obtained in the H_2O_2-treated cells, and was quantitated by formula $2^{-\Delta\Delta Ct}$ (Livak and Schmittgen, 2001). The primer sequences, cycling conditions, and reaction mixture for Q-PCR were shown in Table 1, Table 2, and Table 3, respectively.

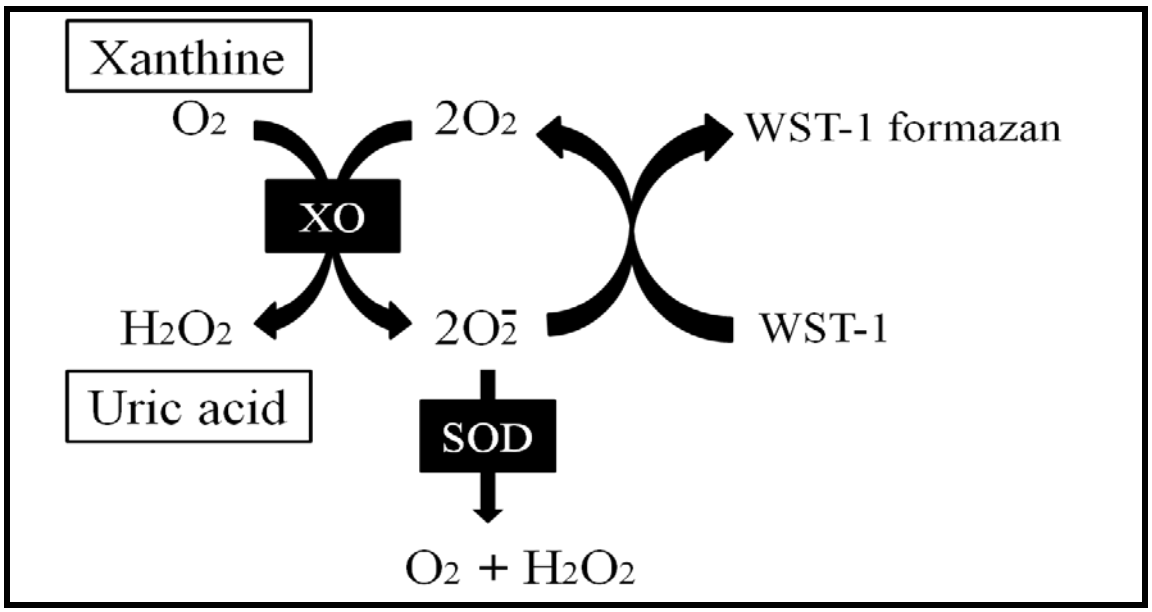

Figure 20. Principle of SOD assay kit

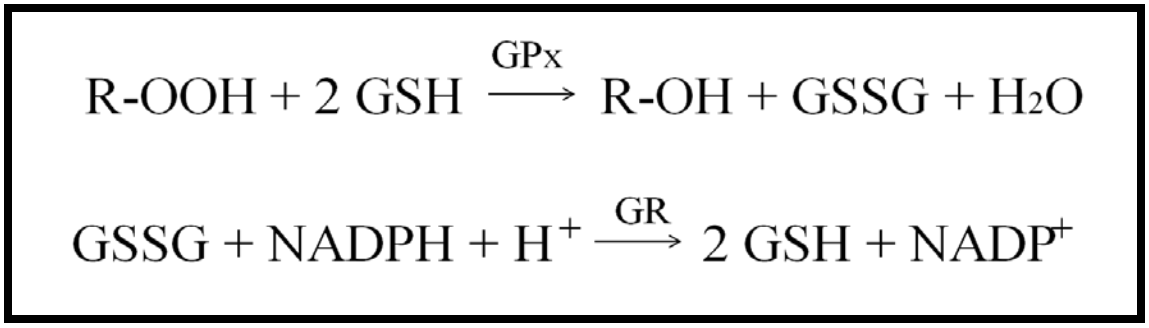

Figure 21. Principle of GPx assay kit

Table 2. Cycling conditions for Q-PCR

Target gene	Reference gene	Denaturation	Annealing	Extension
Bax	HMBS	At 95 °C for 10 seconds	At 51 °C for 45 seconds, 40 cycles	At 72 °C for 10 seconds
Bcl-2	HMBS	At 95 °C for 10 seconds	At 60 °C for 45 seconds, 40 cycles	At 72 °C for 10 seconds
CCL21	HMBS	At 95 °C for 10 seconds	At 45 °C for 45 seconds, 40 cycles	At 72 °C for 10 seconds

Table 3. Reaction mixture for Q-PCR

Reagents	1 reaction (total volume 25 µl)	Final concentration
Water (H_2O)	4.5 µl	-
Sensimix SYBR One-Step	12.5 µl	1x
SYBR green	0.5 µl	1x
$MgCl_2$	-	3 mM
Forward primer	1.0 µl	200 nM
Reverse primer	1.0 µl	200 nM
RNase inhibitor	0.5 µl	10 units
RNA	5.0 µl	20 ng/µL

3.2.15 Flow cytometric analysis of Bax, Bcl-2, and CCL21 protein expression by immunofluorescence staining

The immunoexpression of Bax, Bcl-2, and CCL21 were measured via flow cytometric immunofluorescence staining according to Roussi et al. (2007) with some modifications. Upon pretreatment with (+)-catechin for 2 h followed by H_2O_2 insult for subsequent 10 h, NG108-15 cells were harvested, rinsed with ice-cold PBS, fixed, and permeabilized using intracellular flow cytometry system. Cells were subsequently resuspended in $1.0x10^6$ cells/mL and aliquot into 100 µl using flow cytometry wash buffer. For Bax and Bcl-2 direct staining, cells were incubated for 60 min in dark with 20 µl of FITC-conjugated Bax mouse monoclonal antibody or rabbit IgG isotype control, and PE-conjugated Bcl-2 mouse monoclonal antibody or rabbit IgG isotype control, respectively. For CCL21 staining, rabbit anti-murine exodus-2 CCL21 polyclonal antibody was conjugated directly using Lightning-Link^{TM} fluorescein conjugation kit. Cells were then mixed with 20 µL of FITC-conjugated CCL21 polyclonal antibody or rabbit IgG isotype control and incubated for 60 min in dark. Upon staining, cells were washed twice with flow cytometry wash buffer and resuspended in 500 µl flow cytometry wash buffer. Cells were ready to be measured via flow cytometry.

3.2.16 Data analysis

The experimental results were expressed as mean ± SE of at least two independent experiments with minimum three replicates each. Data were analyzed using Pearson correlation test and one-way analysis of variance (ANOVA) followed by Dunnett's test. (* $p < 0.01$ and ** $p < 0.05$) were considered statistically significant.

CHAPTER 4

RESULTS

4.1. Evaluation of antioxidative activities of the extract and fractions of *L. parasiticus*

4.1.1 LPAF showed the strongest DPPH free radical scavenging activity

From the extraction and fractionation of *L. parasiticus*, LPEE, LPEAF, and LPAF obtained, demonstrated strong DPPH free radical scavenging activity with 50 % inhibitory concentration (IC_{50}) values of 20.51 $\pm$ 0.18 μg/mL, 55.66 $\pm$ 0.55 μg/mL, and 16.82 $\pm$ 0.27 μg/mL, respectively (Table 4). LPAF showed the strongest scavenging ability as compared with LPEE and LPEAF. Moreover, all the *L. parasiticus* extract and fractions (LPEE, LPEAF, and LPAF) resulted in higher antioxidant scavenging activity than the positive control, BHT with IC_{50} value of 57.20 $\pm$ 4.92 μg/mL as shown in Figure 22. Also, the LPAF showed significant ($p < 0.05$) positive correlation ($r = 0.814$) between total phenolic content and DPPH IC_{50} value.

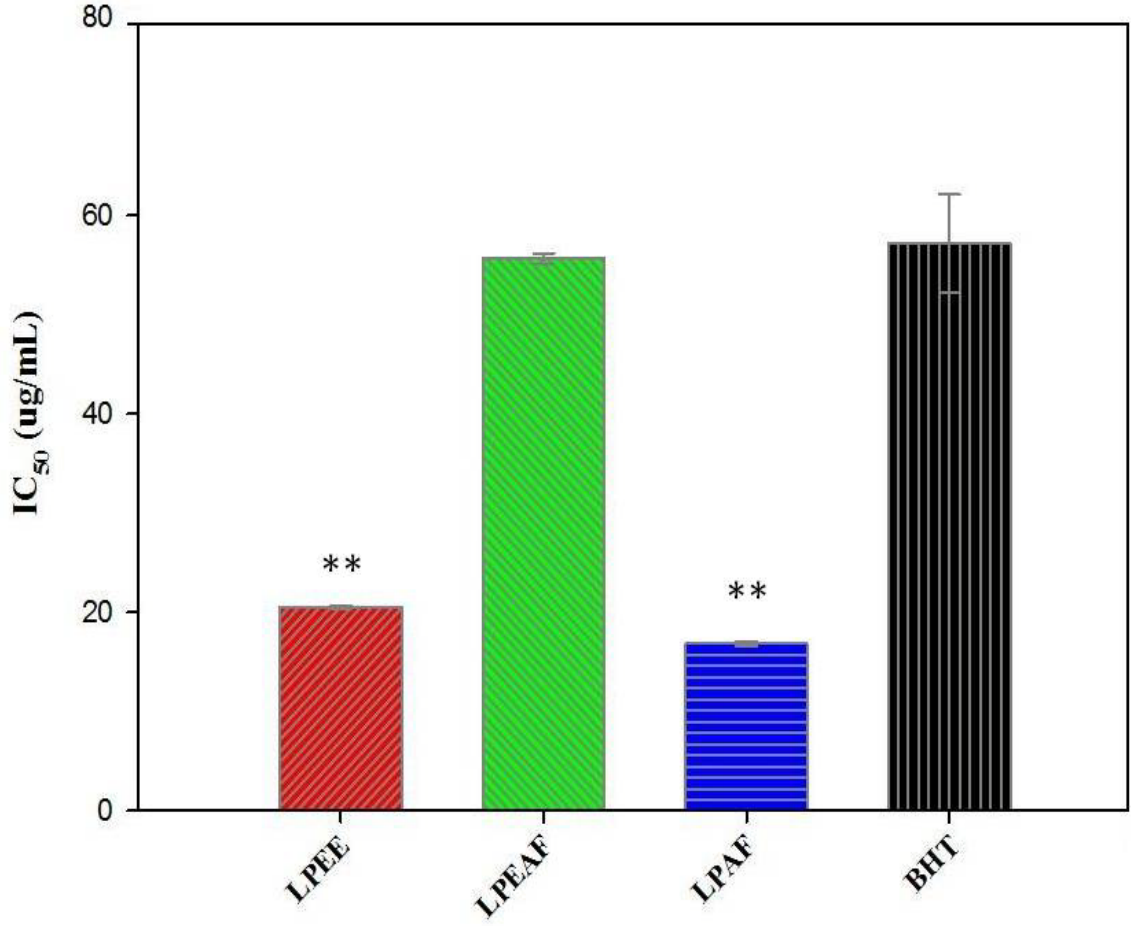

Figure 22. Effects of LPEE, LPEAF, and LPAF on DPPH free radical scavenging activity. 0.2 mM DPPH solution was added in LPEE, LPEAF, and LPAF to incubate for 30 min in dark at ambient temperature. Asterisk (**) represented significant positive correlation between DPPH free radical scavenging assay and total phenolic content ($P<0.05$). Data shown are mean ± SE of at least two independent experiments with minimum three replicates each.

Table 4. Antioxidative properties of *L. parasiticus* extract and fractions (LPEE, LPEAF, and LPAF) in DPPH free radical scavenging activity, lipid peroxidation inhibitory activity, and total phenolic content quantified by Folin-Ciocalteu reaction

Group	DPPH IC_{50} (μg/mL)	Lipid peroxidation IC_{50} (mg/mL)	Total phenolic content (GAE/g_{DW})
LPEE	20.51 ± 0.18**	3.39 ± 0.24**	52.08 ± 1.76
LPEAF	55.66 ± 0.55	7.68 ± 0.37	18.82 ± 0.53
LPAF	16.82 ± 0.27**	1.05 ± 0.04**	56.51 ± 1.43
BHT	57.20 ± 4.92	-	-
Curcumin	-	0.47 ± 0.02	-

BHT and curcumin were employed as positive control in DPPH free radical scavenging activity assay and lipid peroxidation inhibitory activity assay, respectively. Asterisk (**) represented significant positive correlation between DPPH free radical scavenging assay, lipid peroxidation inhibitory assay, and total phenolic content ($P<0.05$). Data shown are mean ± SE of at least two independent experiments with minimum three replicates each.

4.1.2 LPAF possessed the highest reducing power activity

Hydrogen donation from phenolic compounds has the capability to reduce Fe (III) (Shimada et al., 1992), which is also associated with the existence of reductant agents (Duh, 1998). Figure 23 shows the reducing power activity of the LPEE, LPEAF, LPAF, and BHT. LPAF possessed the strongest reducing power followed by the standard positive control, BHT, LPEE, and LPEAF in a descending order. Also, LPAF showed significant ($p < 0.05$) positive correlation ($r = 0.899$) between total phenolic content and reducing power activity. All the *L. parasiticus* extract and fractions (LPEE, LPEAF, and LPAF) showed a dose-dependent reducing power activity as shown in Figure 23.

4.1.3 LPAF exhibited the strongest inhibitory activity in lipid peroxidation

From the results shown in Table 4, the positive control, curcumin, possessed the lowest IC_{50} value of 0.47 $\pm$ 0.02 mg/mL which indicated its ability to inhibit the oxidative degradation of lipids from egg yolk. The highest inhibition was shown by LPAF with IC_{50} value of 1.05 $\pm$ 0.04 mg/mL followed by LPEE and LPEAF with IC_{50} values of 3.39 $\pm$ 0.24 mg/mL and 7.68 $\pm$ 0.37 mg/mL, respectively (Figure 24; Table 4). LPAF showed significant ($p < 0.05$) positive correlation ($r = 0.859$) between total phenolic content and IC_{50} value for lipid peroxidation assay.

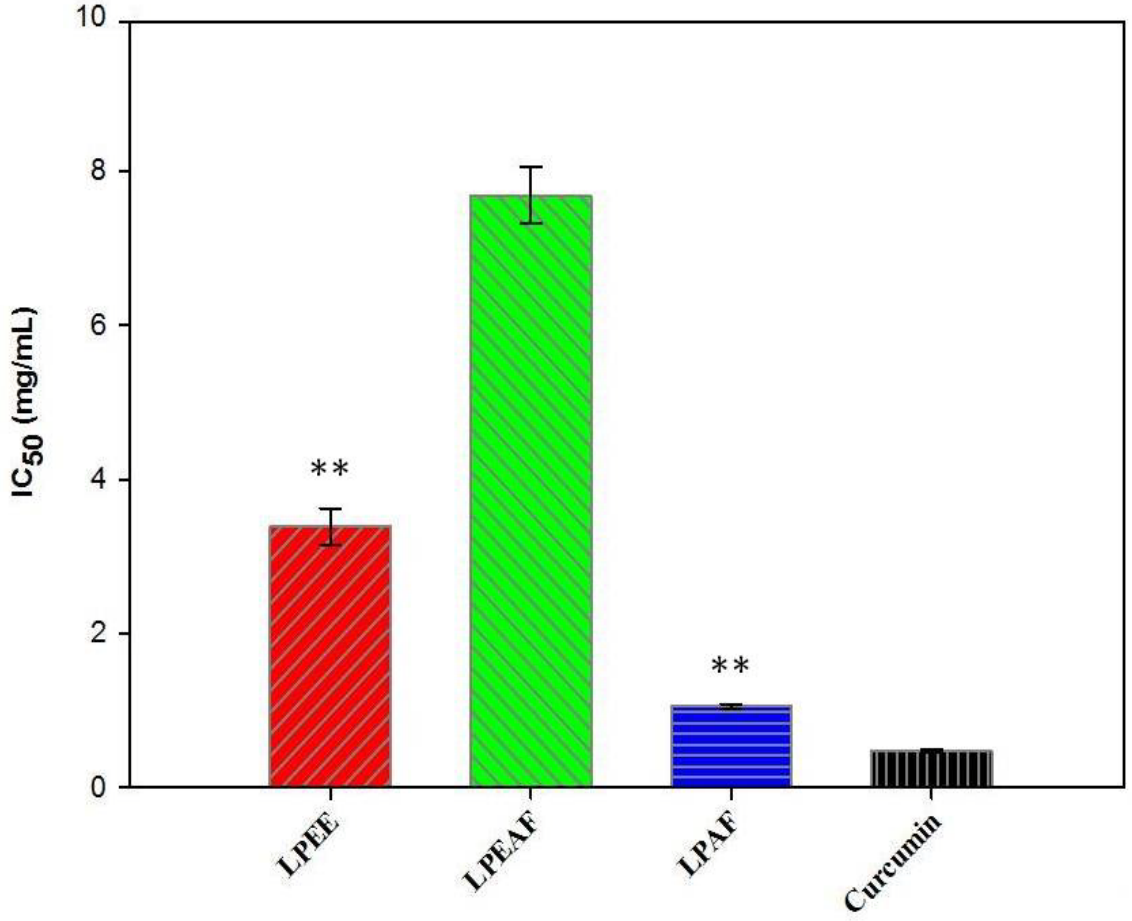

Figure 24. Effects of LPEE, LPEAF, and LPAF on lipid peroxidation inhibitory activity. Egg yolk homogenate was used as an alternative to rodent liver microsomes and linoleic acid in the present lipid peroxidation assay. Asterisk (**) represented signficant positive correlation between lipid peroxidation inhibitory assay and total phenolic content ($P<0.05$). Data shown are mean ± SE of at least two independent experiments with minimum three replicates each.

4.1.4 LPAF yielded the highest phenolic content

Folin-Ciocalteu reagent was determined according to the color measurement that was non-specific on phenol. However, the measurement of color changes after 2 h of incubation in the dark is appropriated to measure the presence of phenol in LPEE, LPEAF, and LPAF. At the concentration of 100 μg/mL, LPAF yielded the highest total phenolic content with 56.51 $\pm$ 1.43 GAE/g_{DW}, followed by LPEE and LPEAF with 52.08 $\pm$ 1.76 GAE/g_{DW} and 18.82 $\pm$ 0.53 GAE/g_{DW}, respectively as shown in Table 4.

4.2 Assessment of neuroprotective effect of the extract and fractions of *L. parasiticus*

4.2.1 Effect of H_2O_2-induced oxidative damage in NG108-15 cells

In order to determine the optimal H_2O_2 concentration to induce oxidative stress in NG108-15 cells, cells were treated with different H_2O_2 concentrations. A significant ($P<0.01$) dose-dependent cell death was observed (Figure 25) when cells were treated with various concentrations of H_2O_2 (0.125 mM - 4.0 mM) for 10 h. Figure 24 showed that the highest percentage of cell death (79.45 $\pm$ 1.03) occurred at the treatment concentration of 4.0 mM H_2O_2. After determination of H_2O_2 concentrations, 2.0 mM of H_2O_2 which killed approximately 50 % of cells was selected and found to be suitable in the present neuroprotection model. The untreated cells were used as the control group which was considered as 100 % cell viability.

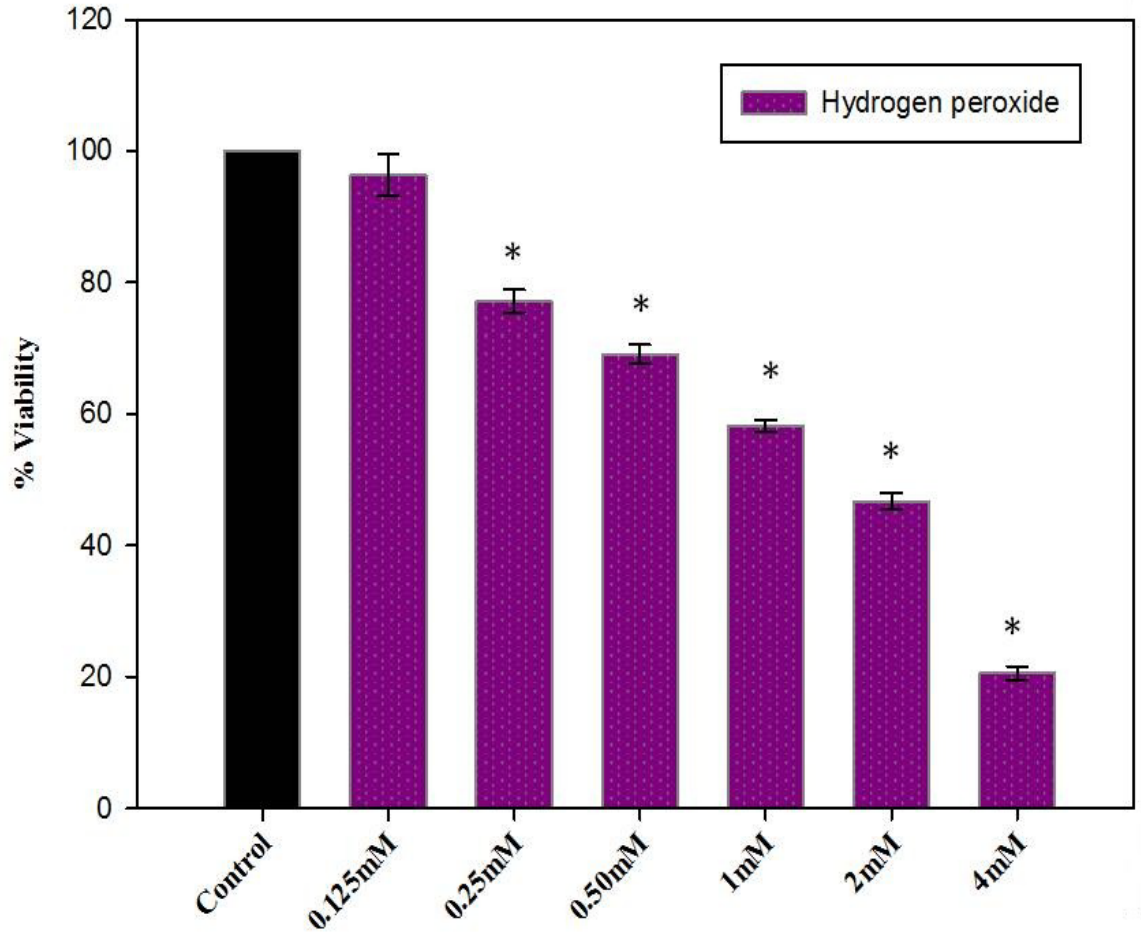

Figure 25. Effects of H_2O_2-induced oxidative stress in NG108-15 cells by MTT cell viability assay. Cells were treated with various concentration of H_2O_2 for 10 h and cell viability was examined via MTT assay. Asterisk (*) represented signficantly di fferent value from untreated control group ($P<0.01$). Data shown are mean ± SE of at least two independent experiments with minimum three replicates each.

4.2.2 LPAF increased the cell viability after H_2O_2 insult

As measured by MTT assay, oxidative damage induced by 2.0 mM H_2O_2 decreased cell viability significantly ($P < 0.01$) by 46.64 $\pm$ 1.29% as compared with the untreated control group (Figure 25). LPAF and LPEE showed the ability to inhibit cell death against H_2O_2 insult dose-dependently (Figure 25). 2 h pretreatment with LPAF exhibited stronger protective activity than LPEE with 78.00 $\pm$ 1.85 % and 67.23 $\pm$ 1.85 % cell viability, respectively. However, LPEAF failed to protect NG108-15 cells against H_2O_2-induced oxidative damage even at the highest treatment concentration of 100 μg/mL (Figure 26). The positive control, resveratrol, showed a dose-dependent increase in the precentage cell viability with 78.49 $\pm$ 1.09 at 100 μg/mL treatment concentration.

4.3 Evaluation of neuroprotective potential of LPAF

4.3.1 LPAF inhibited apoptotic nuclear morphological changes

Morphological apoptotic nuclear alteration which was assessed via DAPI staining, observed in H_2O_2-treated group and such nuclear apoptotic morphogies were greatly decreased in LPAF pretreated NG108-15 cells. In untreated control group, cells were stained less bright blue homogenously and were in round shape (Figure 27a). Nonetheless, a much more condensed and brighter blue staining was observed in cells following H_2O_2 challenge. Also, characteristics of apoptosis such as nuclear shrinkage, fragmentation, and condensation were observed (Figure 27b). Conversely, cells pretreated with 1.0 mg/mL LPAF for 2 h exhibited similar morphologies (Figure 27c) as in untreated control group, indicating the neuroprotective effects afforded by LPAF under oxidative stress conditions.

4.3.2 LPAF attenuated H_2O_2-induced depletion of GSH

In order to investigate the regulation of LPAF on intracellular GSH level in H_2O_2-induced oxidative damaged NG108-15 cells, total GSH content was assessed. Results demonstrated that the intracellular GSH was higher in untreated control group but decreased approximately 3-fold following H_2O_2 insult (Figure 28). Increasing concentration of LPAF significantly ($P < 0.01$) elevated the intracellular GSH level, signifying the neuroprotective role exerted by LPAF against oxidative stress circumstances.

4.3.3 LPAF decreased H_2O_2-induced reactive oxygen species formation

Results demonstrated that H_2O_2-induced oxidative damage leads to an excessive accumulation of reactive oxygen species as compared with untreated control group. Intracellular reactive oxygen species generation by H_2O_2 was significantly ($P < 0.01$) decreased in LPAF pretreated NG108-15 cells as shown in Figure 29.

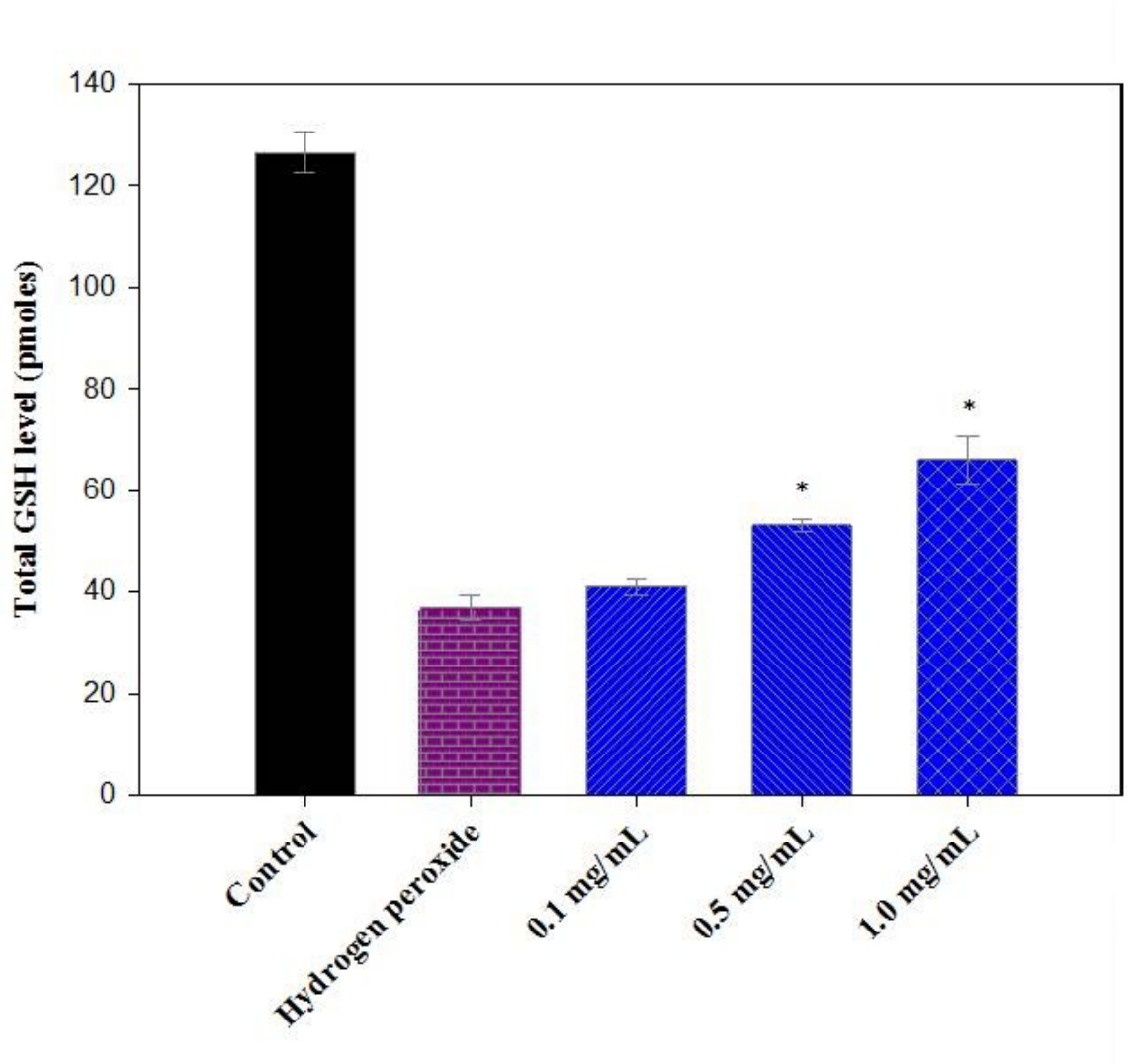

Figure 28. Effect of LPAF against H_2O_2-induced GSH depletion in NG108-15 cells. Cells were pretreated with LPAF for 2 h followed by 10 h H_2O_2 insult. Total intracellular GSH content was measured as picomoles per 0.5 x 10^6 NG108-15 cells based on GSH standard curve. Asterisk (*) represented significantly different value from H_2O_2 treated group ($P<0.01$). Data shown are mean ± SE of at least two independent experiments with minimum three replicates each.

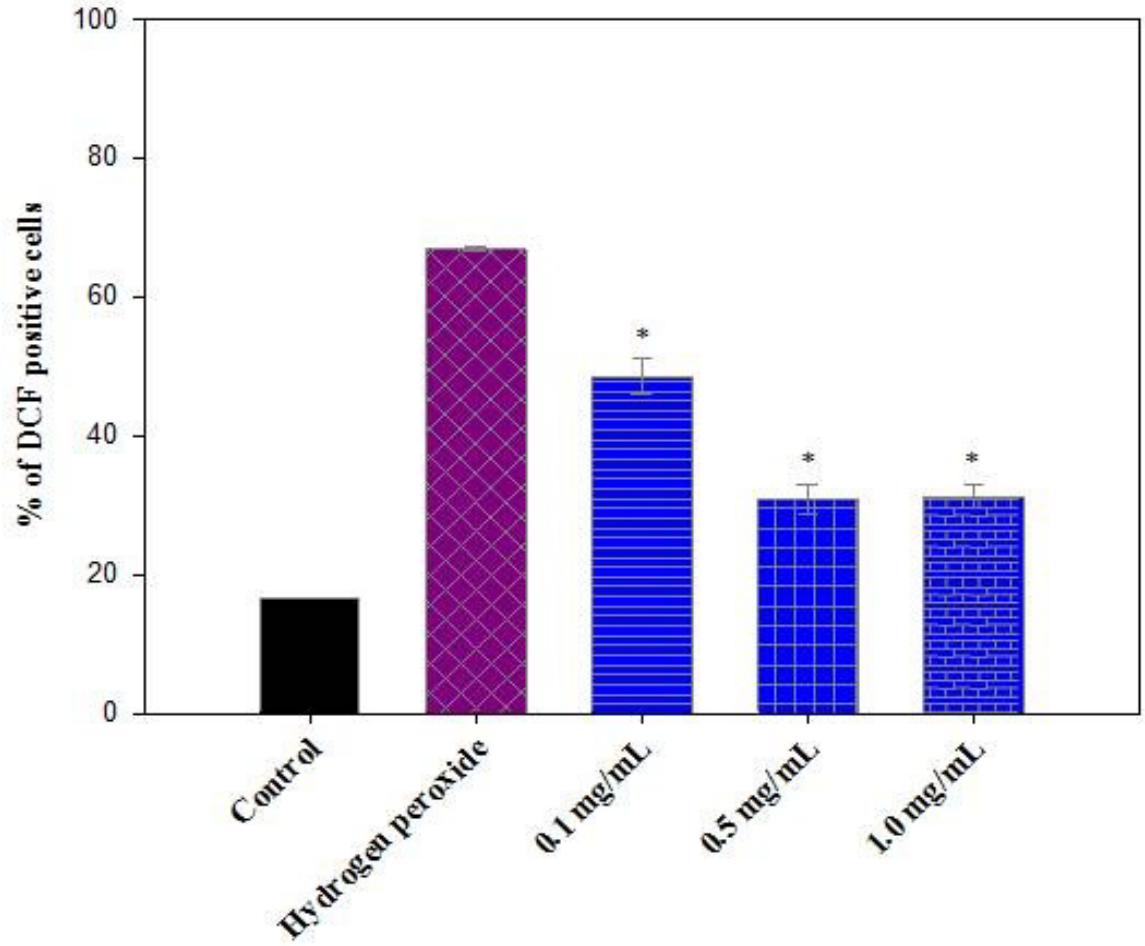

Figure 29. Effect of LPAF on reactive oxygen species formation by H_2O_2 in NG108-15 cells. Cells were pretreated with LPAF for 2 h followed by H_2O_2 insult for subsequent 10 h. Intracellular reactive oxygen species generation resulting from H_2O_2 challenge was determined via DCF-DA fluorescent probe. Asterisk (*) represented significantly different value from H_2O_2 treated group ($P<0.01$). Data shown are mean ± SE of at least two independent experiments with minimum three replicates each.

4.3.4 LPAF mitigated H_2O_2-induced externalization of phosphatidylserine

In the investigation of membrane phosphatidylserine externalization, annexin V stained only (lower right quadrant) cells represented early apoptotic population whereas annexin V and PI stained (upper right quadrant) cells indicated later stage of apoptotic population. Results showed a substantial increase in the percentage of annexin V positive population (lower right and upper right quadrant) in H_2O_2 treated cells as shown in Figure 30a. However, LPAF pretreated cells significantly ($P < 0.01$) decreased the percentage of annexin V positive population dose-dependently (Figure 30b), accounting for 86.27 $\pm$ 0.29 %, 68.67 $\pm$ 0.63 %, and 13.59 $\pm$ 2.03 %, following 2 h pretreatment with 0.1 mg/mL, 0.5 mg/mL, and 1.0 mg/mL LPAF, respectively.

4.3.5 LPAF prevented H_2O_2-induced depolarization of mitochondrial membrane potential

We further evaluated the H_2O_2-induced apoptotic effects as well as the neuroprotective potential of LPAF by assessing the mitochondrial membrane potential via JC-1 fluorescent probe. Results revealed that the majority of the untreated population showing red fluorescence appeared on the upper right quadrant. However, upon the induction of H_2O_2, there was a fluorescence signal shift from the upper right quadrant to the lower right quadrant, representing the loss of red fluorescence (Figure 31a). Conversely, pretreatment with LPAF significantly ($P < 0.01$) increased the red/green fluorescence ratio (60.57 $\pm$ 1.33 %) at 1.0 mg/mL treatment concentration as shown in Figure 31b, as compared with H_2O_2 treated group.

a)

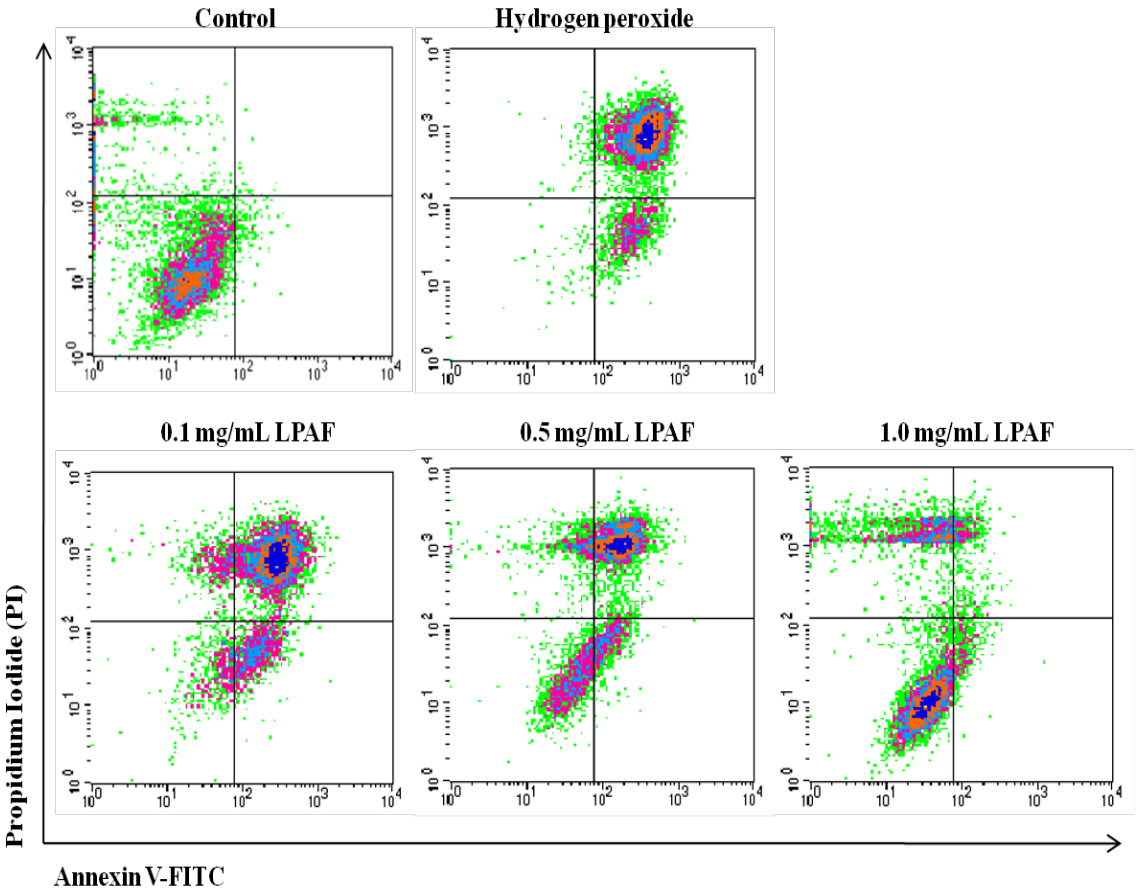
Control
Hydrogen peroxide
0.1 mg/mL LPAF
0.5 mg/mL LPAF
1.0 mg/mL LPAF
Propidium Iodide (PI)
Annexin V-FITC

b)

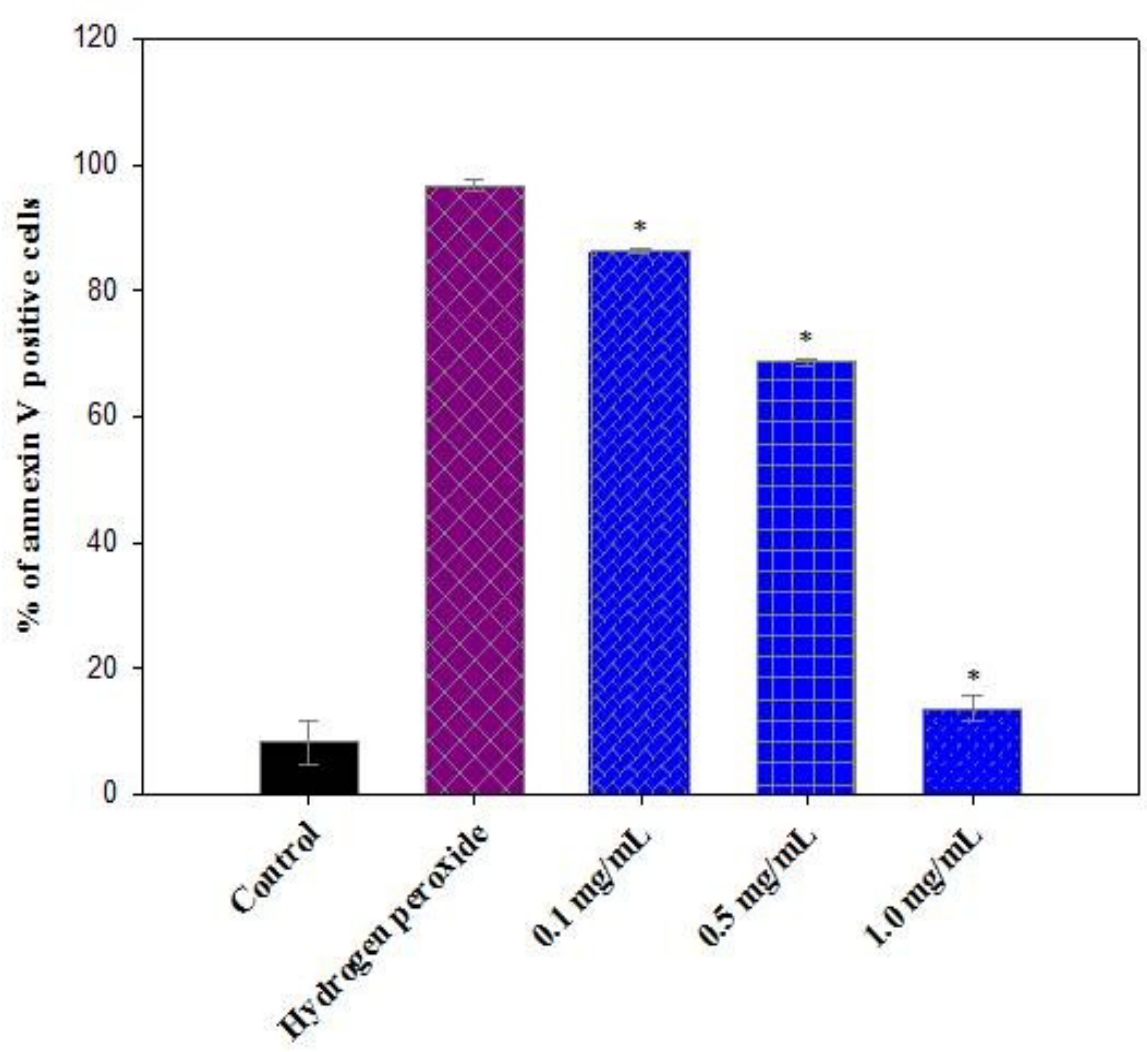

Figure 30. Effect of LPAF against H_2O_2-induced externalization of phosphatidylserine in NG108-15 cells. Cells were pretreated with LPAF followed by H_2O_2-induced oxidative damage. The externalization of phosphatidylserine induced by H_2O_2 was detected using annexin V-FITC/PI double labeled fluorescence dye via flow cytometry analysis. a) Flow cytometric fluorescence patterns of annexin V-FITC/PI double staining. b) Percentage of annexin V positive cells following desired treatment. Asterisk (*) represented significantly different value from H_2O_2 treated group ($P<0.01$). Data shown are mean ± SE of at least two independent experiments with minimum three replicates each.

a)

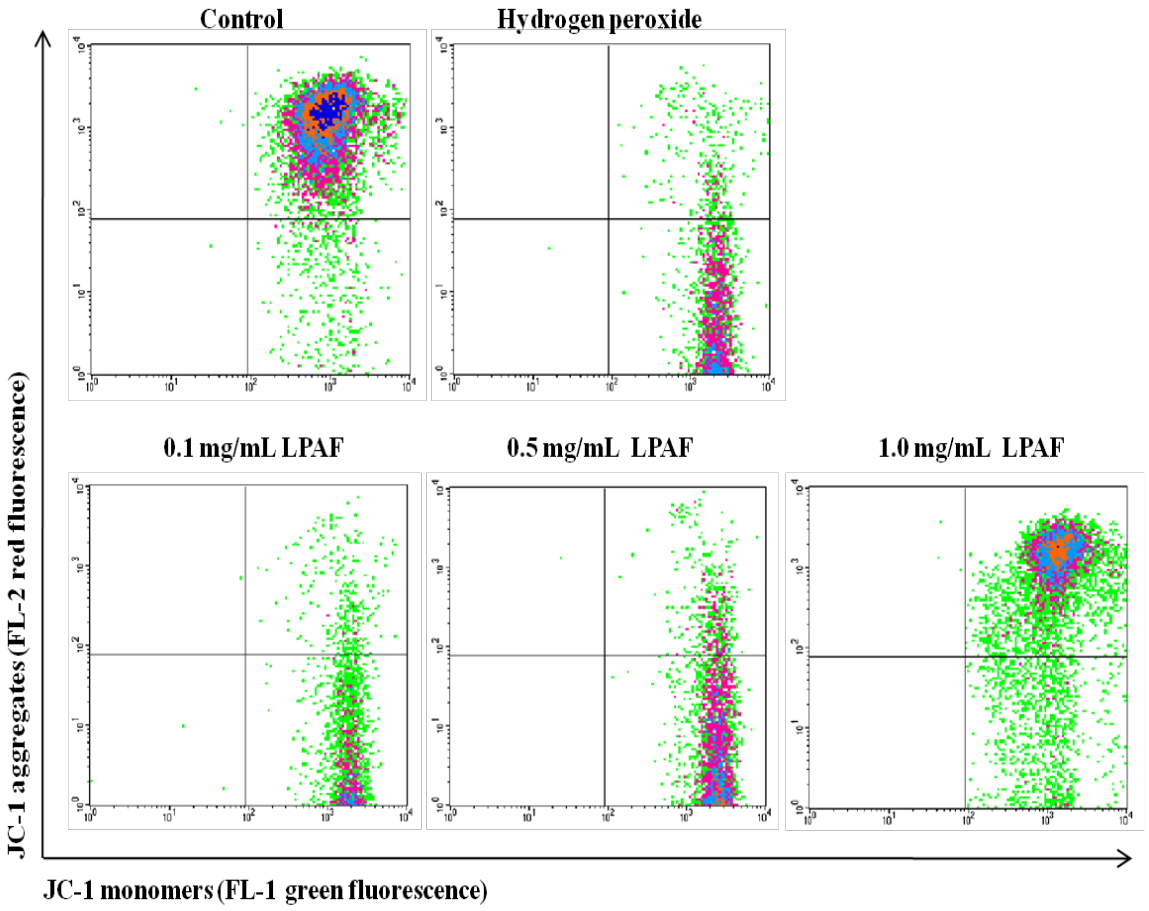
Control
Hydrogen peroxide
0.1 mg/mL LPAF
0.5 mg/mL LPAF
1.0 mg/mL LPAF
JC-1 aggregates (FL-2 red fluorescence)
JC-1 monomers (FL-1 green fluorescence)

b)

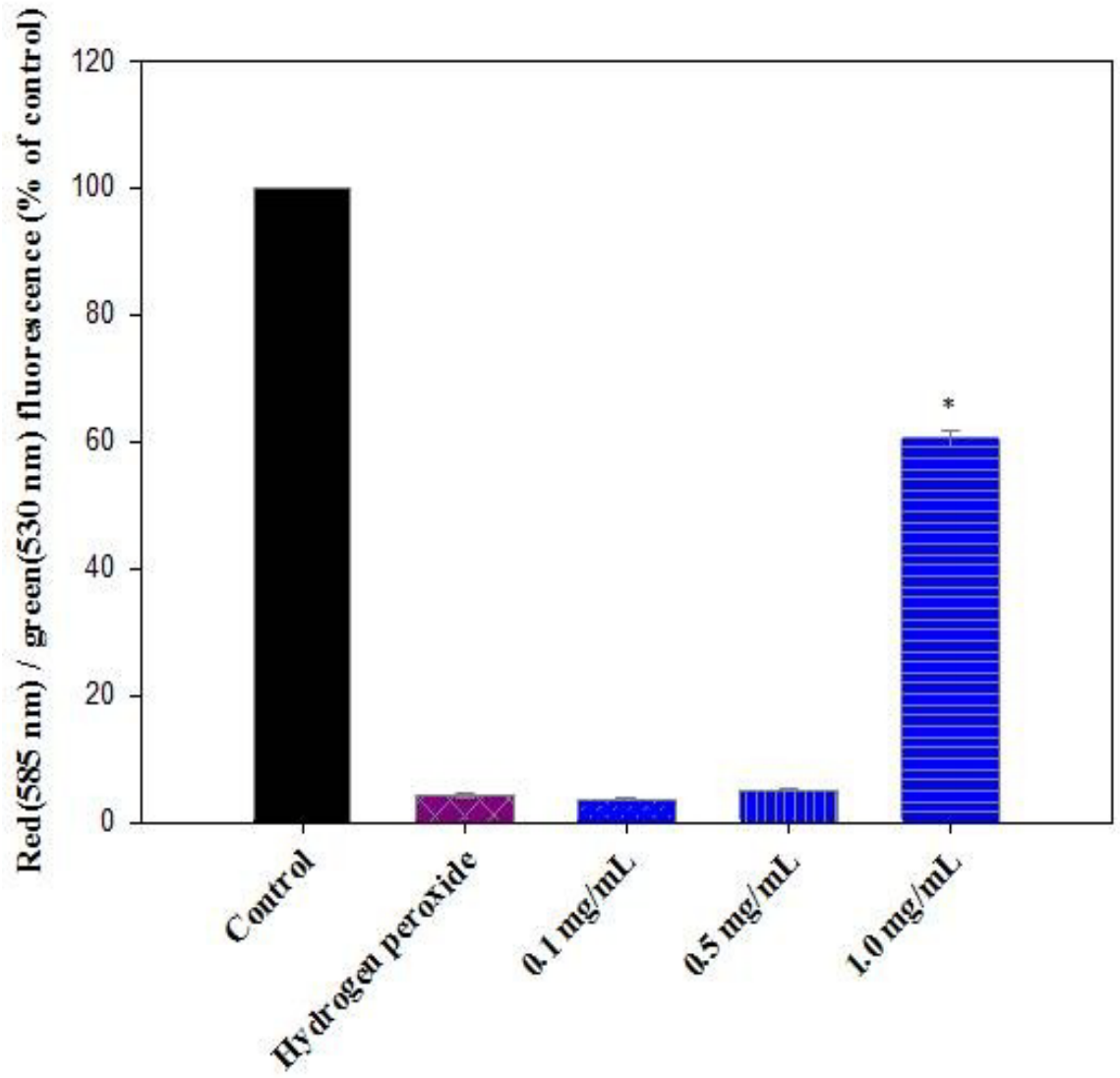

Figure 31. Effect of LPAF on the change of mitochondrial membrane potential following H_2O_2 insult in NG108-15 cells. Cells were pretreated with LPAF for 2 h followed by 10 h H_2O_2-induced oxidative damage. JC-1 fluorescent probe was applied to check the dissipation of mitochondrial membrane potential in the present neuroprotection model. a) Flow cytometric fluorescence pattern analysis of JC-1 staining. b) Quantitative analysis of mitochondrial membrane potential as red (585 nm)/green (530 nm) fluorescence, expressed as percentage of control, indicated the ratio of high/low mitochondrial membrane potential. Asterisk (*) represented significantly different value from H_2O_2 treated group ($P<0.01$). Data shown are mean ± SE of at least two independent experiments with minimum three replicates each.

4.3.6 LPAF abrogated H_2O_2-induced appearance of subG_1-cells

Cell cycle event was elucidated subsequently using flow cytometry via PI staining. Figure 32a showed a substantial increase in sub-G_1 population (54.77 $\pm$ 2.95 %) following H_2O_2-induced oxidative damage, as demonstrated by the appearance of sub-G_1 peak. On the other hand, LPAF significantly ($P < 0.01$) reversed the sub-G_1-induced effect of H_2O_2 in sub-G_1 population (13.58 $\pm$ 0.48 %) at 1.0 mg/mL pretreatment concentration, signifying a neuroprotective role of LPAF.

4.4 Isolation of AC trimer and (+)-catechin via bioacitivity-guided approach

4.4.1 Phytochemical analysis of LPAF

Throughout the fractionation and isolation of LPAF, the percentage cell viability against H_2O_2-induced oxidative damage assessed by MTT assay was compared as shown in Figure 33. Two known proanthocyanidins were isolated and identified from LPAF662 and LPAF762 namely AC trimer (Figure 34) and (+)-catechin (Figure 35), respectively, by evaluating the ^{1}H-NMR and ^{13}C-NMR spectroscopic data with literature values (Nonaka et al., 1981; Nonaka et al., 1983; Cren-Olivé et al., 2002) as shown in Table 5-8. Also, coupling constant and chemical shift values were compared to the literature values (Nonaka et al., 1983) in order to verify the isomer type of (+)-catechin.

a)

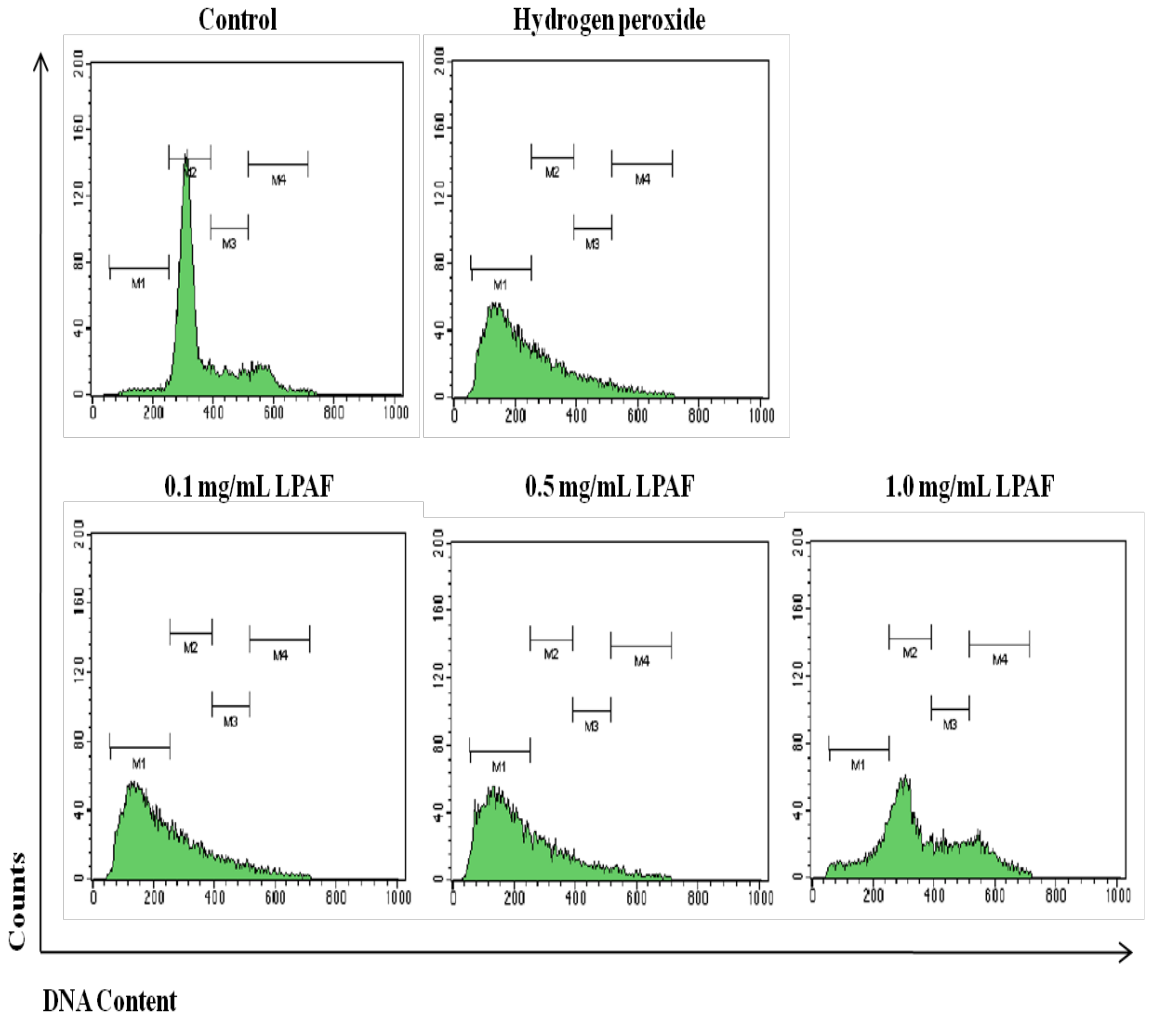
Control
Hydrogen peroxide
0.1 mg/mL LPAF
0.5 mg/mL LPAF
1.0 mg/mL LPAF
M1
M2
M3
M4
Counts
DNA Content

b)

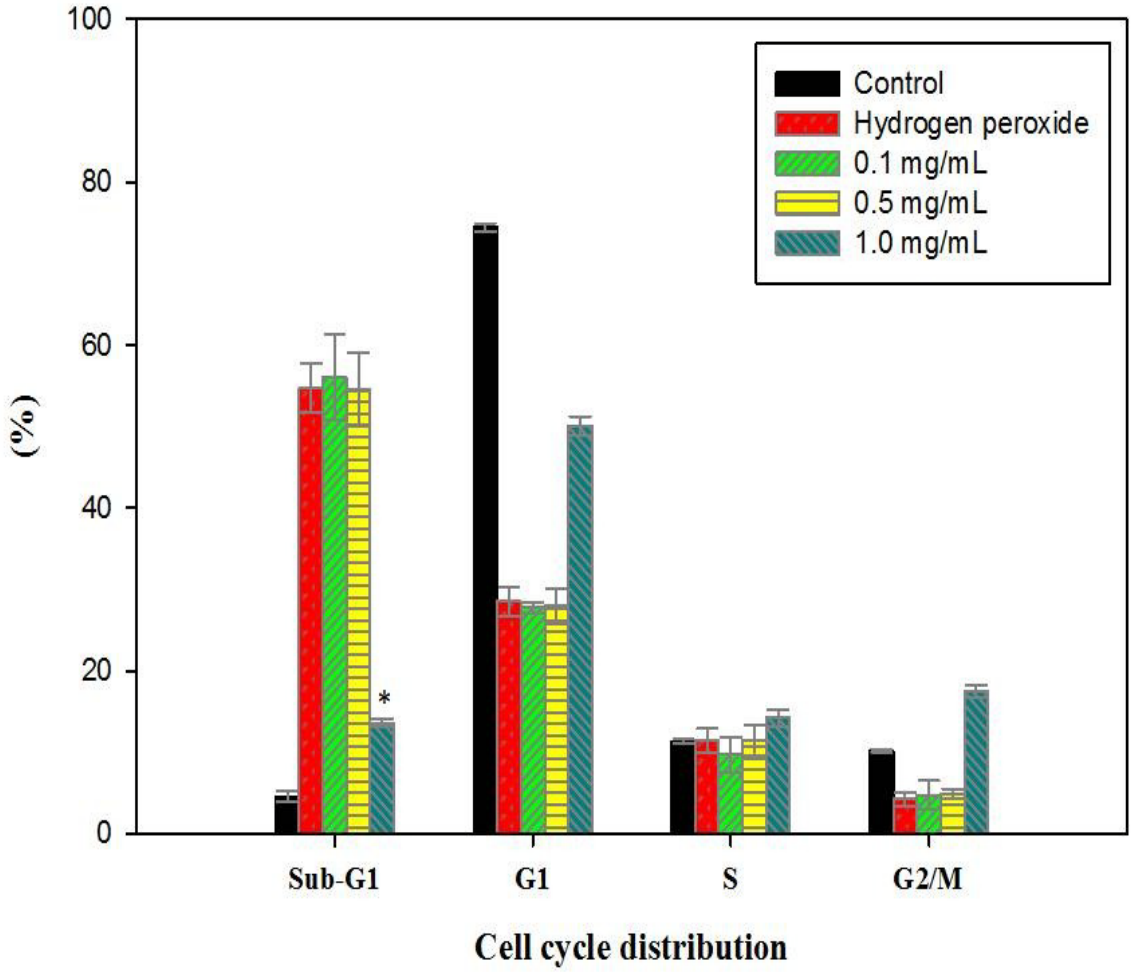

Figure 32. Effect of LPAF on cell cycle event in NG108-15 cells. Cells were pretreated with LPAF followed by H_2O_2-induced oxidative damage. Cellular DNA was stained with PI solution and flow cytometric analysis was carried out. a) Histograms acquired from PI staining and the M1, M2, M3, and M4 regions are corresponding to the cell population with sub-G_1, G_1, S, and G_2/M DNA content, respectively. b) Cell cycle distribution by LPAF upon the oxidative damage induction by H_2O_2. Asterisk (*) represented significantly different value from H_2O_2 treated group ($P<0.01$). Data shown are mean ± SE of at least two independent experiments with minimum three replicates each.

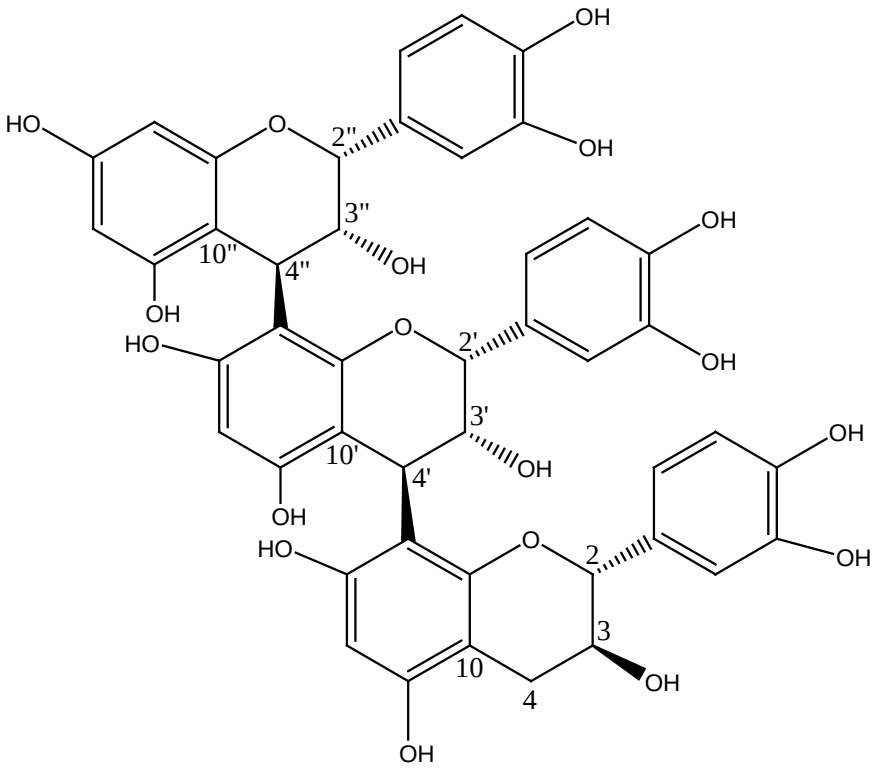

Figure 34. AC trimer isolated from *L. parasiticus*

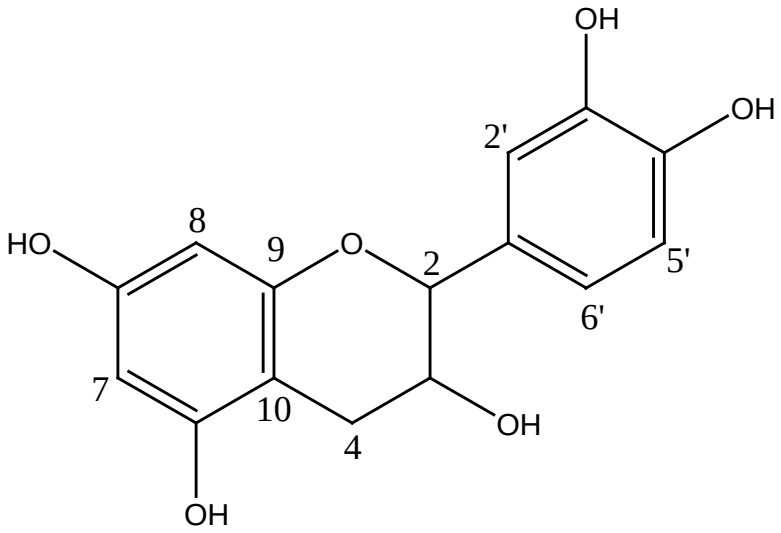

Figure 35. (+)-Catechin isolated from *L. parasiticus*

Table 5. ^{1}H-NMR spectroscopic data of AC trimer

	δ_H	
	Experimental	Literature
H-2	4.88 d (6.0)	4.91 d (6.0)

Table 6. ^{13}C-NMR spectroscopic data of AC trimer

	δ_C	
	Experimental	Literature
C-2	81.6	81.7
C-3	67.5	67.8
C-10	101.4	101.5
C-2'	76.6	76.7
C-3'	71.3	71.5
C-4'	36.8	36.7
C-10'	100.7	100.5
C-2''	76.6	76.7
C-3''	72.8	72.8
C-4''	36.8	36.7
C-10''	100.7	100.5

Table 7. ^{1}H-NMR spectroscopic data of (+)-catechin

	δ_H	
	Experimental	Literature
H-2	4.50 d (7.8)	4.57 d (8)
H-3	3.95 m	3.99 m
H-4a	2.48 dd (8.7, 15.9)	2.52 dd (8.0, 16.0)
H-4b	2.88 dd (5.4, 15.9)	2.92 dd (6.0, 16.0)
H-6	5.83 d (2.4)	5.86 d (2.0)
H-8	5.99 d (2.4)	6.02 d (2.0)
H-2'	6.87 d (1.8)	6.75-6.96 m
H-5'	6.77 d (8.1)	6.75-6.96 m
H-6'	6.71 dd (2.1, 8.1)	6.75-6.96 m

Table 8. ^{13}C-NMR spectroscopic data of (+)-catechin

	δ_C	
	Experimental	Literature
C-2	82.4	83.0
C-3	68.0	68.9
C-4	28.7	28.6
C-5	157.1	157.7
C-6	95.9	96.4
C-7	157.5	157.9
C-8	95.0	95.6
C-9	156.6	157.0
C-10	100.3	100.9
C-1'	131.7	132.3
C-2'	115.1	115.4
C-3'	145.6	146.4
C-4'	145.5	146.3
C-5'	115.5	116.2
C-6'	119.8	120.2

4.4.2 (+)-Catechin exerted stronger neuroprotective activity compared to AC trimer by showing a higher precentage cell viability after H_2O_2 insult

Neuroprotective activites of the isolated AC trimer and (+)-catechin were assessed with varying concentrations of 0.01-1.00 mM in NG108-15 cells. Results demonstrated that both isolated proanthocyanidins significantly ($P<0.01$) alleviated H_2O_2-induced oxidative damage by increasing percentage cell viability of 93.38 $\pm$ 2.36 and 102.41 $\pm$ 3.89 for AC trimer and (+)-catechin, respectively at their highest treatment concentration as shown in Table 9. (+)-Catechin possessed a stronger neuroprotective activity than AC trimer in the present neuroprotection model.

4.5 Neuroprotective mechanism elucidation on (+)-catechin

4.5.1 Effect of (+)-catechin on apoptotic markers

4.5.1.1 (+)-Catechin reduced reactive oxygen species formation

In order to ascertain the neuroprotective mechanism exerted by (+)-catechin, we first introduced the DCF-DA probe to check the H_2O_2-induced intracelular reactive oxygen species level. Upon 10 h treatment, H_2O_2 increased reactive oxygen species production in NG108-15 cells. However, (+)-catechin significantly ($P<0.01$) mitigated the H_2O_2-induced reactive oxygen species generation, indicating a substantial neuroprotection against oxidative stress. Interestingly, a dose-dependent neuroprotective effect was afforded by (+)-catechin as shown in Figure 36.

Table 9. Neuroprotective activities of two isolated proanthocyanidins from LPAF namely AC trimer and (+)-catechin following H_2O_2 insult in NG108-15 cells[a]

Group	Cell viability (%)[b]
Control	100
H_2O_2[c]	47.73 ± 2.72[#]
AC trimer	
0.01 mM	61.74 ± 2.16*
0.05 mM	77.21 ± 2.16*
0.10 mM	88.18 ± 1.69*
0.50 mM	92.51 ± 2.84*
1.00 mM	93.38 ± 2.36*
(+)-Catechin	
0.01 mM	65.34 ± 2.56*
0.05 mM	76.19 ± 2.36*
0.10 mM	81.88 ± 2.22*
0.50 mM	99.07 ± 2.12*
1.00 mM	102.41 ± 3.89*
Resveratrol[d]	78.49 ± 1.09*

[a] NG108-15 cells were pretreated with proanthocyanidins (0.01 mM-1.00 mM) for 2 h. Cells were then exposed to 2.0 mM H_2O_2 for 10 h. After desired incubation period, cells were assessed by MTT to measure the percentage cell viability after oxidative stress-induced neuronal damage;
[b] Cell viability was determined by MTT assay;
[c] H_2O_2 treated alone group differed significantly from the untreated control group at the level of [#] $p < 0.01$;
[d] Resveratrol as positive control.

The values shown are the means ± SE of at least two independent experiments with minimum three replicates each. Results differ significantly from H_2O_2 treated group compared to untreated control group: [#] $p < 0.01$, and significantly from H_2O_2 treated group compared to the proanthocyanidins pretreatment group: [*] $p < 0.01$.

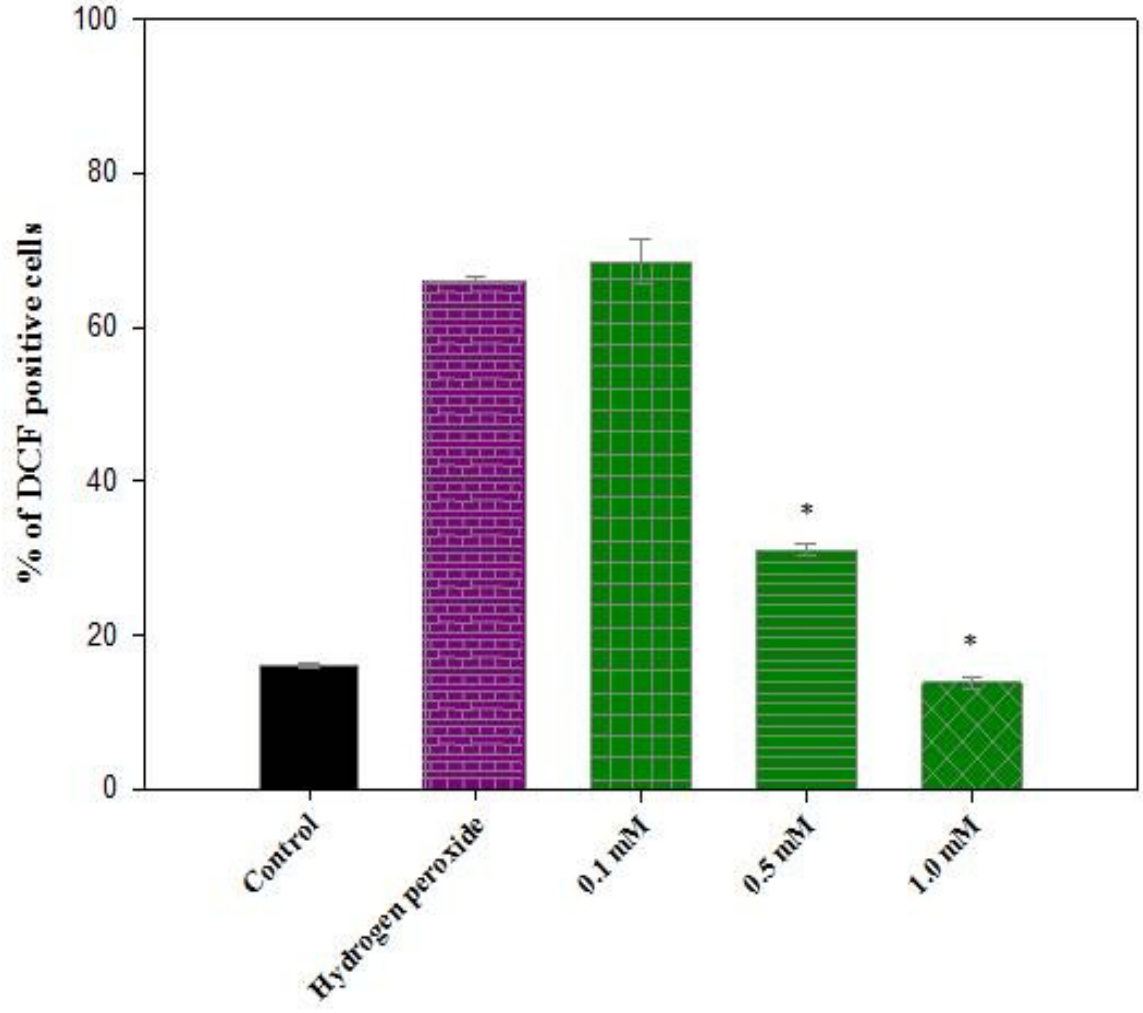

Figure 36. Effect of (+)-catechin on H_2O_2-induced reactive oxygen species formation in NG108-15 cells. DCF-DA fluorescent probe was introduced to detect the intracellular reactive oxygen species level. Cells were pretreated with (+)-catechin followed by H_2O_2-induced oxidative damage. Asterisk (*) represented significantly different value from H_2O_2 treated group ($P<0.01$). Data shown are mean ± SE of at least two independent experiments with minimum three replicates each.

4.5.1.2 (+)-Catechin alleviated externalization of phosphatidylserine

Low level of oxidative stress causes apoptosis wheareas higher level of oxidative stress triggers the occurrence of necrosis (Dypbukt et al., 1994). Therefore, we checked the plasma membrane integrity of the phosphatidylserine externalization as one of the early apoptosis hallmark event in NG108-15 cells. Results revealed that untreated control group showed the total percentage annexin V positive (early and late apoptotic) population of 5.10 $\pm$ 0.20, via fluorescent activated cell sorting (FACS) analysis. After 10 h exposure to H_2O_2, the percentage of population in early and late apoptosis increased to 62.88 $\pm$ 0.07 (Figure 37a). Nevertheless, 2 h pretreatment with 0.1 mM, 0.5 mM, and 1.0 mM (+)-catechin prior to H_2O_2 exposure reduced dose-dependently the total annexin V population to 30.25 $\pm$ 0.29 %, 18.89 $\pm$ 0.37 %, and 14.45 $\pm$ 0.26 %, respectively as shown in Figure 37b. (+)-Catechin significantly ($P<0.01$) reversed the H_2O_2-induced externalization of phosphatidylserine effects, representing its potential neuroprotective role in preventing apoptosis challenged by H_2O_2.

a)

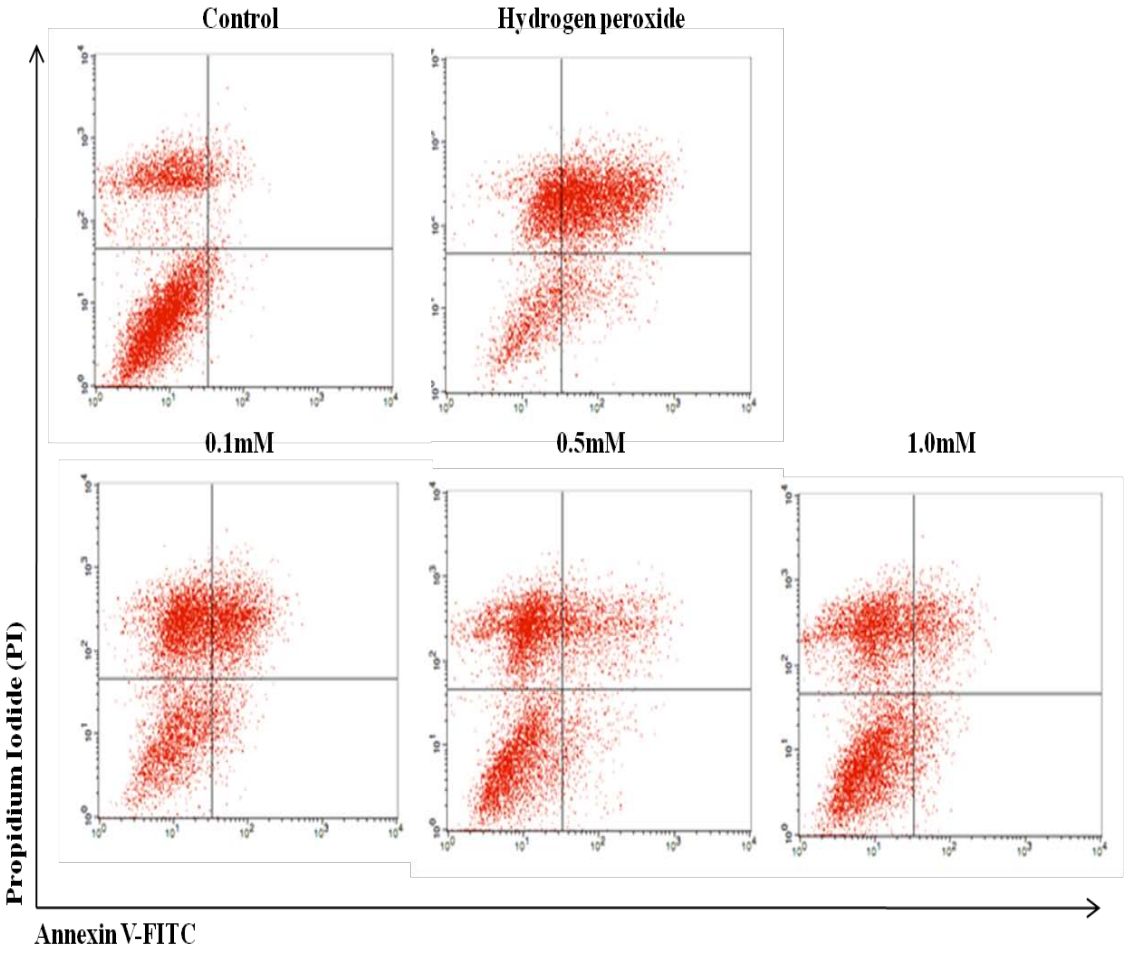
Control
Hydrogen peroxide
0.1mM
0.5mM
1.0mM
Propidium Iodide (PI)
Annexin V-FITC

b)

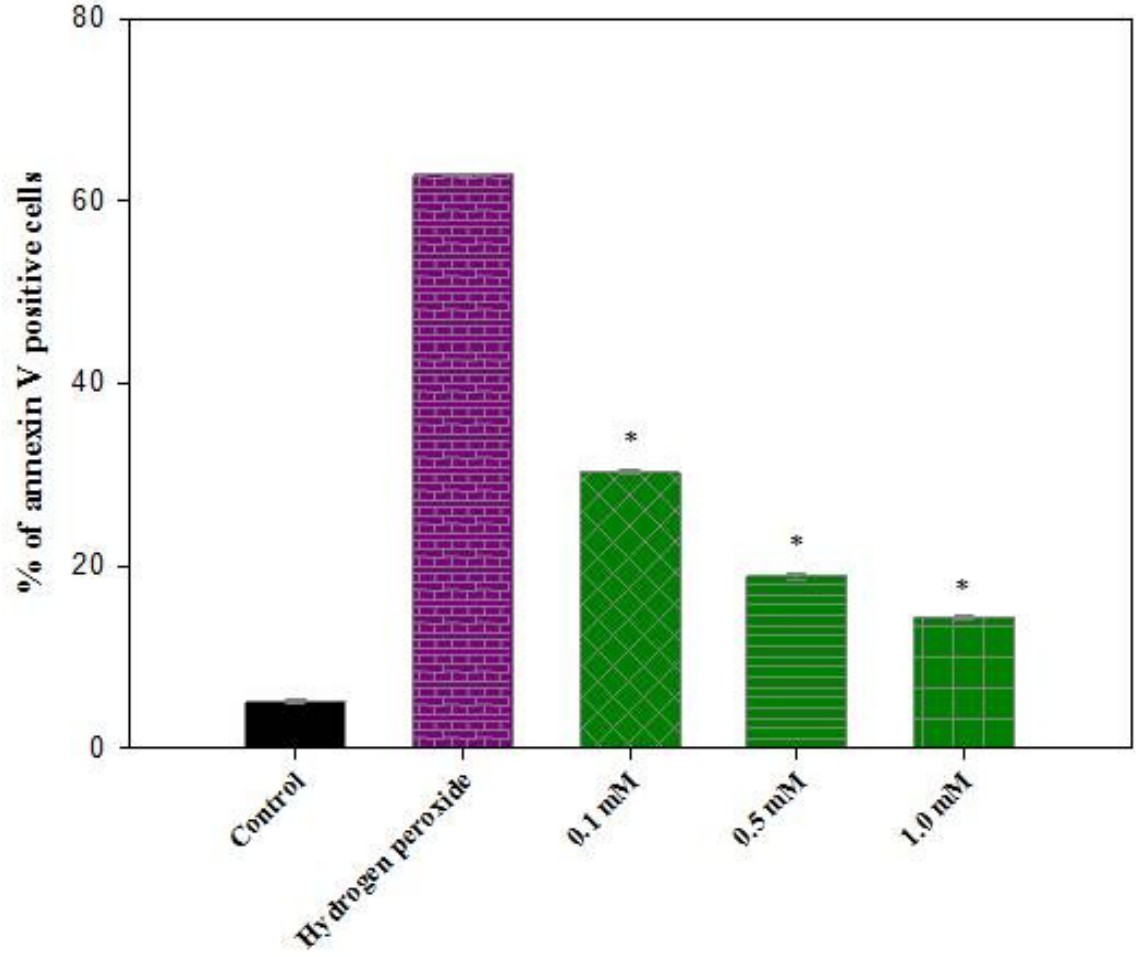

Figure 37. Effect of (+)-catechin on the phosphatidylserine externalization in NG108-15 cells. Dual staining of annexin V/PI was employed in the investigation of phosphatidylserine externalization. Cells were undergoing 2 h pretreatment with (+)-catechin and subsequently 10 h H_2O_2-induced oxidative damage. a) Flow cytometric fluorescence patterns of annexin V/PI dual labeling. b) Percentage of annexin V positive cells upon 2 h pretreatment with (+)-catechin. Asterisk (*) represented significantly different value from H_2O_2 treated group ($P<0.01$). Data shown are mean ± SE of at least two independent experiments with minimum three replicates each.

4.5.1.3 (+)-Catechin attenuated dissipation of mitochondrial membrane potential

Other than the externalization of phosphatidylserine, dissipation of mitochondrial membrane potential has also been demonstrated to be one of the early apoptosis hallmarks in various studies (Zamzami et al, 1995). JC-1 probe was applied to check the disruption of mitochondrial membrane potential in NG108-15 cells. Results showed that upon the oxidative damage induction of H_2O_2, there was a fluorescence signal shift from the upper right quadrant to the lower right quadrant resulting in the H_2O_2 treated cells having lower red fluorescence signal than the untreated control cells, showing the dissipation of mitochondrial membrane potential. Nevertheless, this observation was attenuated dose-dependently by 2 h pretreatment with (+)-catechin as shown in Figure 38a. Pretreatment with 1.0 mM (+)-catechin significantly ($P<0.01$) opposed the effect of H_2O_2-induced depolarization of mitochondrial membrane potential as shown by JC-1 fluorescence ratio (Figure 38b).

a)

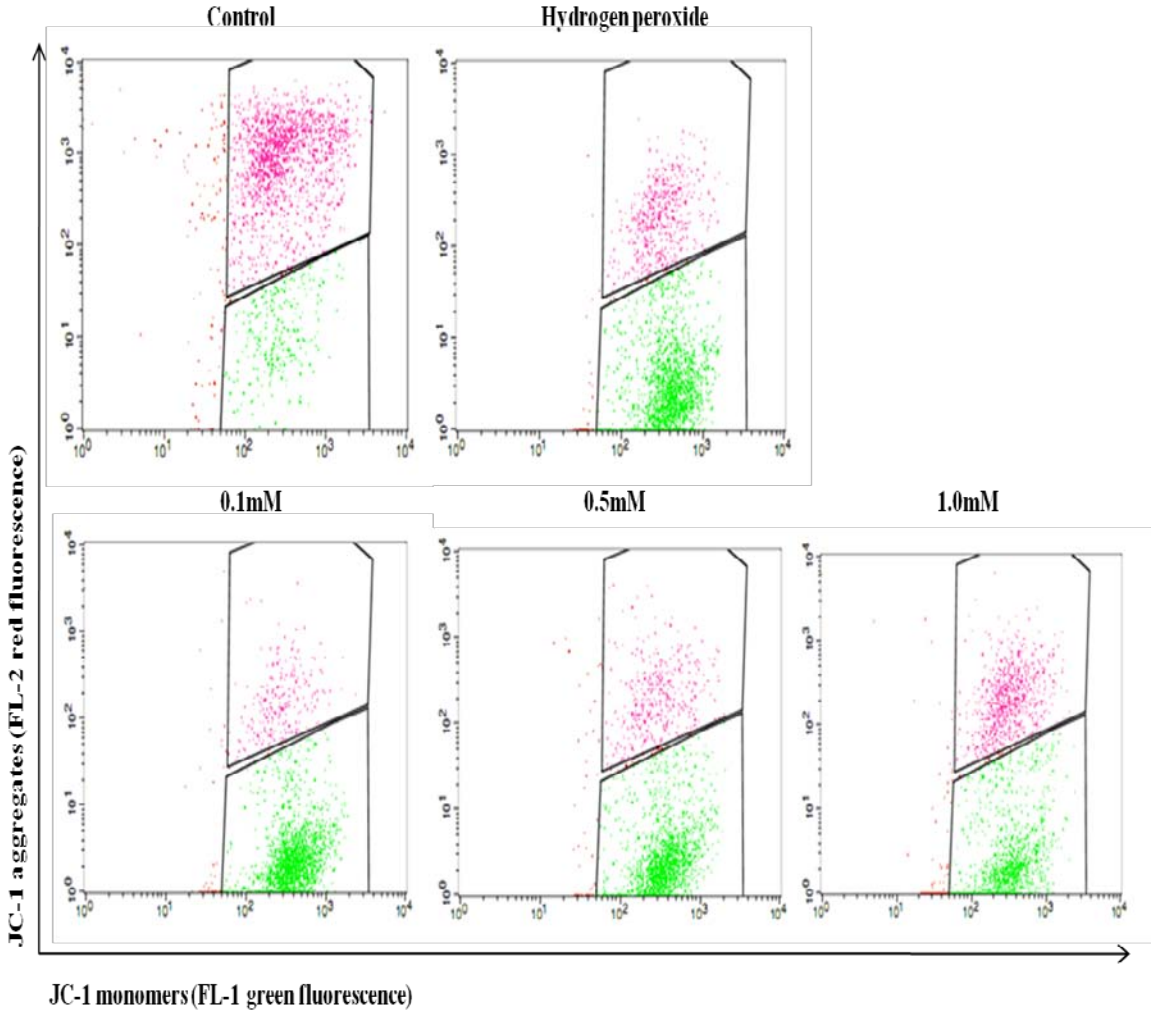
Control
Hydrogen peroxide
0.1mM
0.5mM
1.0mM
JC-1 aggregates (FL-2 red fluorescence)
JC-1 monomers (FL-1 green fluorescence)

b)

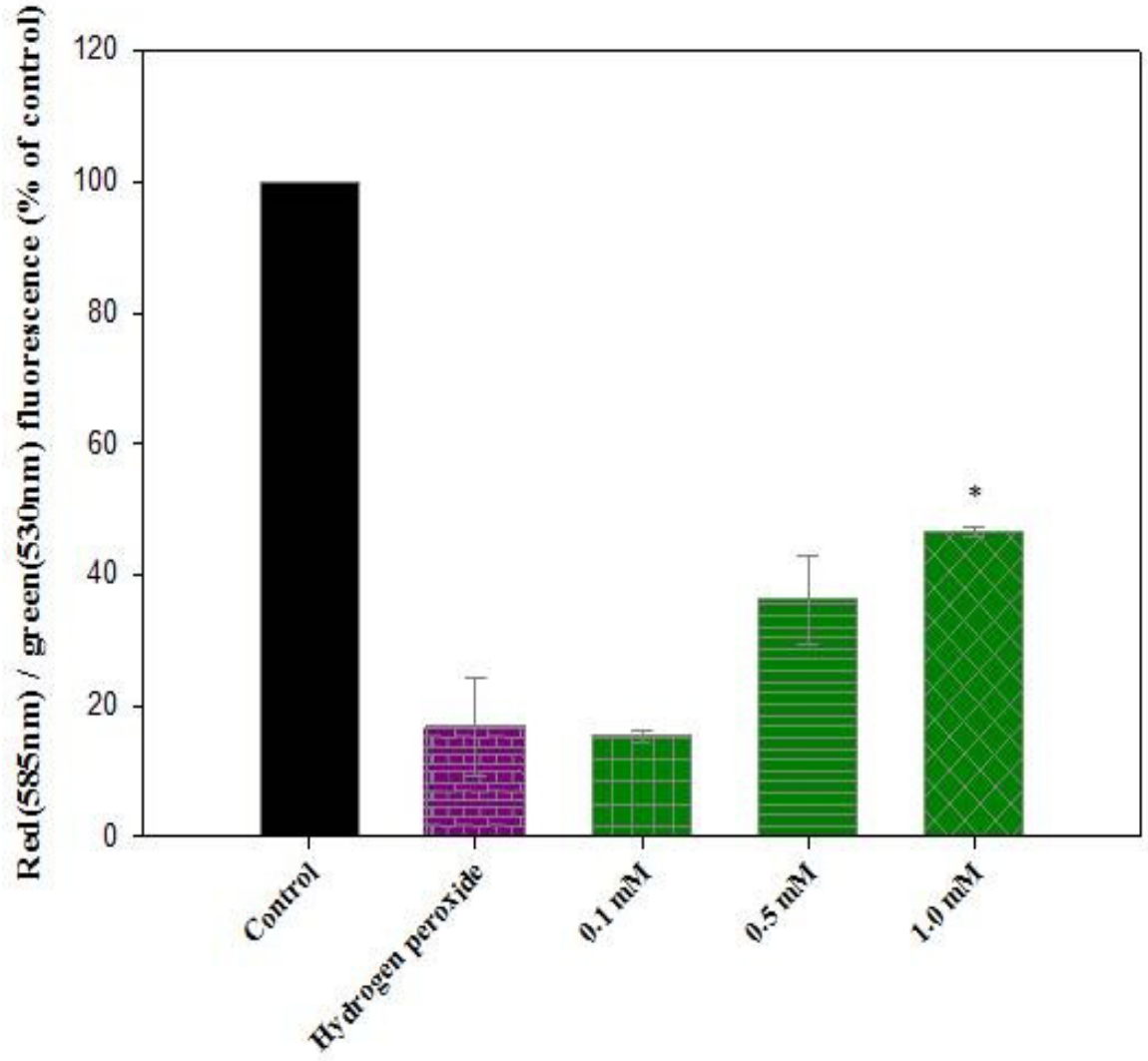

Figure 38. Effect of (+)-catechin on mitochondrial membrane potential in NG108-15 cells. Cells were pretreated with (+)-catechin followed by H_2O_2-induced oxidative damage. Upon desired treatment, cells were stained with JC-1 probe and analyzed via flow cytometry. a) Flow cytometric fluorescence patterns of JC-1 staining. b) Fluorescence ratio of red (585nm)/green (530nm), expressed as percentage of control, indicated the ratio of high/low mitochondrial membrane potential. Asterisk (*) represented significantly different value from H_2O_2 treated group ($P<0.01$). Data shown are mean ± SE of at least two independent experiments with minimum three replicates each.

4.5.1.4 (+)-Catechin blocked accumulation of subG$_1$-cells

We further investigated the cell cycle progression to check the DNA degradation as revealed in sub-G_1 peak in cell cycle DNA histogram. PI fluorescent dye was applied to identify dead cells in a population. We found that in cells treated with 10 h H_2O_2 alone, the sub-G_1 population elevated to 40.26 $\pm$ 0.34 % compared with 1.83 $\pm$ 0.12 % of untreated control population, which was accompanied by a decrease in G_2/M population in H_2O_2 treated group compared with untreated control group (Figure 39a). However, 2 h pretreatment with 1.0 mM (+)-catechin significantly ($P<0.01$) opposed the H_2O_2-induced increase in sub-G_1 peak effects by giving 18.60 $\pm$ 0.55 % in sub-G_1 population, signifying the neuroprotective potential of (+)-catechin by halting the cell cycle arrest at sub-G_1 phase, as shown in cell cycle DNA histogram (Figure 39a).

4.5.2 Effect of (+)-catechin on intracellular antioxidant enzymes

4.5.2.1 (+)-Catechin improved SOD enzyme activity

SOD catalyzes the dismutation of O_2^- to form H_2O_2, which in turn is decomposed to H_2O and oxygen by GPx. These enzymes work together to protect the cells from oxidative stress. 10 h induction of H_2O_2 showed a substantial decrease in SOD enzyme activity, revealing the H_2O_2-induced oxidative damage in the present model (Figure 40). The H_2O_2-induced reduction of SOD activity prompted the cells to be more accessible to oxidative damage. However, SOD enzyme activity was improved significantly ($P<0.01$) in cells pretreated with (+)-catechin (Table 10), presenting the neuroprotection role of (+)-catechin in attenuating H_2O_2-induced oxidative damage.

a)

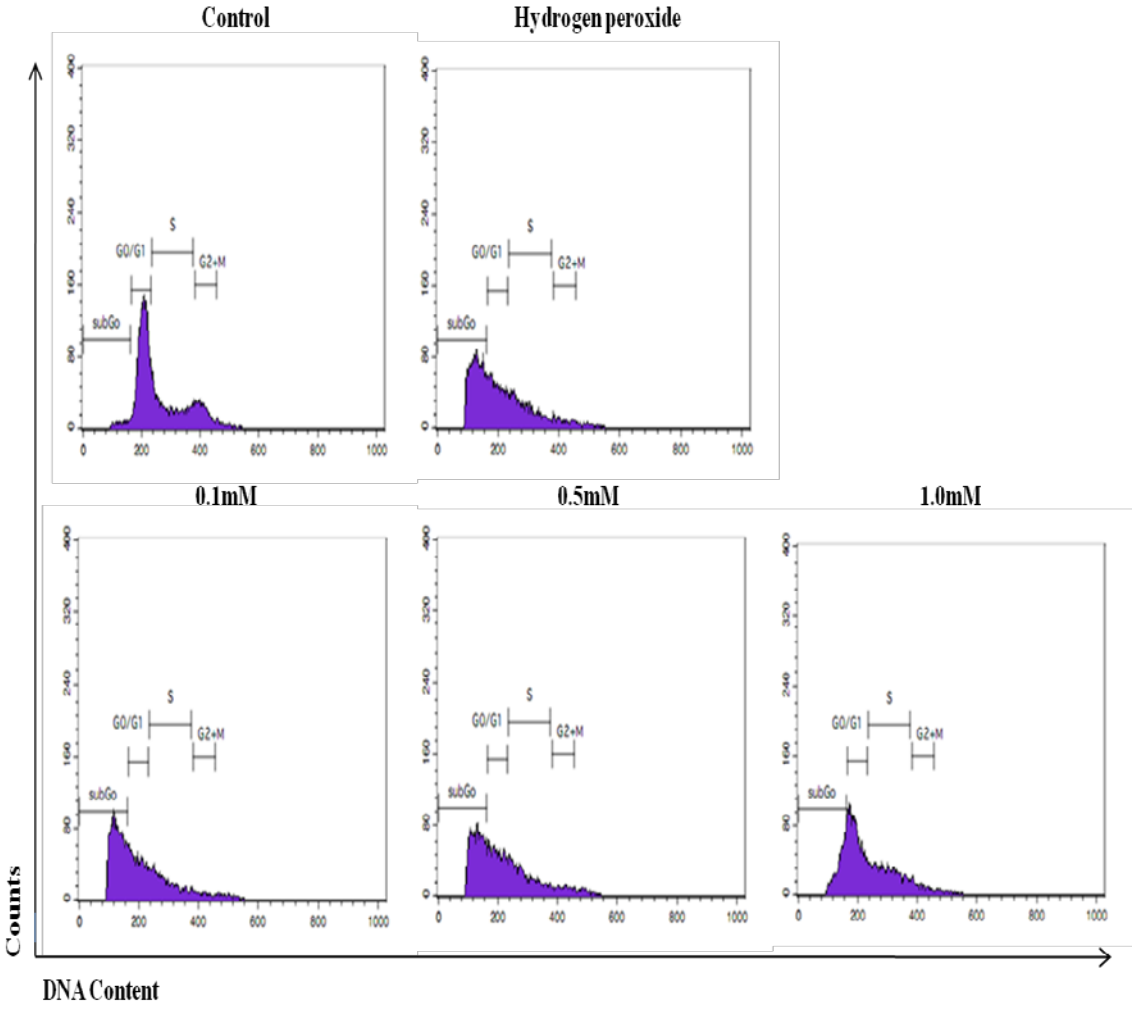
Control
Hydrogen peroxide
0.1mM
0.5mM
1.0mM
Counts
DNA Content
subGo
G0/G1
S
G2+M

b)

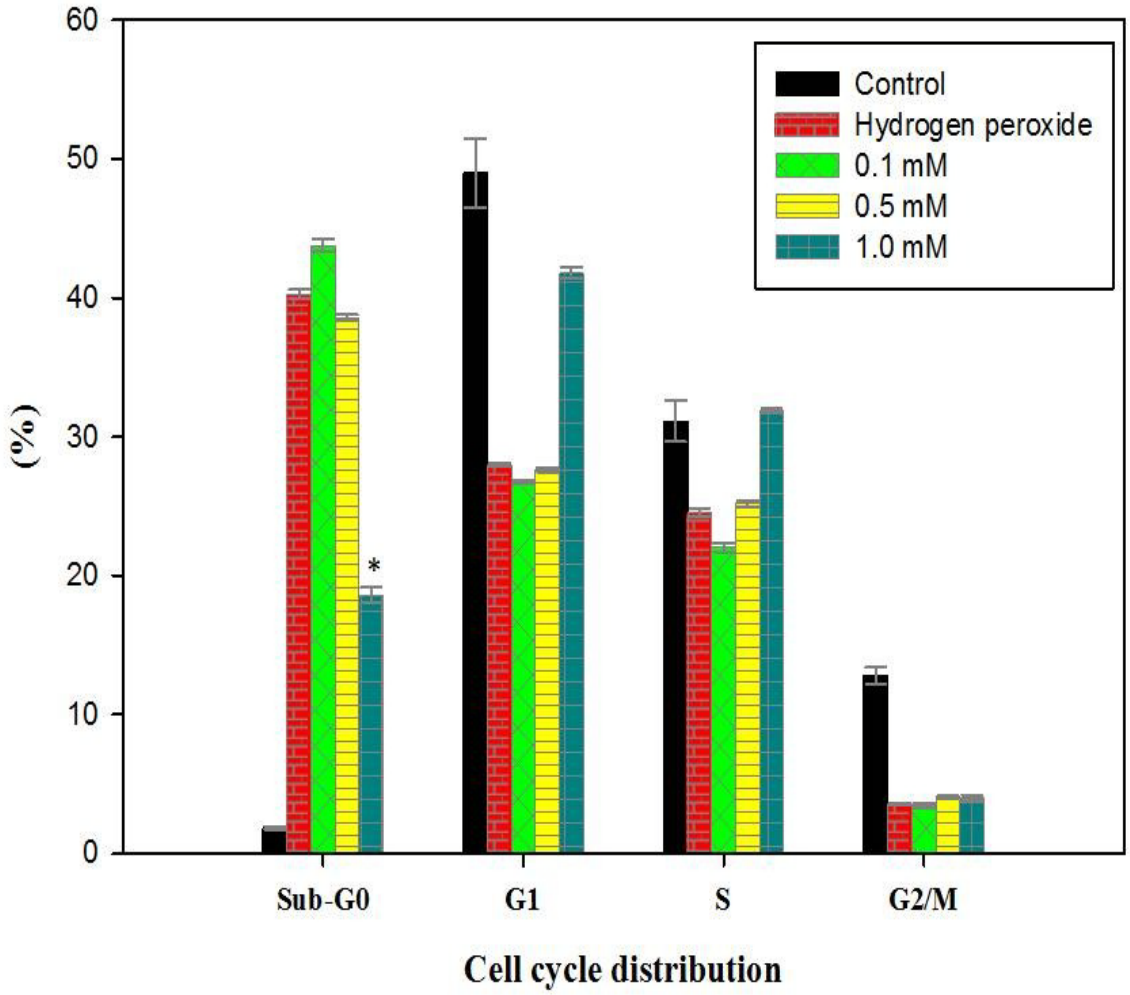

Figure 39. Effect of (+)-catechin on cell cycle distribution in NG108-15 cells. Cells were pretreated with (+)-catechin followed by H_2O_2-induced oxidative damage. Upon treatment, cells were stained with PI solution and analyzed using flow cytometry. a) DNA histograms acquired from PI staining. b) Cell cycle distribution by (+)-catechin against H_2O_2 insult in NG108-15 cells. Asterisk (*) represented significantly different value from H_2O_2 treated group ($P<0.01$). Data shown are mean ± SE of at least two independent experiments with minimum three replicates each.

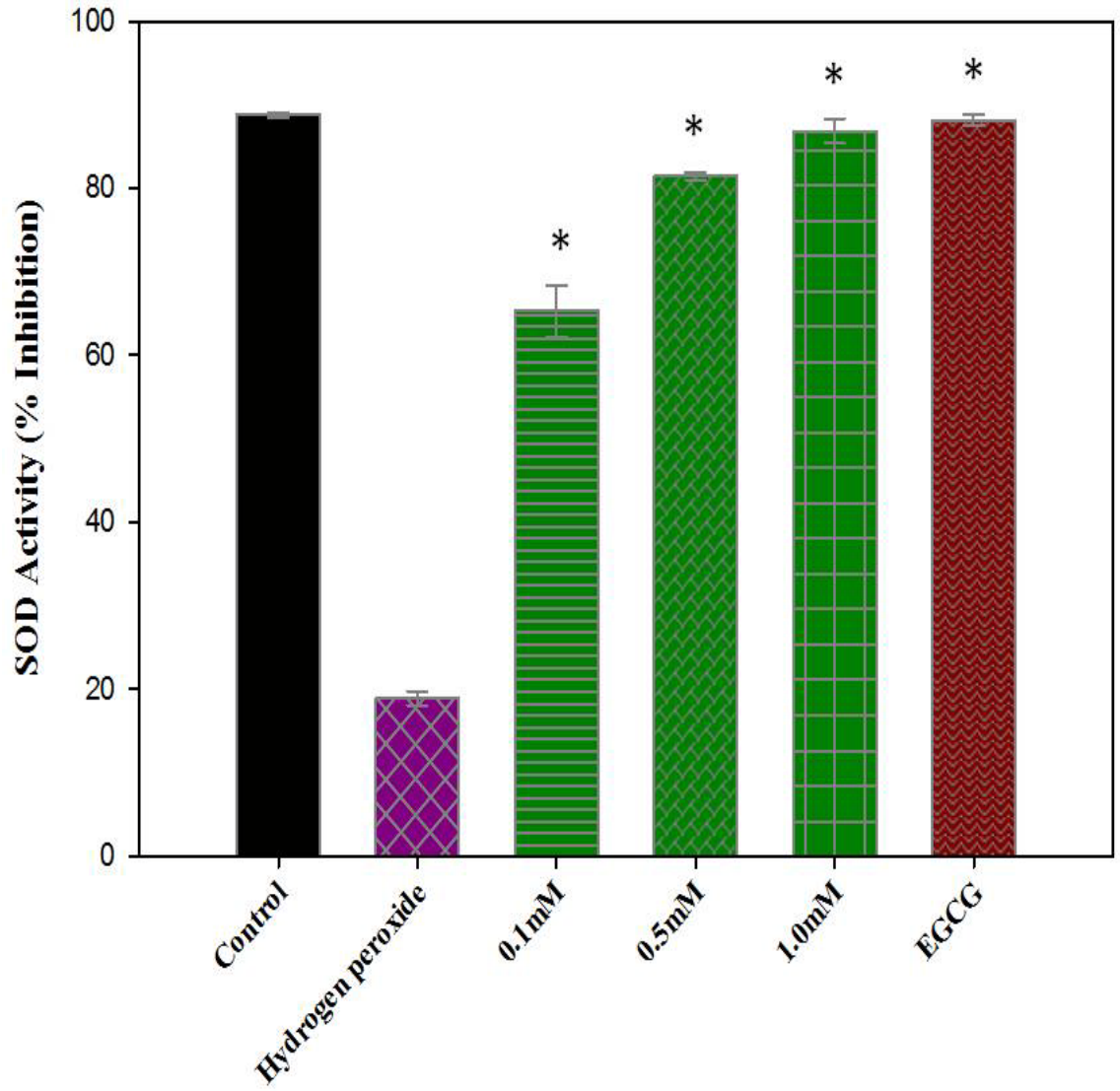

Figure 40. Effect of (+)-catechin on SOD activity in NG108-15 cells. Cells were pretreated with (+)-catechin for 2 h and subsequently by H_2O_2-induced oxidative damage for 10 h. Upon desired treatment, cells were harvested, rinsed, and centrifuged to obtain the supernatant for SOD activity assay. EGCG was used as positive control in the present experiment. Asterisk (*) represented significantly different value from H_2O_2 treated group ($P<0.01$). Data shown are mean ± SE of at least two independent experiments with minimum three replicates each.

4.5.2.2 (+)-Catechin increased GPx enzyme activity

GPx catalyzes the reduction of H_2O_2 to H_2O and O_2 at the expense of GSH. In another word, the increase in GPx enzyme activity advocates the more GSSG is being reduced to GSH. We found that the GPx enzyme activity was greatly reduced upon the 10 h H_2O_2-induced oxidative damage as compared to untreated control group (Figure 41). Conversely, GPx activity was significantly ($P<0.01$) improved in a dose-dependent manner by 2 h pretreatment with (+)-catechin (Table 10), indicating the elevation in GSH recycling by (+)-catechin-induced GPx enzyme activity.

4.5.3 Effect of (+)-catechin on gene expression analysis

4.5.3.1 (+)-Catechin decreased the expression of Bax, increased the expression of Bcl-2, and reduced the ratio of Bax/Bcl-2

Mitochondria are primary cellular source of reactive oxygen species as they generate huge numbers of oxidation-reduction reactions and consume massive amounts of oxygen. Thus, mitochondria are critical to brain cell in response to oxidative stress, with multiple pivotal roles such as ATP production, free radicals generation, and apoptosis regulation. Bcl-2 family members, namely Bcl-2 and Bax play an essential role in the interference of mitochondrial membrane potential and the effect of (+)-catechin on mitochondrial membrane potential have been demonstrated earlier, we therefore analyzed the gene expression of Bax and Bcl-2 in regards to the present neuroprotective activity exerted by (+)-catechin. Our results showed that H_2O_2 increased Bax and decreased Bcl-2 expression in H_2O_2 treated cells whereas a significant ($P <0.01$) reversed effect was observed in (+)-catechin pretreated cells (Figure 42a; Figure 42b). The decrease in Bax and increase in Bcl-2 expression significantly ($P <0.01$) decline the

Bax/Bcl-2 ratio (Figure 42c), indicating neuroprotective role afforded by (+)-catechin in NG108-15 cells.

4.5.3.2 (+)-Catechin attenuated the induction of chemokine CCL21

Neuronal chemokine CCL21, a microglia-activating chemokine, is exclusively found in endangered neurons in brain region which plays a vital role in neuron-microglia communication. Since chemokine CCL21 has been demonstrated to be overexpressed in endangered neruons (Biber et al., 2001) and (+)-catechin is known to exhibit potent antioxidative and neuroprotective effects, therefore, we evaluated the role of (+)-catechin on chemokine CCL21 expression against H_2O_2-induced oxidative damage insult. Q-PCR result revealed a substantial increase in the expression of chemokine CCL21 in H_2O_2 treated cells as compared to untreated control cells. Reversely, 2 h pretreatment with (+)-catechin significantly ($P < 0.01$) decreased the expression of chemokine CCL21 (Figure 43), showing a novel (+)-catechin-mediated neuroprotection via the regulation of chemokine CCL21 against oxidative damage induced by H_2O_2.

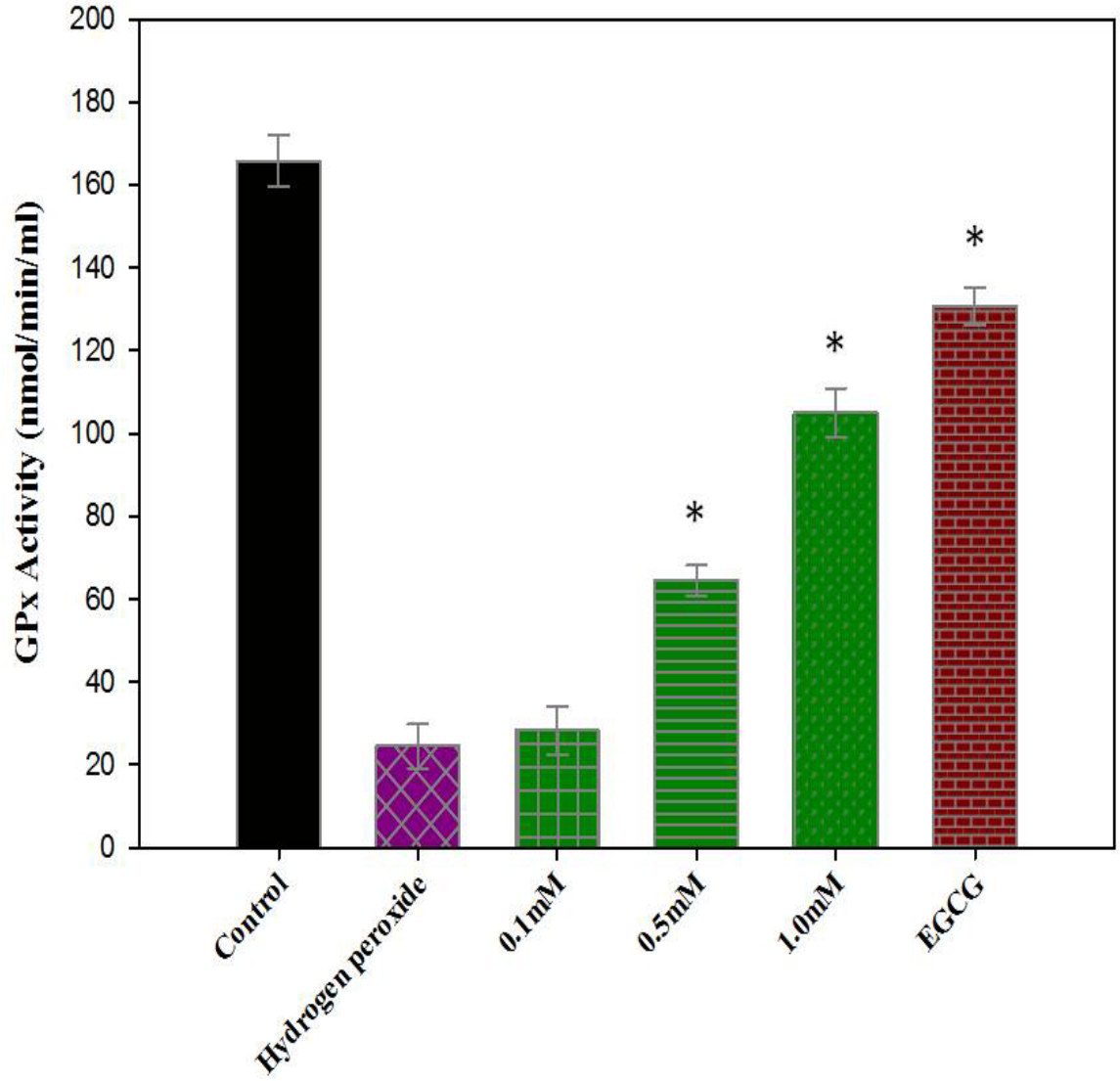

Figure 41. Effect of (+)-catechin on GPx activity in NG108-15 cells. Cells were pretreated for 2 h with (+)-catechin and subsequently to induce oxidative damage for 10 h by H_2O_2. Upon desired treatment, cells were harvested, rinsed, and centrifuged to obtain the supernatant for GPx activity assay. EGCG was used as positive control in the present experiment. Asterisk (*) represented significantly different value from H_2O_2 treated group ($P<0.01$). Data shown are mean ± SE of at least two independent experiments with minimum three replicates each.

Table 10. Alterations in the activities of SOD and GPx by (+)-catechin[a] and EGCG[b] following H_2O_2 exposure in NG108-15[c] cells

Group	SOD Activity (% Inihibtion)	GPx Activity (nmol/min/ml)
Control	88.72 ± 0.20	165.68 ± 6.20
H_2O_2	18.85 ± 0.85	24.52 ± 5.35
(+)-Catechin	86.84 ± 1.47 *	104.99 ± 5.93 *
EGCG	88.14 ± 0.58 *	130.72 ± 4.59 *

[a] (+)-Catechin: The most neuroprotective compound isolated from LPAF.

[b] EGCG as standard positive control.

[c] NG108-15 cells were pretreated with (+)-catechin (0.10 mM-1.00 mM) for 2 h and exposed to 2.0 mM H_2O_2 for subsequent10 h.

Values shown are means ± SE of at least two independent experiments with minimum three replicates each. Results differ significantly from H_2O_2 treated group compared with (+)-catechin pretreated group: * $p < 0.01$.

a)

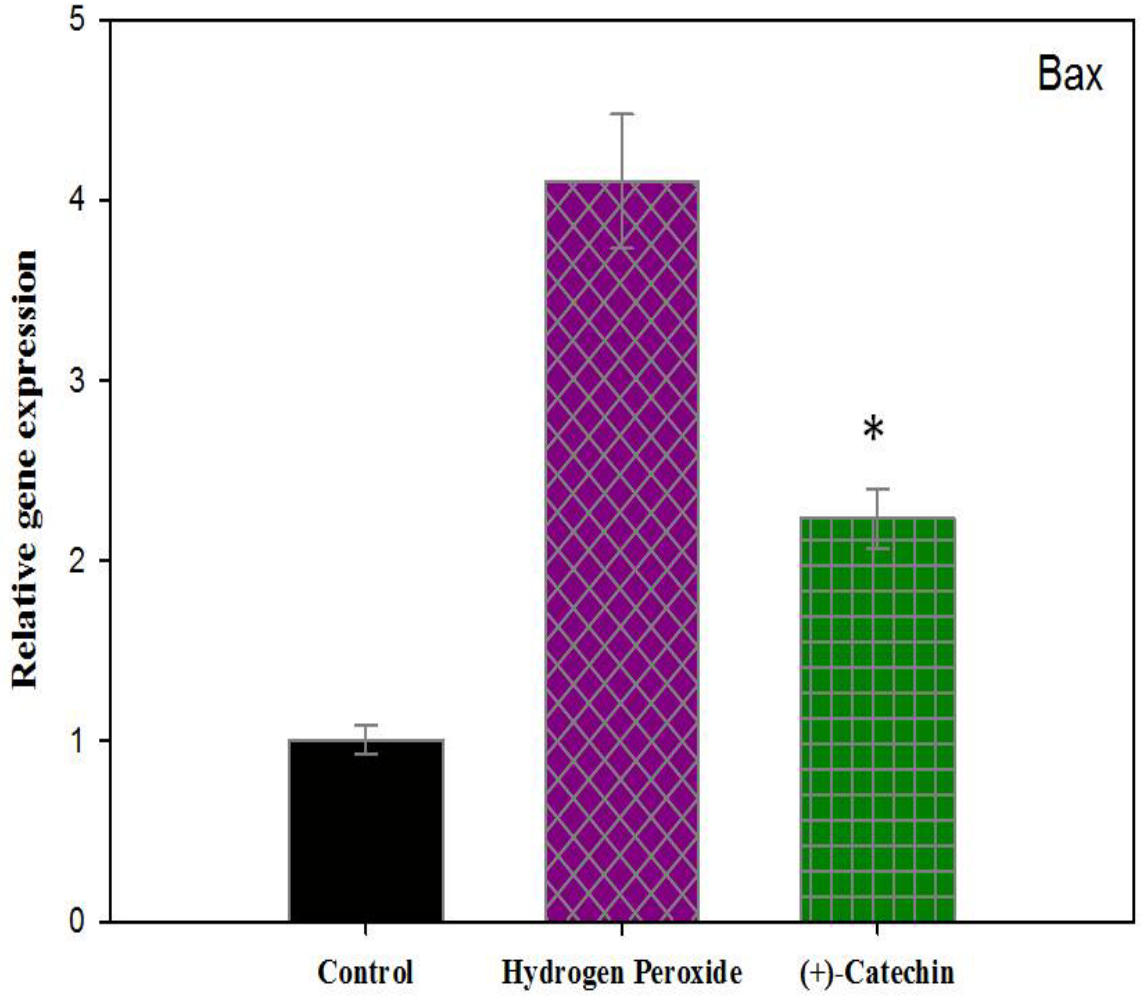
Bax
Relative gene expression
5
4
3
2
1
0
*
Control
Hydrogen Peroxide
(+)-Catechin

b)

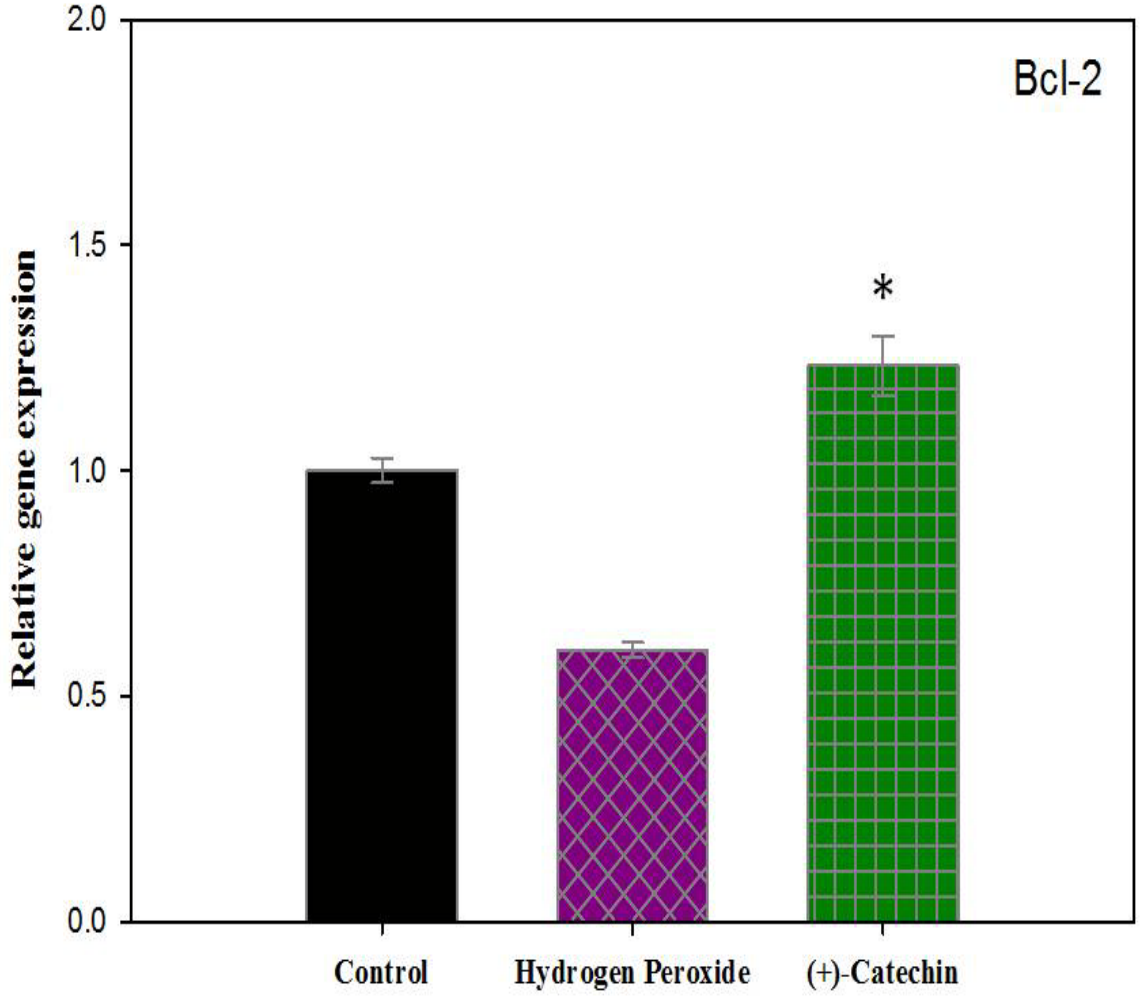
Bcl-2
Relative gene expression
2.0
1.5
1.0
0.5
0.0
*
Control
Hydrogen Peroxide
(+)-Catechin

c)

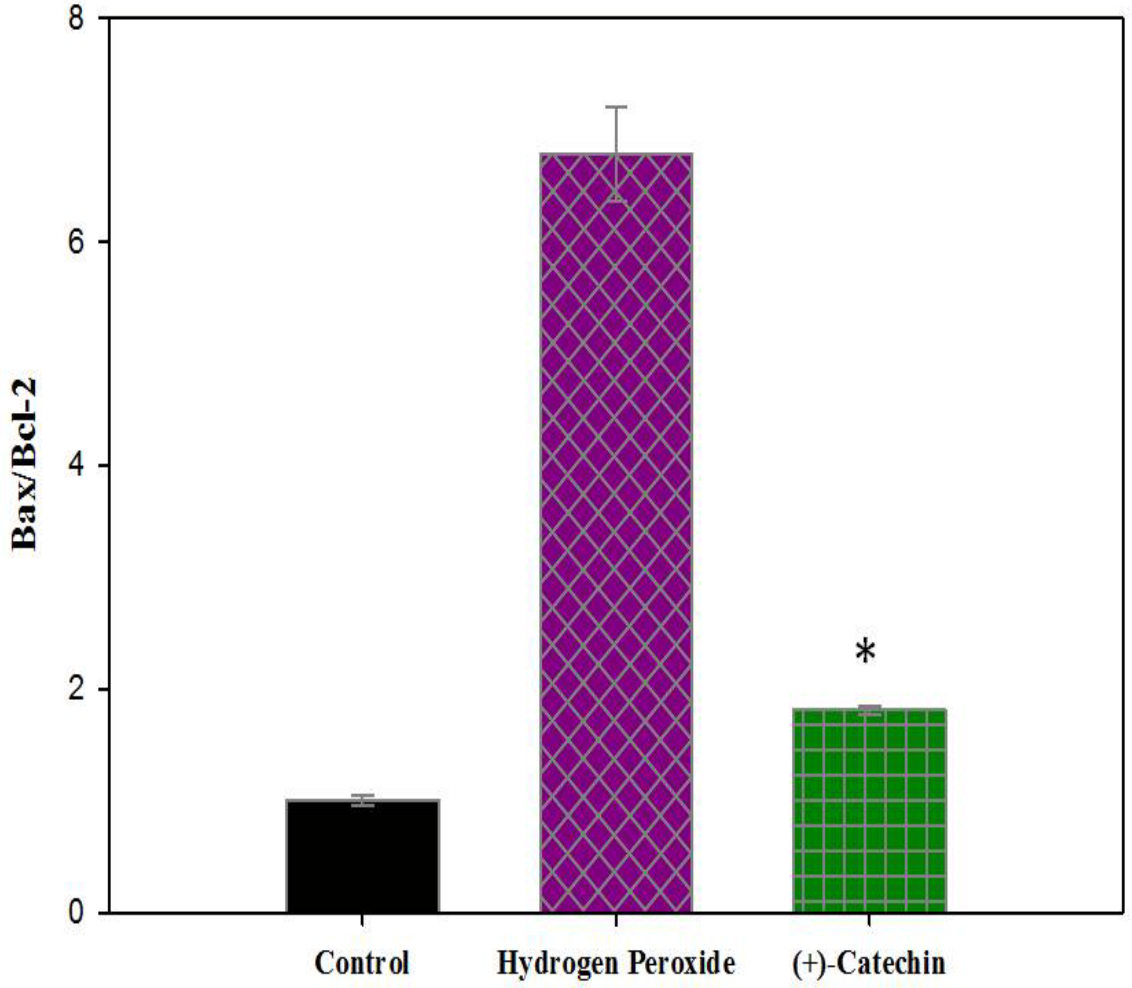

Figure 42. Effect of (+)-catechin on the Bcl-2 and Bax gene expression levels in NG108-15 cells. Upon treatment, cells were harvested, rinsed, and pelleted. Total RNA was extracted subsequently and subjected to one-step SYBR Green relative Q-PCR analysis. a) Relative gene expression level of Bax which was normalized against HMBS expression by $2^{-\Delta\Delta CT}$ formulation. b) Relative gene expression level of Bcl-2 which was normalized against HMBS expression by $2^{-\Delta\Delta CT}$ formulation. c) Bar chart presentation of Bax/Bcl-2 ratio analyzed from Q-PCR. Asterisk (*) represented significantly different value from H_2O_2 treated group ($P<0.01$). Data shown are mean ± SE of at least two independent experiments with minimum three replicates each.

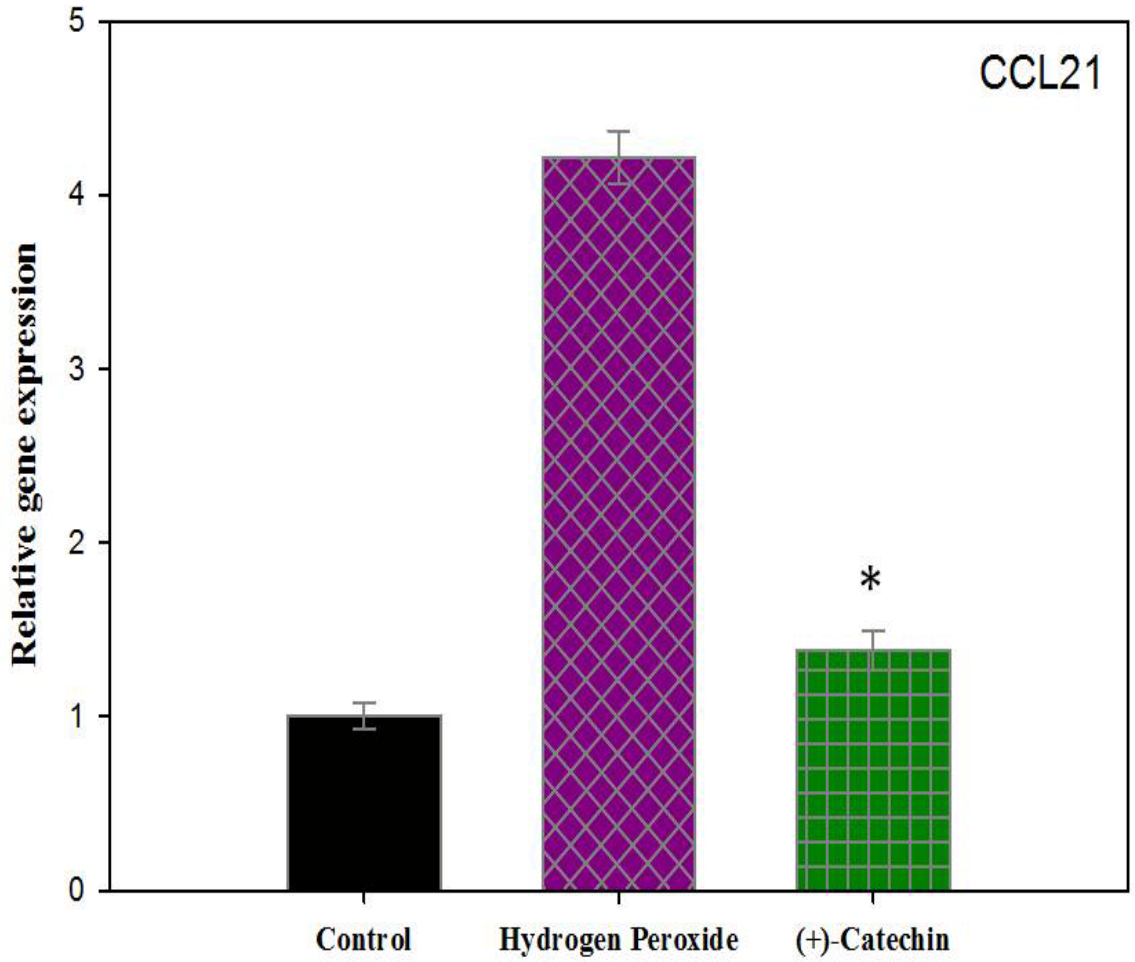

Figure 43. Effect of (+)-catechin on chemokine CCL21 gene expression level in NG108-15 cells. Cells were harvested, rinsed, and pellected after desired treatment. Total RNA was isolated subsequently and subjected to one-step SYBR Green relative Q-PCR analysis. Bar chart showed relative gene expression level of chemokine CCL21 which was normalized against HMBS expression by $2^{-\Delta\Delta CT}$ formulation. Asterisk (*) represented signficantly di fferent value from H_2O_2 treated group ($P<0.01$). Data shown are mean ± SE of at least two independent experiments with minimum three replicates each.

4.5.4 Effect of (+)-catechin on protein expression level

4.5.4.1 (+)-Catechin downregulated Bax expression and upregulated Bcl-2 expression

Next, we employed immunofluorescence staining using flow cytometric approach to verify the Bcl-2 and Bax expression in individual cells. As compared with H_2O_2 treated cells, (+)-catechin pretreated cells profiles shifted to the left in Bax histogram (Figure 44a) whereas (+)-catechin pretreated cells profiles shifted to the right in Bcl-2 histogram (Figure 44b). These immunofluorescence associated-results were in agreement with the gene expression outcomes obtained from Q-PCR, showing that Bax was downregulated and Bcl-2 was upregulated upon the 2 h pretreatment with (+)-catechin following H_2O_2-induced oxidative damage insult.

4.5.4.2 (+)-Catechin downregulated the expression of chemokine CCL21

Subsequently, we further analyzed the expression of chemokine CCL21 in individual cell by flow cytometric immunofluorescence staining detection. We observed a shift to the left in (+)-catechin pretreated cells profiles in CCL21 histogram as compared with H_2O_2-treated cells (Figure 45) which was consistent with CCL21 gene expression result from Q-PCR. Respectively, these findings reflected the novel chemokine CCL21 mediated-neuroprotective pathway as demonstrated by (+)-catechin in the downregulation of chemokine CCL21 against H_2O_2-induced oxidative damage in NG108-15 cells.

a)

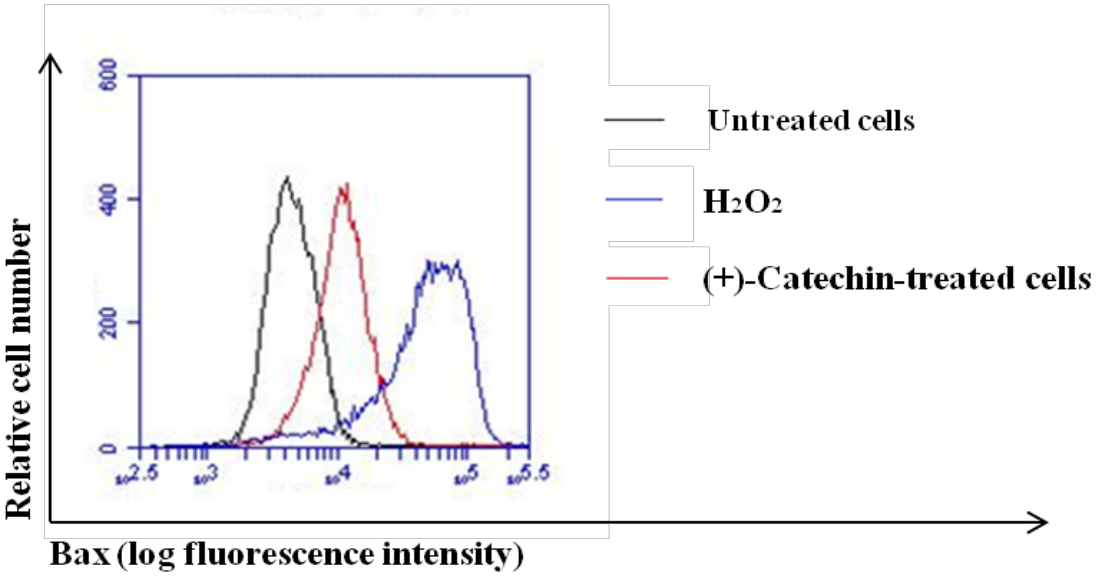

b)

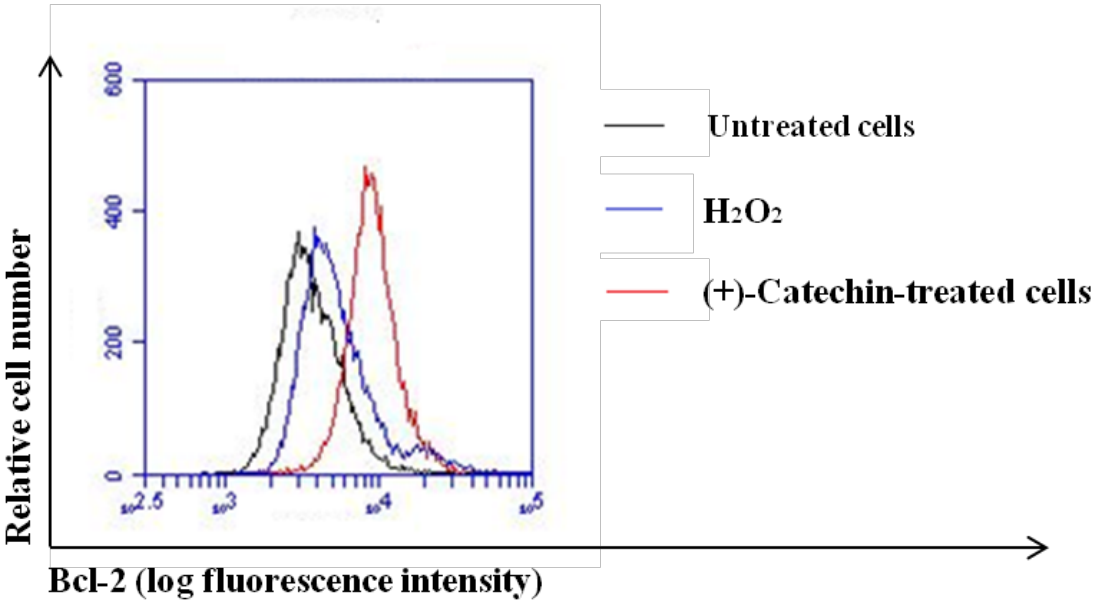

Figure 44. Effect of (+)-catechin on Bcl-2 and Bax protein expression in NG108-15 cells. Cells were washed, fixed and permeabilized using intracellular flow cytometry system. Intracellular levels of Bcl-2 and Bax were subsequently stained directly and examined via flow cytometry. Representative overlay of histograms showing a) Bax and b) Bcl-2-associated immunofluorescence.

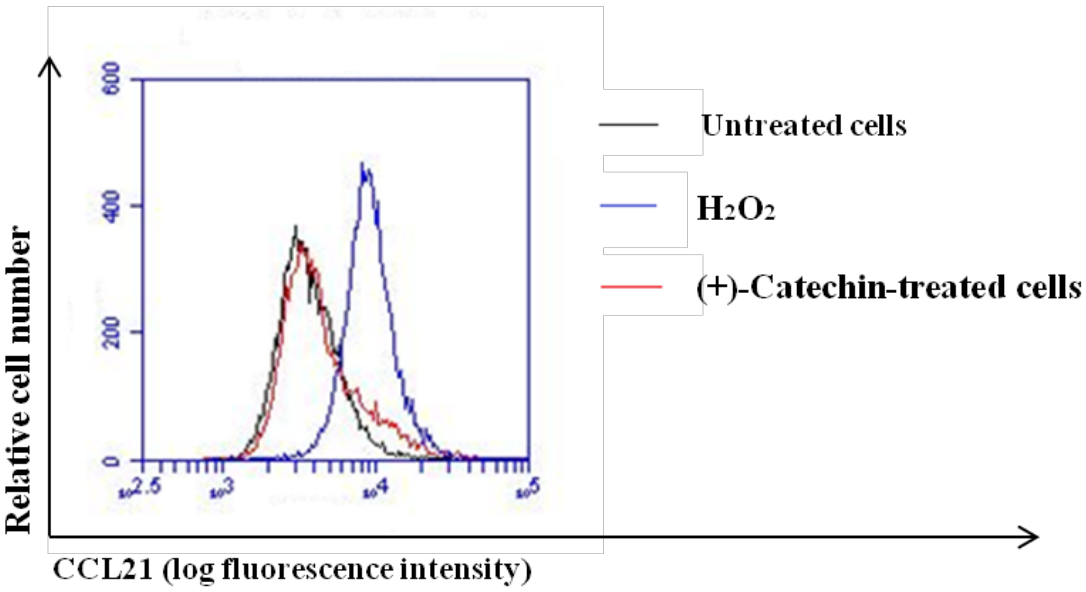

Figure 45. Effect of (+)-catechin on CCL21 protein expression in NG108-15 cells. Upon treatment, cells were washed, fixed and permeabilized using intracellular flow cytometry system. Lightning-Link™ fluorescein conjugation kit was employed in CCL21 direct conjugation staining and analyzed using flow cytometry. Representative overlay of histogram showing chemokine CCL21-associated immunofluorescence.

CHAPTER 5

DISCUSSION

NG108-15, a mouse neuroblastoma-rat glioma hybridoma cell line, has been utilized extensively as a neuronal model in electrophysiology and pharmacology research by possessing both neuronal and glial properties. Among a great variety of reactive oxygen species, H_2O_2 is known to be generated from nearly all sources of oxidative stress in biological condition. Due to its high membrane permeability, exogenous H_2O_2 causes oxidative stress by entering cellular membrane and leads to the generation of highly oxidizing, tissue-damaging radicals such as $OH^{\bullet}$, which is able to induce toxicity to the cellular system. Therefore, H_2O_2 was selected to induce oxidative damage in the present NG108-15 neuroprotection model.

L. parasiticus, a traditional medicinal herb which is known as a supplement for brain diseases was investigated for its antioxidative and neuroprotective ability. DPPH free radical scavenging assay was carried out initially. DPPH, a free radical with an unpaired electron, has been used broadly for the elucidation of antioxidant activity. Due to the unpaired electron, DPPH in ethanol gives a deep color as it absorbs strongly at 517 nm. After the unpaired electron paired off, decolorization occurred as the absorption vanishes, and this is proportional to the number of electrons taken up (Blois, 1958). When DPPH is being scavenged by an antioxidant, it accepts an electron from the antioxidant and becomes a stable yellow substance known as 2,2-diphenyl-1,2-picryhydrazyl. The extent of this reaction depends on the hydrogen or electron donating capability of the antioxidant. In the present study, LPAF showed the highest DPPH radical scavenging activity as shown in Table 4. Even at a low concentration of 16.82 $\pm$ 0.27 μg/mL, LPAF exhibited 50 % antioxidant activity. LPEE possessed the second

highest DPPH radical scavenging activity, followed by LPEAF with the IC_{50} value of 20.51 $\pm$ 0.18 μg/mL and 55.66 $\pm$ 0.55 μg/mL, respectively (Figure 22).

In reducing power assay, the presence of antioxidant reduces ferricyanide ions to ferrocyanide ions, which further react with ferric chloride to form ferric ferrocyanide. This Fe^{3+}-Fe^{2+} transformation gives rise to the Prussian blue complex that absorbs light at 700 nm. The intensity of the colored complex increased with the electron or hydrogen donating ability from the antioxidant. Figure 23 reveals the absorbance of *L. parasiticus* extract and fractions (LPEE, LPEAF, and LPAF) at various concentrations. LPAF exhibited the strongest DPPH free radical scavenging activity as well as reducing power activity compared to LPEE and LPEAF. Hence, LPAF might have the ability to reduce both free radicals and ferric ions, which may due to the main constituents consisting of phenolic acids, polyphenols which are primarily flavonoids and flavonoid glycosides. It has been reported that flavonoids and phenolic acids are the sources of antioxidants in plants (Cook and Samman, 1996). However, LPEE which showed a much lower antioxidant activities may due to the composition of chlorophylls, chlorophyll derivatives, and luteins. LPAF exhibited the strongest reducing power compared to the other fractions but its reducing power was lower than BHT, the standard positive control. Nevertheless, these data indicate that LPAF had a higher potential to act as a reductant or antioxidant.

Lipid peroxidation inhibitory assay was performed subsequently to determine the amount of malondialdehyde formation, in which malondialdehyde is a breakdown product of lipid peroxides (Jentzsch et al., 1996). In the presence of acid and heat, malondialdehyde reacts with TBA to produce a red pigment which has a peak wavelength at 530 nm (Janero, 1990). Since the reaction is not specific to malonaldehyde and therefore results are reported as TBA reactive substances. The present TBA reactive substances assay utilized egg yolk as lipid substrate. It is known

that linoleic acid and linolenic acid are two of the polyunsaturated fatty acids present in this substrate. Upon reaction with oxygen, these fatty acids produce malonaldehyde which reacts with TBA producing a pink color. Results indicated that LPAF was again possessed the highest inhibitory effects towards lipid peroxidation by exhibiting the lowest IC_{50} value of 1.05 $\pm$ 0.04 mg/mL. On the other hand, LPEE also inhibited lipid peroxidation as indicated by low color formation with TBA. However, LPEAF yielded the highest IC_{50} value, showing the least inhibition towards the oxidative degradation of lipids among LPAF and LPEE (Figure 24).

Phenolic compounds are chemical compounds that comprise hydroxyl group attached to an aromatic hydrocarbon group. Among the natural antioxidants isolated from various plants, phenolic compounds are in the forefront due to their wide distribution in the plant kingdom (Duan et al., 2006). There are many types of phenolic compounds found in plants, such as simple phenolics, flavonoids, anthocyanins, phenolic acids, and, hydroxycinnamic acid derivatives. Every phenolic compound possesses the structural requirements of free radical scavengers and serves as potent antioxidant in food (Duan et al., 2006). Folin-Ciocalteu's phenol reagent, a mixture of phosphotungstate and phosphomolybdate has been widely employed for the colorimetric assay of polyphenolic as well as phenolic antioxidants (Singleton et al., 1999). It reacts with phenolic compounds to generate chromogens which can be detected using spectrophotometer. Color development is caused by the transfer of electrons at basic pH to decrease the phosphomolybdate and phosphotungstate complexes and produce chromogens where the metals have lower valence. In this study, a comparison between LPEE, LPEAF, and LPAF for their total phenolic content was assayed at 100 μg/mL as shown in Table 4. LPAF possessed the highest total phenolic content by giving 56.51 $\pm$ 1.43 GAE/g_{DW}, followed by LPEE and LPEAF with 52.08 $\pm$ 1.76 GAE/g_{DW} and 18.82 $\pm$ 0.53 GAE/g_{DW}, respectively. Hence, the highest antioxidant

ability exhibited by LPAF may due to the phenolic compounds which were found to be present the most in LPAF.

It is well acknowledged that neurodegeneration such as in ischemic stroke, Alzheimer's disease and Parkinson's disease, is closely associated with neuronal damage which is mediated by free radicals-induced oxidative stress. The remarkable antioxidative effect of *L. parasiticus* has led to the investigation of its relevancy in neuroprotection. Neuroprotective effect of LPEE, LPEAF, and LPAF were assessed by MTT cell viability assay. MTT is a yellow color tetrazolium salt which can be converted into insoluble purple formazan via mitochondrial enzyme present solely in living cells, succinate dehydrogenase (Lee et al., 2004). Thus, the amount of purple formazan formed is directly proportional to the number of viable cells (Van de Loosdrecht et al., 1994). The decrease in cell viability is due to the conversion of H_2O_2 into $OH^{\bullet}$ through the Fenton reaction in cells. $OH^{\bullet}$, which in turn, damage the proteins, lipids and DNA of the cells, resulting in the cell damage followed by cell death. As determined by MTT assay, 10 h exposure of NG108-15 hybridoma cells to 2.0 mM H_2O_2 significantly ($P<0.01$) revealed oxidative damage (Figure 25). LPAF and LPEE showed significantly ($P<0.01$) ability to protect cell death induced by H_2O_2 with 78.00 $\pm$ 1.85 % and 67.23 $\pm$ 1.85 % cell viability at 100 μg/mL treatment concentration, respectively. LPAF exhibited stronger neuroprotective effect compared with LPEE which may due to the stronger antioxidant capability possessed by LPAF that shown previously and the presence of higher total phenolic content compared with LPEE. A dose-dependency was observed in cells pretreated with both LPAF and LPEE (Figure 26) but the neuroprotective effect of LPEAF was not observed with the percentage cell viability of 45.78 $\pm$ 0.91 at 100 μg/mL treatment concentration which may due to the weak antioxidative activities and low phenolic content presented in LPEAF.

LPAF exhibited the highest neuroprotective activity and presented obvious radical scavenging activity against DPPH with the IC_{50} value of 16.82 $\pm$ 0.27 μg/mL, indicating that LPAF may be a potent neuroprotectant owing to its free radical scavenging activity. LPAF also exhibited strongest reducing power ability and lipid peroxidation inhibitory activity. Moreover, total phenolic content screening showed that LPAF yielded the highest phenolic content of 56.51 $\pm$ 1.43 GAE/g_{DW} which may explain the highest presence of phenolic compounds in LPAF that possessed the strongest antioxidative and neuroprotective activities due to the reactivity of metal ion chelating properties, electron- as well as hydrogen-donating agents (Rice-Evans et al., 1996), and may be the occurrence of synergistic effects from phenolic compounds contained in LPAF that contributes to the potent antioxidant and neuroprotection ability. The presence of the highest phenolic content of LPAF demonstrated the strongest antioxidant capacity compared with LPEE and LPEAF, showed a consistency with many researchers who revealed such positive correlation between antioxidative activity and total phenolic content (Cai et al., 2004; Tawaha et al., 2007; Zheng and Wang, 2001). Additionally, total phenolic concentration of medicinal plants is generally ranging from 0.23 GAE/g_{DW} to 2.85 GAE/g_{DW} (Zheng and Wang, 2001) while the phenolic content of LPAF found in our present study established substantial amount of phenolic concentration which contributed to the effective antioxidant activity.

In view of that, we further analyzed the neuroprotective potential afforded by LPAF through the employment of several apoptosis markers. Apoptosis is initially characterized by morphological features, such as nuclear fragmentation and condensation (Kerr et al., 1972). Exogenous H_2O_2 has been reported to increase oxidative damage despite the neuroprotective ability of endogenous antioxidant defense system and subsequently to induce apoptosis or necrosis in cultured cortical neurons (Koh et al., 1995a; Koh et al., 1995b; Whittemore et al., 1995) and PC12 cell line (Tong

and Perez-Polo, 1996; Maroto and Perez-Polo, 1997). Nevertheless, low level of oxidative damage causes apoptosis whereas high level of oxidative damage triggers necrosis (Dypbukt et al., 1994). Hence, NG108-15 cells were stained with DAPI fluorescent dye to check the nuclear morphologies upon the pretreatment with LPAF following H_2O_2-induced oxidative damage insult. Results showed signs of nuclear shrinkage, fragmentation, and condensation in H_2O_2 treated cells while such morphological changes were not observed in cells pretreated with 1.0 mg/mL LPAF as shown in Figure 27. This indicates the occurrence of apoptosis by H_2O_2 insult and LPAF showed a substantial neuroprotection against oxidative damage in NG108-15 cells.

Depletion and alteration of the intracellular GSH has been reported in the contribution of cellular apoptosis by rendering the cells to be more sensitive and susceptible to apoptotic agents (Macho et al., 1997). Thus, the intracellular GSH content was evaluated against H_2O_2-induced oxidative damage insult. A substantial loss in the intracellular GSH level was observed in H_2O_2 treated group. Nonetheless, pretreatment with LPAF for 2 h opposed the H_2O_2-induced GSH depleting effect, signifying the neuroprotective effect of LPAF against oxidative damage and moreover, a dose-dependent elevation in the intracellular GSH level with the increase in LPAF pretreatment concentration was observed as shown in Figure 28.

Reactive oxygen species formation plays a vital role in the protection, function, and signaling of the immune system. During aerobic metabolism in cells, reactive oxygen species is regularly produced. Nevertheless, excessive formation of reactive oxygen species will initiate a condition called oxidative stress that overwhelms the intracellular antioxidant defense system and subsequently destroys the cellular system. In this investigation, DCF-DA, a cell permeable fluorescent probe was utilized to determine the levels of intracellular reactive oxygen species induced by exogenous

H_2O_2. From the results obtained, LPAF significantly ($P < 0.01$) decreased the reactive oxygen species production by H_2O_2 as shown in Figure 29. Nonetheless, DCF positive population was observed in the untreated control group as well, due to the reason in which, H_2O_2 formed as a natural byproduct of enzymatic oxidase action and serves as an endogenous source of free radicals that contributes to the background level of cellular oxidative stress (Halliwell, 1992; Richardson et al., 1992). Interestingly, when treated with high concentrations of H_2O_2, DCF positive population was not observed but an increase in PI positive population was found. This is probably due to the high degree of H_2O_2 that causes the event of necrosis in NG108-15 cells (Dypbukt et al., 1994). Pretreatment with LPAF exhibited a significant ($P < 0.01$) decreased in DCF positive population as compared with H_2O_2 treated group, indicates its potential relevance in the management of reactive oxygen species-induced neurodegenerative disorders.

The idea of using annexin V to detect apoptosis was derived from a cellular phenomenon, first described by Fadok et al. (1992). They have reported that the exposure of phosphatidylserine on the surface of apoptotic cells which was originally present in the inner leaflet of plasma membrane (Fadok et al., 1992). The event of phosphatidylserine externalization is one of the early apoptosis hallmark occruring well before the detection of DNA fragmentation and nuclear condensation microscopically. FITC-annexin V, a fluorescent dye that binds to the exposed phosphatidylserine to identify the early stage of apoptosis, has been employed in the detection of apoptotic cells (Koopman et al., 1994; Dumont et al., 2000). Flow cytometric analyses, monitoring the appearance of annexin V^+/PI^- apoptotic population, thereby carried out to examine whether H_2O_2-induced oxidative damage, occurring in the existence of LPAF pretreatment, exhibited this apoptotic feature. Results demonstrated that early apoptotic population (annexin V^+/PI^-) and late apoptotic population (annexin V^+/PI^+) were detected in H_2O_2 treated group as shown in Figure 30a. However, pretreatment with

LPAF for 2 h significantly ($P < 0.01$) decreased the percentage of total annexin V positive population (early and late apoptotic cells) dose-dependently (Figure 30b) in which, the percentage of total apoptotic cells continued to reduce with the increasing concentrations of LPAF in NG108-15 cells.

JC-1 fluorescent probe, one of the early apoptosis hallmarks was utilized in the evaluation of mitochondrial membrane potential via flow cytometry. In the mitochondria of healthy cells, with a high mitochondrial membrane potential, JC-1 forms J-aggregates and emits red fluorescence. Upon the induction of apoptosis, with low mitochondrial membrane potential, JC-1 remains in the monomeric form and emits green fluorescence. For that reason, the ratio of red to green fluorescence determines the ratio of high to low mitochondrial membrane potential (Zamzami et al., 1995). JC-1 fluorescent probe was applied to investigate the neuroprotective effect of LPAF on the H_2O_2-induced dissipation of mitochondrial membrane potential in the present neuroprotection model. In the untreated control group, JC-1 forms J-aggregates within the mitochondria, giving a higher level of red fluorescence signal, which corresponded to a polarized mitochondrial membrane potential and appeared in the upper right quadrant. Conversely, H_2O_2 treated group dramatically decreased the red fluorescent J-aggregates signals, leading to a fluorescence signal shifted from the upper right quadrant to the lower right quadrant, presenting a disruption of mitochondrial membrane potential as shown in Figure 31a. H_2O_2 induced a rapid increment of cells with low mitochondrial membrane potential, causing the depolarization of mitochondrial membrane potential as shown by JC-1 fluorescence ratios (Figure 31b). Interestingly, H_2O_2-mediated low mitochondrial membrane potential was abrogated by LPAF in which, pretreatment with highest concentration of 1.0 mg/mL LPAF shifted the fluorescence signal from the lower right quadrant to the upper right quadrant, almost entirely reversing the H_2O_2-induced depolarization of mitochondrial membrane

potential. Altogether, these findings obviously showed that LPAF evoked a significant ($P < 0.01$) suppression in the loss of mitochondrial membrane potential (depolarization) against H_2O_2-induced oxidative damage insult, representing the onset of neuroprotection afforded by LPAF.

LPAF-mediated substantial neuroprotective effects were also observed in cell cycle progression event. Cell cycle arrest at sub-G_1 phase in DNA histogram is an indication of apoptotic cells, representing cells with hypodiploid DNA content and this sub-G_1 population was considered as apoptotic fraction (Darzynkiewicz et al., 1992). Results showed that H_2O_2-induced oxidative damage for 10 h in NG108-15 cells increased the sub-G_1 population, as exhibited by the apoptotic peak which arrested at sub-G_1 phase in DNA histogram. Conversely, 1.0 mg/mL LPAF pretreatment blocked the induction of cell cycle at sub-G_1 phase, resulting in the inhibition of apoptosis (Figure 32a).

Collectively, our findings advocated the significant ($P < 0.01$) antioxidative and neuroprotective effects exerted by LPAF which draw our attention to isolate the most neuroprotective compound from LPAF. Throughout the neuroprotective activity-guided fractionation and isolation from LPAF, repeated sephadex LH-20 as well as diaion HP20SS columns were employed to isolate the most neuroprotective compound via MTT cell viability screening assay (Figure 33). The isolated compounds from LPAF were characterized mainly based on LC-MS and NMR. After comparing the ^{1}H-NMR and ^{13}C-NMR spectral data with literature values (Nonaka et al., 1981; Nonaka et al., 1983), two known proanthocyanidins were isolated and identified from fractions LPAF662 and LPAF762, namely AC trimer (Figure 34) and (+)-catechin (Figure 35), respectively. Next, we continued to examine and compare the neuroprotective activity of AC trimer and (+)-catechin against H_2O_2-induced oxidative damage in NG108-15 cells. Results showed that (+)-catechin revealed higher cell viability (102.41 $\pm$ 3.89 %)

than AC trimer after 10 h H_2O_2 insult at the highest treatment concentration as shown in Table 9. Thus, as our continual study, we keep on to evaluate the possible neuroprotective mechanism afforded by (+)-catechin in our present NG108-15 neuroprotection model.

(+)-Catechin, a natural proanthocyanidin or flavanol which belongs to a class of flavonoids, can be found abundantly in teas, cocoas, vegetables, fruits, and plants. (+)-Catechin has been known for its various biological acivities in the context of pharmacology as well as neuropharmacology such as neuroprotection (Bastianetto et al., 2000), treatment of viral hepatitis (Suzuki et al., 1986), antioxidant (Pedrielli et al., 2001), anti-tumor (Wcyant et al., 2001) as well as anti-bacterial (Bais et al., 2002) properties. Nonetheless, the precise mechanism underlying neuroprotection afforded by (+)-catechin against oxidative stress circumstances stay ambiguous and less explored. Also, there is no report on the mechanism possessed by (+)-catechin in NG108-15 cells against H_2O_2-induced oxidative damage insult. In view of that, the possible neuroprotective mechanism against H_2O_2-induced oxidative damage by the isolated compound, (+)-catechin from LPAF in NG108-15 cells was discussed and demonstrated for the first time.

In order to ascertain the neuroprotective effects exerted by (+)-catechin in NG108-15 cells, intracellular reactive oxygen species level was assessed initially via DCFH-DA fluorescent probe. DCFH-DA is a cell-permeable dye that diffuses through the cell membrane easily to form non-fluorescent DCFH by intracellular esterases and subsequently oxidized to highly fluorescent DCF rapidly in the existence of $OH^{\bullet}$ (Hempel et al., 1999; Royall and Ischiropoulos, 1993). DCF fluorescence intensity is relative to the $OH^{\bullet}$ amount that produced intracellularly. Since exogenous H_2O_2 is known to diffuse into cell nucleus and injure DNA by generating $OH^{\bullet}$ in cultures (Chen et al., 2003), therefore, the intracellular reactive oxygen species level was investigated

to check if (+)-catechin could inhibit the H_2O_2-induced reactive oxygen species formation in the present model. From the results obtained, reactive oxygen species was markedly increased following H_2O_2 insult. Reactive oxygen species have been reported to serve in a range of cellular functions and receptor-mediated signal transduction events (Coffer et al., 1995; Huang et al., 1996; Knebel et al., 1996). Nevertheless, excessive reactive oxygen species formation causes the lipids, proteins, and DNA damage, leading to a cascade of inflammation and subsequently cell death. Our findings exhibited that (+)-catechin significantly ($P<0.01$) attenuated the effects of H_2O_2-induced reactive oxygen species generation in a dose dependent manner in NG108-15 cells, as shown in Figure 36.

Apoptotic neuronal cell injury comprises the early stage of membrane phosphatidylserine externalization as well as the later stage of genomic DNA degradation (Maiese et al., 2009a; Maiese et al., 2009b). Phosphatidylserine refers to a phospholipid which is generally found in the inner leaflet of plasma membrane and externalized upon the onset of early apoptotic event. Therefore, FITC-labeled annexin V/PI double staining was introduced to evaluate the neuroprotective effects of (+)-catechin on the early and late apoptotic NG108-15 cells against H_2O_2 insult. Results showed that untreated control group demonstrated the total annexin V positive (early and late apoptotic cells) population of 5.10 ± 0.20 %, via FACS analysis. Upon the 10 h oxidative induction by H_2O_2, the percentage of total annexin V positive population increased to 62.88 ± 0.07 %. Nevertheless, 2 h pretreatment with (+)-catechin prior to H_2O_2 exposure reduced the total annexin V positive population dose dependently to 30.25 ± 0.29 %, 18.89 ± 0.37 %, and 14.45 ± 0.26 %, respectively as shown in Figure 37b. Hence, (+)-catechin significantly ($P<0.01$) reversed the H_2O_2-induced phosphatidylserine externalization effect to protect NG108-15 cells from oxidative damage.

The disruption of mitochondrial membrane potential represents one of the early apoptotic hallmarks during the onset of cellular apoptosis (Zamzami et al., 1995). JC-1, a lipophilic and cationic fluorescent dye was introduced to signal the loss of mitochondrial membrane potential. Results advocated a fluorescence signal shifted from the upper right quadrant to the lower right quadrant in 10 h H_2O_2 treated group as compared to untreated control group as shown in Figure 38a, resulting in a low red fluorescence signal which indicates the depolarization of mitochondrial membrane potential in H_2O_2 treated group. Nonetheless, 2 h pretreatment with (+)-catechin significantly ($P<0.01$) opposed the effect of H_2O_2-mediated dissipation of mitochondrial membrane potential in a dose dependent manner as shown in JC-1 fluorescence ratio (Figure 38b), signifying a substantial neuroprotective role of (+)-catechin in the regulation of mitochondrial membrane potential.

Next, cell cycle distribution was evaluated by employing PI solution to determine the DNA content. PI is a fluorescent dye that binds to DNA to serve in the identification of dead cells in a population, which is usually excluded from viable cells. During the onset of cellular apoptosis, DNA fragmentation and degradation events occurred which can be detected as sub-G_1 population peak in cell cycle DNA histogram (Darzynkiewicz et al., 1992). For this reason, we elucidate whether (+)-catechin could protect NG108-15 cells against H_2O_2-induced oxidative damage via cell cycle evaluation by determining the sub-G_1 peak in DNA histogram. Flow cytometric analysis demonstrated that the sub-G_1 population increased to 40.26 $\pm$ 0.34 % in H_2O_2 treated group as compared with 1.83 $\pm$ 0.12 % in untreated control group, accompanied by a decrease in G_2/M population in H_2O_2 treated group (Figure 39a). Conversely, 2 h pretreatment with 1.0 mM (+)-catechin significantly ($P<0.01$) opposed the H_2O_2-induced sub-G_1 effect by presenting a drastic decrease in sub-G_1 population (18.60 $\pm$

0.55 %), signifying the neuroprotective role of (+)-catechin by halting the cell cycle arrest at sub-G_1 phase, as shown in DNA histogram (Figure 39a).

Subsequently, the role of (+)-catechin in intracellular antioxidant enzymes, namely SOD and GPx was further analyzed in the present neuroprotection model. SOD is a metalloenzyme that catalyzes the dismutation of O_2^- to form H_2O_2 and oxygen. H_2O_2 is then decomposed to H_2O by GPx (McCord and Fridovich, 1969; Flohé et al., 1972). Empirical studies revealed that each of these enzymes has their specific functional role in maintaining a global cell protection, and the optimal protection of cells could be achieved only when an appropriate balance between the activities of these enzymes is maintained (Hodgson and Fridovich, 1975; Spector, 1995). Results showed that 10 h oxidative insult by H_2O_2 was accompanied by the reduction of SOD and GPx enzyme activities. Nevertheless, 2 h pretreatment with (+)-catechin significantly ($P < 0.01$) increased the SOD and GPx enzyme activities against H_2O_2 insult (Figure 40; Figure 41; Table 10). These results probably can be explained by the free radical scavenging effects and the rapid recycling of GSSG to GSH triggered by (+)-catechin which leads to a significant ($P<0.01$) increase in SOD and GPx activities, respectively. Hence, we addressed that the induction of intracellular antioxidant enzymes namely SOD and GPx, as well as the restoration of intracellular GSH participating in the neuroprotective activity exerted by (+)-catechin in NG108-15 cells.

On the other hand, Bcl-2 family members have been implicated in numerous neuropathological conditions as a key regulator in neuronal cell death. Bcl-2, an anti-apoptotic molecule is the prototypical member of the Bcl-2 family (Korsmeyer, 1999). Bcl-2 plays a crucial role in the regulation of neuronal programmed cell death through several experimental approaches (Mah et al., 1993; Farlie et al., 1995; Allsopp et al., 1993; Garcia et al., 1992; Martinou et al., 1994). Hence, overexpression of Bcl-2 has evidently demonstrated a significant inhibition of neuronal cell death as well as to

promote neuronal survival. Adversely, Bax as a pro-apoptotic molecule reverses the action of Bcl-2. Bax was initially identified as a binding partner for Bcl-2 (Oltvai et al., 1993). Bax regulates the release of cytochrome c from mitochondria via the mitochondrial transition pore formation (Ju¨rgensmeier et al., 1998; Narita et al., 1998). Also, there is evidence advocating that Bcl-2 maintained the mitochondrial integrity, whereas Bax damaged the mitochondrial integrity leading to the loss in mitochondrial membrane potential (Sharpe et al., 2004), which in turn triggered neuronal programmed cell death. As a result, Bax/Bcl-2 ratio measures a cell's life and death vulnerability in response to apoptosis and therefore, directing the cell either to continue to survive or to undergo cell death (Chang et al., 2005; Wall et al., 1999). In view of that, since (+)-catechin has been implicated in the interference of mitochondrial membrane potential in this study and therefore, mitochondria-mediated neuroprotective mechanism through the gene expression of Bcl-2 and Bax was investigated subsequently. From the results obtained via Q-PCR, H_2O_2 treated group demonstrated a marked increase in the Bax expression (Figure 42a) and a drastic decrease in the expression of Bcl-2 (Figure 42b). However, 2 h pretreatment with (+)-catechin reversed the effects of H_2O_2 treated group through the downregulation of bax and upregulation of Bcl-2, leading to a significant ($P < 0.01$) reduction in Bax/Bcl-2 ratio (Figure 42c). Subsequently, immunofluorescence staining exhibited a shift to the left in Bax histogram and a shift to the right in Bcl-2 histogram in (+)-catechin pretreated cells profiles (Figure 44), reflecting an increase and decrease of Bcl-2 and Bax-associated immunofluorescence which was in agreement with the gene expression outcome. Taken together, these results delivered the notion that (+)-catechin protects NG108-15 cells significantly ($P < 0.01$) via the downregulation of Bax and upregulation of Bcl-2 against H_2O_2-induced oxidative damage in the present neuroprotection model.

Chemokines are small chemotaxis cytokines which regulate the peripheral immune cell trafficking under both pathological and physiological circumstances (Baggiolini, 1998; Moser and Loetscher, 2001; Rot and von Andrian, 2004). Apart from their chemotaxis effect on immune cells, chemokines have been known to serve in various cellular functions like tumor growth (Rossi and Zlotnik, 2000), metastasis (Zlotnik, 2006), asthma (Murray et al., 2006), angiogenesis (Benelli et al., 2006; Mackay, 2001), allergic (Pease and Williams, 2006), pain and analgesia (Rittner and Brack, 2006) as well as wound healing (Charo and Ransohoff, 2006; Kunkel, 1999). On the other hand, several studies have revealed that chemokines are also expressed in the central nervous system besides their existence in the periphery which plays a pivotal role in both pathological and physiological circumstances (Ubogu et al., 2006; Charo and Ransohoff, 2006; Bertollini et al., 2006). Therefore, chemokines constitutively exist in glial cells as well as neuronal cells in the brain, other than appearing and expressed during neuroinflammation circumstances. For that reason, chemokines might play its significant role in neuroprotection. Additionally, overexpression of chemokine CCL21 has been evidenced in endangered neurons. In view of that, here for the first time, a novel neuroprotective role afforded by (+)-catechin via chemokine CCL21-mediated neuroprotective pathway against H_2O_2-induced oxidative damage in NG108-15 cells was speculated. Q-PCR results revealed an increase expression of chemokine CCL21 in H_2O_2-treated cells while a significant ($P < 0.01$) decreased expression of chemokine CCL21 was observed upon 2 h pretreatment with (+)-catechin (Figure 43). This finding was in accordance with chemokine CCL21 immunofluorescence staining whereby a shift to the left was witnessed in CCL21 histogram in (+)-catechin pretreated cells profiles (Figure 45). Hence, chemokine CCL21 was overexpressed in H_2O_2-treated cells while (+)-catechin as a known powerful antioxidant and neuroprotectant candidate, presented a novel neuroprotective pathway by downregulating chemokine CCL21

against H_2O_2-induced oxidative damage in the present NG108-15 neuroprotection model, for the first time.

Collectively, the present findings have demonstrated that *L. parasiticus* exerts substantial antioxidative effects through the DPPH free radical scavenging activity, reducing power activity, lipid peroxidation inhibitory activity and total phenolic content assessment. H_2O_2-induced apoptotic effect has been confirmed in our present NG108-15 neuroprotection model. Also, *L. parasiticus* has been subsequently shown to exhibit signficant neuroprotective activity against H_2O_2-induced apoptotic cell death by inhibiting the H_2O_2-induced apoptotic nuclear morphological changes, attenuating the fall in intracellular GSH, decreasing intracellular reactive oxygen species formation, reducing apoptotic features such as externalization of phosphatidylserine, depolarization of mitochondrial membrane potential and appearance of sub-G_1 apoptotic population, leading to the isolation of the most potent neuroprotective compound, (+)-catechin via the bioassay-guided fractionation approach. Our data revealed that (+)-catechin significantly protected cells by reducing H_2O_2-induced cell loss, decreasing the intracellular reactive oxygen species generation, mitigating the externalization of phosphatidylserine, attenuating the dissipation of mitochondrial membrane potential, blocking the cell cycle arrest at sub-G_1 apoptotic fraction, increasing the intracellular antioxidant enzymes activity namely SOD and GPx, reducing the Bax/Bcl-2 ratio and downregulating the H_2O_2-induced overexpression of neuronal chemokine CCL21. The antioxidative and neuroprotective properties of *L. parasiticus* have been investigated and validated successfully in this present etiology, in which an antioxidant mediating free radical scavenging effect, various apoptotic markers in neuroprotection elucidation, and more importantly a novel role of neuronal chemokine CCL21 associated with neuroprotection signaling pathway has been established. Therefore, the present research

supports the use of *L. parasiticus* in treating and preventing neurodegenerative diseases where oxidative stress is implicated.

CHAPTER 6

CONCLUSION

According to the current neurobiology research, apparently the hectic environmental and lifestyle factors cause the formation of free radicals which subsequently leads to a condition known as oxidative stress. However, excessive oxidative damage prompts significant pathological changes in neuronal cells particularly in central nervous system. Therefore, a need in the management of free radical-induced oxidative damage is crucial to maintain the highest possible integrity in the brain. Here, we have demonstrated that *L. parasiticus* exhibited substantial antioxidative as well as neuroprotective activities against H_2O_2-induced oxidative damage in our present NG108-15 neuroprotection model. Moreover, a novel neuronal chemokine CCL21-mediated neuroprotective mechanism has been illustrated by the most potent isolated neuroprotective compound, (+)-catechin, for the first time. In view of that, these findings provide a basis for future studies to investigate the impact of (+)-catechin on vesicle-mediated transport and release of chemokine CCL21 in oxidative damaged neurons, as well as to activate the microglia via chemokine receptor CXCR3, throughout the entire neuronal process. A clear and precise neuroprotective mechanism afforded by (+)-catechin to induce chemokine CCL21-mediated neuroprotection signaling pathway is recommended to provide a novel role of (+)-catechin in its contribution to neuroprotection via chemokine CCL21.

BIBLIOGRAPHY

Adams, J. M. and Cory, S. (1998). The Bcl-2 protein family: arbiters of cell survival. *Science*, 281, 1322-1326.

Agar, N. S., Sadrzadeh, S. M., Hallay, P. E. and Eaton, J. W. (1986). Erythrocyte catalase. A somatic oxidant defense? *Journal of Clinical Investigation*, 77, 319-321.

Alkhatib, G., Combadiere, C., Broder, C. C., Feng, Y., Kennedy, P. E., Murphy, P. M., et al. (1996). CC CKR5: a RANTES, MIP-1alpha, MIP-1beta receptor as a fusion cofactor for macrophage-tropic HIV-1. *Science*, 272, 1955-1958.

Allsopp, T. E., Wyatt, S., Paterson, H. F. and Davies, A. M. (1993). The proto-oncogene bcl-2 can selectively rescue neurotrophic factor-dependent neurons from apoptosis. *Cell*, 73, 295-307.

Anjaneyulu, A. S. R., Row, L. R. and Reddy, D. S. (1977). Chemical constituents of *Loranthus falcatus* Linn. *Current Science*, 46, 850-851.

Antonsson, B. and Martinou, J. C. (2000). The Bcl-2 protein family. *Experimental Cell Research*, 256, 50-57.

Azzouz, M., Hottinger, A., Paterna, J. C., Zurn, A. D., Aebischer, P. and Bueler, H. (2000). Increased motoneuron survival and improved neuromuscular function in transgenic ALS mice after intraspinal injection of an adeno-associated virus encoding Bcl-2. *Human Molecular Genetics*, 9, 803-811.

Baggiolini, M. (1998). Chemokines and leukocyte traffic. *Nature*, 392, 565-568.

Baggiolini, M. and Dahinden, C. A. (1994). CC chemokines in allergic inflammation. *Immunology Today*, 15, 127-133.

Bains, J. S. and Shaw, C. A. (1997). Neurodegenerative disorders in humans: the role of glutathione in oxidative stress-mediated neuronal death. *Brain Research Reviews*, 25, 335-358.

Bais, H. P., Walker, T. S., Stermitz, F. R., Hufbauer, R. A. and Vivanco, J. M. (2002). Enantiomeric-Dependent Phytotoxic and Antimicrobial Activity of (±)-Catechin. A Rhizosecreted Racemic Mixture from Spotted Knapweed. *Plant Physiology*, 128, 1173-1179.

Balkwill, F. (1998). The molecular and cellular biology of the chemokines. *Journal of Viral Hepatitis*, 5, 1-14.

Bastianetto, S., Zheng, W. H. and Quirion, R. (2000). Neuroprotective abilities of resveratrol and other red wine constituents against nitric oxide related toxicity in cultured hippocampal neurons. *British Journal of Pharmacology*, 131, 711-720.

Batistatou, A., Merry, D. E., Korsmeyer, S. J. and Greene, L. A. (1993). Bcl-2 affects survival but not neuronal differentiation of PC12 cells. *Journal of Neuroscience*, 13, 4422-4428.

Behl, C., Davis, J. B., Lesley, R. and Schubert, D. (1994). Hydrogen peroxide mediates amyloid beta protein toxicity. *Cell*, 77, 817-827.

Bei, W., Peng, W., Ma, Y. and Xu, A. (2005). Flavonoids from the leaves of Diospyros kaki reduce hydrogen peroxide-induced injury of NG108-15 cells. *Life sciences*, 76, 1975-1988.

Bei, W. J., Pen, W. L., Ma, Y. and Xu, A. L. (2004). NaoXinQing, an anti-stroke herbal medicine, reduces hydrogen peroxide-induced injury in NG108-15 cells. *Neuroscience Letters*, 363, 262-265.

Benelli, R., Lorusso, G., Albini, A. and Noonan, D. M. (2006). Cytokines and chemokines as regulators of angiogenesis in health and disease. *Current Pharmaceutical Design*, 12, 3101-3115.

Berger, M. M. (2005). Can oxidative damage be treated nutritionally? *Clinical Nutrition*, 24, 172-183.

Bernardi, P. and Azzone, G. F. (1981). Cytochrome c as an electron shuttle between the outer and inner mitochondrial membranes. *Journal of Biological Chemistry*, 256, 7187-7192.

Bertollini, C., Ragozzino, D., Gross, C., Limatola, C. and Eusebi, F. (2006). Fractalkine/CX3CL1 depresses central synaptic transmission in mouse hippocampal slices. *Neuropharmacology*, 51, 816-821.

Biber, K., Rappert, A., Kettenmann, H., Brouwer, N., Copray, S. C. V. M. and Boddeke, H. W. G. M. (2002). Neuronal SLC (CCL21) expression: implications for the neuron-microglial signaling system. *Ernst Schering Research Foundation Workshop*, 45-60.

Biber, K., Sauter, A., Brouwer, N., Copray, S. C. and Boddeke, H. W. (2001). Ischemia-induced neuronal expression of the microglia attracting chemokine secondary lymphoid tissue chemokine (SLC). *Glia*, 34, 121-133.

Blois, M. S. (1958). Antioxidant determination by the use of a stable free radical. *Nature*, 181, 1199-1200.

Bonfoco, E., Zhivotovsky, B., Rossi, A. D., Aguilar-Santelises, M., Orrenius, S., Lipton, S. A., et al. (1996). Bcl-2 delays apoptosis and PARP cleavage induced by NO donors in GT1-7 cells. *Neuroreport*, 8, 273-276.

Bouayed, J., Piri, K., Rammal, H., Dicko, A., Desor, F., Younos, C., et al. (2006). Comparative evaluation of the antioxidant potential of some Iranian medicinal plants. *Food Chemistry*, 104, 364-368.

Brookes, P. S., Land, J. M., Clark, J. B. and Heales, S. J. (1998). Peroxynitrite and brain mitochondria: evidence for increased proton leak. *Journal of Neurochemistry*, 70, 2195-2202.

Brown, J. E., Khodr, H., Hider, R. C. and Rice-Evans, C. A. (1998). Structural dependence of flavonoid interactions with Cu^{2+} ions: implications for their antioxidant properties. *Biochemical Journal*, 330, 1173-1178.

Browne, S. E., Bowling, A. C., MacGarvey, U., Baik, M. J., Berger, S. C., Muqit, M. M., et al. (1997). Oxidative damage and metabolic dysfunction in Huntington's disease: selective vulnerability of the basal ganglia. *Annals of Neurology*, 41, 646-653.

Bruce-Keller, A. J., Begley, J. G., Fu, W., Butterfield, D. A., Bredesen, D. E., Hutchins, J. B., et al. (1998). Bcl-2 protects isolated plasma and mitochondrial membranes against lipid peroxidation induced by hydrogen peroxide and amyloid beta-peptide. *Journal of Neurochemistry*, 70, 31-39.

Bu, B., Klunemann, H., Suzuki, K., Li, J., Bird, T., Jin, L. W., et al. (2002a). Niemann-Pick disease type C yields possible clue for why cerebella neurons do not form neurofibrillary tangles. *Neurobiology of Disease*, 11, 285-297.

Bu, B., Li, J., Davies, P. and Vincent, I. (2002b). Deregulation of cdk5, hyperphosphorylation, and cytoskeletal pathology in the Niemann–Pick type C murine model. *Journal of Neuroscience*, 22, 6515-6525.

Bush, A. I. (2000). Metals and neuroscience. *Current Opinion in Chemical Biology*, 4, 184-191.

Busser, J., Geldmacher, D. S. and Herrup, K. (1998). Ectopic cell cycle proteins predict the sites of neuronal cell death in Alzheimer's disease brain. *Journal of Neuroscience*, 18, 2801-2807.

Butterfield, D. A., Castegna, A., Lauderback, C. M. and Drake, J. (2002). Evidence that amyloid β-peptide induced lipid peroxidation and its sequelae in Alzheimer's disease brain contribute to neuronal death. *Neurobiology of Aging*, 23, 655-664.

Cadet, J. L. (1998). Free radical mechanisms in the central nervous system: an overview. *International Journal of Neuroscience*, 40, 13-18.

Cai, Y., Luo, Q., Sun, M. and Corke, H. (2004). Antioxidant activity and phenolic compounds of 112 traditional Chinese medicinal plants associated with cancer. *Life Sciences*, 74, 2157-2184.

Cai, Y. Z., Sun, M. and Corke, H. (2003). Antioxidant activity of betalains from plants of the amaranthaceae. *Journal of Agricultural and Food Chemistry*, 51, 2288-2294.

Cain, K., Bratton, S. B. and Cohen, G. M. (2002). The Apaf-1 apoptosome: a large caspase-activating complex. *Biochimie*, 84, 203-214.

Canals, S., Casarejos, M. J., De Bernardo, S., Rodriquez Martin, E., and Mena, M. A. (2001). Glutathione depletion switches nitric oxide neurotrophic effects to cell death in midbrain cultures: implications for Parkinson's disease. *Journal of Neurochemistry*, 79, 1183-1195.

Cao, Y., Shibata, T. and Rainov, N. (2002). Liposome-mediated transfer of the bcl-2 gene results in neuroprotection after in vivo transient focal cerebral ischemia in an animal model. *Gene Therapy*, 9, 415-419.

Cassarino, D. S., Fall, C. P., Swerdlow, R. H., Smith, T. S., Halvorsen, E. M., Miller, S. W., et al. (1997). Elevated reactive oxygen species and antioxidant enzyme activities in animal and cellular models of Parkinson's disease. *Biochimica et Biophysica Acta*, 1362, 77-86.

Cha, E. E., Kim, B. S., Kim, D. H., Lee, Y. K., Kim, Y. J. and Kang, J. S. (2003). Study on antioxidant action of *Loranthus parasiticus* (L.) Merr. *Korean Journal of Oriental Physiology and Pathology*, 7, 939-945.

Chance, B., Sies, H. and Boveris, A. (1979). Hydroperoxide metabolism in mammalian organs. *Physiological Reviews*, 59, 527-605.

Chang, J. S., Hsu, Y. L., Kuo, P. L., Kuo, Y. C., Chiang, L. C. and Lin, C. C. (2005). Increase of Bax/Bcl-XL ratio and arrest of cell cycle by luteolin in immortalized human hepatoma cell line. *Life Sciences*, 76, 1883-1893.

Charo, I. F. and Ransohoff, R. M. (2006). The many roles of chemokines and chemokine receptors in inflammation. *The New England Journal of Medicine*, 354, 610-621.

Chen, X., Nishida, H. and Konishi, T. (2003). Baicalin promoted the repair of DNA single strand breakage caused by H_2O_2 in cultured NIH3T3 fibroblasts. *Biological and Pharmaceutical Bulletin*, 26, 282-284.

Cheng Chew, S. B., Leung, P. Y. and Fiscus, R. R. (2003). Preincubation with atrial natriuretic peptide protects NG108-15 cells against the toxic/proapoptotic effects of the nitric oxide donor S-nitroso-N-acetylpenicillamine. *Histochemistry and cell biology*, 120, 163-171.

Chipuk, J. E. and Green, D. R. (2005). Do inducers of apoptosis trigger caspase independent cell death? *Nature Reviews Molecular Cell Biology*, 6, 268-275.

Clancy, R. M., Levartovsky, D., Leszczynska-Piziak, J., Yegudin, J. and Abramson, S. B. (1994). Nitric oxide reacts with intracellular glutathione and activates the hexose monophosphate shunt in human neutrophils: evidence for S-nitrosoglutathione as a bioactive intermediary. *Proceedings of the National Academy of Sciences of the United States of America*, 91, 3680-3684.

Coffer, P. J., Burgering, B. M. T., Peppelenbosch, M. P., Bos, J. L. and Kruijer, W. (1995). UV activation of receptor tyrosine kinase activity. *Oncogene*, 11, 561-569.

Comhair, S. A. A. and Erzurum, S. C. (2005). The regulation and role of extracellular glutathione peroxidase. *Antioxidants and Redox Signalling*, 7, 72-79.

Commandeur, J. N., Stijntjes, G. J. and Vermeulen, N. P. (1995). Enzymes and transport systems involved in the formation and disposition of glutathione S-conjugates. Role in bioactivation and detoxication mechanisms of xenobiotics. *Pharmacological Reviews*, 47, 271-330.

Conte, A., Pellegrini, S. and Tagliazucchi, D. (2003). Effect of resveratrol and catechin on PC12 tyrosine kinase activities and their synergistic protection from beta-amyloid toxicity. *Drugs Under Experimental and Clinical Research*, 29, 243-255.

Cook, N. C. and Samman, S. (1996). Flavonoids-chemistry, metabolism cardioprotective effects, and dietary sources. *Journal of Nutritional Biochemistry*, 7, 66-76.

Cooper, A. J. and Kristal, B. S. (1997). Multiple roles of glutathione in the central nervous system. *Journal of Biological Chemistry*, 378, 793-802.

Cory, S. and Adams, J. M. (2002). The Bcl2 family: regulators of the cellular life-or-death switch. *Nature Reviews Cancer*, 2, 647-656.

Cotelle, N., Bernier, J. L., Catteau, J. P., Pommery, J., Wallet, J. C. and Gaydou, E. M. (1996). Antioxidant properties of hydroxyflavones. *Free Radical Biology and Medicine*, 20, 35-43.

Cren-Olivé, C., Wieruszeski, J. M., Maes, E. and Rolando, C. (2002). Catechin and epicatechin deprotonation followed by ^{13}C NMR. *Tetrahedron Letters*, 43, 4545-4549.

Cuzzocrea, S., Riley, D. P., Caputi, A. P. and Salvemini, D. (2001). Antioxidant therapy: a new pharmacological approach in shock, inflammation, and ischemia/reperfusion injury. *Pharmacological Reviews*, 53, 135-159.

Dakshinamurti, K., Sharma, S. K. and Jonathan, D. G. (2003). Neuroprotective actions of pyridoxine. *Biochimica et Biophysica Acta-Proteins and Proteomics*, 1647, 225-229.

Dalton, T. P., Shertzer, H. G. and Puga, A. (1999). Regulation of gene expression by reactive oxygen. *Annual Review of Pharmacology and Toxicology*, 39, 67-101.

Danial, N. N. (2007). Bcl-2 family proteins: critical checkpoints of apoptotic cell death. *Clinical Cancer Research*, 13, 7254-7263.

Darzynkiewicz, Z., Bruno, S., Del Bino, G., Gorczyca, W., Hotz, M. A., Lassota, P., et al. (1992). Features of apoptotic cells measured by flow cytometry. *Cytometry*, 13, 795-808.

De Haan, J. B., Bladier, C., Griffiths, P., Kelner, M., O'Shea, R. D., Cheung, N. S., et al. (1998). Mice with a homozygous null mutation for the most abundant glutathione peroxidase, Gpx1, show increased susceptibility to the oxidative stress-inducing agents paraquat and hydrogen peroxide. *Journal of Biological Chemistry*, 273, 22528-22536.

De Jong, E. K., Dijkstra, I. M., Hensens, M., Brouwer, N., van Amerongen, M., Liem, R. S., et al. (2005). Vesicle- mediated transport and release of CCL21 in endangered neurons: a possible explanation for microglia activation remote from a primary lesion. *Journal of Neuroscience*, 25, 7548–7557.

Debatin, K. M. and Krammer, P. H. (2004). Death receptors in chemotherapy and cancer. *Oncogene*, 23, 2950-2966.

Demopoulos, H. B., Flamm, E. S., Pietronegro, D. D. and Seligman, M. L. (1980). The free radical pathology and the microcirculation in the major central nervous system disorders. *Acta physiologica Scandinavica. Supplementum*, 492, 91-119.

Deng, G., Soriano, E., Smyth, C., Parge, H. E., Ahmed, A., Roses, A. D., et al. (1993). Amyotrophic lateral sclerosis and structural defects in Cu, Zn superoxide dismutase. *Science*, 261, 1047-1051.

Dhavan, R. and Tsai, L. H. (2001). A decade of CDK5. *Nature Reviews Molecular Cell Biology*, 2, 749-759.

Di Giovanni, S., Movsesyan, V., Ahmed, F., Cernak, I., Schinelli, S., Stoica, B., et al. (2005). Cell cycle inhibition provides neuroprotection and reduces glial proliferation and scar formation after traumatic brain injury. *Proceedings of the National Academy of Sciences of the United States of America*, 102, 8333-8338.

Didier, M., Bursztajn, S., Adamec, E., Passani, L., Nixon, R. A., Coyle, J. T., et al. (1996). DNA strand breaks induced by sustained glutamate excitotoxicity in primary neuronal cultures. *The Journal of Neuroscience*, 16, 2238-2250.

Dijkstra, I. M., Hulshof, S., van der Valk, P., Boddeke, H. W. and Biber, K. (2004). Cutting edge: activity of human adult microglia in response to CC chemokine ligand 21. *Journal of Immunology*, 172, 2744-2747.

Distelhorst, C. W., Lam, M. and McCormick, T. S. (1996). Bcl-2 inhibits hydrogen peroxide-induced ER Ca21 pool depletion. *Oncogene*, 12, 2051-2055.

Dragic, T., Litwin, V., Allaway, G. P., Martin, S. R., Huang, Y., Nagashim, K. A., et al. (1996). HIV-1 entry into $CD4^+$ cells is mediated by the chemokine receptor CC-CKR-5. *Nature*, 381, 667-673.

Dringen, R. (2000). Metabolism and functions of glutathione in brain. *Progress in Neurobiology*, 62, 649-671.

Duan, X. J., Zhang, W. W., Li, X. M. and Wang, B. G. (2006). Evaluation of antioxidant property of extract and fractions obtained from a red alga, *Polysiphonia urceolata*. *Food Chemistry*, 95, 37-43.

Duh, P. D. (1998). Antioxidant activity of Budrock (*Arctium laooa* Linn) its scavenging effect on free radical and active oxygen. *Journal of the American Oil Chemists' Society*, 75, 455-461.

Dumont, A., Hehner, S. P., Hofmann, T. G., Ueffing, M., Droege, W. and Schmitz, M. L. (1999). Hydrogen peroxide-induced apoptosis is CD95-independent, requires the release of mitochondria-derived reactive oxygen species and the activation of NF-kappa B. *Oncogene*, 18, 747-757.

Dumont, E. A. W. J., Hofstra, L., Van Heerde, W. L., Eijnde, S. V. D., Doevendans, P. A. F., DeMuinck, E., et al. (2000). Cardiomyocyte death induced by myocardial ischemia and reperfusion: measurement with recombinant human annexin-V in a mouse model. *Circulation*, 102, 1564-1568.

Dypbukt, J. M., Ankarcrona, M., Burkitt, M., Sjoholm, A., Strom, K., Orrenius, S., et al. (1994). Different prooxidant levels stimulate growth, trigger apoptosis, or produce necrosis of insulin-secreting RINm5F cells. The role of intracellular polyamines. *Journal of Biological Chemistry*, 269, 30553-30560.

Emdadul Haque, M., Asanuma, M., Higashi, Y., Miyazaki, I., Tanaka, K. and Ogawa, N. (2003). Apoptosis-inducing neurotoxicity of dopamine and its metabolites via reactive quinone generation in neuroblastoma cells. *Biochimica et Biophysica Acta*, 1619, 39-52.

Enokido, Y. and Hatanaka, H. (1993). Apoptotic cell death occurs in hippocampal neurons cultured in a high oxygen atmosphere. *Neuroscience*, 57, 965-972.

Fadok, V. A., Voelker, D. R., Campbell, P. A., Cohen, J. J., Bratton, D. L. and Henson, P. M. (1992). Exposure of phosphatidylserine on the surface of apoptotic lymphocytes triggers specific recognition and removal by macrophages. *The Journal of Immunology*, 148, 2207-2216.

Farlie, P. G., Dringen, R., Rees, S. M., Kannourakis, G. and Bernard, O. (1995). Bcl-2 transgenic expression can protect neurons against developmental and induced cell death. *Proceedings of the National Academy of Sciences of the United States of America*, 92, 4397-4401.

Feng, Y., Broder, C. C., Kennedy, P. E. and Berger, E. A. (1996). HIV-1 entry cofactor: functional cDNA cloning of a seven-transmembrane, G protein-coupled receptor. *Science*, 272, 872-877.

Fernandez, E. J. and Lolis, E. (2002). Structure, function, and inhibition of chemokines. *Annual Review of Pharmacology and Toxicology*, 42, 469-499.

Ferrari, C. K. B. (2000). Free radicals, lipid peroxidation and antioxidants in apoptosis: implications in cancer, cardiovascular and neurological diseases. *Biologia*, 55, 581-590.

Ferrer, I. and Planas, A. M. (2003). Signaling of cell death and cell survival following focal cerebral ischemia: life and death struggle in the penumbra. *Journal of Neuropathology and Experimental Neurology*, 62, 329-339.

Fiskum, G. (2000). Mitochondrial participation in ischemic and traumatic neural cell death. *Journal of Neurotrauma*, 17, 843-855.

Flohé, L., Loschen, G., Günzler, W. A. and Eichele, E. (1972). Glutathione Peroxidase, V. The kinetic mechanism. *Hoppe-Seyler´s Zeitschrift für physiologische Chemie*, 353, 987-1000.

Floyd, R. A. (1999). Antioxidants, oxidative stress, and degenerative neurological disorders. *Proceedings of the Society for Experimental Biology and Medicine*, 222, 236-245.

Floyd, R. A. and Carney, J. M. (1992). Free radical damage to protein and DNA: Mechanism involved and relevant observations on brain undergoing oxidative stress. *Annals of Neurology*, 32, 522-527.

Folio, F. Turrens. (2003). Mitochondrial formation of reactive oxygen species. *Journal of Physiology*, 552, 335-344.

Forloni, G., Chiesa, R., Smiroldo, S., Verga, L., Salmona, M., Tagliavini, F., et al. (1993). Apoptosis mediated neurotoxicity induced by chronic application of beta-amyloid fragment 25-35. *NeuroReport*, 4, 523-526.

Friberg, H., Connern, C., Halestrap, A. P. and Wieloch, T. (1999). Differences in the activation of the mitochondrial permeability transition among brain regions in the rat correlate with selective vulnerability. *Journal of Neurochemistry*, 72, 2488-2497.

Friberg, H., Ferrand-Drake, M., Bengtsson, F., Halestrap, A. P., Wieloch, T. and Cyclosporin, A. (1998). Cyclosporin A, but not FK 506, protects mitochondria and neurons against hypoglycemic damage and implicates the mitochondrial permeability transition in cell death. *Journal of Neuroscience*, 18, 5151-5159.

Fuentes-Prior, P. and Salvesen, G. S. (2004). The protein structures that shape caspase activity, specificity, activation and inhibition. *Biochemical Journal*, 384, 201-232.

Furie, M. B. and Randolph, G. J. (1995). Chemokines and tissue injury. *American Journal of Pathology*, 146, 1287-1301.

Gabbita, S. P., Lovell, M. A. and Markesbery, W. R. (1998). Increased nuclear DNA oxidation in the brain in Alzheimer's disease. *Journal of Neurochemistry*, 71, 2034-2040.

Gan, R. Y., Kuang, L., Xu, X. R., Zhang, Y., Xia, E. Q., Song, F. L., et al. (2010). Screening of natural antioxidants from traditional Chinese medicinal plants associated with treatment of rheumatic disease. *Molecules*, 15, 5988-5997.

Garcia, I., Martinou, I., Tsujimoto, Y. and Martinou, J. C. (1992). Prevention of programmed cell death of sympathetic neurons by the Bcl-2 protooncogene. *Science*, 258, 302-304.

Gilgun-Sherki, Y., Melamed, E. and Offen, D. (2001). Oxidative stress induced neurodegenerative diseases: the need for antioxidants that penetrate the blood brain barrier. *Neuropharmacology*, 40, 959-975.

Giustarini, D., Rossi, R., Milzani, A., Colombo, R. and Dalle-Donne, I. (2004). S-glutathionylation: from redox regulation of protein functions to human diseases. *Journal of Cellular and Molecular Medicine*, 8, 201-212.

Gomez-Sintes, R., Hernandez, F., Lucas, J. J. and Avila J. (2011). GSK-3 mouse models to study neuronal apoptosis and neurodegeneration. *Frontiers in Molecular Neuroscience*, 4, 45.

Good, P. F., Werner, P., Hsu, A., Olanow, C. W. and Perl, D. P. (1996). Evidence of neuronal oxidative damage in Alzheimer's disease. *American Journal of Pathology*, 149, 21-28.

Graham, H. N. (1992). Green tea composition, consumption, and polyphenol chemistry. *Preventive Medicine*, 21, 334-350.

Green, D. R. and Kroemer, G. (2004). The pathophysiology of mitochondrial cell death. *Science*, 305, 626-629.

Griffith, O. W. (1980). Determination of glutathione and glutathione disulfide using glutathione reductase and 2-vinylpyridine. *Analytical Biochemistry*, 106, 207-212.

Gul, M., Kutay, F. Z., Temocin, S. and Hanninen, O. (2000). Cellular and clinical implications of glutathione. *Indian Journal of Experimental Biology*, 38, 625-634.

Gutteridge, J. M. C. and Halliwell, B. (2000). Free radicals and antioxidants. *Annals of the New York Academy of Sciences*, 899, 136-147.

Halliwell, B. (1992). Reactive oxygen species and the central nervous system. *Journal of Neurochemistry*, 59, 1609-1623.

Halliwell, B. (1994). Free radicals, antioxidants, and human disease: curiosity, cause, or consequence? *Lancet*, 344, 721-724.

Halliwell, B. (2001). Role of free radicals in neurodegenerative diseases: therapeutic implications for antioxidant treatment. *Drugs and Aging*, 18, 685-716.

Halliwell, B. and Gutteridge, J. M. C. (1999). Free Radicals in Biology and Medicine. *Oxford University Press New York.*

Hamprecht, B., Glaser, T., Reiser, G., Bayer, E. and Propst, F. (1985). Culture and characteristics of hormone-responsive neuroblastoma X glioma hybrid cells. *Methods in Enzymology*, 109, 316-341.

Han, Z., Yang, L., MacLellan, W. R., Weiss, J. N. and Qu, Z. (2005). Hysteresis and cell cycle transitions: how crucial is it? *Biophysical Journal*, 88, 1626-1634.

Haque, A. M., Hashimoto, M., Katakura, M., Tanabe, Y., Hara, Y. and Shido, O. (2006). Long-term administration of green tea catechins improves spatial cognition learning ability in rats. *Journal of Nutrition*, 136, 1043-1047.

Hara, H., Fink, K., Endres, M., Friedlander, R. M., Gagliardini, V., Yuan, J. Y., et al. (1997). Attenuation of transient focal cerebral ischemic injury in transgenic mice expressing a mutant ICE inhibitory protein. *Journal of Cerebral Blood Flow and Metabolism*, 17, 370-375.

Harman, D. (1956). Aging: a theory based on free radical and radiation chemistry. *Journal of Gerontology*, 11, 298-300.

Harvala, E., Exner, J. and Becker, H. (1984). Flavonoids of *Loranthus europaeus*. *Journal of Natural Products*, 47, 1054-1055.

Harvey, A. L. (1984). The pharmacology of nerve and muscle in tissue culture. New York: Alan R. Liss, Inc.

Hedrick, J. A. and Zlotnik, A. (1997). Identification and characterization of a novel beta chemokine containing six conserved cysteines. *Journal of Immunology*, 159, 1589-1593.

Hempel, S. L., Buettner, G. R., O'Malley, Y. Q., Wessels, D. A. and Flaherty, D. M. (1999). Dihydrofluorescein diacetate is superior for detecting intracellular oxidants: comparison with 2',7'-dichlorodihydrofluorescein diacetate, 5(and 6)-carboxy-2',7'-dichlorodihydrofluorescein diacetate, and dihydrorhodamine 123. *Free Radical Biology and Medicine*, 27, 146-159.

Hensley, K., Hall, N., Subramaniam, R., Cole, P., Harris, M., Aksenov, M., et al. (1995). Brain regional correspondence between Alzheimer's disease histopathology and biomarkers of protein oxidation. *Journal of Neurochemistry*, 65, 2146-2156.

Hensley, K., Maidt, M. L., Yu, Z., Sang, H., Markesbery, W. R. and Floyd, R. A. (1998). Electrochemical analysis of protein nitrotyrosine and dityrosine in the Alzheimer brain indicates region-specific accumulation. *Journal of Neuroscience*, 18, 8126-8132.

Hider, R. C., Liu, Z. D. and Khodr, H. H. (2001). Metal chelation of polyphenols. *Methods in Enzymology*, 335, 190-203.

Hockenbery, D. M. (1995). Bcl-2, a novel regulator of cell death. *BioEssays*, 17, 631-638.

Hockenbery, D., Nuffez, G., Milliman, C., Schreiber, R. D. and Korsmeyer, S. J. (1990). Bcl-2 is an inner mitochondrial membrane protein that blocks programmed cell death. *Nature*, 348, 334-336.

Hockenbery, D. M., Oltvai, Z. N., Yin, X. M., Milliman, C. L. and Korsmeyer, S. J. (1993). Bcl-2 functions in an antioxidant pathway to prevent apoptosis. *Cell*, 75, 241-251.

Hodgson, E. K. and Fridovich, I. (1975). The interaction of bovine erythrocyte superoxide dismutase with hydrogen peroxide: chemiluminescence and peroxidation. *Biochemistry*, 14, 5299-5303.

Hoglinger, G. U., Breunig, J. J., Depboylu, C., Rouaux, C., Michel, P. P., Alvarez-Fischer, D., et al. (2007). The pRb/E2F cell-cycle pathway mediates cell death in Parkinson's disease. *Proceedings of the National Academy of Sciences of the United States of America*, 104, 3585-3590.

Hosaka, S., Akahoshi, T., Wada, C. and Kondo, H. (1994). Expression of the chemokine superfamily in rheumatoid arthritis. *Clinical and Experimental Immunology*, 97, 451-457.

Hromas, R., Kim, C. H., Klemsz, M., Krathwohl, M., Fife, K., Cooper, S., et al. (1997). Isolation and characterization of Exodus-2, a novel C-C chemokine with a unique 37-amino acid carboxyl-terminal extension. *Journal of Immunology*, 159, 2554-2558.

Huang, R. P., Wu, J. X., Fan, Y. and Adamson, E. D. (1996). UV activates growth factor receptors via reactive oxygen intermediates. *The Journal of Cell Biology*, 133, 211-220.

Hussain, S., Slikker, W. Jr. and Ali, S. F. (1996). Role of metallothionein and other antioxidants in scavenging superoxide radicals and their possible role in neuroprotection. *Neurochemistry International*, 29, 145-152.

Hyman, M. S. (2004). Redox neurology: Visions of an emerging subspecialty. *Annals of the New York Academy of Sciences*, 1012, 342-355.

Inanami, O., Watanabe, Y., Syuto, B., Nakano, M., Tsuji, M. and Kuwabara, M. (1998). Oral administration of (+)-catechin protects against ischemia-reperfusion-induced neuronal death in the gerbil. *Free Radical Research*, 29, 359-365.

Indrani, N., Rao, V. S., Balasubramanian, K., Reddy, K. K. and Vijayaramayya, T. (1980). Studies on *Loranthus longiflorus* Desr. Tannins. *Leather Science Madras*, 27, 438-439.

Ivins, K. J., Ivins, J. K., Sharp, J. P. and Cotman, C. W. (1999). Multiple pathways of apoptosis in PC12 cells: CrmA inhibits apoptosis induced by beta-amyloid. *Journal of Biological Chemistry*, 274, 2107-2112.

Janaky, R., Ogita, K., Pasqualotto, B. A., Bains, J. S., Oja, S. S., Yoneda, Y., et al. (1999). Glutathione and signal transduction in the mammalian CNS. *Journal of Neurochemistry*, 73, 889-902.

Janaky, R., Varga, V., Hermann, A., Saransaari, P. and Oja, S. S. (2000). Mechanisms of L-cysteine neurotoxicity. *Neurochemical Research*, 25, 1397-1405.

Janero, D. R. (1990). Malondialdehyde and thiobarbituric acid-reactivity as diagnostic indices of lipid peroxidation and peroxidative tissue injury. *Free Radical Biology and Medicine*, 9, 515-540.

Jentzsch, A. M., Bachmann, H., Furst, P. and Biesalski, H. K. (1996). Improved analysis of malondialdehyde in human body fluids. *Free Radical Biology and Medicine*, 20, 251-256.

Jeon, S. E., Choi Kwon, S., Park, K. A., Lee, H. J., Park, M. S., Lee, J. H., et al. (2003a). Dietary supplementation of (+)-catechin protects against UVB-induced skin damage by modulating antioxidant enzyme activities. *Photodermatology, Photoimmunology and Photomedicine*, 19, 235-241.

Jeon, S. Y., Bae, K., Seong, Y. H. and Song, K. S. (2003b). Green tea catechins as a BACE1 (beta-secretase) inhibitor. *Bioorganic Medicinal Chemistry Letters*, 13, 3905-3908.

Jones, G. M., Sanford, K. K., Parshad, R., Gantt, R., Price, F. M. and Tarone, R. E. (1985). Influence of added catalase on chromosome stability and neoplastic transformation of mouse cells in culture. *British Journal of Cancer*, 52, 583-590.

Jordan-Sciutto, K. L., Dorsey, R., Chalovich, E. M., Hammond, R. R. and Achim, C. L. (2003). Expression patterns of retinoblastoma protein in Parkinson disease. *Journal of Neuropathology and Experimental Neurology*, 62, 68-74.

Ju¨rgensmeier, J. M., Xie, Z., Deveraux, Q., Ellerby, L., Bredesen, D. E. and Reed, J. C. (1998). Bax directly induces release of cytochrome c from isolated mitochondria. *Proceedings of the National Academy of Sciences of the United States of America*, 95, 4997-5002.

Kalfon, L., Youdim, M. B. and Mandel, S. A. (2007). Green tea polyphenol (-)-epigallocatechin-3-gallate promotes the rapid protein kinase C and proteasome-mediated degradation of Bad: implications for neuroprotection. *Journal of Neurochemistry*, 100, 992-1002.

Kane, D. J., Sarafian, T. A., Anton, R., Hahn, H., Butler Gralla, E., Selverstone Valentine, J., et al. (1993). Bcl-2 inhibition of neural death: decreased generation of reactive oxygen species. *Science*, 262, 1274-1277.

Kang, S. S., Lee, J. Y., Choi, Y. K., Kim, G. S. and Han, B. H. (2004). Neuroprotective effects of flavones on hydrogen peroxide-induced apoptosis in SH-SY5Y neuroblostoma cells. *Bioorganic & Medicinal Chemistry Letters*, 14, 2261-2264.

Karawita, R., Siriwardhana, N., Lee, K., Heo, M., Yeo, I., Lee, Y., et al. (2005). Reactive oxygen species scavenging, metal chelation, reducing power and lipid peroxidation inhibition properties of different solvent fractions from *Hizikia fusiformis*. *European Food Research and Technology*, 220, 363-371.

Kawpoomhae, K., Sukma, M., Ngawhirunpat, T., Opanasopit, P. and Sripattanaporn, A. (2010). Antioxidant and neuroprotective effects of standardized extracts of *Mangifera indica* leaf. *Thai Journal of Pharmaceutical Sciences*, 34, 32-43.

Kehrer, J. P. (2000). The Haber-Weiss reaction and mechanisms of toxicity. *Toxicology*, 149, 43-50.

Kerr, J. F., Wyllie, A. H. and Currie, A. R. (1972). Apoptosis: a basic biological phenomenon with wide-ranging implications in tissue kinetics. *British Journal of Cancer*, 26, 239-257.

Klaus, A. and Heribert, H. (2004). Reactive oxygen species: Metabolism, oxidative stress, and signal transduction. *Annual Review of Plant Biology*, 55, 373-399.

Knebel, A., Rahmsdorf, H. J., Ullrich, A. and Herrlich, P. (1996). Dephosphorylation of receptor tyrosine kinases as target of regulation by radiation, oxidants or alkylating agents. *EMBO Journal*, 15, 5314-5325.

Koh, J. Y., Gwag, B. J., Lobner, D. and Choi, D. W. (1995a). Potentiated necrosis of cultured cortical neurons by neurotrophins. *Science*, 268, 573-575.

Koh, J. Y., Wie, M. B., Gwag, B. J., Sensi, S. L., Canzoniero, L. M. T., Demaro, J., et al. (1995b). Staurosponine-induced neuronal apoptosis. *Experimental Neurology*, 135, 153-159.

Koh, S. H., Lee, S. M., Kim, H. Y., Lee, K. Y., Lee, Y. J., Kim, H. T., et al. (2006). The effect of epigallocatechin gallate on suppressing disease progression of ALS model mice. *Neuroscience Letters*, 395, 103-107.

Kohn, K. W. (1999). Molecular interaction map of the mammalian cell cycle control and DNA repair systems. *Molecular Biology of the Cell*, 10, 2703-2734.

Koopman, G., Reutelingsperger, C. P., Kuijten, G. A., Keehnen, R. M., Pals, S. T. and Van Oers, M. H. (1994). Annexin V for flow cytometric detection of phosphatidylserine expression on B cells undergoing apoptosis. *Blood*, 84, 1415-1420.

Koppal, T., Drake, J., Yatin, S., Jordan, B., Varadarajan, S., Bettenhausen, L., et al. (1999). Peroxynitrite-induced alterations in synaptosomal membrane proteins: insight into oxidative stress in Alzheimer's disease. *Journal of Neurochemistry*, 72, 310-317.

Korsmeyer, S. J. (1992). Bcl-2: a repressor of lymphocyte death. *Immunology Today*, 13, 285-288.

Korsmeyer, S. J. (1999). Bcl-2 gene family and the regulation of programmed cell death. *Cancer Research*, 59, 1693-1700.

Kroemer, G. and Martin, S. J. (2005). Caspase-independent cell death. *Nature Medicine*, 11, 725-730.

Kroemer, G., Dallaporta, B. and Resche-Rigon, M. (1998). The mitochondrial death/life regulator in apoptosis and necrosis. *Annual Review of Physiology*, 60, 619-642.

Kroemer, G., Zamzami, N. and Susin, S. A. (1997). Mitochondrial control of apoptosis. *Immunology Today*, 18, 44-51.

Ksenzenko, M., Konstantinov, A. A., Khomutov, G. B., Tikhonov, A. N. and Ruuge, E. K. (1983). Effect of electron transfer inhibitors on superoxide generation in the cytochrome bc1 site of the mitochondrial respiratory chain. *FEBS Letters*, 155, 19-24.

Kuan, C. Y., Schloemer, A. J., Lu, A., Burns, K. A., Weng, W. L., Williams, M. T., et al. (2004). Hypoxia-ischemia induces DNA synthesis without cell proliferation in dying neurons in adult rodent brain. *Journal of Neuroscience*, 24, 10763-10772.

Kukielka, G. L., Youker, K. A., Michael, L. H., Kumar, A. G., Ballantyne, C. M., Smith, C. W., et al. (1995). Role of early reperfusion in the induction of adhesion molecules and cytokines in previously ischemic myocardium. *Molecular and cellular biochemistry*, 147, 5-12.

Kumamoto, M., Sonda, T., Nagayama, K. and Tabata, M. (2001). Effects of pH and metal ions on antioxidative activities of catechins. *Bioscience, Biotechnology, and Biochemistry*, 65, 126-132.

Kunkel, S. L. (1999). Through the looking glass: the diverse in vivo activities of chemokines. *The Journal of Clinical Investigation*, 104, 1333-1334.

Kuppusamy, U. R., Indran, M. and Balraj, B. R. S. (2002). Antioxidant effect of local fruits and vegetable extracts. *Journal of Tropical Medicinal Plants*, 3, 47-52.

Kusumoto, I. T., Shimada, I., Kakiuchi, N., Hattori, M., Namba, T. and Supriyatna, S. (1992). Inhibitory effects of Indonesian plant extracts on reverse transcriptase of an RNA tumor virus. *Phytotherapy Research*, 6, 241-244.

Laing, K. J. and Secombes, C. J. (2004). Chemokines. *Developmental and Comparative Immunology*, 28, 443-460.

Larson, R. A. (1988). The antioxidants of higher plants. *Phytochemistry*, 27, 969-978.

Laudanna, C. and Alon, R. (2006). Right on the spot. Chemokine triggering of integrin-mediated arrest of rolling leukocytes. *Journal of Thrombosis and Haemostasis*, 95, 5-11.

LeBrun, D. P., Warnke, R. A. and Cleary, M. L. (1993). Expression of bcl-2 in fetal tissues suggests a role in morphogenesis. *American Journal of Pathology*, 142, 743-753.

Lee, J. Y., Wang, W. I. H. and Lim, S. T. (2004). Antioxidant and anticancer activities of organic extracts from *Platycodon grandiflorum* A. De Candolle roots. *Journal of Ethnopharmacology*, 93, 409-415.

Lepoivre, M., Flaman, J. M., Bobé, P., Lemaire, G. and Henry, Y. (1994). Quenching of the tyrosyl free radical of ribonucleotide reductase by nitric oxide. *Journal of Biological Chemistry*, 269, 21891-21897.

Levites, Y., Amit, T., Mandel, S. and Youdim, M. B. (2003). Neuroprotection and neurorescue against amyloid beta toxicity and PKC-dependent release of non-amyloidogenic soluble precursor protein by green tea polyphenol (-)-epigallocatechin-3-gallate. *FASEB Journal*, 17, 952-954.

Levites, Y., Youdim, M. B., Maor, G. and Mandel, S. (2002). Attenuation of 6-hydroxydopamine (6-OHDA)-induced nuclear factor-kappaB (NF-kappaB) activation and cell death by tea extracts in neuronal cultures. *Biochemical Pharmacology*, 63, 21-29.

Lewis, W. (1985). Establishment of mouse cells lines homozygous for temperature-sensitive mutation in catalastic gene. *Somatic Cell and Molecular Genetics*, 11, 319-324.

Li, L. Y., Luo, X. and Wang, X. (2001). Endonuclease G is an apoptotic DNase when released from mitochondria. *Nature*, 412, 95-99.

Li, S. Z. (1975). Material Medica Principles: describes 1,892 kinds of medical material in 1578 AD. In The Great Pharmacopoeia (Ben-Cao Gang-mu). *In People's Health Publication Beijing*, 1-52.

Liao, S. (2001). The medicinal action of androgens and green tea epigallocatechin gallate. *Hong Kong Medical Journal*, 7, 369-374.

Lin, J. H. and Lin, Y. T. (1999). Flavonoids from the leaves of *Loranthus kaoi* (chao) kiu. *Yaowu Shipin Fenxi*, 7, 185-190.

Linnik, M. D., Zobrist, R. H. and Hatfield, M. D. (1993). Evidence supporting a role for programmed cell death in focal cerebral ischemia in rats. *Stroke*, 24, 2002-2008.

Livak, K. J. and Schmittgen, T. D. (2001). Analysis of relative gene expression data using real-time quantitative PCR and the 2-ΔΔCT method. *Methods*, 25, 402- 408.

Lo, L. and Anderson, D. J. (1995). Postmigratory neural crest cells expressing c-RET display restricted developmental and proliferative capacities. *Neuron*, 15, 527-539.

Loo, D. T., Copani, A., Pike, C. J., Whittemore, E. R., Walencewicz, A. J. and Cotman, C. W. (1993). Apoptosis is induced by beta-amyloid in cultured central nervous system neurons. *Proceedings of the National Academy of Sciences of the United States of America*, 90, 7951-7955.

Loschen, G., Azzi, A., Richter, C. and Flohe, L. (1974). Superoxide radicals as precursors of mitochondrial hydrogen peroxide. *FEBS Letters*, 42, 68-72.

Lossi, L. and Merighi, A. (2003). In vivo cellular and molecular mechanisms of neuronal apoptosis in the mammalian central nervous system. *Progress in Neurobiology*, 69, 287-312.

Macho, A., Hirsch, T., Marzo, I., Marchetti, P., Dallaporta, B., Susin, S. A., et al. (1997). Glutathione depletion is an early and calcium elevation is a late event of thymocyte apoptosis. *The Journal of Immunology*, 158, 4612-4619.

Mackay, C. R. (2001). Chemokines: immunology's high impact factors. *Nature Immunology*, 2, 95-101.

MacManus, J. P., Hill, I. E., Huang, Z. G., Rasquinha, I., Xue, D. and Buchan, A. M. (1994). DNA damage consistent with apoptosis in transient focal ischaemic neocortex. *NeuroReport*, 5, 493-496.

Mah, S. P., Zhong, L. T., Liu, Y., Roghani, A., Edwards, R. H. and Bredesen, D. E. (1993). The protooncogene bcl-2 inhibits apoptosis in PC12 cells. *Journal of Neurochemistry*, 60, 1183-1186.

Mahakunakorn, P., Tohda, M., Murakami, Y., Matsumoto, K. and Watanabe, H. (2004). Antioxidant and free radical-scavenging activity of Choto-san and its related constituents. *Biological and pharmaceutical bulletin*, 27, 38-46.

Maher, P. (2005). The effects of stress and aging on glutathione metabolism. *Ageing Research Reviews*, 4, 288-314.

Maiese, K. (1998). From the bench to the bedside: the molecular management of cerebral ischemia. *Clinical Neuropharmacology*, 21, 1-7.

Maiese, K., Chong, Z. Z., Hou, J. and Shang, Y. C. (2009a). The vitamin nicotinamide: translating nutrition into clinical care. *Molecules*, 14, 3446-3485.

Maiese, K., Chong, Z. Z., Hou, J. and Shang, Y. C. (2009b). New strategies for Alzheimer's disease and cognitive impairment. *Oxidative Medicine and Cellular Longevity*, 2, 279-290.

Malik, B., Currais, A., Andres, A., Towlson, C., Pitsi, D., Nunes, A., et al. (2008). Loss of neuronal cell cycle control as a mechanism of neurodegeneration in the presenilin-1 Alzheimer's disease brain. *Cell Cycle*, 7, 637-646.

Malstrom, B., Andreasson, L. and Reinhammer, B. (1975). The Enzymes. *X11B, Academic Press, New York*, 533.

Manach, C., Morand, C., Crespy, V., Demign´e, C., Texier, O., R´eg´erat, F., et al. (1998). Quercetin is recovered in human plasma as conjugated derivatives which retain antioxidant properties. *FEBS Letters*, 426, 331-336.

Mandel, S. and Youdim, M. B. H. (2004). Catechin polyphenols: neurodegeneration and neuroprotection in neurodegenerative diseases. *Free Radical Biology and Medicine*, 37, 304-317.

Mandel, S., Reznichenko, L., Amit, T. and Youdim, M. B. (2003). Green tea polyphenol (-)-epigallocatechin-3-gallate protects rat PC12 cells from apoptosis induced by serum withdrawal independent of P13-Akt pathway. *Neurotoxicology Research*, 5, 419-424.

Mandel, S., Weinreb, O., Amit, T. and Youdim, M. B. H. (2004). Cell signaling pathways in the neuroprotective actions of the green tea polyphenol (-)-epigallocatechin-3-gallate: implications for neurodegenerative diseases. *Journal of Neurochemistry*, 88, 1555-1569.

Manning, J. and Roberts, J. C. (2003). Analysis of catechin content of commercial green tea products. *Journal of Herbal Pharmacotherapy*, 3, 19-32.

Marchetti, P., Castedo, M., Susin, S. A., Zamzami, N., Hirsch, T., Macho, A., et al. (1996). Mitochondrial permeability transition is a central coordinating event of apoptosis. *The Journal of Experimental Medicine*, 184, 1155-1160.

Maroto, R. and Perez-Polo, J. R. (1997). Bcl-2-related protein expression in apoptosis: Oxidative stress versus serum deprivation in PC12 cells. *Journal of Neurochemistry*, 69, 514-523.

Martinou, J. C., Dubois-Dauphin, M., Staple, J. K., Rodriguez, I., Frankowski, H., Missotten, M., et al. (1994). Overexpression of Bcl-2 in transgenic mice protects neurons from naturally occurring cell death and experimental ischemia. *Neuron*, 13, 1017-1030.

Mattson, M. P. (2000). Apoptosis in neurodegenerative disorders. *Nature Reviews Molecular Cell Biology*, 1, 120-130.

Mattson, M. and Kroemer, G. (2003). Mitochondria in cell death: novel targets for neuroprotection and cardioprotection. *Trends in Molecular Medicine*, 9, 196-205.

Maxwell, S. R. J. (1995). Prospects for the use of antioxidant therapies. *Drugs*, 49, 345-361.

McCord, J. M. and Fridovich, I. (1969). An enzymic function for erythrocuprein (Hemocuprein). *Journal of Biological Chemistry*, 244, 6049-6055.

McCorkle, C. M., Mathias-Mundy, E. and Schillhorn van Veen, T. W. (1996). In: ethnoveterinary research and development. *Intermediate Technology Publications*, 137-147.

Mecocci, P., Beal, M. F., Cecchetti, R., Polidori, M. C., Cherubini, A., Chionne, F., et al. (1997a). Mitochondrial membrane fluidity and oxidative damage to mitochondrial DNA in aged and AD human brain. *Molecular and Chemical Neuropathology*, 31, 53-64.

Mecocci, P., Cherubini, A. and Senin, U. (1997b). Increased oxidative damage in lymphocytes of Alzheimer's disease patients. *Journal of the American Geriatrics Society*, 45, 1536-1537.

Mecocci, P., MacGarvey, U. and Beal, M. F. (1994). Oxidative damage to mitochondrial DNA is increased in Alzheimer's disease. *Annals of Neurology*, 36, 747-751.

Mehlen, P. and Bredesen, D. E. (2004). The dependence receptor hypothesis. *Apoptosis*, 9, 37-49.

Meister, A. (1988). On the discovery of glutathione. *Trends in Biochemical Sciences*, 13, 185-188.

Melkova, Z. S., Lee, B., Rodriguez, D. and Esteban, M. (1997). Bcl-2 prevents nitric oxide-mediated apoptosis and poly (ADP-ribose) polymerase cleavage. *FEBS Letters*, 403, 273-278.

Mellado, M., Rodríguez-Frade, J. M., Vila-Coro, A. J., Fernández, S., de Ana, A. M., Jones, D. R., et al. (2001). Chemokine receptor homo- or heterodimerization activates distinct signaling pathways. *EMBO Journal*, 20, 2497-2507.

Merad-Boudia, M., Nicole, A., Santiard-Baron, D., Saille, C. and Ceballos-Picot, I. (1998). Mitochondrial impairment as an early event in the process of apoptosis induced by glutathione depletion in neuronal cells: relevance to Parkinson's disease. *Biochemical Pharmacology*, 56, 645-655.

Merad-Saidoune, M., Boitier, E., Nicole, A., Marsac, C., Martinou, J. C., Sola, B., et al. (1999). Overproduction of Cu/Zn-superoxide dismutase or Bcl-2 prevents the brain mitochondrial respiratory dysfunction induced by glutathione depletion. *Experimental Neurology*, 158, 428-436.

Mitchell, P. and Moyle, J. (1965a). Evidence discriminating between the chemical and the chemiosmotic mechanisms of electron transport phosphorylation. *Nature*, 208, 1205-1206.

Mitchell, P. and Moyle, J. (1965b). Stoichiometry of proton translocation through the respiratory chain and adenosine triphosphatase systems of rat liver mitochondria. *Nature*, 208, 147-151.

Mo, J. Q., Hom, D. G. and Anderson, J. K. (1995). Decreases in protective enzymes correlates with increased oxidative damage in the aging mouse brain. *Mechanisms of Ageing and Development*, 81, 73-82.

Moosmann, B. and Behl, C. (2002). Antioxidants as treatment for neurodegenerative disorders. *Expert Opinion on Investigational Drugs*, 11, 1407-1435.

Moser, B. and Loetscher, P. (2001). Lymphocyte traffic control by chemokines. *Nature Immunology*, 2, 123-128.

Mosmann, T. (1983). Rapid colorimetric assay for cellular growth and survival: application to proliferation and cytotoxicity assays. *Journal of Immunological Methods*, 65, 55-63.

Mostafapour, S. P., del Puerto, N. M. and Rubel, E. W. (2002). Bcl-2 overexpression eliminates deprivation-induced cell death of brainstem auditory neurons. *Journal of Neuroscience*, 22, 4670-4674.

Murphy, P. M. (2002). International Union of Pharmacology. XXX. Update on chemokine receptor nomenclature. *Pharmacological Reviews*, 54, 227-229.

Murray, L. A., Syed, F., Li, L., Griswold, D. E. and Das, A. M. (2006). Role of chemokines in severe asthma. *Current Drug Targets*, 7, 579-588.

Nagira, M., Imai, T., Hieshima, K., Kusuda, J., Ridanpää, M., Takagi, S., et al. (1997). Molecular cloning of a novel human CC chemokine secondary lymphoid-tissue chemokine that is a potent chemoattractant for lymphocytes and mapped to chromosome 9p13. *Journal of Biological Chemistry*, 272, 19518-19524.

Nair, U., Bartsch, H. and Nair, J. (2003). Prevention of degehnerative diseases; clues from studies investigating oxidative stress. *Mutagenesis*, 18, 477-483.

Namiki, M., Yamashita, K. and Osawa, T. (1993). Food-related antioxidants and their activities in vivo. In: active oxygen, lipid peroxidases and antioxidants. *Japan Science Society Press*, 319-332.

Nanjo, F., Goto, K., Seto, R., Suzuki, M., Sakai, M. and Hara, Y. (1996). Scavenging effects of tea catechins and their derivatives on 1,1-diphenyl-2-picrylhydrazyl radical. *Free Radical Biology and Medicine*, 21, 895-902.

Narita, M., Shimizu, S., Ito, T., Chittenden, T., Lutz, R. J., Matsuda, H., et al. (1998). Bax interacts with the permeability transition pore to induce permeability transition and cytochrome c release in isolated mitochondria. *National Academy of Sciences of the United States of America*, 95, 14681-14686.

Nesic-Taylor, O., Cittelly, D., Ye, Z., Xu, G. Y., Unabia, G., Lee, J. C., et al. (2005). Exogenous Bcl-xL fusion protein spares neurons after spinal cord injury. *Journal of Neuroscience Research*, 79, 628-637.

Neves, S. R., Ram, P. T. and Iyengar, R. (2002). G protein pathways. *Science*, 296, 1636-1639.

Nguyen, M. D., Lariviere, R. C. and Julien, J. P. (2001). Deregulation of Cdk5 in a mouse model of amyotrophic lateral sclerosis: toxicity alleviated by perikaryal neurofilament inclusions. *Neuron*, 30, 135-147.

Nicoletti, I., Migliorati, G., Pagliacci, M., Grignani, F. and Riccardi, C. (1991). A rapid and simple method for measuring thymocyte apoptosis by propidium iodide staining and flow cytometry. *Journal of immunological methods*, 139, 271-279.

Nobre Junior, H. V., Cunha, G. M., Maia, F. D., Oliveira, R. A., Moraes, M. O. and Rao, V. S. (2003). Catechin attenuates 6-hydroxydopamine (6-OHDA)-induced cell death in primary cultures of mesencephalic cells. *Comparative Biochemistry and Physiology Part C: Toxicology & Pharmacology*, 136, 175-180.

Nohl, H., Gille, L., SchÖnheit, K. and Liu, Y. (1996). Conditions allowing redox-cycling ubisemiquinone in mitochondria to establish a direct redox couple with molecular oxygen. *Free Radical Biology and Medicine*, 20, 207-213.

Nonaka, G., Hsu, F. L. and Nishioka, I. (1981). Structures of dimeric, trimeric, and tetrameric procyanidins from *Areca catechu* L. *Journal of Chemical Society and Chemical Communication*, 15, 781-783.

Nonaka, G., Kawahara, O. and Nishioka, I. (1983). Tannins and related compounds. XV. A new class of dimeric flavan-3-olgallates, theasinensins A and B, and proanthocyanidin gallates from green tea leaf. *Chemical and Pharmaceutical Bulletin*, 31, 3906-3914.

Novack, D. V. and Korsmeyer, S. J. (1994). Bcl-2 protein expression during murine development. *American Journal of Pathology*, 145, 61-73.

Nunez, G., London, L., Hockenbery, D., Alexander, M., McKearn, J. P. and Korsmeyer, S. J. (1990). Deregulated Bcl-2 gene expression selectively prolongs survival of growth factor-deprived hemopoietic cell lines. *Journal of Immunology*, 144, 3602-3610.

Okamoto, M., Matsumoto, M., Ohtsuki, T., Taguchi, A., Mikoshiba, K., Yanagihara, T., et al. (1993). Internucleosomat DNA cleavage involved in ischemia-induced neuronal death. *Biochemical and Biophysical Research Communications*, 196, 1356-1362.

Okuda, T., Yoshida, T., Chen, X. M., Xie, J. X. and Fukushima, M. (1987). Corianin from *Coriaria japonica* A. Gray and sesquiterpene lactones from *Loranthus parasiticus* Merr used for treatment of schizophrenia. *Chemical & Pharmaceutical Bulletin*, 35, 182-187.

Oltvai, Z. N., Milliman, C. L. and Korsmeyer, S. J. (1993). Bcl-2 heterodimerizes in vivo with a conserved homolog, Bax, that accelerates programmed cell death. *Cell*, 74, 609-619.

Osuga, H., Osuga, S., Wang, F., Fetni, R., Hogan, M. J., Slack, R. S., et al. (2000). Cyclin-dependent kinases as a therapeutic target for stroke. *Proceedings of the National Academy of Sciences of the United States of America*, 97, 10254-10259.

Palluy, O. and Rigaud, M. (1996). Nitric oxide induces cultured cortical neuron apoptosis. *Neuroscience Letters*, 208, 1-4.

Pandolfo, M. (1998). Molecular genetics and pathogenesis of Friedreich ataxia. *Neuromuscular Disorders*, 8, 409-415.

Pease, J. E. and Williams, T. J. (2006). Chemokines and their receptors in allergic disease. *Journal of Allergy and Clinical Immunology*, 118, 305-318.

Pedrielli, P., Holkeri, L. M. and Skibsted, L. H. (2001). Antioxidant activity of (+)-catechin. Rate constant for hydrogen-atom transfer to peroxyl radicals. *European Food Research and Technology*, 213, 405-408.

Plotkin, M. J. (1992). Ethnomedicine: past, present and future. In: natural resources and human health: plants of medicinal and nutritional value. *Proceedings of Elsevier Amsterdam*, 79-86.

Polidori, M. C., Mecocci, P., Browne, S. E., Senin, U. and Beal, M. F. (1999). Oxidative damage to mitochondrial DNA in Huntington's disease parietal cortex. *Neuroscience Letters*, 272, 53-56.

Poot, M., Teubert, H., Rabinovitch, P. S. and Kavanagh, T. J. (1995). De novo synthesis of glutathione is required for both entry into and progression through the cell cycle. *Journal of Cellular Physiology*, 163, 555-560.

Putcha, G. V. and Johnson, E. M. (2004). Men are but worms: neuronal cell death in *C elegans* and vertebrates. *Cell Death and Differentiation*, 11, 38-48.

Rahman, Atta-ur., Khan, M. A. and Khan, N. H. (1973). Loranthol. New pentacyclic triterpenoid from *Loranthus grewinkii*. *Phytochemistry*, 12, 3004-3006.

Ranganathan, S. and Bowser, R. (2003). Alterations in G1 to S phase cell-cycle regulators during amyotrophic lateral sclerosis. *American Journal of Pathology*, 162, 823-835.

Rappert, A., Bechmann, I., Pivneva, T., Mahlo, J., Biber, K., Nolte, C., et al. (2004). CXCR3-dependent microglial recruitment is essential for dendrite loss after brain lesion. *Journal of Neuroscience*, 24, 8500-8509.

Rappert, A., Biber, K., Nolte, C., Lipp, M., Schubel, A., Lu, B., et al. (2002). Secondary lymphoid tissue chemokine (CCL21) acti- microglia. *Journal of Immunology*, 168, 3221-3226.

Rauhala, P., Lin, A. M. and Chiueh, C. C. (1998). Neuroprotection by S-nitrosoglutathione of brain dopamine neurons from oxidative stress. *Federation of American Societies for Experimental Biology Journal*, 12, 165-173.

Reddy, P. H. (2006). Mitochondrial oxidative damage in ageing and Alzheimer's disease: implications for mitochondrially targeted antioxidant therapeutics. *Journal of Biomedicine and Biotechnology*, 1155, 1-13.

Reddy, P. H. and Beal, M. F. (2005). Are mitochondria critical in the pathogenesis of Alzheimer's disease? *Brain Research*, 9, 618-632.

Reers, M., Smiley, S. T., Mottola-Hartshorn, C., Chen, A., Lin, M. and Chen, L. B. (1995). Mitochondrial membrane potential monitored by JC-1 dye. *Methods in Enzymology*, 260, 406-417.

Reiter, R. J. (1995). Oxidative processes and antioxidative defense mechanisms in the aging brain. *FASEB Journal*, 9, 526-533.

Rezai-Zadeh, K., Shytle, D., Sun, N., Mori, T., Hou, H., Jeanniton, D., et al. (2005). Green tea epigallocatechin-3-gallate (EGCG) modulates amyloid precursor protein cleavage and reduces cerebral amyloidosis in Alzheimer transgenic mice. *Journal of Neuroscience*, 25, 8807-8814.

Reznichenko, L., Amit, T., Youdim, M. B. and Mandel, S. (2005). Green tea polyphenol (-)-epigallocatechin-3-gallate induces neurorescue of long-term serum deprived PC12 cells and promotes neurite outgrowth. *Journal of Neurochemistry*, 93, 1157-1167.

Rice-Evans, C. A., Miller, N. J. and Paganga, G. (1996). Structure antioxidant activity relationship of flavonoids and phenolic acids. *Free Radical Biology and Medicine*, 20, 933-956.

Richardson, J. S., Subbarao, K. V. and Ang, L. C. (1992). On the possible role of iron-induced free radical peroxidation in neural degeneration in Alzheimer's disease. *Annals of the New York Academy of Sciences*, 648, 326-327.

Rittner, H. L. and Brack, A. (2006). Chemokines and pain. *Current Opinion in Investigational Drugs*, 7, 643-646.

Robberecht, W., Sapp, P., Viaene, M. K., Rosen, D., McKenna-Yasek, D., Haines, J., et al. (1994). Cu/Zn superoxide dismutase activity in familial and sporadic amyotrophic lateral sclerosis. *Journal of Neurochemistry*, 62, 384-387.

Rosen, D. R., Siddique, T., Patterson, D., Figlewicz, D. A., Sapp, P., Hentati, A., et al. (1993). Mutations in Cu/Zn superoxide dismutase gene are associated with familial amyotrophic lateral sclerosis. *Nature*, 362, 59-62.

Rossi, D. and Zlotnik, A. (2000). The biology of chemokines and their receptors. *Annual Review of Immunology*, 18, 217-242.

Rot, A. and von Andrian, U. H. (2004). Chemokines in innate and adaptive host defense: basic chemokinese grammar for immune cells. *Annual Review of Immunology*, 22, 891-928.

Rotig, A., de Lonlay, P., Chretien, D., Foury, F., Koenig, M., Sidi, D., et al. (1997). Aconitase and mitochondrial iron–sulphur protein deficiency in Friedreich ataxia. *Nature Genetics*, 17, 215-217.

Roussi, S., Gosse, F., Aoude-Werner, D., Zhang X., Marchioni, E., Geoffroy, P., et al. (2007). Mitochondrial perturbation, oxidative stress and lysosomal destabilization are involved in 7β-hydroxysitosterol and 7β-hydroxycholesterol triggered apoptosis in human colon cancer cells. *Apoptosis*, 12, 87-96.

Royall, J. A. and Ischiropoulos, H. (1993). Evaluation of 2',7'-dichlorofluorescin and dihydrorhodamine 123 as fluorescent probes for intracellular H_2O_2 in cultured endothelial cells. *Archives of Biochemistry and Biophysics*, 302, 348-355.

Sadik, G., Islam, R., Rahman, M. M., Khondkar, P., Rashid, M. A. and Sarker, S. D. (2003). Antimicrobial and cytotoxic constituents of *Loranthus globosus*. *Fitoterapia*, 74, 308-311.

Sagara, J. and Makino, N. (2008). Glutathione induces neuronal differentiation in rat bone marrow stromal cells. *Neurochemical Research*, 33, 16-21.

Salganik, R. I. (2001). The benefits and hazards of antioxidants: Controlling apoptosis and other protective mechanisms in cancer patients and the human population. *Journal of the American College of Nutrition*, 20, 464-472.

Sato, M., Horinouchi, T., Sakurai, M., Murakami, N., Sato, S. and Kato, M. (2003). Cyclosporin A reduces delayed motor neuron death after spinal cord ischemia in rabbits. *The Annals of Thoracic Surgery*, 75, 1294-1299.

Satoh, T., Sakai, N., Enokido, Y., Uchiyama, Y. and Hatanaka, H. (1996). Free radical-independent protection by nerve growth factor and Bcl-2 of PC12 cells from hydrogen peroxide-triggered apoptosis. *Journal of Biochemistry*, 120, 540-546.

Scaffidi, C., Fulda, S., Srinivasan, A., Friesen, C., Li, F., Tomaselli, K. J., et al. (1998). Two CD95 (APO-1/Fas) signaling pathways. *European Molecular Biology Organization Journal*, 17, 1675-1687.

Schafer, F. Q. and Buettner, G. R. (2001). Redox environment of the cell as viewed through the redox state of the glutathione disulfide/glutathione couple. *Free Radical Biology and Medicine*, 30, 1191-1212.

Schaffer, S., Eckert, G. P., Schmitt-Schillig, S. and Muller, W. F. (2006). Plant foods and brain aging: a critical apparaisal. *Forum of Nutrition*, 59, 86-115.

Schapira, A. H. (1998). Mitochondrial dysfunction in neurodegenerative disorders. *Biochimica et Biophysica Acta*, 1366, 225-233.

Seaton, T. A., Cooper, J. M. and Schapira, A. H. (1997). Free radical scavengers protect dopaminergic cell lines from apoptosis induced by complex I inhibitors. *Brain Research*, 777, 110-118.

Sentman, C. L., Shutter, R. H., Hockenbery, D., Kanagawa, O. and Korsmeyer, S. J. (1991). Bcl-2 inhibits multiple forms of apoptosis but not negative selection in thymocytes. *Cell*, 67, 879-888.

Sharpe, J. C., Arnoult, D. and Youle, R. J. (2004). Control of mitochondrial permeability by Bcl-2 family members. *Biochimica et Biophysica Acta-Molecular Cell Research*, 1644, 107-113.

Shimada, K., Fujikawa, K., Yahara, K. and Nakamura, T. (1992). Antioxidative properties of xanthan on the autoxidation of soyabean oil in cyclodextrin emulsion. *Journal of Agricultural and Food Chemistry*, 40, 945-948.

Sies, H. (1985). Oxidative stress: introductory remarks. In: Oxidative stress, ed. SIES H. *Academic Press London*, 1-8.

Sies, H. (1997). Oxidative stress: Oxidants and antioxidants. *Experimental Physiology*, 82, 291-295.

Simonati, A., Tosati, C., Rosso, T., Piazzola, E. and Rizzuto, N. (1999). Cell proliferation and death: morphological evidence during corticogenesis in the developing human brain. *Microscopy Research and Technique*, 45, 341-352.

Singh, R. J., Hogg, N., Joseph, J. and Kalyanaraman, B. (1996). Mechanism of nitric oxide release from S-nitrosothiols. *Journal of Biological Chemistry*, 271, 18596-18603.

Singh, R. P., Sharad, S. and Kapur, S. (2004). Free radicals and oxidative stress in neurodegenerative diseases: relevance of dietary antioxidants. *Journal, Indian Academy of Clinical Medicine*, 5, 218-225.

Singleton, V. L., Orthofer, R. and Lamuela-Raventós, R. M. (1999). Analysis of total phenols and other oxidation substrates and antioxidants by means of Folin-Ciocalteu reagent. *Methods in Enzymology*, 299, 152-178.

Slater, A. F., Stefan, C., Novel, I., Van Den Dobbelsteen, D. J. and Orrenius, S. (1995). Signaling mechanisms and oxidative stress in apoptosis. *Toxicology Letters*, 82-83, 149-153.

Smith, M. A., Richey Harris, P. L., Sayre, L. M., Beckman, J. S. and Perry, G. (1997). Widespread peroxynitrite-mediated damage in Alzheimer's disease. *Journal of Neuroscience*, 17, 2653-2657.

Smith, T. S. and Bennett, J. P. Jr. (1997). Mitochondrial toxins in models of neurodegenerative diseases. I: in vivo brain hydroxyl radical production during systemic MPTP treatment or following microdialysis infusion of methylpyridinium or azide ions. *Brain Research*, 765, 183-188.

Soto, H., Wang, W., Strieter, R. M., Copeland, N. G., Gilbert, D. J., Jenkins, N. A., et al. (1998). The CC chemokine 6Ckine binds the CXC chemokine receptor CXCR3. *Proceedings of the National Academy of Sciences of the United States of America*, 95, 8205-8210.

Spear, N., Estevez, A. G., Johnson, G. V., Bredesen, D. E., Thompson, J. A. and Beckman, J. S. (1998). Enhancement of peroxynitrite-induced apoptosis in PC12 cells by fibroblast growth factor-1 and nerve growth factor requires p21 Ras activation and is suppressed by Bcl-2. *Archives of Biochemistry and Biophysics*, 356, 41-45.

Spector, A. (1995). Oxidative stress-induced cataract: mechanism of action. *FASEB Journal*, 9, 1173-1182.

Steller, H. (1995). Mechanisms and genes of cellular suicide. *Science*, 267, 1445-1449.

Stokes, A. H., Lewis, D. Y., Lash, L. H., Jerome III, W. G., Grant, K. W., Aschner, M., et al. (2000). Dopamine toxicity in neuroblastoma cells: role of glutathione depletion by L-BSO and apoptosis. *Brain Research*, 858, 1-8.

Su, J. H., Deng, G. and Cotman, C. W. (1997). Neuronal DNA damage precedes tangle formation and is associated with up-regulation of nitrotyrosine in Alzheimer's disease brain. *Brain Research*, 774, 193-199.

Sugaya, K., Chouinard, M., Greene, R., Robbins, M., Personett, D., Kent, C., et al. (1996). Molecular indices of neuronal and glial plasticity in the hippocampal formation in a rodent model of age-induced spatial learning impairment. *Journal of Neuroscience*, 16, 3427-3443.

Sukma, W. and Siripong, T. (2006). Antioxidative and neuroprotective activities of extracts from the fruit hull of mangosteen (*Garcinia mangostana* Linn). *Medical Principles and Practice*, 15, 281-287.

Suma, C., Hayashi, S., Ukai, Y., Yoshikuni, Y. and Kimura, K. (1997). Na^{+} and high-voltage-activated Ca^{2+} channel blocking actions of NS-7, a novel neuroprotective agent, in NG108-15 cells. *European journal of pharmacology*, 336, 283-290.

Susin, S. A., Lorenzo, H. K., Zamzami, N., Marzo, I., Brenner, C., Larochette, N., et al. (1999). Mitochondrial release of caspase-2 and -9 during the apoptotic process. *Journal of Experimental Medicine*, 189, 381-393.

Suzuki, H., Yamamoto, S., Hirayama, C., Takino, T., Fujisawa, K. and Oda, T. (1986). Cianidanol therapy for HBs-antigen-positive chronic hepatitis: a muticentre, double-blind study. *Liver*, 6, 35-44.

Tanaka, K., Fujita, N., Yoshioka, M. and Ogawa, N. (2001). Immunosuppressive and non-immunosuppressive immunophilin ligands improve H_2O_2-induced cell damage by increasing glutathione levels in NG108-15 cells. *Brain Research*, 889, 225-228.

Tateishi, N., Higashi, T., Naruse, A., Nakashima, K. and Shiozaki, H. (1977). Rat liver glutathione: possible role as a reservoir of cysteine. *Journal of Nutrition*, 107, 51-60.

Tawaha, K., Alali, F. Q., Gharaibeh, M., Mohammad, M. and El-Elimat, T. (2007). Antioxidant activity and total phenolic content of selected Jordanian plant species. *Food Chemistry*, 104, 1372-1378.

Tetich, M., Leśkiewicz, M., Budziszewska, B., Basta-Kaim, A., Kutner, A. and Lasoń, W. (2003). The third multidisciplinary conference on drug research, Piła 2002. Effects of 1alpha, 25-dihydroxyvitamin D3 and some putative steroid neuroprotective agents on the hydrogen peroxide-induced damage in neuroblastoma-glioma hybrid NG108-15 cells. *Acta poloniae pharmaceutica*, 60, 351-355.

Thomas, B., Muralikrishnan, D. and Mohanakumar, K. P. (2000). In vivo hydroxyl radical generation in the striatum following systemic administration of 1-methyl-4-phenyl-1,2,3,6- tetrahydropyridine in mice. *Brain Research*, 852, 221-224.

Tian, L., Cai, Q. and Wei, H. (1998). Alterations of antioxidant enzymes and oxidative damage to macromolecules in different organs of rats during aging. *Free Radical Biology and Medicine*, 24, 1477-1484.

Timsit, S., Rivera, S., Ouaghi, P., Guischard, F., Tremblay, E., Ben-Ari, Y., et al. (1999). Increased cyclin D1 in vulnerable neurons in the hippocampus after ischemia and epilepsy: a modulator of in vivo programmed cell death? *European Journal of Neuroscience*, 11, 263-278.

Tong, L. and Perez-Polo, J. R. (1996). Effect of nerve growth factor on AP-1, NF-kB, and Oct DNA binding activity in apoptotic PC12 cells: extrinsic and intrinsic elements. *Journal of Neuroscience Research*, 45, 1-12.

Tseng, K. F. and Chen, Z. L. (1957). Studies of the chemical compositions of *Loranthus parasiticus*. II. Isolation of quercetin and its glucoside in Kwang chi-shen. *Yaoxue Xuebao*, 5, 317-325.

Turrens, J. F., Alexandre, A. and Lehninger, A. L. (1985). Ubisemiquinone is the election donor for superoxide formation by complex III of heart mitochondria. *Archives of Biochemistry and Biophysics*, 237, 408-414.

Ubogu, E. E., Cossoy, M. B. and Ransohoff, R. M. (2006). The expression and function of chemokines involved in CNS inflammation. *Trends in Pharmacological Sciences*, 27, 48-55.

Vajragupta, O., Boonchoong, P., Watanabe, H., Tohda, M., Kummasud, N. and Sumanont, Y. (2003). Manganese complexes of curcumin and its derivatives: evaluation for the radical scavenging ability and neuroprotective activity. *Free Radical Biology and Medicine*, 35, 1632-1644.

Van Acker, S. A., Van Den Berg, D. J., Tromp, M. N., Griffioen, D. H., Van Bennekom, W. P., Van Der Vijgh, W. J., et al. (1996). Structural aspects of antioxidant activity of flavonoids. *Free Radical Biology and Medicine*, 20, 331-342.

Van de Loosdrecht, A. A., Beelen, R. H. J., Ossenkoppele, G. J., Broekhoven, M. G. and Langenhuijsen, M. M. A. C. (1994). A tetrazolium-based colorimetric MTT assay to quantitate humanmonocyte mediated cytotoxicity against leukemic cells from cell lines and patients with acute myeloid leukemia. *Journal of Immunological Methods*, 174, 311-320.

Vaux, D. L., Cory, S. and Adams, J. M. (1988). Bcl-2 gene promotes haemopoietic cell survival and cooperates with c-myc to immortalize pre-B cells. *Nature*, 335, 440-442.

Velioglu, Y. S., Mazza, G., Gao, L. and Oomah, B. D. (1998). Antioxidant activity and total phenolics in selected fruits, vegetables, and grain products. *Journal of Agricultural and Food Chemistry*, 46, 4113-4117.

Vincent, A. M. and Maiese, K. (1999). Nitric oxide induction of neuronal endonuclease activity in programmed cell death. *Experimental Cell Research*, 246, 290-300.

Vincent, I., Jicha, G., Rosado, M. and Dickson, D. W. (1997). Aberrant expression of mitotic cdc2/cyclin B1 kinase in degenerating neurons of Alzheimer's disease brain. *Journal of Neuroscience*, 17, 3588-3598.

Wall, N. R., Mohammad, R. M. and Al-Katib, A. M. (1999). Bax: Bcl-2 ratio modulation by bryostatin 1 and novel antitubulin agents is important for susceptibility to drug induced apoptosis in the human early pre-B acute lymphoblastic leukemia cell line, Reh. *Leukemia Research*, 23, 881-888.

Wang, F. P. and Yuan, Y. P. (1980). Isolation of some chemical constituents from *Loranthus parasiticus* (L) Merr. *Chung Tsao Yao*, 11, 345.

Warita, H., Hayashi, T., Murakami, T., Manabe, Y. and Abe, K. (2001). Oxidative damage to mitochondrial DNA in spinal motoneurons of transgenic ALS mice. *Molecular Brain Research*, 89, 147-152.

Wcyant, M. J., Carothers, A. M., Danncnberg, A. J. and Bertagnolli, M. M. (2001). (+)-Catechin inhibits intestinal tumor formation and suppresses focal adhesion kinase activation in the min/+ mouse. *Cancer Research*, 61, 118-125.

Weinreb, O., Mandel, S. and Youdim, M. B. (2003). Gene and protein expression profiles of anti- and pro-apoptotic actions of dopamine, R-apomorphine, green tea polyphenol (-)-epigallocatechine-3-gallate, and melatonin. *Annals of the New York Academy of Sciences*, 993, 351-361.

Weiss, R. F. and Fintelmann, V. (2000). In: herbal Medicine. *Thieme Stuttgart*, 3-20.

Whittemore, E. R., Loo, D. T., Watt, J. A. and Cotman, C. W. (1995). A detailed analysis of hydrogen peroxide-induced cell death in primary neuronal culture. *Neuroscience*, 67, 921-932.

Wiedau-Pazos, M., Goto, J. J., Rabizadeh, S., Gralla, E. B., Roe, J. A., Lee, M. K., et al. (1996). Altered reactivity of superoxide dismutase in familial amyotrophic lateral sclerosis. *Science*, 271, 515-518.

Winterbourn, C. C. and Metodiewa, D. (1994). The reaction of superoxide with reduced glutathione. *Archives of Biochemistry and Biophysics*, 314, 284-290.

Wolter, K. G., Hsu, Y. T., Smith, C. L., Nechushtan, A., Xi, X. G. and Youle, R. J. (1997). Movement of Bax from the cytosol to mitochondria during apoptosis. *Journal of Cell Biology*, 139, 1281-1292.

Wu, C. Y. and Zhang, G. D. (1984). Quantitative analysis of sesquiterpene lactones in *Loranthus parasiticus* (L) Merr. parasiting on *Coriaria sinica* maxim and in seeds of *Coriaria sinica* maxim. *Yaoxue Xue bao*, 19, 56-62.

Wu, C. Y., Zhang, G. D. and Liu, H. Y. (1982). Colorimetric method for microdetermination of tutin in *Loranthus parasiticus* (or *L. yadoriki*) and in injections. *Zhong Cao Yao*, 13, 536-539.

Wyllie, A. H. (1980). Glucocorticoid-induced thymocyte apoptosis is associated with endogenous endonuclease activation. *Nature*, 284, 555-556.

Xie, C., Lovell, M. A. and Markesbery, W. R. (1998). Glutathione transferase protects neuronal cultures against four hydroxynonenal toxicity. *Free Radical Biology and Medicine*, 25, 979-988.

Yang, C. S. (1999). Tea and health. *Nutrition*, 15, 946-949.

Yang, Y. and Herrup, K. (2007). Cell division in the central nervous system: protective response or lethal event in post-mitotic neurons? *Biochimica et Biophysica Acta*, 1772, 457-466.

Yao, C. H., Tsai, H. M., Chen, Y. S. and Liu, B. S. (2005). Fabrication and evaluation of a new composite composed of tricalcium phosphate, gelatin, and Chinese medicine as a bone substitute. *Journal of Biomedical Materials Research Part B: Applied Biomaterials*, 2, 277-288.

Yim, H. S., Kang, J. H., Chock, P. B., Stadtman, E. R. and Yim, M. B. (1997). A familial amyotrophic lateral sclerosis-associated A4V Cu, Zn-superoxide dismutase mutant has a lower Km for hydrogen peroxide. Correlation between clinical severity and the Km value. *The Journal of Biological Chemistry*, 272, 8861-8863.

Yim, M. B., Kang, J. H., Yim, H. S., Kwak, H. S., Chock, P. B. and Stadtman, E. R. (1996). A gain-of-function of an amyotrophic lateral sclerosis-associated Cu, Zn-superoxide dismutase mutant: an enhancement of free radical formation due to a decrease in Km for hydrogen peroxide. *Proceedings of the National Academy of Sciences USA*, 93, 5709-5714.

Yin, X. M., Oltvai, Z. N. and Korsmeyer, S. J. (1994). BH1 and BH2 domains of Bcl-2 are required for inhibition of apoptosis and heterodimerization with Bax. *Nature*, 369, 321-323.

Yoon, Y., Kim, K. S., Hong, S. G., Kang, B. J., Lee, M. Y. and Cho, D. W. (2000). Protective effects of *Orostachys japonicus* A. Berger (Crassulaceae) on H_2O_2-induced apoptosis in GT1-1 mouse hypothalamic neuronal cell line. *Journal of Ethnopharmacology*, 69, 73-78.

Yoshida, R., Nagira, M., Kitaura, M., Imagawa, N., Imai, T. and Yoshie, O. (1998). Secondary lymphoid-tissue chemokine is a functional ligand for the CC chemokine receptor CCR7. *Journal of Biological Chemistry*, 273, 7118-7122.

Yoshimura, T., Matsushima, K., Tanaka, S., Robinson, E. A., Appella, E., Oppenheim, J. J., et al. (1987). Purification of a human monocyte-derived neutrophil chemotactic factor that has peptide sequence similarity to other host defense cytokines. *Proceedings of the National Academy of Sciences of the United States of America*, 84, 9233-9237.

Zaleska, M. M. and Floyd, R. A. (1985). Regional lipid peroxidation in rat brain in vitro: possible role of endogenous iron. *Neurochemical Research*, 10, 397-410.

Zamzami, N., Larochette, N. and Kroemer, G. (2005). Mitochondrial permeability transition in apoptosis and necrosis. *Cell Death and Differentiation*, 2, 1478-1480.

Zamzami, N., Marchetti, P., Castedo, M., Zanin, C., Vayssiere, J. L., Petit, P. X., et al. (1995). Reduction in mitochondrial potential constitutes an early irreversible step of programmed lymphocyte death in vivo. *The Journal of Experimental Medicine*, 181, 1661-1672.

Zamzami, N., Susin, S. A., Marchetti, P., Hirsch, T., Go´mez-Monterrey, I., Castedo, M., et al. (1996). Mitochondrial control of nuclear apoptosis. *The Journal of Experimental Medicine*, 183, 1533-1544.

Zaveri, N. T. (2006). Green tea and its polyphenolic catechins: Medicinal uses in cancer and noncancer applications. *Life Sciences*, 78, 2073-2080.

Zheng, W. and Wang, S. Y. (2001). Antioxidant activity and phenolic compounds in selected herbs. *Journal of Agricultural and Food Chemistry*, 49, 5165-5170.

Zhong, L. T., Sarafian, T., Kane, D. J., Charles, A. C., Mah, S. P., Edwards, R. H., et al. (1993). Bcl-2 inhibits death of central neural cells induced by multiple agents. *Proceedings of the National Academy of Sciences of the United States of America*, 90, 4533-4537.

Zlotnik, A. (2006). Involvement of chemokine receptors in organspecific metastasis. *Contributions to Microbiology*, 13, 191-199.

Zoratti, M. and Szabo, I. (1995). The mitochondrial permeability transition. *Biochimica et Biophysica Acta*, 1241, 139-176.

APPENDIX

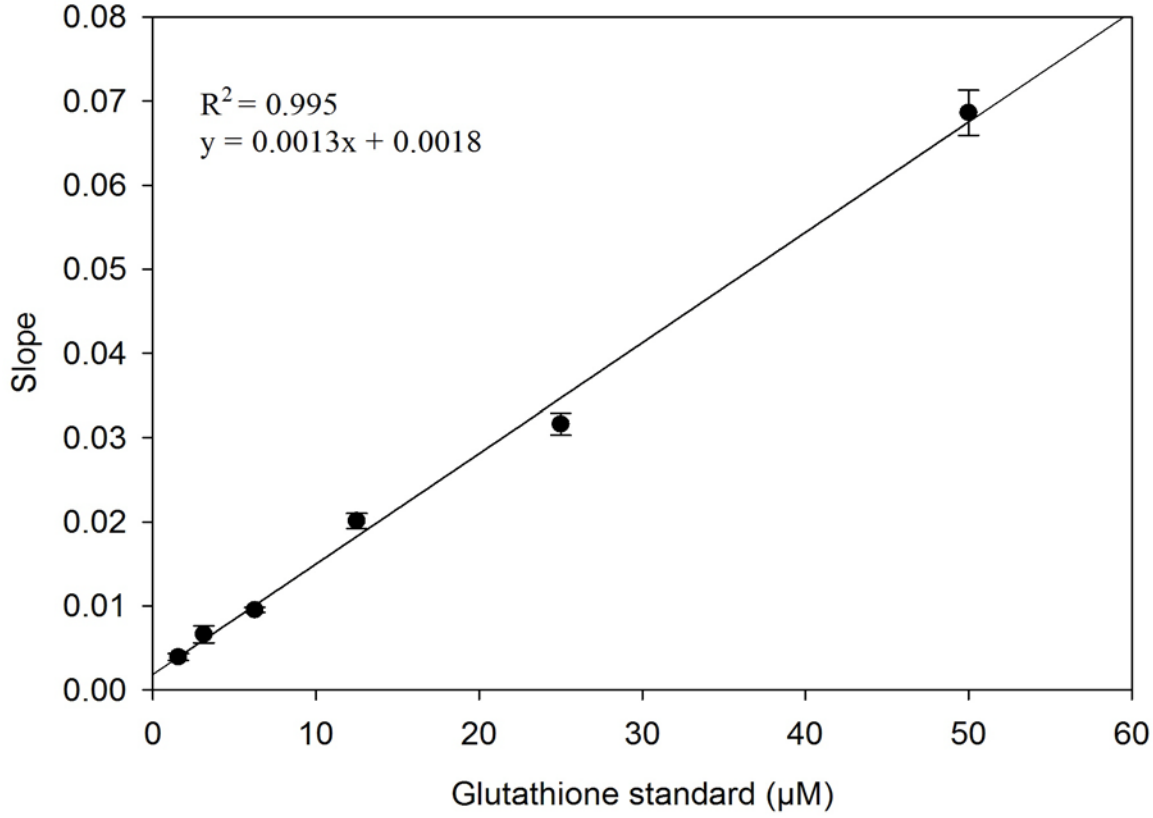

Appendix 1. Standard curve of GSH

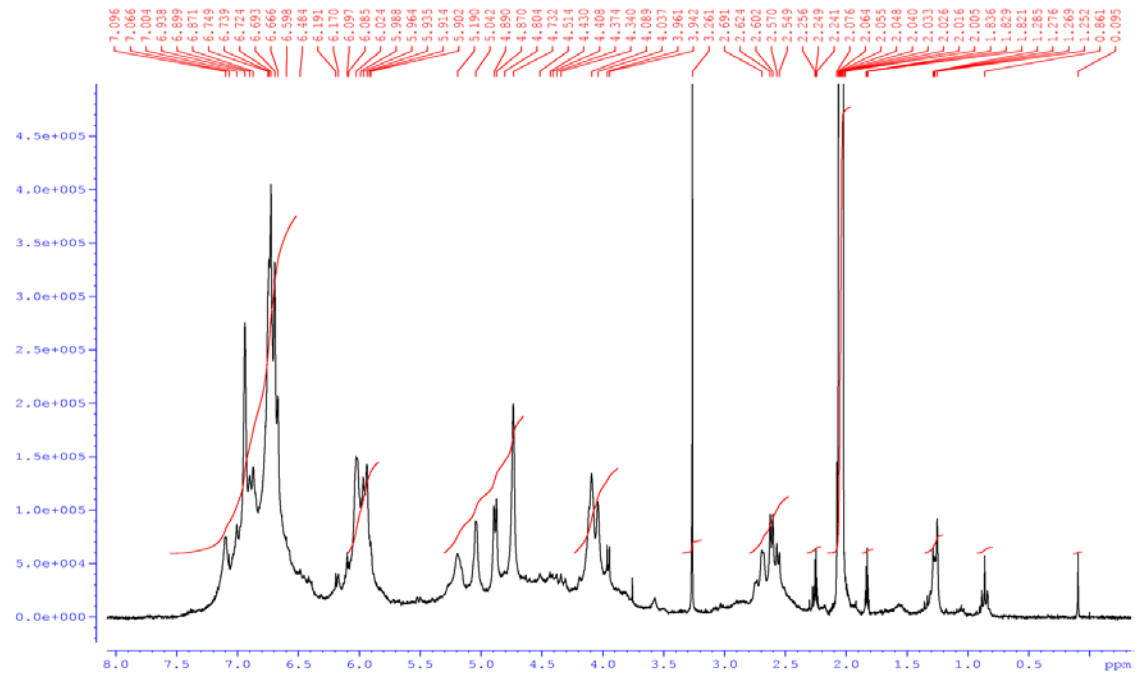

Appendix 2. H represents ^{1}H-NMR spectrum for AC Trimer

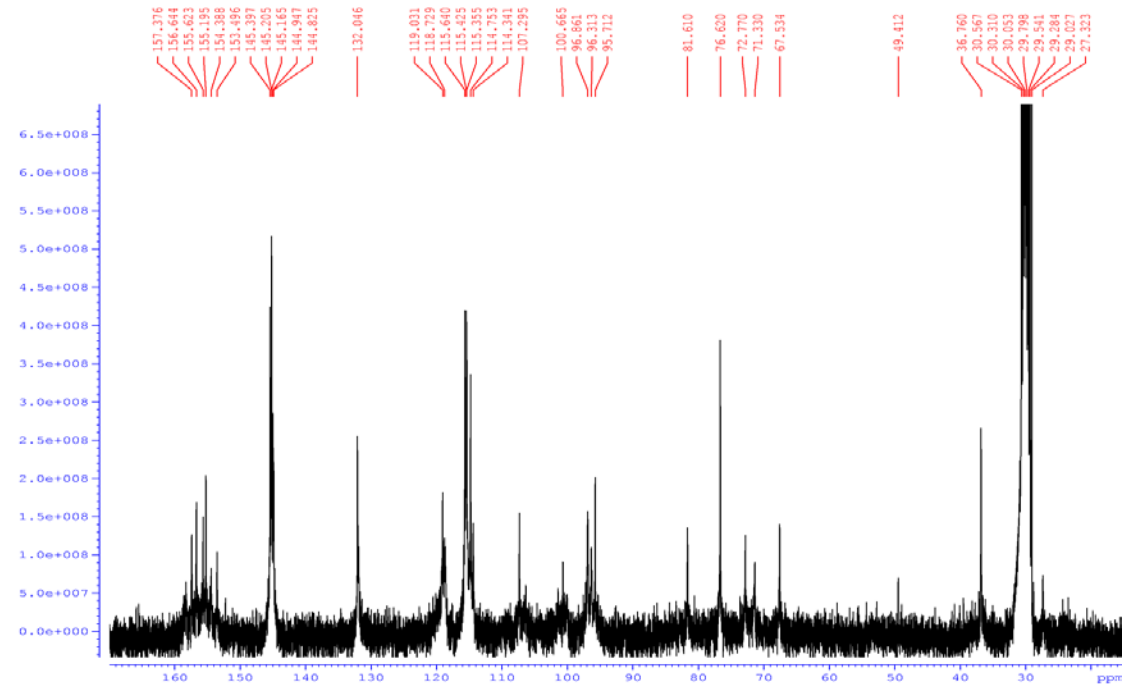

Appendix 3. C represents ^{13}C-NMR spectrum for AC Trimer

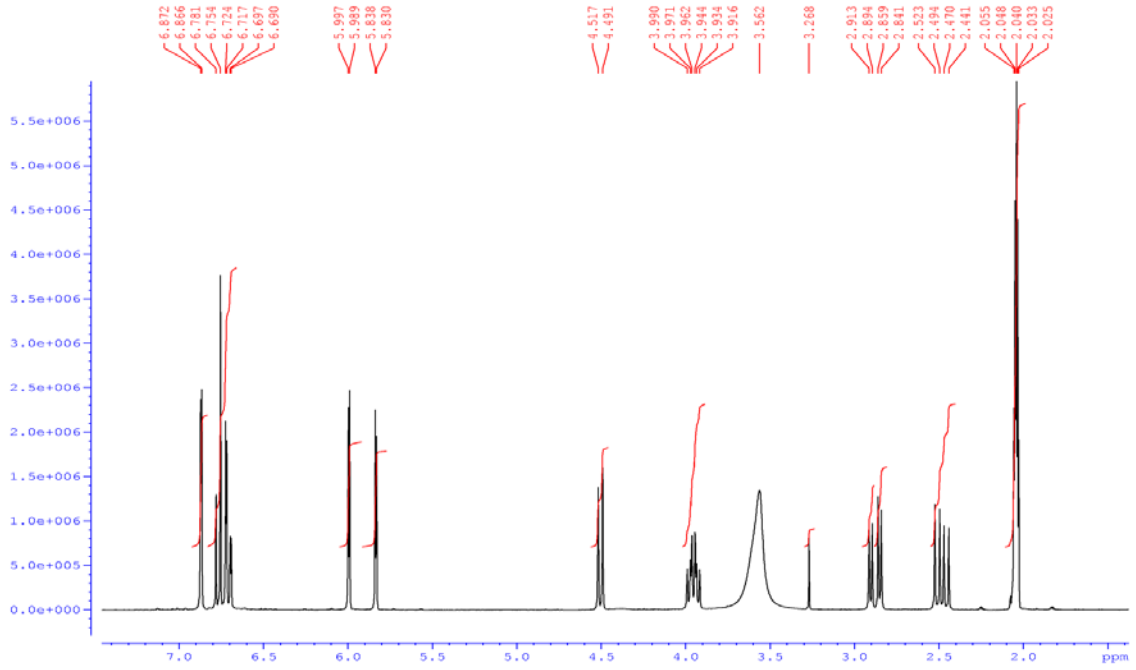

Appendix 4. H represents ^{1}H-NMR spectrum for (+)-catechin

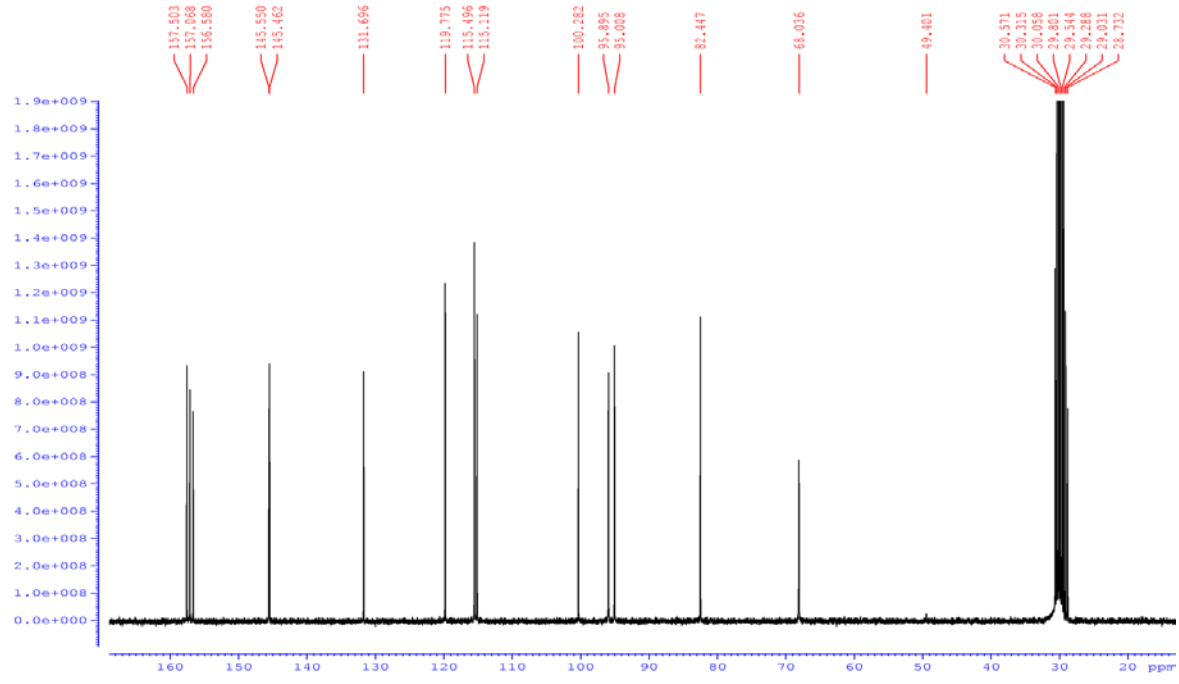

Appendix 5. C represents ^{13}C-NMR spectrum for (+)-catechin

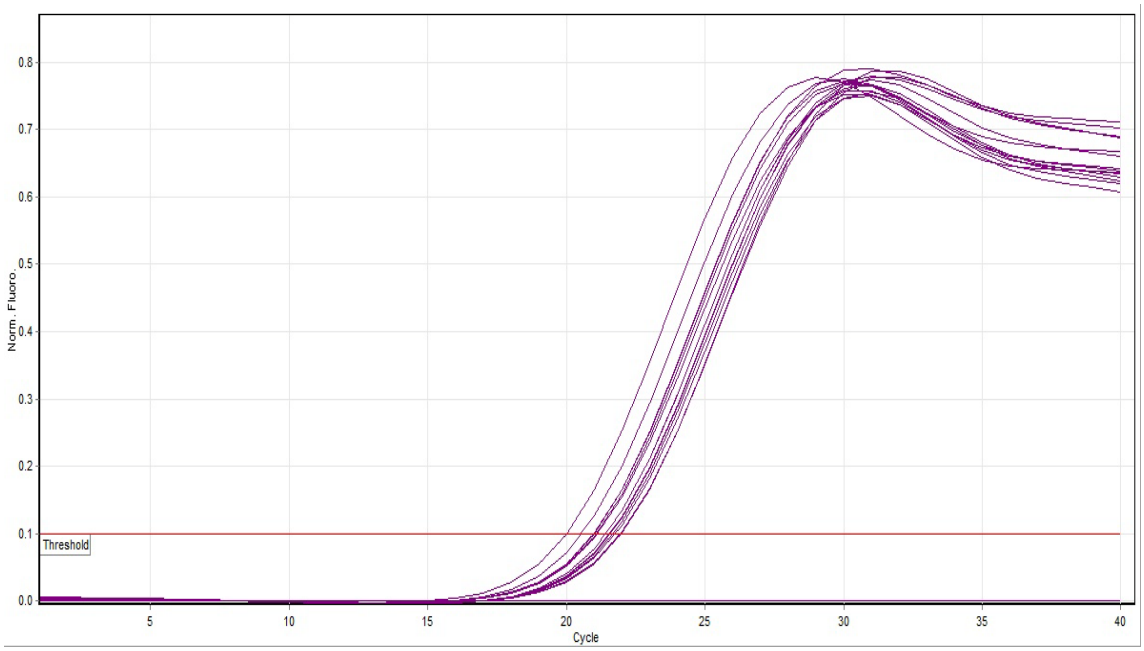

Appendix 6. Amplification curve of Bax

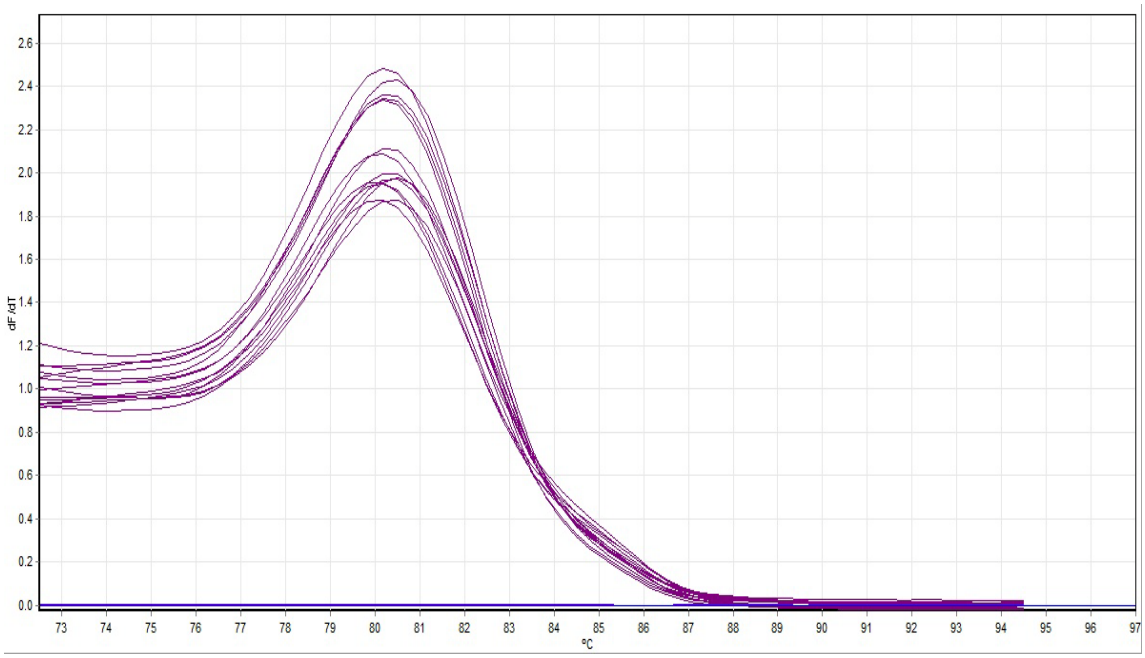

Appendix 7. Melt curve of Bax

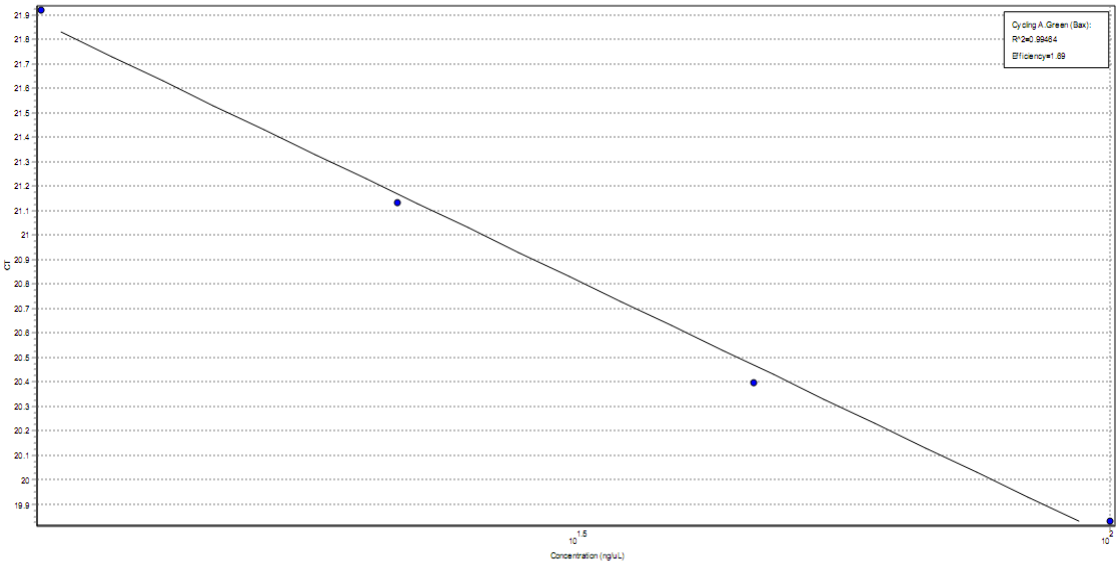

Appendix 8. Standard curve of Bax

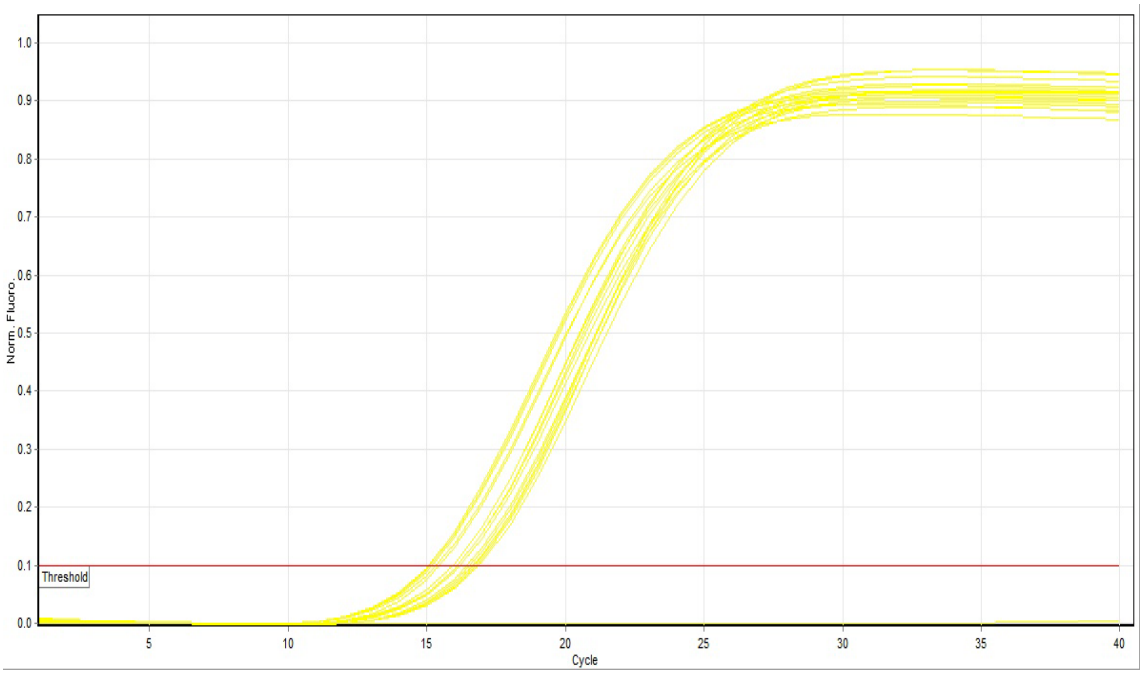

Appendix 9. Amplification curve of HMBS

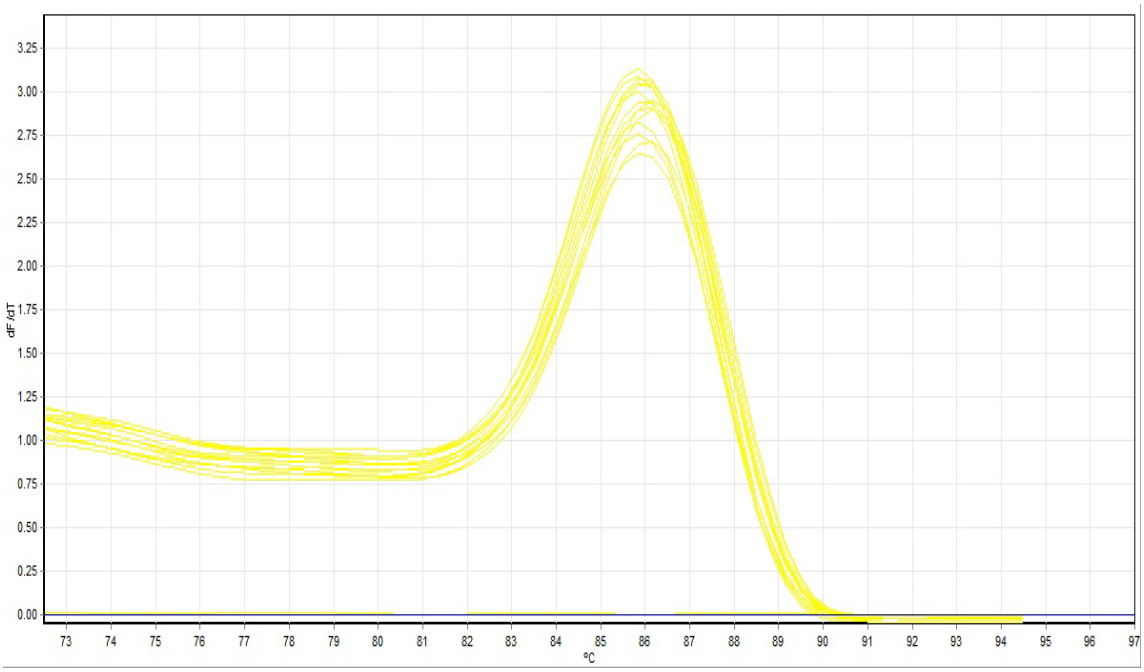

Appendix 10. Melt curve of HMBS

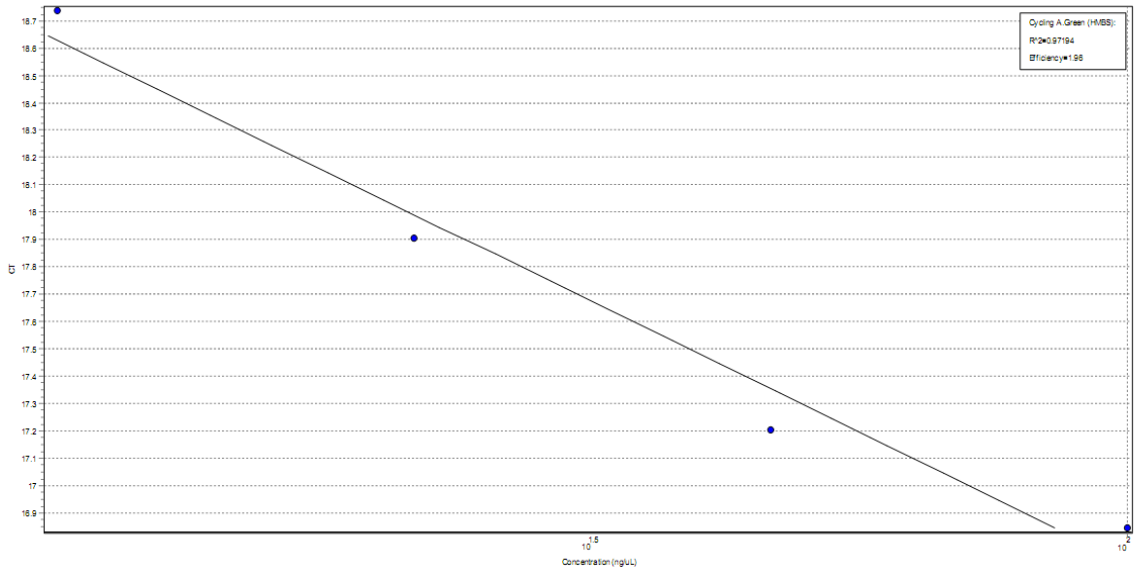

Appendix 11. Standard curve of HMBS

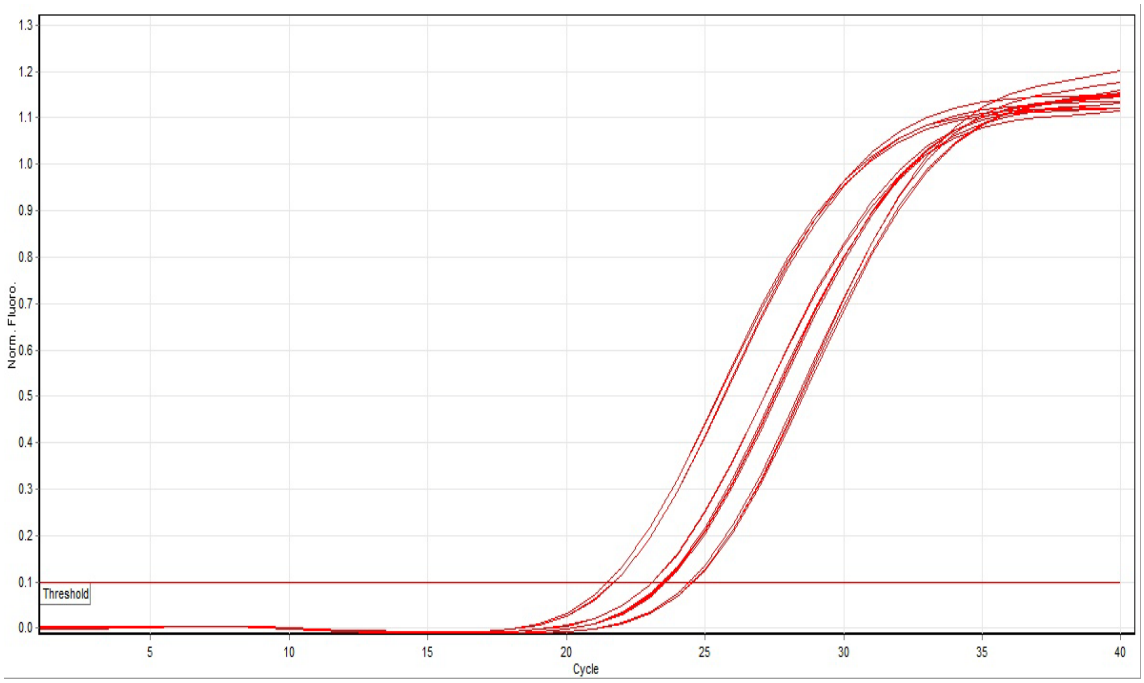

Appendix 12. Amplification curve of Bcl-2

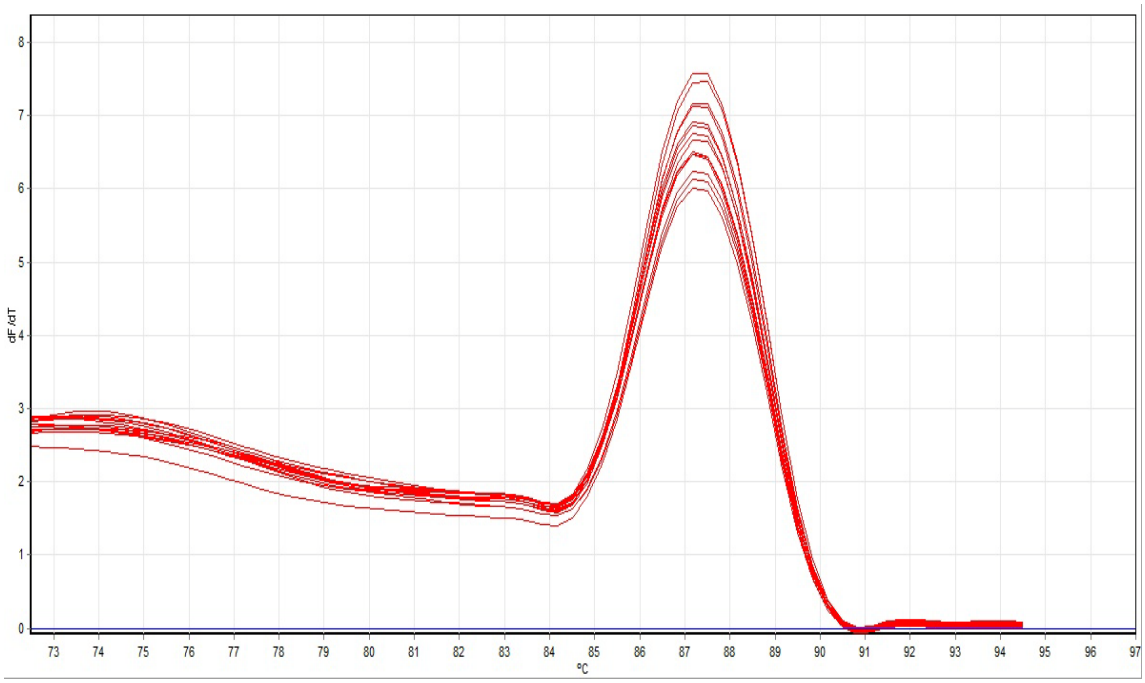

Appendix 13. Melt curve of Bcl-2

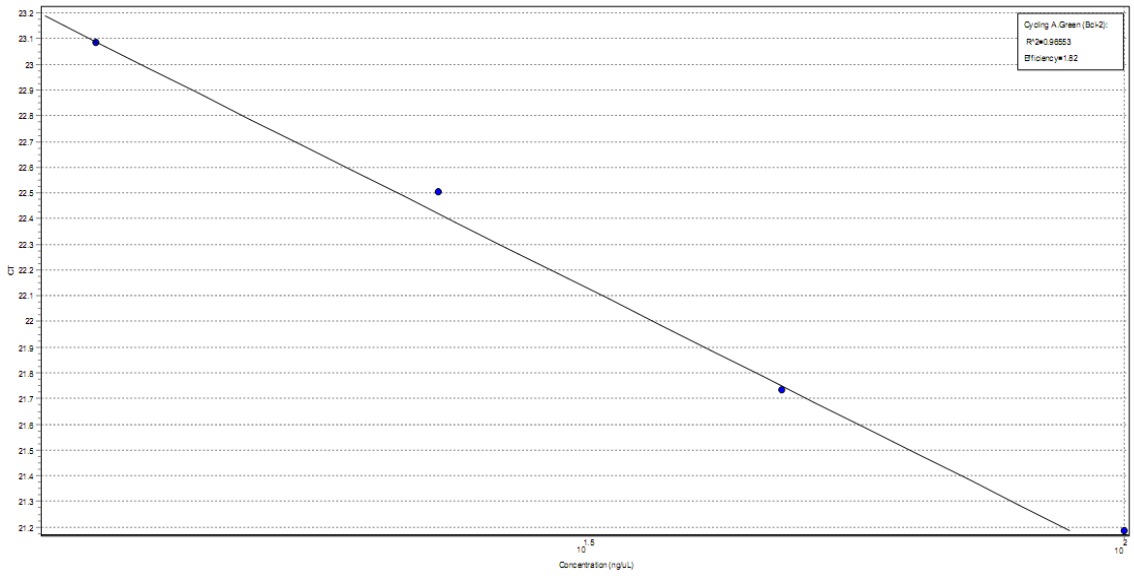

Appendix 14. Standard curve of Bcl-2

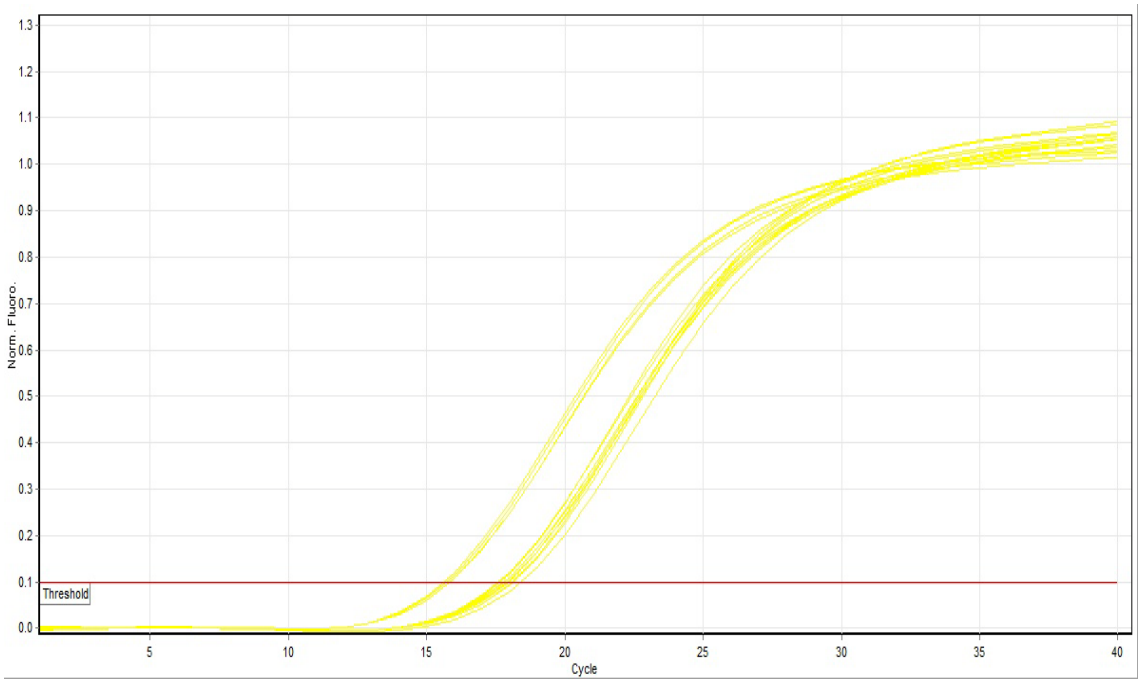

Appendix 15. Amplification curve of HMBS

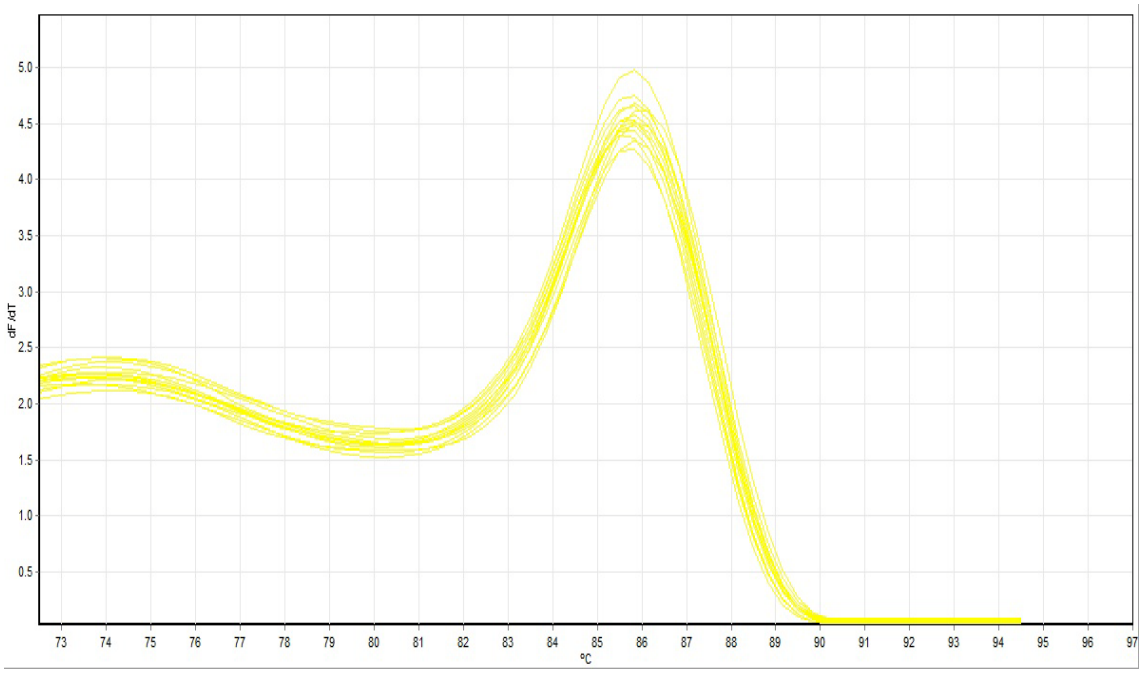

Appendix 16. Melt curve of HMBS

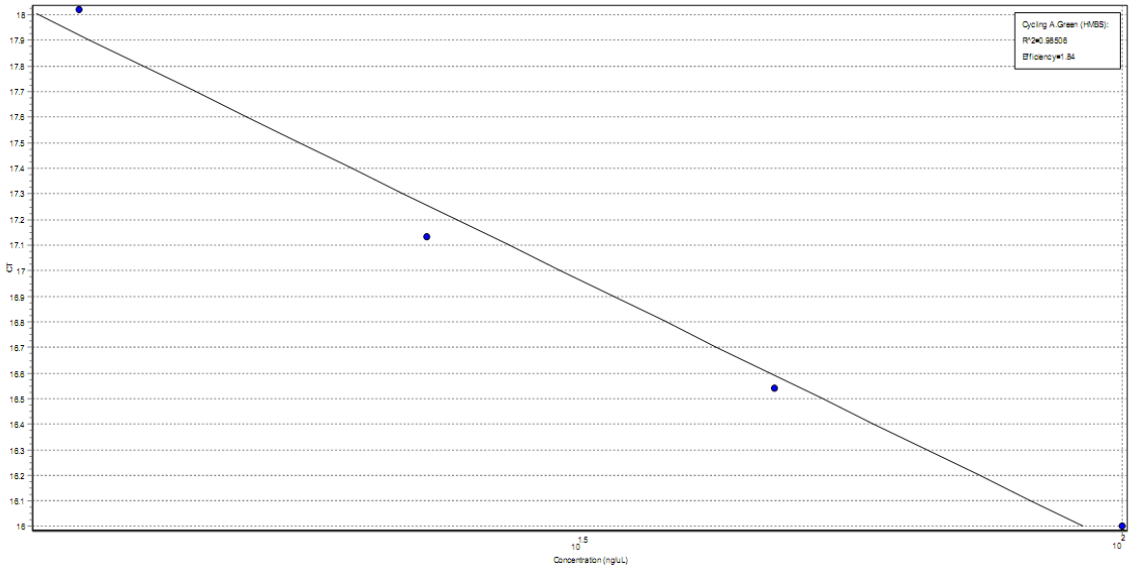

Appendix 17. Standard curve of HMBS

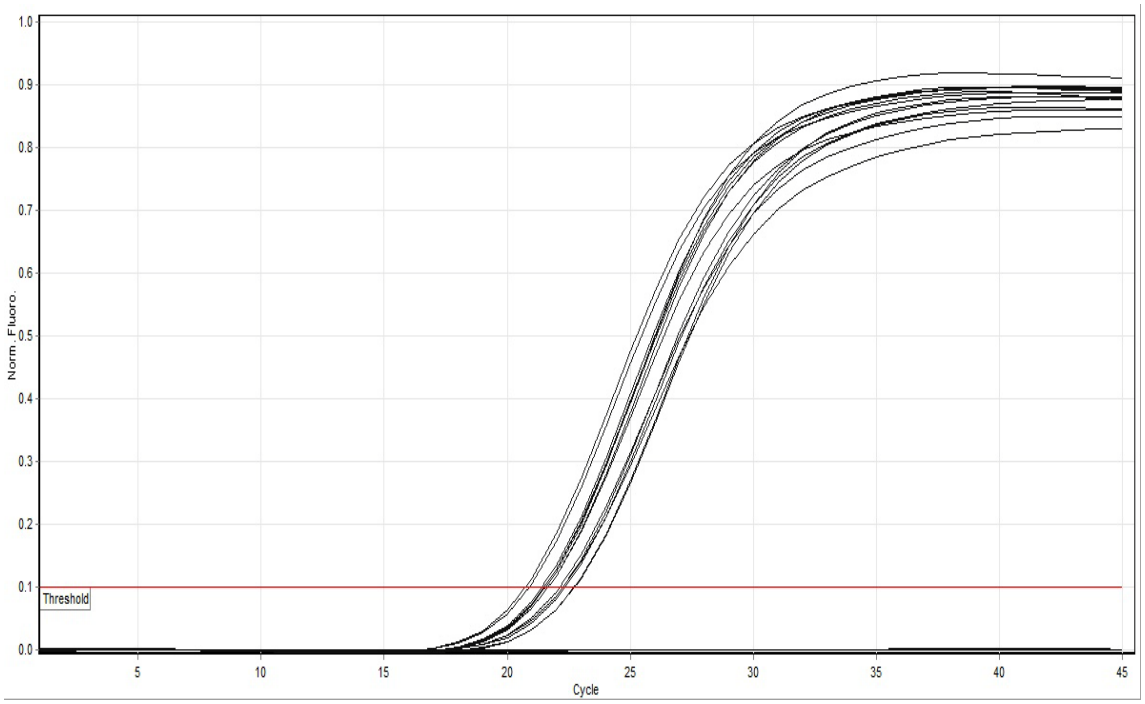

Appendix 18. Amplification curve of CCL21

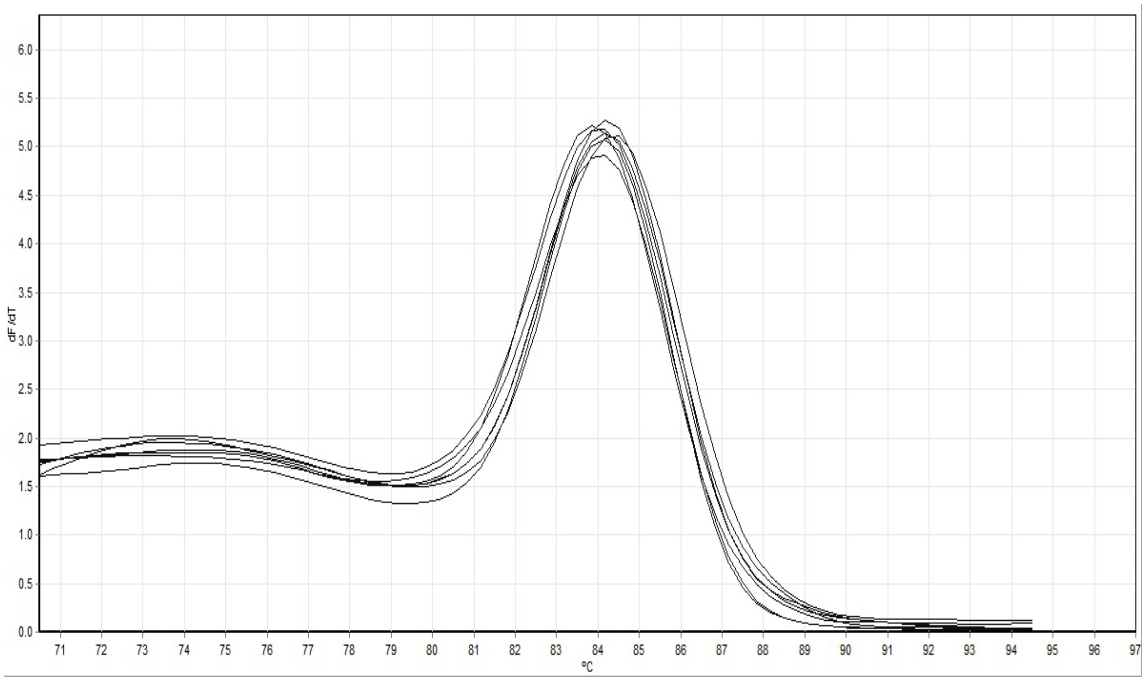

Appendix 19. Melt curve of CCL21

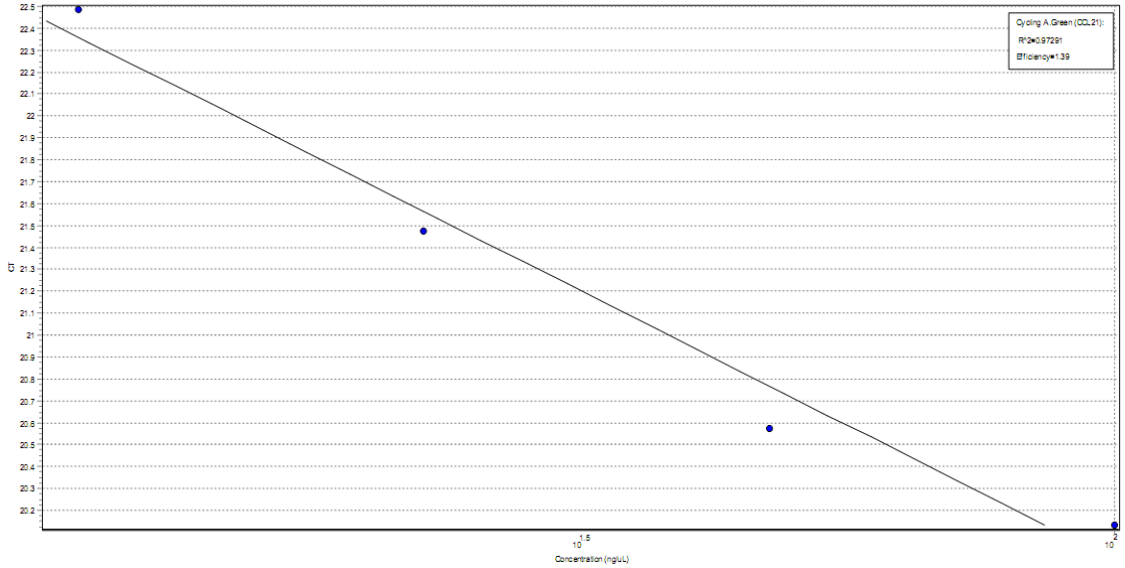

Appendix 20. Standard curve of CCL21

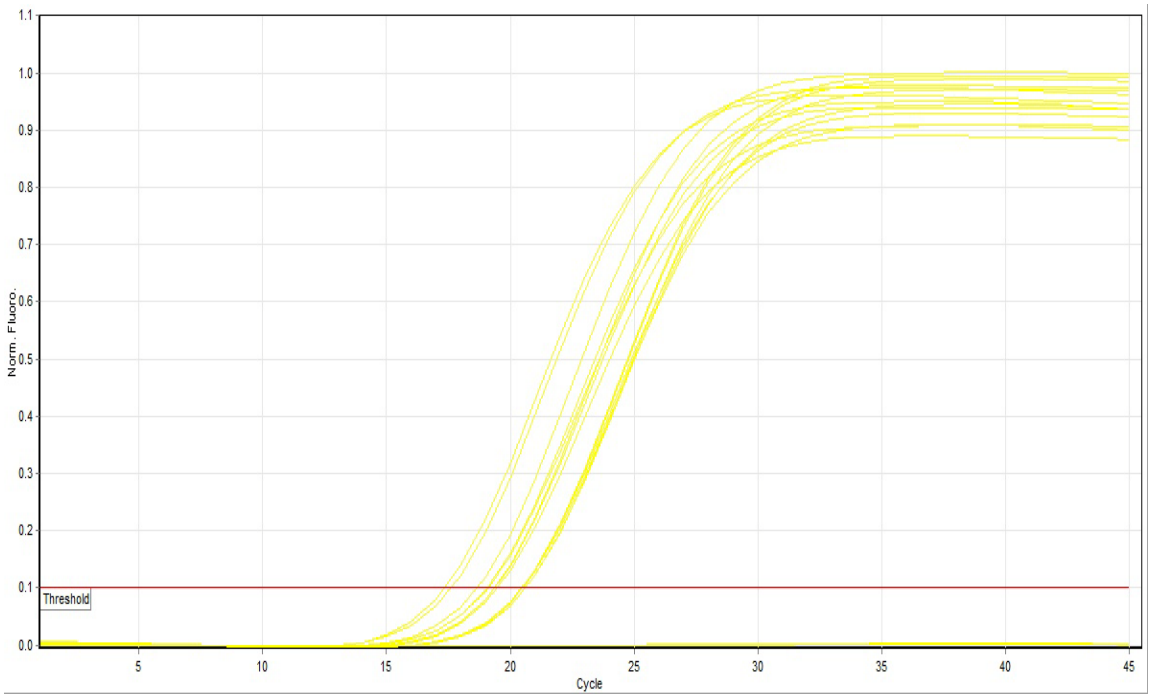

Appendix 21. Amplification curve of HMBS

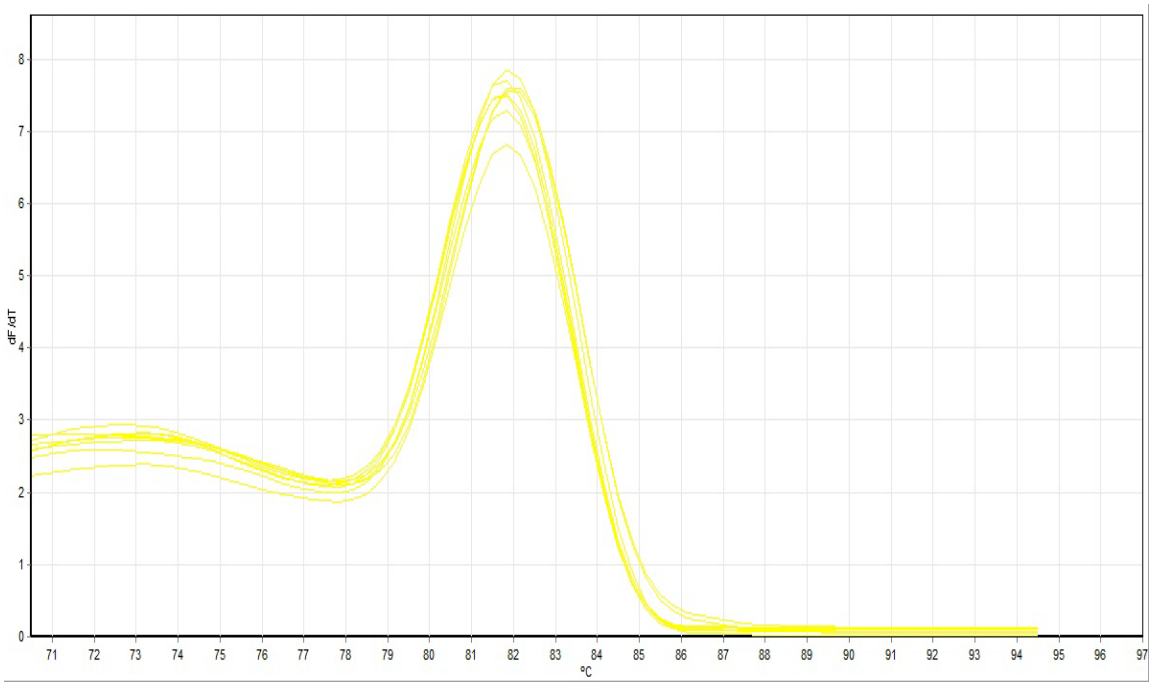

Appendix 22. Melt curve of HMBS

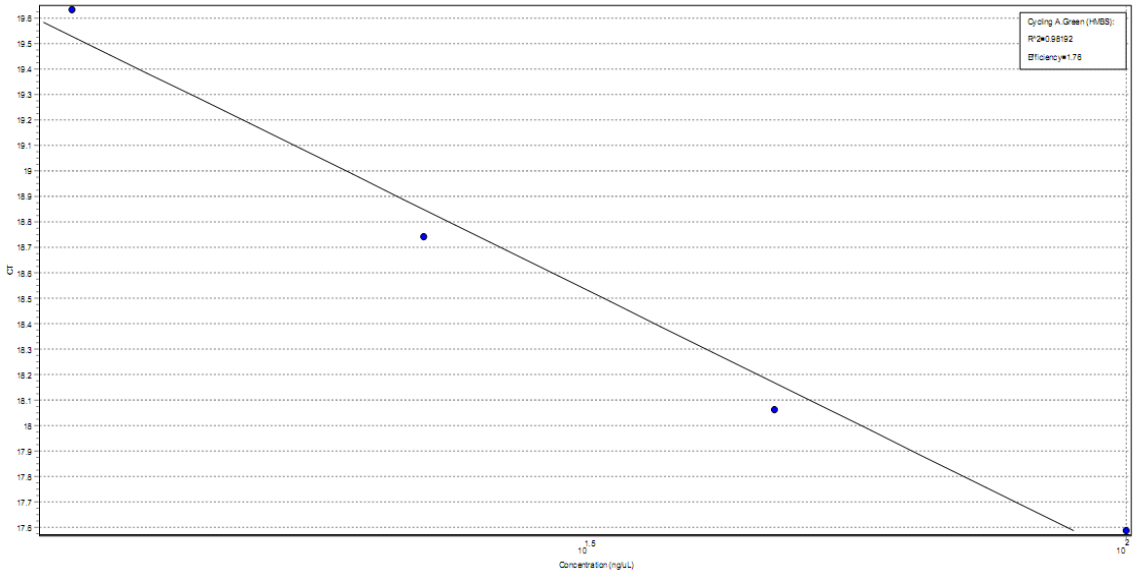

Appendix 23. Standard curve of HMBS